Universidad de Huelva

Departamento de Ingeniería Química, Química Física y Ciencia de los Materiales

Desarrollo de bioplásticos a partir de subproductos agroalimentarios con aplicaciones en envases y matrices de difusión

Memoria para optar al grado de doctora
presentada por:

Diana Patricia Gómez Martínez

Fecha de lectura: 20 de febrero de 2013

Bajo la dirección de los doctores:

Pedro Partal López

Inmaculada Martínez García

Huelva, 2013

Universidad de Huelva

2013

DESARROLLO DE BIOPLÁSTICOS A PARTIR DE SUBPRODUCTOS AGROALIMENTARIOS CON APLICACIONES EN ENVASES Y MATRICES DE DIFUSIÓN

Programa de Doctorado
Ingeniería de Fluidos Complejos

Diana Patricia Gómez Martínez

DESARROLLO DE BIOPLÁSTICOS A PARTIR DE SUBPRODUCTOS AGROALIMENTARIOS CON APLICACIONES EN ENVASES Y MATRICES DE DIFUSIÓN

DEVELOPMENT OF PROTEIN-BASED BIOPLASTICS FOR POTENCIAL APPLICATION IN PACKAGING AND CONTROLLED RELEASE

Universidad de Huelva

Departamento de Ingeniería Química, Química Física y Química Orgánica

Memoria de Tesis presentada por Dña. Diana Patricia Gómez Martínez, Ingeniera Agroindustrial, para aspirar al Grado de Doctor con Mención Internacional del Programa de Doctorado de Ingeniería de Fluidos Complejos.

Huelva, 4 de Junio de 2013

Fdo. Diana Patricia Gómez Martínez

Universidad de Huelva

Departamento de Ingeniería Química,
Química Física y Química Orgánica

Esta Tesis ha sido dirigida por los Profesores Dr. Pedro Partal López y Dra. Inmaculada Martínez García del Departamento de Ingeniería Química, Química Física y Química Orgánica de la Universidad de Huelva.

Huelva, 4 de Junio de 2013

Fdo. Dr. Pedro Partal López

Fdo. Dra. Inmaculada Martínez García

Universidad de Huelva

Departamento de Ingeniería Química,
Química Física y Química Orgánica

This work is part of a research project sponsored by OX-CTA, by "Consejería de Innovación, Ciencia y Empresa de la Junta de Andalucía" (Ref. P06–TEP–02126) and by "Ministerio de Economía y Competitividad" (Ref. MAT2011-29275-C02-01). The author gratefully acknowledges their financial support.

Agradecimientos/Acknowlegements

Primero que todo me gustaría agradecer en gran manera a Dios por haber hecho posible que este gran sueño se convirtiera en realidad. Sobre todo, porque ha puesto en mi camino personas maravillosas que han contribuido de manera directa e indirecta en la consecución de este sueño y también en mi formación personal, profesional e incluso espiritual.

Agradezco al Prof. Crispulo Gallego por darme la oportunidad de pertenecer al Grupo de Ingeniería de Fluidos Complejos y desde entonces comenzar en el mundo de la investigación científica.

Especialmente expreso mi gratitud a mis directores de tesis Pedro Partal López e Inmaculada Martínez García, por llevarme de la mano en estos años de doctorado. Por vuestro tiempo, dedicación y paciencia al compartir sus conocimientos y sabios consejos conmigo. Muchas gracias por ser mis padres de la ciencia y por creer en mí.

A todos mis colegas y amigos de trabajo del Grupo de Ingeniería de Fluidos Complejos, por su ayuda oportuna en las tareas de investigación, por sus consejos y soporte en los momentos que lo he necesitado, por todos los momentos vividos.

A todo el personal del Departamento de Ingeniería Química y la Universidad de Huelva por brindarme amablemente el soporte y los medios necesarios para el desarrollo de este Trabajo.

Inmensa gratitud a mi familia (Los Gómez Vides), mi Padre y Evita por formarme con valores cristianos y darme las herramientas necesarias para ser la persona que soy hoy día. Infinitas gracias por todo su amor y apoyo incondicional.

Muchas gracias a mis amigos por aceptarme con mis defectos y virtudes, por escucharme, por gozarse con mis alegrías y darme animo en mis momentos de debilidad.

Sist men inte minst, till min stora kärlek Magnus Heincke för all sin kärlek, tålamod och stöd. Dessa år med dig har varit de lyckligaste i mitt liv.

A mi familia: Los Gómez Vides,

mi Padre y Evita

Och min största kärlek Magnus

LIST OF PUBLICATIONS

I. Gluten-based bioplastics with modified controlled-release and hydrophilic properties. Gomez-Martinez, D.; Partal, P.; Martinez, I.; Gallegos, C. Industrial Crops and Products. **2013**, 43, pag. 704-710.

II. Modelling of pyrolysis and combustion of gluten–glycerol-based bioplastics. Gomez-Martinez, D.; Barneto, A.; Martinez, I., Partal, P. Bioresource Technology. **2011**, 102. Pag. 6246-6253.

III. Rheological behaviour and physical properties of controlled-release gluten-based bioplastics. Gomez-Martinez, D.; Partal, P.; Martinez, I.; Gallegos, C. Bioresource Technology. **2009**, 100, Pag. 1828-1832.

IV. Rhelogical and release behaviour of gluten-based bioplastics. Gomez-Martinez, D.; Partal, P.; Martinez, I.; Gallegos, C. Book: Rheology in product design and engineering. Edited by : A. Guerrero, J. Muñoz and J.M. Franco. Grupo Español de Reología RSEQ. **2008.**

RELATED PUBLICATION NOT INCLUDED IN THE THESIS

V. Correlation between viscoelasticity, microstructure and molecular properties of zein and pennisetin melts. Journal of Applied Polymer Science. Gómez-Martínez, D, Altskär, A. Stading, M. DOI: 10.1002/app.36454 .

NON-RELATED PUBLICATION

VI. Viscoelasticity and microstructure of a hierarchical soft composite based on nano-cellulose and κ-carrageenan. Gómez-Martínez, Stading, M., Hermansson, A-M. Rheol Acta Journal. Submitted.

PATENT

VII. New materials to obtain biodegradable films and bags by extrusion blow molding, and their method of preparation. D. Gómez-Martínez; I. Martínez, M. García-Morales, P. Partal; C. Gallegos. P200901035. Spain **2009**.

CONTENTS

I. INTRODUCTION

Non-renewable plastics have serious drawbacks, most of them related to the raw material availability, also non-renewable, and volatility of the crude oil world market. Thus, the growing demand of petroleum and the political circumstances in many of the most important oil-producing countries have increased petroleum prices far away from those of the previous decades (Shawkat and Li, 2004). In addition, synthetic polymers have the serious disadvantage of their low biodegradability, which means that, once discarded, these materials must be stored in landfills for long periods of time (years or even decades) leading to the gradual accumulation of waste volume.

As a consequence, the development of new biodegradable materials able to substitute synthetic polymers has become a relevant challenge nowadays. Such biodegradable plastics can be manufactured not only from bio-based feedstock but also from petrochemical raw materials. But bio-based plastics or bioplastics, defined as plastics that are fully or partially produced from renewable raw materials, have a more relevant role in the domain of biodegradable plastics. Such bioplastics are mixtures of biopolymers and plasticizers, whose characteristics resemble a thermoplastic (or thermosetting) synthetic polymer with similar roles in certain applications. In addition, they have the advantage of their biodegradability, which adds an extra value to materials developed from them (Domenek et al., 2004). According to Biodegradable Products Institute, bioplastics from renewable resources do not generate waste since they decompose in a reasonable time into carbon dioxide and water.

Currently, many bioplastics are still in the developmental stage, but important applications are beginning to emerge in the areas of packaging, food production and medicine. Bioplastics can be used as adhesives, absorbents, lubricants, soil conditioners, cosmetics, drug delivery vehicles, textiles, high-strength structural materials, and even computational switching devices (Chen and Tan, 2006; Archambault et al., 2004; Lörck et al., 2000; Suda et al., 2000; Kinney and Scranton, 1994). Some biopolymers can directly replace synthetically

derived materials in traditional applications, whereas others possess unique properties that could open up a range of new commercial opportunities.

Among others, biopolymers from agricultural resources are becoming an interesting alternative not only as biodegradable films, suitable for food packaging, but also as plastic stuffs which require improved mechanical properties. As a result, novel biopolymer compounds are being investigated by established agricultural and chemical firms, as well as small biotechnology enterprises. In recent years the growing interest in using natural biopolymers has focused on those obtained from animal and plant raw materials such as proteins, lipids, polysaccharides and other compounds synthesized from living organisms (Irissin-Mangata et al., 2001; De Graaf, 2000).

In particular, plant-derived proteins are renewable raw materials that are produced by kilotonnes per year, for example, wheat gluten, soy protein, pea etc. Moreover, these biopolymers represent a great opportunity to give new value to what is often an important byproduct of the food industry. Likewise, the uses described above are also remarkable for their potentially high value in applications such as the development of intelligent packaging (including the formulation of food preservatives), as matrices controlling the diffusion of active species (drugs, antibiotics, pesticides, etc.) and superabsorbent materials (with applications in agriculture, controlling the dissemination of water for irrigation, fertilizer release and continuous rehydration ability, as fillers for hygiene products, etc.) (Shen et al., 2009).

The overall objective of this work has been the development of new bioplastics with appropriate mechanical and biodegradability properties to be an alternative to current materials manufactured from synthetic polymers. Specifically, this monograph aims to provide a scientific and technological approach to the development of protein-based bioplastics that, depending on their final uses, should exhibit improved water resistance, antimicrobial activity, water absorption-rehydration and/or controlled-released properties. Those materials might find applications in packaging, active food packing, agriculture, personal hygiene products, water pollution control, etc. This work will lead to the development of two types of materials:

A) Biodegradable materials exhibiting improved water resistance for packaging, in non-food applications or with antimicrobial activity for active food packaging. To that end, different natural biocides have been incorporated to the bioplastics formulation and assessed their antimicrobial activity.

B) Hydrophilic protein-based bioplastics with enhanced water absorption, rehydration and controlled-release capabilities. Specifically, bioplastics obtained should be able to carry out a controlled-release of active agents such as agricultural micronutrients or natural bioicides.

II. LITERATURE REVIEW

1. Bioplastics

The European Bioplastics Association has defined a bioplastic as having two differentiated categories (European-Bioplastics.htm):

a. Compostable plastics certified according to EN13432 and based on renewable (biobased) and/or non-renewable (fossil) resources. The focus here is on their functionality "compostability": A large proportion of plastics compostable are included in this concept, such as starch based materials (starch blends), PLA (polylactide), PHA (polyhydroxyalkanoate) type polyesters e.g. PHB, PHV, cellulosic materials from chemically modified cellulose; other materials produced from chemically modified cellulose; specific synthetic polyesters made from crude oil or natural gas. The compostability of plastics therefore must be proven by recognized testing standards (Europe: EN 13432, the legally binding standard for the compostability of plastics in all EU member states or EN 14995, USA: ASTM D-6400, other countries: ISO 17088).
b. Biobased plastics produced on the basis of renewable resources. The focus here is their raw materials basis: Bio-based polymers come from renewable resources such as sugar, starch, vegetable oils or cellulose in production. Corn, potatoes, cereals, sugar cane and wood are the most commonly used feedstocks. The proportion of renewable carbon used in the product can be determined using analytical methods e.g. ASTM D-6866. Bio-based polymers are not in all cases biodegradable and compostable.

1.1 Composition of bioplastics

Bioplastics are mainly composed of renewable raw materials (Biopolymers) and plasticizer. The result of this mixture is a material with thermomechanical properties similar to those of plastics coming from petroleum-based synthetic polymers and, thanks to their thermomechanical properties, may play the role of synthetic plastics in certain applications.

The formulation of a bioplastic involves the use of at least one component, and biopolymers that can form a matrix that imparts enough cohesion and uniformity. Such polymers may have the properties of a crystalline or amorphous structure (Almeida et al., 2004). In addition, a plasticizer is usually required to reduce polymer fragility and allow material processing.

1.2 Biopolymers

The three main classes of biopolymers are polysaccharides, lipids and proteins.

a. Polysaccharides

Polysaccharides are polymers or macromolecules composed of simple sugars. Polysaccharides have two principal functions. Some, such as starch, store energy for cell activity, and others, such as cellulose, serve as structural materials in living systems. After proteins, polysaccharides are among the most diverse and complex group of biopolymers. This is because the bonds linking the sugar monomers can be formed at different positions on the sugar units. By simply linking glucose monomers together at different positions, polymers with very different properties are produced. At least 20 different sugars have been identified in a variety of polysaccharides from biological sources, and thus a great range of polymer structures can be created. Many polysaccharides contain branched structures and are chemically modified by the addition of other molecules.

Starch was one of the first generation of biopolymers, and is commonly used in packaging and agriculture. It is cheap, widely available and relatively easy to mold. Moreover, there are other polysaccharides such as cellulose, lignin, starch, alginates and chitosans widely used in different applications (Almeida et al., 2004; Brescia et al., 1977).

b. Lipids

Lipids are biomolecules that remain insoluble in water, and can be extracted from cells with low polarity organic solvents such as ether and chloroform. These materials cover a wide range of structural types including the following: carboxylic acids (fatty acids), triacylglycerols (or neutral fats), phospholipids, glycolipids, waxes, and steroids tarpenos.

Most carboxylic acids and lipids are esters of glycerol, i.e. triglycerides. The triglycerides are oils and fats of vegetable or animal, including substances as common as peanut oil, olive oil, soybean oil, corn oil, flaxseed oil, butter, lard and tallow. Those triglycerides liquid at room temperature are generally referred to as oils, and those which are solid are called fats or tallow (Brescia et al., 1977).

Lipids and their derivatives are used for their good water barrier properties and also their low cost. Their properties are utilized in the use of controlled release matrices for fertilizers (Brescia et al., 1977).

c. Proteins

Proteins, also referred to as polypeptides are complex copolymers composed of up to 20 different amino acid building blocks. Proteins can contain a few hundred of amino-acid units or thousands of units. Each protein has a specific chemical composition and three-dimensional shape.

Therefore, proteins are a renewable, biodegradable/edible resource with great potential to improve the quality and stability of a large range of food products by using a number of processing techniques. For a long time, proteins have been used to produce edible materials, but understanding of the precise physical and chemical mechanisms of protein interactions continues to evolve (Pommet et al., 2005; Redl et al., 1999a; Li and Lee 1996).

Proteins can be classified according to the animal (casein, whey, keratin, collagen and gelatin) and plant (wheat gluten, corn, rice, millet, sorghum, potato, peas, etc.).

Plasticizers

Plasticizer is a necessary component to prevent the material from becoming fragile and breakage occurring during handling and storage. Plasticizer reduces the intermolecular forces and increases the mobility of polymer chains. In addition, the plasticizer reduces the glass

transition temperature of these materials thus resulting in increased flexibility of the bioplastic (lowering the elastic modulus of protein). They also produce an increase in the elongation of bioplastics, and a decrease in their hardness (Cuq et al., 1998; Gontard et al., 1992).

The most commonly used plasticizers are glycerol, sorbitol, propylene glycol, sucrose, polyethylene glycol, fatty acids and monoglycerides. Water also acts as a significant plasticizer as it has the ability to modify the structure of the polymer. This means that the moisture content of the material, subject to the relative humidity which it experiences, has an important effect on its properties (Cuq et al., 1998; Gontard et al., 1992).

According to Gontard (1991), hydrophilic compounds of low molecular weight polyols (glycerol, sorbitol, propylene glycol) and fatty acids of low volatility, are capable of modifying the three dimensional structure of proteins (Matveev et al., 2000, Pouplin et al., 1999), and can be considered from this point of view as good plasticizers. However, they also reduce the ability to act as a barrier to moisture, oxygen, odors and oils. It also reduces the values of elongation during aging, which is a result of plasticizer migration into the environment (Cuq et al., 1998).

Hydrophobic substances of high molecular weight as waxes, oils, monoglycerides and fatty acids have an antiplastifying effect on these types of materials, reducing their flexibility. However, they reduce the water vapor permeability (WVP) of these materials, and also can help hydrophobic plasticizer migration, avoiding the aging of the material and thereby improving their extensibility (Park, 1994).

1.3 Proteins

Proteins are heteropolymers, with α-amino acids being their monomer units. With the 20 amino acids most commonly found in proteins, an almost unlimited number of sequential arrangements with a wide range of interactions and chemical reactions are possible (Pommet et al., 2003; Stevens, 1999; McMurry, 1994). During heat processing, proteins disaggregate, denature, dissociate, unravel, and align in the direction of the flow. These changes allow the protein molecules to recombine and cross-link through specific linkages (Redl et al., 1999a). The crosslinking reactions can result in a high glass transition temperature and high melt viscosity, which require addition of plasticizers to increase free volume and mobility of the molecules. As temperature increases above the glass transition, the plasticized proteins turn

into a soft and rubbery material that can be shaped into desired forms. Upon cooling, the matrix network gets fixed into the desired structure (Pommet et al., 2003).

1.3.1 Molecular structure of proteins

a. Primary Structure

Proteins are polymers of amino acids. Amino acids are primary amines that contain an alpha carbon that is connected to an amino (NH_3) group, a carboxyl group (COOH), and a variable side group (*R*) (Figure 1.1). The side group gives each amino acid its distinctive properties and helps dictate the folding of the protein.

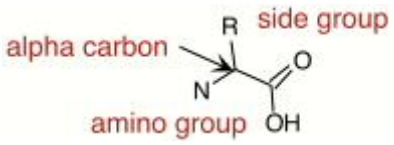

Figure 1.1 General amino acid.

Polymers of amino acids are created by linking an amino group to a carboxyl group on another amino acid. This is termed a peptide bond (Figure 1.2)

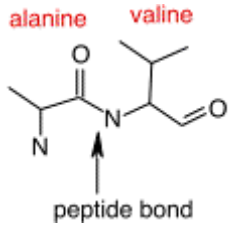

Figure 1.2 Peptide bond.

There are 20 common amino acids found in proteins and these amino acids can be classified into 3 groups; polar, non-polar and charged. Polar and charged amino acids will most often be found on the surface of a protein, interacting with the surrounding water, while the non-polar (or hydrophobic) amino acids will bury themselves in the interior. The number and position of these types of amino acids in protein can greatly influence its function. Figure 1.3 shows the chemical structure of the amino acids.

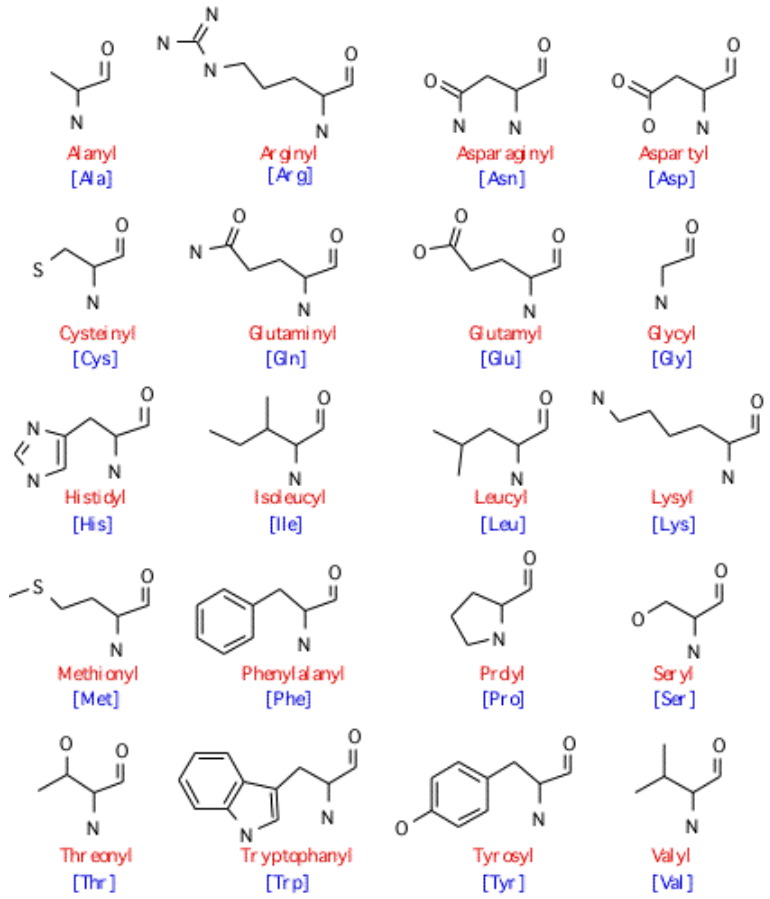

Figure 1.3 The common amino acids.

Peptides and proteins are formed when a ribosome and the rest of the translation machinery link 10 – 10.000 amino acids together in a long polymer. This long chain is termed the primary sequence. The properties of the protein are determined, for the most part, by this primary sequence. In many cases an alteration of any amino acid in the sequence will result in a loss of f unction for the protein (a mutation).

b. Secondary Structure

- **Basic attractive forces**

During and after synthesis, the primary sequence will associate in a fashion that leads to the most stable, "comfortable" structure for the protein. How a protein folds is largely dictated by the primary sequence of amino acids. Each amino acid in the sequence will associate with other amino acids to conserve the most energy. This structure is stabilized by hydrogen bonds, hydrophobic interactions, ionic interactions, and sulfhydryl linkages.

- **Sulfhydryl linkages**

These are covalent bonds between cysteine groups. Cysteine is a unique amino acid that has a sulfur group available for binding to other groups. Often in proteins, adjacent sulfhydryl groups on cysteines will form a covalent link in a protein (Figure 1.4) and are often crucial for the mature protein to perfom its function.

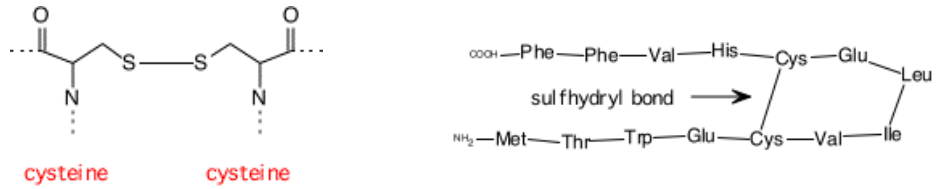

The chemical structure of a sulhydryl bond *A sulfhydryl bond in a peptide*

Figure 1.4 Two views of sulfhydryl linkages.

c. Tertiary Structure

During and after synthesis, a protein folds into alpha helices and beta sheets. These areas of secondary structure are connected by bridging sequences that will cause the protein to fold in specific ways. At the completion of this process, the protein takes on its final shape. The mature stable structure of a single peptide sequence is termed its tertiary structure. Figure 1.5 shows the tertiary structure of ribulose bisphosphate carboxylase (RubisCo), one of the most important enzymes on this planet. Life would not exist without it. This enzyme takes energy, obtained most often from the sun, and uses it to convert carbon dioxide into carbohydrate. It is found in many photosynthetic organisms and is probably the most abundant protein on Earth. Notice in Figure 1.5 the alpha helices throughout the protein and the beta sheet near the bottom of the protein.

d. Quaternary Structure

Many enzymes and structures are actually complexes of several polypeptides. The arrangement of these polypeptides is termed the quaternary structure of a protein. Proteins complexes can contain several copies of an identical protein or they may consist of any number of polypeptides in various ratios.

Ribbon *Space Filling*

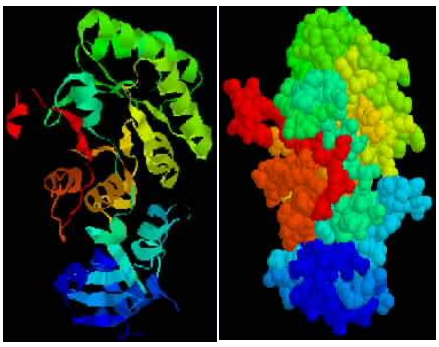

Figure 1.5 The tertiary structure of ribulose bisphosphate carboxylase (RubisCo).

Figure 1.6, notices the hemoglobin groups associated with each polypeptide (the light blue group that is surrounded by the dark blue protein). These heme groups contain iron and the iron is the atom that actually binds the oxygen. Heme iron has an even greater affinity for carbon monoxide.

Ribbon *Space Filling*

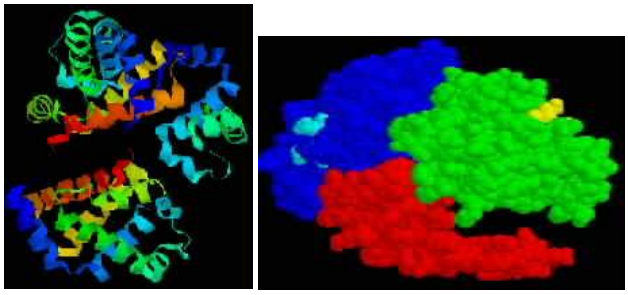

Figure 1.6 Hemoglobin-Only 3 of the four subunits are visible.

1.3.2 Protein desnaturation

Protein denaturation has been defined in several ways, for example as a change in solubility (Mirsky, 1941) or by simultaneous changes in chemical, physical and biological properties (Neurath et al., 1944; Langmuir, 1938) under some standard reference set of conditions (Timasheff and Gibbs, 1957). These changes in physical and to a lesser extent chemical properties are manifestations of configurational changes taking place in the polypeptide chains. The denaturation process presumably involves an unfolding or at least an alteration in the nature of the folded structure (Foster and Samsa, 1951). Most denaturation changes consist of changes in secondary bonds: ion-dipole, hydrogen and Van der Waals, and

in the rotational positions around single bonds which are controlled by the secondary bond structure (Lumry and Eyring, 1954). The term denaturation denotes the response of the native protein to heat, acid, alkali, and a variety of other chemical and physical agents which cause marked changes in the protein structure. Rice et al., (1958) suggested denaturation to mean a class of reactions which lead to changes in the structure of the macromolecule with no change in molecular weight. Timasheff and Gibbs (1957), pointed out that the approaches used to define the concept of denaturation can be classified into two types:

- Molecular, in terms of actual structural changes taking place on the molecule.
- Operational, in terms of changes in measurable properties.

The temperatures at which various proteins unfold vary enormously. Most proteins unfold at elevated temperatures, and some unfold at very low temperatures. Many proteins unfold at temperatures only a few degrees higher than those at which they function. Others are stable to much higher temperatures such as the gluten proteins. The unfolding of the protein exposes the buried non-polar amino acid residues. Their intermolecular clustering leads to aggregation of the denatured protein. Consequently, heat denaturation is essentially irreversible.

1.3.3 Protein-Protein Interactions

Protein-protein interactions are generally favoured under conditions which reduce the net charge on the molecules, i.e. pH values near the isoelectric point. High ionic strength tends to reduce electrostatic repulsion between proteins due to the shielding of ionizable groups by mobile ions. Protein-protein association involves the specific complementary recognition of two macromolecules to form a stable assembly (Jones and Thornton, 1995). Fundamental to the stabilization of protein association is the hydrophobic interaction (Chothia and Janin, 1975). The term hydrophobic interaction is used to describe the gain in free energy which occurs when non-polar residues of proteins associate in an aqueous environment (Kauzmann, 1959). The process of folding and protein-protein aggregation reduces the surface area in contact with water. When the protein-solvent interaction is attractive, the protein can reduce its total energy by surrounding itself with solvent molecules, conversely, when the interaction is repulsive, the solvent is excluded (Tanaka, 1981). The aggregation of protein subunits buries the hydrophobic residues of the proteins, and hence minimizes the

number of thermodynamically unfavourable solute-solvent interactions as found when SWP is hydrated in distilled water at room temperature (Friedli, 1996).

1.3.4 Wheat gluten

Wheat gluten is an amorphous polymer composed of gliadins and glutenins. Gliadin and glutenins, accounting for 80-90% of the total wheat flour proteins, are the two primary classes of storage proteins, being necessary for producing an appropriate balance of viscous and elastic properties in gluten and flour dough, it is widely accepted that gliadins confer viscous properties whilst glutenins impart strength and elasticity (Shewry et al., 1986).

Gliadin is soluble in alcohol, while glutenin is soluble in acid solutions. Gliadins are monomers that interact by noncovalent forces, and are classified into four groups according to their mobility (α, β, γ and ω). The faster fraction called α- gliadin, and the slower one ω. These proteins have molecular weights between 30 - 80 kDa. The formation of a three-dimensional network when they are hydrated gives elastic and strength characteristics to gluten (Carceller and Aussenac, 1999). The high molecular weight in glutenin can be attributed to the presence of intermolecular disulfide bonds, joining individual protein chains and resulting in a larger polymer (Krochta 1997; Kokini et al., 1994). Glutenins are composed of low molecular weight glutenin subunits (LMW-GS) and high molecular weight glutenin subunits (HMW-GS) of 12-60 kDa and 60-120 kDa, respectively.

Gliadins and glutenins are responsible for gluten extensibility (viscosity) and strength (elasticity), respectively. The ratios of low molecular weight glutenin subunits (LMW-GS) to hight molecular weight glutenin subunits (HMW-GS) are approximately 3 to 1, although variations exist between wheat cultivars (Cornec et al., 1994; Park et al., 1994; Popineau et al., 1994; Shewry et al., 1986).

Gluten is not a grid system, although the glutenin molecules can be very large, these are discrete molecules which can be solubilized. Aggregation of wheat proteins through disulfide bonding is facilitated by increasing temperatures and moisture contents (Park et al., 1994; Weegels et al., 1994 a,b). The crosslinking reactions of both gliadins and glutenins are highly dependent on temperature (Kokini et al., 1994, 1995). Gliadins and glutenins achieve maximum structure buildup at 120ºC and 135ºC while softening occurs at temperatures above 130ºC and 150ºC, respectively. When thermal treatment is applied between 20-40ºC, it does not induce irreversible changes in mechanical properties. However, when applied at higher

temperatures, the rheological behavior is irreversible because of sulfide/disulfide (SH/SS) interaction. Thermal treatment at 20-40ºC does not induce irreversible changes in mechanical properties. At higher temperatures, however, rheological behavior changes irreversibly due to sulphydryl/disulfide (SH/SS) exchange, (Lefèvre and Subirade, 2000; Aguilera, 1995).

The viscoelasticities of gluten are related to glutenins, gliadin/glutenin ratio and HMW-GS/LMW-GS ratio (Popineau et al., 1994). HMW-GS and subunit composition influence the viscoelasticity by modifying the size distribution and the protein aggregation through crosslinking. The glutenin aggregation leads to a significant rise in elastic plateau modulus of the network (Cornec et al., 1994; Popineau et al., 1994).

1.3.5 Rice protein

It is known that rice storage proteins include albumin, globulin, prolamin and glutelin, of which glutelin accounts for 85-95% of the total storage proteins. Glutelin, prolamin and globulin have been extensively studied with respect to parameters such as size, amino acid composition and charge heterogeneity in rice. It has been studied different types of rice such as *Oryza sativa* L. japonica; cv. lebonnet, cv. briggs M-201, cv. koshhikari, cv. Akenohoshi and cv. mangetsumochi (Kim, 1988; Shyur et al., 1988; Higuchi and Fukazawa, 1987; Takaiwa et al., 1987; Wang et al., 1987; Chen and Cheng, 1986; Krishnan and Okita, 1986; Takaiwa et al., 1986).

Rice glutelins, when analyzed by SDS-PAGE, reveal 2 major subgroups of proteins, having molecular weights of 34-39 kDa and 21-23 kDa. These proteins are the proteolytic products of a larger precursor protein (Krishnan and Okita, 1986; Wen and Luthe, 1985; Luthe, 1983; Zhao et al., 1983). Because of their abundance, the rice glutelins have been the subject of many biochemical and molecular genetic studies (Okita et al., 1989).

Rice seeds also store significant amounts of alcohol-soluble proteins, the prolamines, in the endosperm tissue. They have molecular weights of about 12-17 kDa and contain a high mole percentage of glutamine residues (Kim and Okita, 1988; Padhye and Salunkhe, 1979; Mandac and Juliano, 1978). The rice globulins, which are sulfur-rich and account for 8% of the total seed proteins (Perdon and Juliano, 1978; Cagampang et al., 1976; Houston and Mohammad, 1970) have not been extensively studied.

Among the numerous studies published on the amino acid composition of rice grain (Chung and Pomeranz, 1985; Juliano, 1985; Bechtel and Pomeranz, 1980; Eggum, 1979;

Juliano, 1978; Juliano, 1972), several deal mainly with samples from different varieties having various nitrogen contents N (in g N/100 g grain dry matter) (Khoi et al., 1987; Kennedy et al., 1974; Juliano et al., 1973; Bressani et al., 1971; Houston et al., 1969; Vidal and Juliano, 1967; Cagampang et al., 1966).

1.3.6 Potato protein

Potato protein is mainly composed of patatin and protease inhibitors. Potato proteins were shown to unfold between 55 and 75ºC, decreasing enzyme activities and causing loss of solubility. At mildly acidic pH the solubility was dependent on ionic strength and the presence of unfolded patatin. The use of organic solvents combined with a moderate lowering of pH resulted in potato protein precipitates with good solubility characteristics at neutral pH (Van Koningsveld et al., 2001). However, the presence of ethanol significantly reduced the denaturation temperature of potato proteins, implying that the isolation should be performed at low temperature in order to retain a high solubility.

The ability to form and stabilize foams is an important functional property of food proteins. In whipping tests less foam was formed from untreated patatin than from the protease inhibitors, but patatin foam was much more stable (Van Koningsveld et al., 2002). The foam-forming properties of patatin could be improved greatly by partial unfolding of the protein, suggesting that the way the protein is isolated influences the foaming properties. Proteins are also used in many food products as emulsifiers and emulsion stabilizers (Singh and Kaur, 2009; Van Koningsveld et al., 2006).

The process separates two fractions. The high molecular fraction, mainly composed of patatin, results in a dry food ingredient with protein content of 90–95%. The low molecular fraction comprises the protease inhibitors in liquid product. Potato protein has a high content of amino acids with hydrophobic functional groups, in particular, with branched (isoleucine, leucine, and valine) and aromatic (phenylalanine and tyrosine) side chains (Refstie and Tiekstra, 2003).

1.4 Plasticizers

Plasticizers are generally added to the protein matrix to improve processability and to modify the properties of the final structure. As opposed to “internal” plasticizers, which are copolymerized or reacted with the polymer, “external” plasticizers consist of low molecular

weight, low volatility substances that interact with the polymer chains to produce swelling (Sothornvit and Krochta, 2005).

The action of a plasticizer is generally to interpose itself between the polymer chains and alter the force holding the chains together. As a result, the glass transition temperature (T_g) of the material is depressed. Polymer plasticization enables thus to reduce the shaping temperature of the thermoplastic process and to impart adequate flexibility to the material (Cuq et al., 1998; Gontard et al., 1992; Brescia et al., 1977).

Water is the most effective plasticizer in biopolymer materials, enabling them to undergo the glass transition, facilitating deformation, and processability of the biopolymer matrix. Without water addition, the temperature region of thermal degradation would be easily reached before films could be formed (Tolstoguzov 1993). Besides water, common plasticizers for edible films include monosaccharides, oligosaccharides, polyols, lipids, and derivatives are generally used as proteins plasticizer (Sothornvit and Krochta 2005; Park et al., 1994).

1.4.1 Glycerol

Glycerol is an organic compound, which has three hydrophilic hydroxyl groups that are responsible for its solubility in water and its hygroscopic nature. The glycerol substructure is a central component of many lipids. Glycerol has the following structure (Figure 1.7):

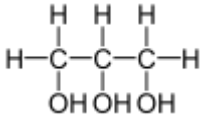

Figure 1.7 Glycerol.

Glycerol ($C_3H_8O_3$) is a low molecular weight, hydrophilic plasticizer that has been widely used in the thermoplastic processing of proteins (Hernandez-Izquierdo 2007; Sothornvit et al., 2007, 2003; Pommet et al., 2005, 2003; Zhang et al., 2001; Cunningham et al., 2000; Redl et al., 1999a). Its high plasticizing effect has been attributed to the ease with which glycerol can insert and position itself within the 3-dimensional biopolymer network (Di Gioia and Guilbert, 1999). Pommet et al., (2005) tested several compounds with different chemical functions, number of functional groups, and degree of hydrophobicity as wheat gluten plasticizers. From this study, the critical factors for a good plasticizer were found to be

low melting point, low volatility, and protein compatibility. In addition to these characteristics, permanence in the film and amount of plasticizer needed should be taken into account when choosing a good plasticizer (Sothornvit and Krochta, 2001; Di Gioia and Guilbert, 1999).

1.4.2 Polyethylene Glycol

Polyethylene glycol (PEG) is a polyether compound with many applications ranging from industrial manufacturing to medicine. PEG is soluble in water, methanol, benzene, dichloromethane and is insoluble in diethyl ether and hexane. It is coupled to hydrophobic molecules to produce non-ionic surfactants. Depending on their molecular weights PEGs are prepared by polymerization of ethylene oxide and are commercially available over a wide range of molecular weights from 300 g/mol to 10.000.000 g/mol. Their melting points vary depending on the formula weight of the polymer. PEG has the following structure (Figure 1.8):

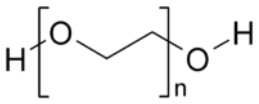

Figure 1.8 Polyethylene glycol.

The numbers that are often included in the names of PEGs indicate their average molecular weights, e.g., a PEG with n=9 would have an average molecular weight of approximately 400 daltons and would be labeled PEG 400. Most PEGs include molecules with a distribution of molecular weights; i.e., they are polydisperse. The size distribution can be characterized statistically by its weight average molecular weight (Mw) and its number average molecular weight (M_n), the ratio of which is called the polydispersity index (M_w/M_n). Mw and Mn can be measured by mass spectrometry (Kahovec et al., 2002).

Polyethylene glycol has a higher molecular weight and hence much lower volatility. It is freely soluble in water, but it is much less hygroscopic than other agents like glycerol (Goswami and Maiti, 1998). There are a variety of molecular weights (M_w) of polyethylene glycol (PEG), include PEG 300 (Gioia et al., 1998), PEG 600 (Gioia et al., 1998; Guo, 1993), PEG 4000 (Turhan et al., 2001; Heinamaki et al., 1994; Guo, 1993), PEG 8000 (Donhove and Fennema, 1993), used as plasticizers depending on the biopolymer materials studied.

Polyethylene glycol and its derivatives are widely used in the industry as dispersant, binder and plasticizer agent for different fields (Tunç and Duman, 2007). They also are used in industry as surfactants, including foods, cosmetics, and pharmaceutics; in biomedicine, as dispersing agents, solvents, ointment, and suppository bases; in vehicles; as tablet excipients; and as laxatives.

1.5 Modifying agents

Modifiying agents are compounds which might change bioplastic material microstructure, improving their properties. An important trend in recent years has been the investigation of different approaches for enhancing the barrier, mechanical, and solubility properties of protein bioplastics. Generally, these approaches involve modification of protein structure and/or interactions among protein molecules.

Amphiphilic lipidic molecules such as hexanoic, hydroxyhexanoic, octanoic, palmitic, and oleic acids, dibutyl tartrate, and phthalate, and diacetyl tartaric acid ester of mono-diglycerides show some effects of plasticization of wheat gluten (WG), zein, and corn gluten (Di Gioia et al., 1999; Lai and Padua, 1998; Kalichevsky et al., 1992). Moisture barrier properties of protein based films can be significantly improved through incorporation of hydrophobic ingredients such as waxes, long-chain saturated fatty acids, monoglycerides and triglycerides, or through emulsion or lamination technology (Liu et al., 2006; Talens and Krochta, 2005; Handa et al., 1999; Krochta and McHugh, 1996; Derksen et al., 1995; Gontard et al., 1995, 1994; Ennadios et al., 1993; Gennadios et al., 1993). Incorporating lipid or wax may interfere with polymer chain-to-chain interactions and/or provide flexible domains, resulting in a reduction in strength (Shellhammer and Krochta, 1997; Gontard et al., 1994).

2. Processing of proteins

According to Gontard et al., (1991) processing of bioplastics, films, coating, or other materials based on polymer from agricultural resources requires three steps:

a. Breaking of intermolecular bridges (non-covalent or covalent if applicable) to stabilize the polymer in its native form, using chemical or physical agents. In this way the polymer chains gain mobility.
b. Ordering and orientation of mobile polymer chains into the desired shape.

c. Allowing the formation of new intermolecular interactions that stabilize the new three-dimensional network obtained. The shape obtained in the previous step is maintained by removing the agents used in the first step to break the intermolecular bridges.

Based on these three steps, two technological manufacturing processes are used to make protein-based material:

1. The "physicochemical processing" is based on dispersing and solubilizing in various solvents and then casting, spraying, or dipping followed by drying.
2. The "thermoplastics processing" or "thermomechanical processing" is based in thermoplasticization of proteins. The use of plasticizers, shear and temperature allows for passing through the glass transition of proteins with formation of a rubbery mass that can be shaped and stabilized by cooling, heating and/or by eliminating volatile plasticizers. Thermoplastics processing includes mixing and extrusion. The "thermomechanical processing" involves a mixing stage followed by thermomoulding.

2.1 Thermoplastic processing of protein based bioplastics

Thermoplastics processing is carried out by directly mixing the protein with the plasticizer in a mixer or extruder. To accomplish this blend it is necessary to provide mechanical energy, called Specific Mechanical Energy (SME) and it requires the application of a minimum SME to obtain a material with appropriate thermomechanical properties (Jerez et al., 2005a; Redl et al., 1999a; Mitchell et al., 1994).

The Specific Mechanical Energy (SME) involved during mixing process can be computed from the torque curve, as follows:

$$SME = \frac{\Omega}{m} \int_0^{tmix} M(t)\partial(t) \qquad [2.1]$$

where Ω is the rotor speed (in rad/s), m the sample mass (in g), M(t) the torque at time t(in Nm) and t_{mix} the mixing (in s). SME is expressed in kJ/kg.

a. Mixing process

Mixing has three distinct functions in the development of the dough; distribution of materials, hydration, and energy input to develop a protein structure (Bloksma and Bushuk, 1998). Therefore, understanding the role of mixing energy is an essential step towards optimizing wheat dough development (Schluentz et al., 2000). During the mixing process, dough is formed by a combination of shear and elongation deformation at high strain rates (MacRitchie, 1986).

Protein-based biopolymers can be produced by blending or mixing different natural polymers. By varying the composition of the blend and processing conditions and its miscibility with proteins, the morphology and therefore, the functional and structural properties can be regulated efficiently which in turn allows the design of the most important mechanical and functional properties of these materials, improving the efficiency of biodegradable packages. Besides, as with synthetic polymers, the composition, microstructure and functional properties of films based on biopolymers determine their possible applications, (Galicia-García et al., 2011).

b. Extrusion process

The most important processing method for thermoplastic materials is probably extrusion which is used to produce films, sheets and assigned profiles. Extrusion of proteins is, therefore, in general only possible in a limited window of operating conditions and the material properties of extrudates depend on the processing conditions in a quite complex way (Redl et al., 1999b; Mitchell et al., 1994).

During extrusion, proteins are exposed to high temperature and shear and undergo structural changes such as denaturation, melting and fractionation. The ability to process protein and the resulting physical properties depend on the extent of structural changes of the protein. However, the way in which proteins interact together during extrusion remains obscure. The extrudate structure is believed to result from a complete restructuring of the polymeric material in an oriented pattern. The formation of the final molecular network involves the dissociation and unfolding of the macromolecules, which allow them to recombine and to crosslink through specific linkages (Redl et al., 1999b; Mitchell et al., 1994). Several attempts have been made in order to establish comprehensive models of the

melt viscosity of biopolymers for flow modelling in extruders. In general, these viscosity models include a term for shear rate, temperature, plasticizer content and eventually a term for the time temperature and the strain history of the material.

During extrusion, the sulfydryl–disulfide interchange interaction causes the molecular structure to change (Rebello and Schaich, 1999; Schaich and Rebello, 1999). Heating plays an important role in the processing of plant protein-based products (Cuq et al., 2000; Mo et al., 1999) by affecting the molecular conformations of proteins, their polymeric state and their molecular interaction (Domenek et al., 2002).

c. Thermomechanical manufacture of protein based bioplastics

Thermal treatment has a significant influence on the structure and properties of the protein films. However, thermal treatment usually reduces the extensibility of the films due to the aggregation and crosslinking between protein molecules through hydrophobic interactions and disulfide/sulfhydryl interchange reaction (Kokini et al., 1995).

A thermomechanical processing, consists of a mixing stage followed by the material moulding through a combination of pressure and temperature. Compared to the "physicochemical" or "casting" processing of films, wheat gluten films or bioplastics obtained through thermomechanical processing show higher thermal susceptibility and similar microstructure (Jerez et al., 2005a; Mangavel et al., 2004). Extrusion and thermomoulding have been applied to process gluten plastics or dough (Pommet et al., 2003; Redl et al., 1999b). Heating plays a relevant role in the processing of plant protein-based products (Cuq et al., 2000; Mo et al., 1999) by affecting the molecular conformations of proteins, their polymeric state and their molecular interaction (Domenek et al., 2002).

Drying temperature also affects mechanical and physical properties of gluten films (Kayserilioglu et al., 2003). At relative humidity 30%, tensile strength increases with increasing drying temperature from 20 to 80 ºC. Thermal treatment reduces water vapor permeability and affects color properties of gluten films (Ali et al., 1997). Thermal treatment at temperatures above 70 and 85ºC improves water barrier properties for glutenin- and gliadin-rich films and improves resistance to disintegration in water for gliadin-rich films (Hernandez-Muñoz et al., 2004).

The crosslinking through sulfydryl–disulfide interchange reactions between protein macromolecules should be highly dependent on temperature so that the moulding temperature

has significant interactive effects on the curing quality of soy proteins (Mo et al., 1999). These authors found that the maximum strength and strain at break of the cured proteins occur at moulding temperatures close temperature 40ºC. There is little research focused on the effects of moulding temperature on the properties of wheat gluten plastics (Cuq et al., 2000).

Wheat gluten is able to form network upon thermosetting (Sarwin et al., 1993; Strecker et al., 1995) so that it can be processed into films and plastics conveniently through thermoplastic moulding (Cuq et al., 2000; Mangavel et al., 2004; Pommet et al., 2005). Thermo-molded wheat gluten films might present a tensile strength higher than that of casting films with the same amount of plasticizer (Mangavel et al., 2004). Glutenins and gliadins are unfolded on heating up to 75ºC, which facilitates the sulfydryl–disulfide interchange (Schofield et al.,1983). The proteins are then 'locked' into the denatured state upon cooling. Aggregation of wheat proteins through disulfide bonding is facilitated by increasing temperatures and moisture contents (Weegels et al., 1994 a,b). In a previous work (Sun et., 2007), it studied the effect of crosslinking types on the properties of thermo-molded gluten plastics containing glycerol as a plasticizer and found that crosslinking through disulfide bonding results in a high degree of phase separation, giving rise to a high glass transition temperature of the gluten-rich phase. The information avaible about processed of protein by mixing, extrusion or thermal moulding have been focus mainly about gluten, there is nothing related with use of rice and potato protein to obtain bioplastics by theses procedure.

3. Market

Bioplastics have such appealing characteristics and benefits that they are often a feasible alternative to conventional plastics made from fossil resources. Since many conventional plastics can be substituted with bioplastics, features of and predictions within the conventional plastic market are also relevant for the bioplastic market. Moreover, the rising cost of oil means that bioplastics are increasingly being viewed as a viable and cost-competitive share of the market (bioplastics42.htm; Shen et al., 2009).

There is a potential for a consumption of 12.000-20.000 tons of degradable plant pots and 1.500 tons of mulch foil per year. COPA (Committee of Agricultural Organisation in the European Union) and COGEGA (General Committee for the Agricultural Cooperation in the European Union) have made an assessment of the potential of bioplastics in different sectors of the European economy as show in Table 3.1.

European Bioplastics estimated that in 2007, all bioplastics applications comprised approximately 75.000-100.000 tons of the total 48 million ton European plastics market. Annual growth is considerably higher than 20%. Market figures currently published by European Bioplastics are based on information which includes member surveys and publications including market studies and expert opinion. More detailed facts and figures (statistics) on market development will become available as the bioplastics' market share increases. Experts regard a technical application potential of 5-10% of the total plastics market as realistic. This estimation is based on biodegradable polymers, which have been on the market for several years. It does not take into account bio-based PE (polyethylene), which was announced to start production in 2009.

Table 3.1 Potential for Bioplastics in Europe (Estimation by COPA and COGECA, 2001).

Catering products	450.000 t/a
Organic waste bags	100.000 t/a
Biodegradable mulch foils	130.000 t/a
Biodegradable foils for diapers	80.000 t/a
Diapers, 100% biodegradable	240.000 t/a
Foil packaging	400.000 t/a
Vegetable packaging	400.000 t/a
Tyre components	200.000 t/a
Total	2.000.000 t/a

(Sources: COPA, COPEGA, European Bioplastics)

The EU countries with comparably advanced market development are England, Italy, Netherlands and Germany, followed by Belgium, France, Austria, Switzerland and Scandinavia. Market introduction of bioplastic products has already started in most of the EU countries.

The increased use of bioplastics and biopackaging by consumers in Europe shows that the price differentials can be accepted in specific application fields, e.g. packaging for organic food. Users are also considering other factors for their buying decision, such as technical performance (e.g. longer product life), image-creation and, if feasible, reduced disposal costs in the composting of used products. As a result, the price of bioplastics has continued to fall over the past ten years. Their competitiveness over conventional plastics should also continue to improve into the future through more effective processes, possible economies of scale and simultaneous increasing competition from new market players.

Whereas biofuels production has reached a multi-million ton level in the EU, the bioplastics market is still in its infancy (approx. 100,000 tons in Europe). The cultivation area needed to supply the bioplastics industry is currently very small. About 2-3 tons of bioplastics can be produced from one hectare of corn or wheat (using their starch), thus the area cultivated for the production of bioplastics can be estimated at approx. 30,000 ha in EU compared with a total agricultural area in Europe of more than 162,000,000 ha according the European Commission.

The bioplastic industry will grow on average by 19% per year up to 2020. The European capacity of bio-based plastics is projected to rise from 0.14 Mtons in 2007 to 0.44 Mtons in 2013 and 1.65 Mtons in 2020. This is equivalent to average annual growth rate of 16% p.a between 2007 and 2020. The growth in Europe is expected to evolve more steadily (about 50 ktons p.a) compared to the world-wide situation. As a further difference to the projection for the world, the production of bio-based plastics in Europe is dominated by starch plastics for the entire period until 2020, with PLA coming into play after 2013. In 2007, 10 ktons of cellulose films were produced in Europe and the volume is expected to increase to (at least) 20 ktons until 2020.

Table 3.2 Worldwide share of bio-based plastics by types and players in 2020.

Type of bioplastics	Share of global bioplastics capacity in 2020	Production capacity major players in Europe in 2020
Starch plastics	89%	Novamont: 200ktons Biotec: 150 ktons Rodenburg: 40 ktons Cereplast: 225 ktons Livan: 100 ktons
PLA	8%	Pyramid 60kt'PURARC TOTAL-Galactic: pilot scales
Cellulose films	2%	Innovia: 20 ktons
Bio-based monomers	1%	Solvay: 10 ktons (ECH)
Total	100%	

(Sources: Shen, L.; Haufe, J.; Patel, M.; Final report, 2009)

The capacity additions for starch plastics are very substantial if compared to the historical development. Unlike the world-wide production in the future, which is expected to become more diverse regarding the types of polymers/monomers (e.g. more capacity announcements are seen for PHA, bio-based PE, and bio-based monomers), the bio-based

plastics production in Europe seems to be only starch plastics (90%), except for one company's vision of a large-scale PLA plant in Europe (See Table 3.2).

The maximum potential of bio-based polymers for technical substitution of their petrochemical counterpart is estimated at 270 Mtons, or 90% of the total polymers that were consumed in 2007 worldwide. It will not be possible to exploit this technical substitution potential in the short to medium term. The main reasons are economic barriers, technical challenges in scale-up, the short-term availability of bio-based feedstocks and the need for the plastics conversion sector to adapt to the new plastics. Nevertheless, this exercise shows that, from a technical point of view, there are very large opportunities for the replacement of petrochemical bio-based bioplastics.

4. Potential applications

According European Bioplastics Association (2008), bioplastics are generally used where functionally and environmental performance offer benefit. Market studies have revealed a generally very high consumer acceptance of bioplastics in many countries. Compostable waste bags, biodegradable mulch film, catering products, film and rigid packaging and many other products are application or products which exhibit high growth rates.

Since the introduction of plastic films in the 1930's and 1940's for greenhouse coverings, fumigation and mulching, agricultural applications of polymers have grown at an enormous rate. All principal classes of polymers, i.e. plastics, coatings, elastomers, fibres and water-soluble polymers are presently utilized in applications which include the controlled release of pesticides and nutrients, soil conditioning, seed coatings, gel plantings and plant protection. However, degradable plastics are also of interest as agricultural mulches and agricultural planting containers. Ultimate biodegradability, as in composting, is also of some interest as it would permit degradable plastics to be combined with other biodegradable materials and converted into useful soil-improving materials. The development of durable products such as those in consumer electronic, in leisure and in the automobile industry is in an early state of market penetration. In the field of medical technology, special biodegradable plastics are in use for some time as stitching materials and for decades for screw or implants.

4.1 Controlled release matrices

Controlled release (CR) is a method in which biologically active chemicals are made available to target species, at a specified rate and for a predetermined time. The polymer serves primarily to control the rate of delivery, mobility, and period of effectiveness of the chemical component. The principal advantage of control release formulations is that less chemicals are used for a given time period, thus lowering the impact on non-target species and limiting leaching, volatilization, and degradation. The macromolecular nature of polymers is the key to limiting chemical losses through these processes.

Controlled release polymeric systems can be divided into two broad categories. In the first, the active agent is dissolved, dispersed, or encapsulated by the polymeric matrix or coating. Release generally occurs by diffusion processes or by the biological or chemical breakdown of the matrix. In the second category polymers contain the active agent as part of the macromolecular backbone or pendent side chain. Release results from biological or chemical cleavage of the bond between the bioactive agents and the polymer.

The release of the active ingredient is governed by a number of factors that are dependent on the polymer, the active ingredient and the matrix itself. The former can include the type of polymer (insoluble, soluble pH - dependent), its molecular weight and crystalline state. Among the parameters related to release of the active agent highlighted the solubility of itself and its molecular weight. Finally, factors dependent on the matrix itself are, for example, the type of internal structure (reservoir or matrix) and the theoretical content of active ingredient with respect to the polymer (Khatkar et al., 1995).

The modified release matrices are those designed in such a way as to adjust the speed or place of release of active agent, compared to immediate release dosage forms of the same pure active agent (Madeka and Kokini, 1994).

- **Delayed release:** The active ingredient is released at a time different from the administration, but the effect is not prolonged. They are enteric-coated forms, in which the active ingredient is released in a particular area.
- **Controlled release:** The active substance is released in stages over time (release rate is limiting in the absorption process). These systems can be classified into several categories according to the release mechanism:

- **Diffusion-controlled systems**, where the active agent is released from the solution by diffusion through a polymer membrane or embedded in a polymer matrix which controls the release rate of the system.
- **Erosion controlled systems**, where the release of the active agent is activated by the dissolution, disintegration or biodegradation of the polymer.
- **Via osmotic controlled systems**, where the content of the active agent is released by the speed of water osmotic absorption of the medium.

At present, interest about research on transport systems and release of an active agent is clearly increased due to a number of reasons, among them its high added value in the development of intelligent packaging (including food preservatives in their formulation) as matrices controlling the diffusion of active species (drugs, antibiotics, pesticides, etc.) and superabsorbent materials (with applications in agriculture to control the spread of irrigation water, fertilizers and continuous rehydration ability, as fillings hygiene products, etc.).

4.2 Active packaging

Definitions stated in Regulation 1935/2004/EC and in Regulation 450/2009/EC consider active materials as ‘‘materials and articles that are intended to extend the shelf-life or to maintain or improve the condition of packaged food”. They are designed to deliberately incorporate components that would release or absorb substances into or from the packaged food or the environment surrounding the food (Brody, 2001; Floros et al., 1997). On the other hand, intelligent materials and articles means: ‘‘materials and articles which monitor the condition of packaged food or the environment surrounding the food”.

- Regulation 1935/2004/EC

The Framework Regulation authorized the use of active and intelligent packaging, to enhance the safety, quality and shelf-life of the packaged foods.

- Regulation 450/2009/EC

General requirements stated in Regulation 1935/2004/EC for the safe use of active and intelligent packaging have been recently integrated by Regulation 450/2009/EC.

Thus, active packaging can be defined as any technique that seeks some sort of favorable interactions between the packaging and product, in order to improve the quality and acceptability. Active materials change certain conditions or food processes that play a role in the life of the product. Also, active packaging systems that absorb/remove or regulate

compounds as oxygen, ethylene, moisture or compounds causing bad odors and tastes in food. Other systems release antimicrobial agents, antioxidants, flavourings, flavours or colours.

Usually an active package is developed based on biodegradable polymers, nanobiocomposites, proteins, polysaccharides and biopolymers from microorganisms; they all have the ability to control the release of substances (Coma, 2008). The interest in the development of active packaging with this type of natural compounds is to increase food shelf life and ensure their safety. There are two ways to apply the active component to the package:

- Active component inside the package**:** The uses of small bags or envelopes containing the active ingredient are the most developed and used. These bags are made from a porous material, on the one hand, the active compound can act and, secondly, it prevents contact with food. They must be resistant to breakage and must be properly identified to prevent drink their contents. It cans also use tags that are placed on the inside of the container.

- Active component included in the packaging material: As an alternative to using bags are developing packaging materials, synthetic and edible films, which contain the active ingredient in its structure is based on desirable migration phenomena and packaged goods that yield the substances of interest.

An additional advantage of the latter technique is that ensures that the entire surface of the active component is in contact with the product and the consumer does not find any foreign element. There are several types of active systems as oxygen absorbers ("scavengers"), absorbers and emitters of carbon dioxide, ethylene absorbers, absorbing moisture and humidity regulators, absorbing odours and flavours, releasing antimicrobial systems and other active systems.

4.2.1 Antimicrobial packaging

Antimicrobial packaging is a form of active packaging that could extend the shelf-life of product and provides microbial safety for consumers (Rooney, 1995). It acts to reduce, inhibit, or retard the growth of pathogen microorganisms in packed foods and packaging material (Vermeiren et al., 1999). In order to control undesirable microorganisms on food surfaces: (1) volatile and non-volatile antimicrobial agents can be incorporated into polymers

or (2) coating or adsorbing antimicrobial onto polymer surfaces can be applied (Appendini and Hotchkiss, 2002).

Among the compounds released by microbial action are: CO_2, ethanol, sulfur dioxide, chlorine dioxide, essential oils, silver, chelating compounds (EDTA), and bioactive compounds such as organic acids, enzymes (glucose oxidase, muramidase), bacteriocins, etc. There are different forms of presentation such as envelopes, plastic film antimicrobial, antimicrobial edible films, etc. (Coma, 2006).

Several compounds have been proposed for antimicrobial activity in food packaging, including organic acids, enzymes such as lysozyme, and fungicides such as benomyl, imazalil and natural antimicrobial compounds such as spices (Tharanathan, 2003; Weng and Hotchkiss, 1992). These compounds carry mostly antimicrobial and some antioxidant properties. Natural compounds, such as nisin and lysozyme, have been studied as potential food preservatives added to the edible films that are safe for human consumption (Min et al., 2005; Cagri et al., 2004; Dawson et al., 2002; Hoffman et al., 2001; Padget et al., 2000; Padgett et al., 1998).

Many studies have demonstrated that antimicrobial agents when incorporated into the packaging films could be effective for reducing levels of foodborne organisms (Cutter, 2006; Quintavalla and Vincini, 2002). In order to meet consumer demands for more natural, disposable, potentially biodegradable and recyclable food packaging materials, research has focused on the incorporation of natural antimicrobial compounds such as plant extracts and bacteriocins into the biobased packaging materials instead of plastic films (Cutter, 2006; Devlieghere et al., 2004; Lopez-Rubio et al., 2004). Within the biobased packaging materials, edible films and coatings have drawn attention in recent years and a variety of edible films and coatings has been developed for fresh and further processed meats and poultry due to their numerous advantages (Beverlya et al., 2008; Cutter, 2006; Oussalah et al., 2006; Cagri et al., 2004; Han, 2000). Some spice essential oils incorporated into packaging materials can control microbial contamination in beef muscle by reducing the growth of Escherichia coli O157:H7 and Pseudomonas spp. (Oussallah et al., 2004). Essential oil fractions of oregano and pimento are efficient against various foodborne bacteria such as Salmonella (Helander et al., 1998; Paster et al., 1990), E. coli O157:H7 (Burt and Reinders, 2003). Spice extracts from oregano, sage, rosemary, garlic, thyme and pimento are also reported to possess antioxidant properties (Dorman and Deans, 2000; Hammer et al., 1999).

Plant essential oils (EOs) and oil compounds (OCs) have been previously evaluated for their ability to protect food against pathogenic bacteria contaminating apple juice (Friedman et al., 2004) and other foods (Seydim and Sarikus, 2006; Burt, 2004). However, little published data exist on the incorporation of EOs and OCs into edible films. Many essential oils (EOs) possess antimicrobial activity and those that contain high level of phenolic groups, such as carvacrol, eugenol or thymol, are usually the most effective ones. Both oregano and clove EOs have been shown to be effective against food pathogen. Carvacrol is the major compound of oregano EO while eugenol is the major compound of clove EO (Paster et al., 1995).

The ability of plant essential oils to protect foods against pathogenic and spoilage microorganisms have been reported by several researchers (Rojas-Graü et al., 2007; Burt and Reinders, 2003; Hao et al., 1998; Lis-Balchin et al., 1997; Nelson, 1997). In order to achieve effective antimicrobial activity in direct food applications, high concentrations of essential oils are generally needed, which might impact inappropriate flavors and odors in the product (Gutierrez et al., 2009; Seydim and Sarikus 2006). Therefore, recent research should focus on incorporation of essential oils to edible films as a supplementary application in food packaging (Seydim and Sarikus 2006). Generally, the essential oils possessing the strongest antibacterial properties against foodborne pathogens contain higher concentrations of phenolic compounds such as carvacrol, eugenol (2-methoxy-4-(2-propenyl) phenol) and thymol (Burt, 2004). These compounds exhibit a wide range of biological effects including antioxidant and antimicrobial properties.

Some published works suggested the possibility of using essential oils such as cinnamon and clove as natural antimicrobials in milk (Cava et al., 2007), lemon, sage, and thyme to preserve cheese (Gammariello et al., 2008), and coriander oil as a food ingredient (Burdock and Carabin, 2009).

There are some studies dealing with the antimicrobial properties of films based on milk-proteins, chitosan or alginates incorporated with various essential oils (oregano, rosemary, garlic, pimento, cinnamon) (Oussalah et al., 2006, 2004; Seydim and Sarikus, 2006; Zivanovic et al., 2005) with good results. In this regard, chitosan is a valuable component for producing biodegradable packaging films, among other reasons because of its filmforming capability as well as its antioxidant and antimicrobial properties (López-Caballero et al., 2005; Jeon et al., 2002). Some studies have considered the incorporation of aqueous plant extracts into the formulation of gelatin edible films (Gómez-Estaca et al., 2007) and the

formulation of plastic films incorporated with clove essential oil (López et al., 2007). The effect of catfish gelatin coating containing oregano oil on some pathogenic bacteria (Salmonella typhimurium and Escherichia coli) was also reported (Min and Oh, 2009).

Despite of the broad application of protein based bioplastics, there is nothing related to use of bioplastics containing antimicrobial agents (essential oil and their active agents) manufactured by mixing, extrusion or thermomoulding.

5. Rheological, thermal and microstructural characterization of bioplastics

5.1 Rheological behaviour

Fluids can be firstly classified as "compressible" and "incompressible" according to their response to the externally applied pressure, i.e. whether or not the volume of an element of fluid is dependent on its pressure. A second classification of fluids may be according to their response to an applied shear stress or shear rate, leading to the so call "Newtonian" and "non-Newtonian" fluids (Chabra and Richardson, 1999). While compressibility influences the flow characteristics of gases, liquids can normally be regarded as incompressible and their response to shear forces is the main goal of this chapter.

General classification of solids and fluids

Regarding incompressible materials (not only fluids), they are considered in a more general classification attending their behaviour under a force or a deformation. Thus, the simplest and probably the first relation between force and deformation is Hook' law, the force is proportional to deformation as follows (Barnes et al, 1993):

$$\sigma = G\gamma \qquad [5.1]$$

where σ is the force per unit area or stress and γ is the relative change of strain and G is the constant of proportionality called de elastic modulus, which is an intrinsic property of a solid. According to this, Hookean materials do not flow and are linearly elastic and therefore, stress remains constant until the strain is removed and the material returns to its original shape. Hooke's law can be used to describe the behaviour of many solids (steel, egg shell, dry pasta, etc.) when subjected to small strains, typically less than 0.01. However, the strain range over which the relationship is linear varies greatly, e.g., ≈2-3 for rubbers, ≈0.2-1 for most polymer gels, ≈1 for gelatin gels, ≈0.003-0.03 for many particle gels (yoghurt), and ≈0.0002 for bread dough, margarine, and cast iron. Only brittle materials such as cast iron,

ceramic products, potato crisps, and several hard biscuits, are linearly elastic up to the point where they fracture (Van Vliet and Lyklema, 2005). Robert Hooke developed his "True Theory of Elasticity" in 1678 and proposed that "the power of any spring is in the same proportion with the tension thereof", i.e. a double tension leads to a double extension. This forms the basic premise behind the theory of classical (infinitesimal-strain) elasticity (Barnes et al., 1993).

At the other end of the spectrum, Isaac Newton, in the "Principia" published in 1687, proposed the following hypothesis for liquids: "The resistance which arises from the lack of slipperiness of the parts of the liquid, other things being equal, is proportional to the velocity with which the parts of the liquid are separated from one another" (Barnes et al., 1993). Thus, for a Newtonian fluid in laminar flow, Newton's law has the following form:

$$\sigma = \mu \dot{\gamma} \qquad [5.2]$$

where, the shear rate, $\dot{\gamma}$, may be expressed as the velocity gradient in the direction perpendicular to that of the shear force. The force per unit area required to produce the motion is F/A and is denoted by σ and is proportional to the "velocity gradient" (or shear rate). The constant of proportionality, μ, is known as the coefficient of viscosity and results from the lack of slipperiness. Gases, simple organic liquids, solutions of low molecular weight inorganic salts, molten metals and salts are all Newtonian fluids.

Although Newton introduced these ideas, it was not until the nineteenth century that Navier and Stokes independently developed a consistent three-dimensional theory for what is now called a Newtonian viscous liquid (Barnes et al., 1993). The governing equations for such a fluid are called the Navier-Stokes equations. Moreover, a Newtonian fluid possesses a constant viscosity and it also satisfies the complete Navier-Stokes equations. Thus, for instance, the well-known Boger fluids display constant shear viscosity but, also, normal stress during flow (Prilutski et al., 1983; Boger, 1977). For that reason, they are considered as non-Newtonian fluids.

As a result, two limiting elastic and viscous behaviours can be considered in terms of the laws of Hooke and Newton. Both of them are linear laws, which assume direct proportionality between stress and strain, or strain rate, whatever the stress. However, phenomenologically, it is possible to provide a wider classification of materials according their rheological behaviour. However, the range of stress over which materials behave linearly is invariably limited. In other words, material properties such as rigidity modulus and

viscosity can change with the applied stress. The change can occur either instantaneously or over a long period of time, and it can appear as either an increase or a decrease of the material parameter.

In that sense, material properties often depend on strain or strain rate (non-linear behaviour). Moreover, the properties of a material may depend on the deformation time, resulting in non-equilibrium behaviour. As result, for many materials the effect of a stress or strain generally consists of a partly viscous contribution and a partly elastic one; they are viscoelastic. The ratio between these two contributions mostly depends on the speed of deformation. A general classification of solid and fluid are shown in Figure 5.1.

Moreover, a given material can behave like a solid or a liquid depending on the time scale of the deformation process. Then, it will be possible to include a given material in more than one of these classifications depending on the experimental conditions. The scaling of time in rheology is achieved by means of the "Deborah number", which was defined by Professor Marcus Reiner, and may be introduced as follows (Barnes et al., 1993):

$$De = \frac{\tau_{rel}}{t_{obs}} \qquad [5.3]$$

where t_{obs} is a characteristic time of the deformation process being observed and τ_{rel} is a characteristic time of the material. The rheological behaviour of materials with one single relaxation time can be classified according to their Deborah numbers as follows: purely elastic or solid behaviour when De are very high, purely viscous or liquid behaviour when De are very low, and viscoelastic behaviour for intermediate values of De. The important conclusion is that the distinction between solid and fluid behaviour not only depends on an intrinsic property of the material but also on the duration of observation (Van Vliet and Lyklema, 2005).

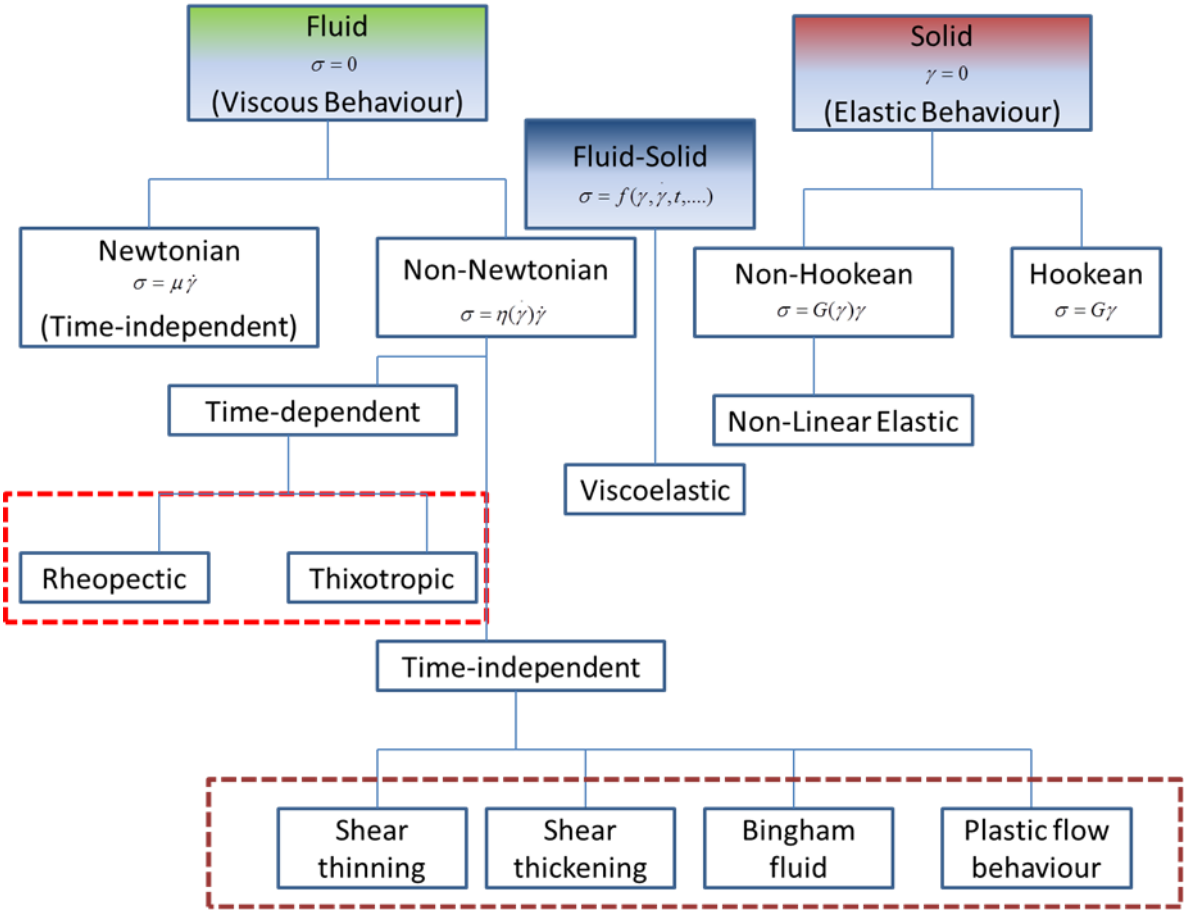

Figure 5.1 Material classification in simple shear.

Accordingly, a solid may be defined as a material that will not continuously change its shape when subjected to a given stress, i.e. for a given stress there will be a fixed final deformation, which may or may not be reached instantaneously on application of the stress. On the other hand, a liquid as a material that will continuously change its shape, that is, it will flow when subjected to a given stress, irrespective of the magnitude that stress.

In the same way, the term "viscoelasticity" may be used to describe behaviour which falls between the classical extremes of Hookean elastic response and Newtonian viscous behaviour (Figure 5.1). In terms of ideal material response, a solid material with viscoelasticity is invariably called a "viscoelastic solid" in the literature. In the case of liquids, there is more ambiguity so far as terminology is concerned. The terms "viscoelastic liquid", "elastic-viscous liquid", "elastic liquid" are all used to describe a liquid showing viscoelastic properties. In recent years, the term "memory fluid" has also been used in this connection. Moreover, liquids whose behaviour cannot be described on the basis of the Navier-Stokes equations are called "non-Newtonian liquids". Such liquids may or may not possess

viscoelastic properties. This means that all viscoelastic liquids are non-Newtonian, but not all non-Newtonian liquids are viscoelastic (Barnes et al., 1993).

Regarding its flow behaviour, a non-Newtonian fluid is one whose flow curve shows an apparent viscosity, shear stress divided by shear rate, which is shear rate dependent and, sometime, dependent upon time of shear. Accordingly, such materials may be conveniently grouped as follows (Chabra and Richardson, 1999):

- Fluids for which the rate of shear at any point is determined only by the value of the shear stress at that point at any instant; these fluids are known as "time independent", "equilibrium behaviour", "purely viscous" or "inelastic" fluids.
- More complex fluids for which the relation between shear stress and shear rate depends, in addition, upon the duration of shearing and their kinematic history; they are called "time-dependent fluids" or "non-equilibrium behaviour".

Steady state viscous behaviour

a. Shear thinning/thickening and structured fluids

Figure 5.2 shows a graphical overview of basic relationships between stress and shear rate for fluids and fluid-like materials subjected to shear deformation. In practice, a combination of these simple relationships can often be observed, particularly when the mechanical behaviour is studied over a large range of shear rates or stresses.

The simplest relationship between shear stress and shear rate is a linear viscous fluid (Figure 5.2). Fluids obeying such behaviour are called Newtonian fluids. Only one material parameter, the Newtonian viscosity, μ, suffices to define fully their rheological behaviour under shear. The viscosity is given by the slope of the line, and is independent of shear rate and shear time.

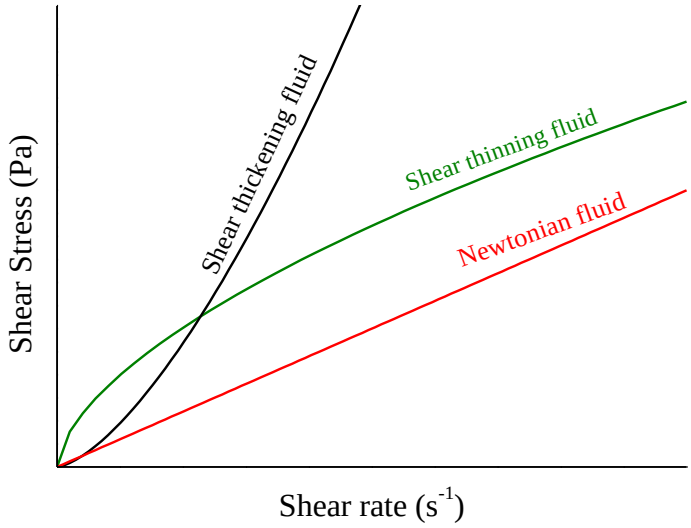

Figure 5.2 Steady flow behaviour of Newtonian and non-Newtonian fluids.

Regarding non-Newtonian fluids, the relationship between shear rate and stress is not linear (Figure 5.2). Then, a shear rate-dependent viscosity is obtained, called apparent viscosity, $\eta=\sigma/\dot{\gamma}$. If the fluid viscosity decreases with increasing shear rate the observed behaviour is known as shear-thinning, on the contrary when viscosity increases a shear-thickening behaviour develops (Figure 5.3) (Van Vliet and Lyklema, 2005; Barnes et al., 1993).

Probably, the most common type of time-independent non-Newtonian fluid behaviour observed is shear-thinning. However, most shear-thinning fluids with a complex microstructure also exhibit Newtonian behaviours at low and high shear rates. The resulting values of the apparent viscosity at very low and high shear rates are known as the zero-shear-rate-limiting viscosity, η_o, and the high-shear-rate-limiting viscosity, η_∞. Thus, the apparent viscosity of a shear-thinning fluid decreases from η_o to η_∞, with increasing shear rate. Theses fluids are known as "structured fluids" because shear rate affects material microstructure and their viscous behaviour changes according to such a microstructure. Data in a sufficiently wide range of shear rates may illustrate this complete viscous behaviour (Figure 5.4).

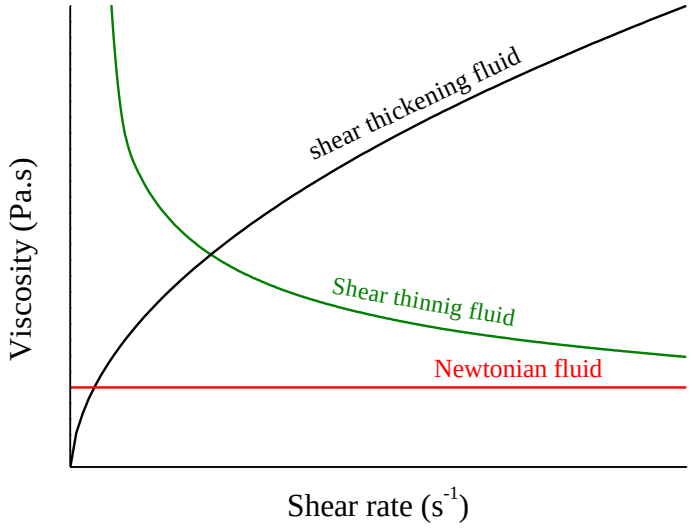

Figure 5.3 Plot on linear-scale of the steady viscous behaviour of Newtonian and non-Newtonian fluids.

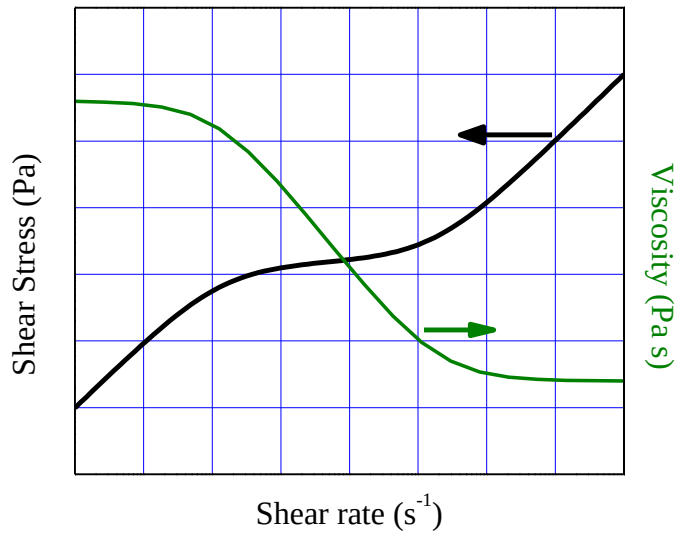

Figure 5.4 Log-log scale plot of the flow behaviour of structured fluids.

Examples of structured fluids are most of concentrated food emulsions, which show a marked non-Newtonian behaviour. This behaviour has been related to droplet deformation, flocculation or the non-Newtonian behaviour of the dispersed phase (Pal, 1998). The general evolution of viscosity with shear rate (or shear stress) shows three different regions, a constant

viscosity, η_o , at low shear rates (or shear stress), a power-law decrease in viscosity, and finally a constant viscosity, η_∞ , at high shear rates, characteristic of an unflocculated system.

However, structured fluid behaviour, showing those three regions, is difficult to obtain and, normally, several measurement instruments are often required to achieve this objective. An alternative procedure is the use of a master curve.

b. Viscoplastics fluids

Many common materials such as margarine, tomato ketchup, buttermilk, etc. behave like solids under small stresses and are fluid-like under large stresses. An effective flow is only noticed above a certain threshold stress value, the so-called yield stress. These fluids are known as viscoplastics and undergo a plastic flow behaviour, characterized by a shear-thinning character above the yield stress. However, the yield stress value often depends on many different factors. This implies that, depending on the purpose for which one wants to know yield stress values, one may have to accept different values for the same material. However, this does not imply that yield stress cannot be a useful material characteristic (Barnes 1999, Steffe 1996).

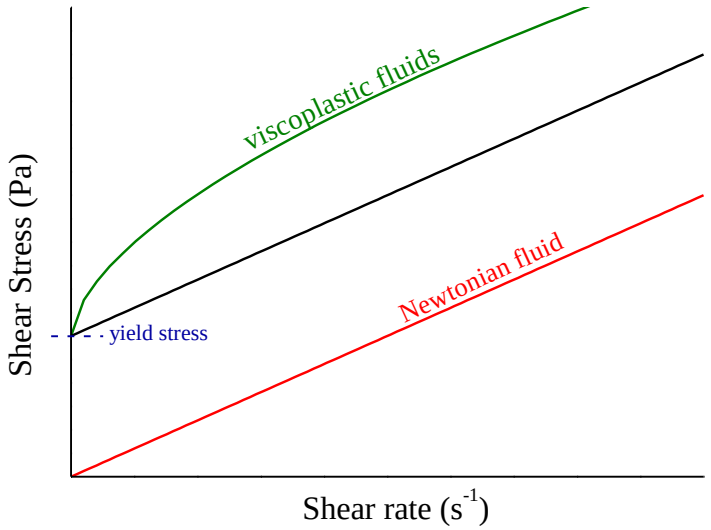

Figure 5.5. Steady flow behaviour of viscoplastic fluids.

A typical stress versus shear rate plot shows that this type of fluid behaviour is characterised by the existence of a yield stress (σ_o) which must be exceeded before the fluid will deform or flow. Once the magnitude of the external stress has exceeded the value of the

yield stress, the flow curve may be linear or non-linear but will not pass through origin (Figure 5.5).

A fluid with a linear flow curve for $\sigma>\sigma_0$ is called a Bingham plastic fluid and is characterised by a constant plastic viscosity (the slope of the shear stress versus shear rate curve) and a yield stress. On the other hand, a substance possessing a yield stress as well as a non-linear flow curve on linear coordinates (for $\sigma > \sigma_0$), is called a 'yield-shear-thinning' material.

Strictly speaking, it is virtually impossible to make certain whether any real material has a true yield stress or not, but nevertheless the concept of a yield stress has proved to be convenient in practice because some materials closely approximate to this type of flow behaviour (Evans, 1992; Astarita, 1990; Schurz, 1990; Barnes and Walters, 1985). The answer to the question whether a fluid has a yield stress or not seems to be related to the choice of a time scale of observation (Chhabra and Richardson, 1999). Common examples of viscoplastic fluid behaviour include particulate suspensions, emulsions, foodstuffs, blood and drilling muds, etc. (Barnes, 1999).

Time-dependent viscous behaviour

Up to now, rheological characterization has been performed on the assumption that the viscosity only depends on the applied shear rate or shear stress. However, in many cases, it is also a function of the length of time that the shear rate or stress is applied to the liquid being measured. A common way of measuring time-dependent effects during viscous flow is to perform a loop test; that is to say, to increase the shear rate (or sometimes shear stress) of a test linearly from zero to a maximum value, and then to return at the same rate to zero (Figure 5.6).

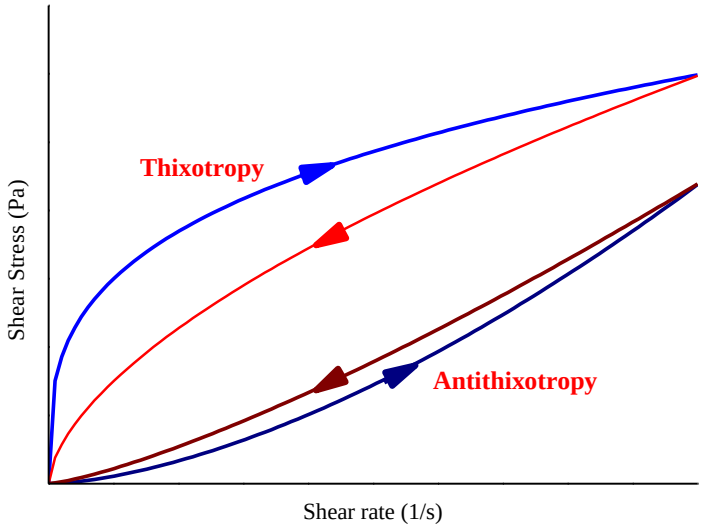

Figure 5.6 Thixotropic loop test.

As may be deduced from Figure 5.6, viscosity may depends on both share rate and shear time in different ways. The measured viscosity can either increase or decrease with time of shear. Such changes can be reversible or irreversible. However, in most cases the viscosity decreases towards an equilibrium value as the liquid microstructure adjusts itself to the particular shear rate. If then the shear rate is decreased (or set to zero), the microstructure begins to rebuild itself towards a value appropriate to the new shear rate. All these effects are manifested as changes in the indicated viscosity, and, when these time effects are significant, they are known as thixotropy or antithixotropy phenomenon (Barnes, 1997).

All liquids with microstructure can show thixotropy, because thixotropy only reflects the finite time taken to move from one state of microstructure to another and back again. The driving force for microstructural changes related to shear is the result of the competition between break-down due to flow stresses, build-up due to in-flow collisions and Brownian motion (Figure 5.6). Thixotropy invariably occurs in circumstances where the liquid is shear-thinning (in the sense that viscosity levels decrease with increasing shear rate).

Very occasionally situations arise when existing weakly attached microstructural elements (brought together by collision during shear) that are slowly torn apart by the constant action of the random Brownian motion. In that case, the opposite to thixotropy is seen, i.e., antithixotropy (or rheopexy), where flow structures and rest destructures the material (Barnes, 1997). In the same way, rheopexy is usually associated with shear-

thickening behaviour. The way that either phenomenon manifests itself depends on the type of test being undertaken.

The occurrence of thixotropy implies that the flow history must be taken into account when making predictions of flow behaviour. For instance, flow of a thixotropic material down a long pipe is complicated by the fact that the viscosity may change with distance down the pipe (Barnes et al., 1993).

Thixotropy has found practical application, for instance, in the following areas (Tropea et al., 2007; Barnes, 1997):

- In paints, inks and coatings by allowing the easy application by thixotropic breakdown of paint and avoiding material draining by a quick microstructure rebuilding.
- Lubricating greases are thixotropic because of the flocculation of the dispersed material (a soap) suspended in an oil phase. The breakdown of the extended three dimensional network is very important in lubricating situations where the grease has to break on shearing so that no unwanted extra drag is experienced in bearings.
- Many food and biological systems are well known examples of thixotropy, where flow makes them thinner, but leaving them to rest thereafter thickens them again.
- Storage stability and applicability of creams and pharmaceuticals products are given by their thixotropic behaviour. Here the original meaning of thixotropy of conferring gel-like properties is still very often the controlling idea.

On the other side, relatively few fluids display rheopexy or negative thixotropy, for which the apparent viscosity or shear stress increases with shear time. In this case, hysteresis effects are observed in the flow curve but inverted, as compared with a thixotropic material (Figure 5.6). In these fluids the structure builds up by shear and breaks down when the material is at rest. However, it is common for the same dispersion to display both thixotropy as well as rheopexy depending upon the shear rate and/or the concentration of solids (Keller and Keller Jr, 1990; Tanner, 1988; Steg and Katz, 1965).

5.1.1 Viscosity

Viscosity is a measure of the resistance of a fluid which is being deformed by either shear stress or tensile stress (Keith, 1971). In everyday terms (and for fluids only), viscosity is "thickness" or "internal friction". Thus, water is "thin", having a lower viscosity, while honey

is "thick", having a higher viscosity (Keith, 1971). Refering to Figure 1.5.9, it could define viscosity as the ratio of the imposed *shear stress (*τ) (force F, applied tangentially, divided by the area (A), and the *shear rate (*$\dot{\gamma}$*).*

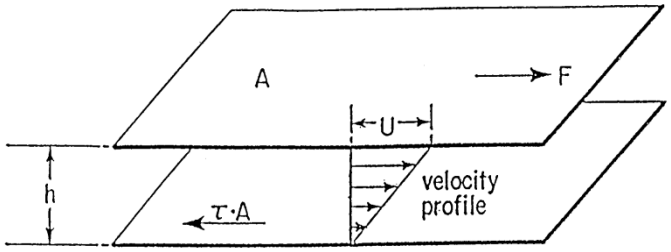

Figure 5.7 Simple shear flow.

One remarkable property of polymeric liquids is their *shear-thinning* behavior (also known as pseudo-plastic behaviour). If it increases the rate of shearing (i.e., extrude faster through a die), the viscosity becomes smaller, as shown in Figure 5.3. This reduction of viscosity is due to molecular alignments and disentanglements of the long polymer chains. The most frequently used model to express the shear-thinning behaviour of polymer is the power law. Viscosity can be measured by either capillary or rotational viscometers.

Mathematical relations

For unidirectional flows, the shear rate is simply the derivative of velocity (V_x) with respect to distance *y*, perpendicular to the flow direction.

$$\dot{\gamma} = \frac{dV_x}{dy} \qquad [5.4]$$

For the drag flow shown in Figure 5.7, the velocity profile is linear (due to the no-slip assumption at top and bottom plates).

$$V_x = \frac{U}{h} y \qquad [5.5]$$

and the shear rate

$$\dot{\gamma} = \frac{dV_x}{dy} = \frac{U}{h} \qquad [5.6]$$

For pressure driven axial flow (z direction) of a Newtonian fluid in a tube of radius R, the velocity profile is parabolic

$$V_z = V_{max}\left(1 - \frac{r^2}{R^2}\right) \quad [5.7]$$

and the absolute value of shear rate

$$\dot{\gamma} = \left|\frac{dV_z}{dr}\right| = 2\frac{r}{R^2}V_{max} \quad [5.8]$$

varies between zero at the axis of symmetry (r=0) to a maximum value at the wall at $r=R$, $\dot{\gamma}_w$

$$\dot{\gamma}_w = \frac{2}{R}V_{max} \quad [5.9]$$

The relation between maximum velocity and average, V_{avg}, in tube flow is

$$V_{max} = 2\,V_{avg} \quad [5.10]$$

Therefore

$$\dot{\gamma}_w = \frac{4}{R}V_{avg} \quad [5.11]$$

and since the volume flow rate Q is related to the average velocity by

$$Q = V_{avg}\pi R^2 \quad [5.12]$$

$$\dot{\gamma}_w = \frac{4Q}{\pi R^3} \quad [5.13]$$

Although this relation is strictly valid for Newtonian fluids, it is also useful for non-Newtonian fluids (see below).

The shear stress is determined from the pressure drop by the equation

[5.14]

$$\tau = \frac{\Delta P}{2L} \mathrm{r}$$

which varies linearly from zero on the capillary axis (r = 0) to a maximum value at the wall (r = R), τ_w

$$\tau_w = \frac{\Delta P}{2L} \mathrm{R} \qquad [5.15]$$

Therefore, for flow through a tube or between two flat plates, the shear stress varies linearly from zero along the central axis to a maximum value along the wall (Figure 5.8).

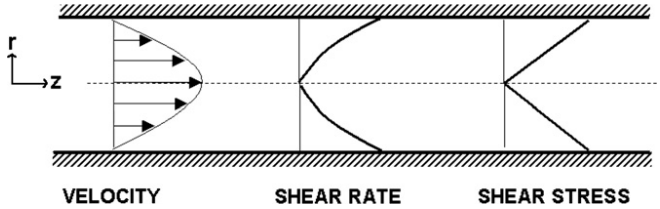

Figure 5.8 Velocity, shear rate and shear stress profiles for flow between two flat plates.

On the other hand, the shear rate varies nonlinearly from zero along the central axis to a maximum along the wall. The velocity profile is quasi-parabolic with a maximum at the plane of symmetry and zero at the wall as shown in Figure 5.8. Thus, for a power law fluid shear stress is

$$\tau = k\left(-\frac{dV_z}{dr}\right)^n \qquad [5.16]$$

By substituting of Equation 5.16 in Equation 5.14 and integrating the resulting expression, the velocity profile for a power law model is obtained as follows,

$$V_z = V_{max}\left[1 - \left(\frac{r}{R}\right)^{\frac{n+1}{n}}\right] \qquad [5.17]$$

where the relation between maximum velocity and average velocity is now

$$V_{max} = \frac{3n+1}{n+1} V_{avg} \qquad [5.18]$$

Then, for the power law model the wall shear rate becomes

[5.19]

$$\dot{\gamma}_w = \frac{3n+1}{4n}\,\frac{4Q}{\pi R3}$$

Previously, the so-called Weissenberg–Rabinowitch correction must be taken into account:

$$m = \frac{d(log\tau_p)}{d(log\tau_\gamma)} \approx n \qquad [5.20]$$

where m is the power law index obtained from pressure drop tests performed on pipes.

Then, the ratio of the measured wall shear stress and the corresponding wall shear rate gives the viscosity

$$\eta = \frac{\tau_w}{\dot{\gamma}_w} \qquad [5.21]$$

where τ_w can be calculated from Equation 5.15. However, for a capillary rheometer, the pressure drop ΔP is measured in the reservoir (Figure 5.9) and at the entrance to the capillary there is an additional pressure drop ΔP_e.

Usually, the entrance pressure drop is evaluated experimentally from the measurement data of at least two, preferably three, capillaries of same diameter but different length. This is accomplished by plotting the pressure drop (ΔP) at constant shear rate versus capillary L/D and fitting a linear fit on the data. The linear Bagley plot is then extrapolated to zero and the point at which the line intersects with y axis is the entrance pressure drop (ΔP_e). True shear stress (τ_w) can be calculated as

$$\tau_w = \frac{\Delta P - \Delta P_e}{2L/R} \qquad [5.22]$$

where L/R represents the capillary length to radius ratio. Without the Weissenberg-Rabinowitsch and Bagley corrections there can be significant errors in viscosity data obtained from capillary instruments.

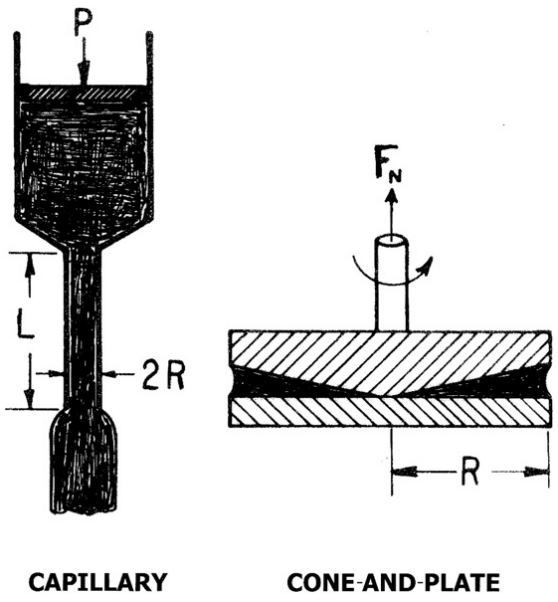

Figure 5.9 Schematic representation of capillary and cone and plate viscometer.

With rotational viscometers (cone-and-plate or parallel plate), the shear stress is determined from the applied torque and the shear rate from the rotational speed and the gap where the fluid is sheared. For the cone-and-plate geometry of Figure 5.9, the shear rate is given by stress by

$$\dot{\gamma} = \frac{\Omega'}{\alpha} \qquad [5.23]$$

and the shear stress by

$$\tau = \frac{3M}{2\pi R^3} \qquad [5.24]$$

where Ω' is rate of rotation; α is the cone angle (usually less than 5º); M is the measured torque; and R is the plate radius.

Capillary viscometers are usually used for the shear rate range from 1 s^{-1} to 3000 s^{-1}. Rotational viscometers are usually used for the range 10^{-5} to 100 s^{-1}. At higher rotational speeds, secondary flows and instabilities may occur which invalidate the simple shear assumption.

Viscosity modeling

Power-Law / Ostwald-de Waele model:

The most frequently used model to express the shear-thinning behavior is the power-law.

$$\eta = k \cdot (\dot{\gamma})^n \qquad [5.25]$$

where k and n are the consistency ($Pa \cdot s^n$) and flow indexes, respectively.

Two other models are frequently used for better fitting of data over the entire shear rate range:

Carreau viscosity equation

Carreau put forward the following viscosity model which incorporates both shear-rate-limiting viscosities η_o and η_∞:

$$\frac{\eta - \eta_\infty}{\eta_o - \eta_\infty} = \frac{1}{[1 + (\lambda\dot{\gamma})^2]^s} \qquad [5.26]$$

Parameter $\lambda = 1/\dot{\gamma}_c$, where $\dot{\gamma}_c$ is a critical shear rate for the onset of the shear-thinning region and "s" is a parameter related to the slope of the power-low region. This model can describe shear-thinning behaviour over wide ranges of shear rates but only at the expense of the added complexity of four parameters.

Cross Model

Cross model also predicts a Newtonian region at low shear rates, shear thinning region at intermediate shear rate values and, finally a constant viscosity (Newtonian region) in the high shear rate regimen:

$$\frac{\eta - \eta_\infty}{\eta_o - \eta_\infty} = \frac{1}{1 + (t_1\dot{\gamma})^P} \qquad [5.27]$$

where η_o and η_∞ are the zero-shear-rate-limiting and high-shear-rate-limiting viscosities respectively. Parameter p is derived from power law as n=1-p when $\eta_o >> \eta >> \eta_\infty$ and t1 is a characteristic time, whose inverse is related to the shear rate at which the apparent viscosity is given by $\eta=\eta_o + \eta_\infty/2$. This four-parameter model may be used in the same shear rate range as the Carreau model.

5.1.2 Oscillatory measurements

Bioplastics are viscoelastic materials, and it is therefore very important to know the ratio of viscous to elastic properties at different temperatures. The characteristic of polymers can by studied by Small-Amplitude Oscillatory Shear (SAOS) when subjected to a sinusoidal stress or strain at different frequencies.

The viscoelastic properties of biopolymers are determined by the effects of many different variables, including temperature, pressure and time. Other important variables include chemical composition, molecular weight and weight distribution, degree of branching branching and crystallinity, types of functionality, component concentration, dilution with solvents or plasticizers, and mixture with other materials to form composite systems. With guidance by molecular theory, the dependence of viscoelastic properties on these variables can be simplified by introducing additional concepts such as the free volume, the monomeric friction coefficient, and the spacing between entanglement to provide a qualitative understanding and in many cases a quantitative prediction of how to achieve desired physical and chemical properties and ultimate microstructure.

Thus, unlike constant rotation (shear) measurements, oscillation is a non-destructive technique which is ideal for investigating structure/structural changes in materials. The oscillation technique involves applying a sinusoidal oscillating stress (σ) wave to a material and measuring the resulting strain wave (γ).

A purely elastic (Hookean solid) material will retain all of the deformation energy applied to it and will therefore have a phase difference (phase angle) of 0^o, (Figure 5.10). Conversely, a purely viscous (Newtonian) fluid dissipates all of the applied energy and will have a phase angle of 90^o, (Figure 5.11). Polymeric materials are visco-elastic and as such their responses fall somewhere between these two limits (Figure 5.12). Polymeric materials that are partly viscous and partly elastic (viscoelastic) will be $0 \leq \delta \leq 90°$ out of phase.

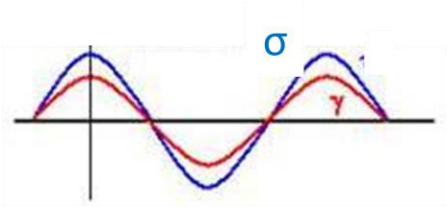

Figure 5.10 Hookean solid responce- Phase angle =0.

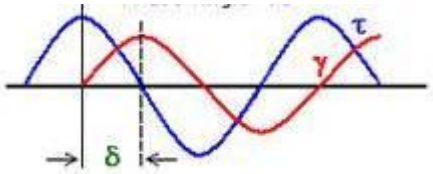

Figure 5.11 Hookean solid response- Phase angle =90.

Figure 5.12 Hookean solid response- Phase angle = 0><90.

Measurements are made over a range of frequencies and a family of curves is generated. The data of most interest that derive from these oscillation strain control measurements are complex viscosity (η*), phase angle (δ), and shear storage and loss moduli (G' and G"), as a function of frequency. The ratio of the elastic stress to strain is the elastic (or storage) modulus G'; the ratio of the viscous stress to strain is the viscous (or loss) Modulus G". The complex modulus $|G^*|^2 = |G'|^2 + |G"|^2$ reflects the contribution of both elastic and viscous components to the material's stiffness. The complex viscosity η* is a measure of the material's overall resistance to flow as a function of shear rate. The ratio of the viscous modulus to the elastic modulus, G"/G'= tan δ, is known as loss tangent.

The limiting viscosity reached at low frequency is indicative of a material's zero shear viscosity and therefore it is related to its molecular weight. The point at which the G' and G" curves cross over can also be a good indication of magnitude of molecular weight and molecular weight distribution, (Figure 5.13). The relationship of G' to G" describes the visco-elastic response of the material. Phase angle, δ, or tan δ is a good indicator of phase transitions (e.g. T_g) when measurements are made as a function of temperature.

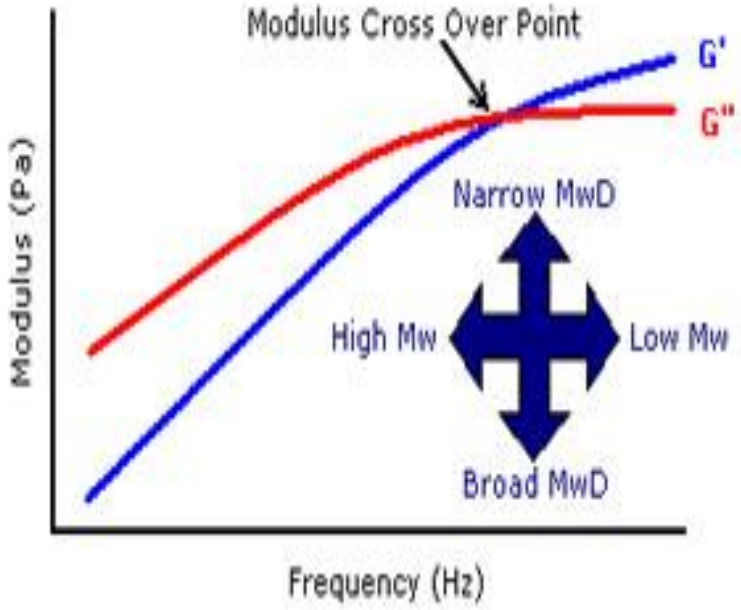

Figure 5.13 Typical plots - Frequency sweep test.

5.2 Thermal properties

Thermal analysis can be defined as the extent of physical and chemical properties of materials as a function of temperature (the most common parameters are: enthalpy, heat capacity, mass and coefficient of thermal expansion).The term thermal analysis is applied to a set of tests, including DSC (differential scanning calorimetry), TGA (Thermogravimetric analysis), and DMTA (dynamic mechanical thermal analysis).

5.2.1 Differential Scanning Calorimetry

Differential Scanning Calorimetry is a thermoanalytical technique in which the difference in the amount of heat required to increase the temperature of a sample and reference is measured as a function of temperature. Both the sample and reference are maintained at nearly the same temperature throughout the experiment (Figure 5.14). Generally, the temperature program for a DSC analysis is designed such that the sample holder temperature increases linearly as a function of time. The reference sample should have a well-defined heat capacity over the range of temperatures to be scanned.

For example, as a solid sample melts to a liquid it will require more heat flowing to the sample to increase its temperature at the same rate as the reference. This is due to the absorption of heat by the sample as it undergoes the endothermic phase transition from solid to liquid. Likewise, as the sample undergoes exothermic processes (such as crystallization) less heat is required to raise the sample temperature. By observing the difference in heat flow between the sample and reference, differential scanning calorimeters are able to measure the amount of heat absorbed or released during such transitions. Differential Scanning Calorimetry may also be used to observe more subtle phase changes, such as glass transitions. It is widely used in industrial settings as a quality control instrument due to its applicability in evaluating sample purity and for studying polymer curing (Skoog et al., 1998; Dean, 1995; Pungor, 1995).

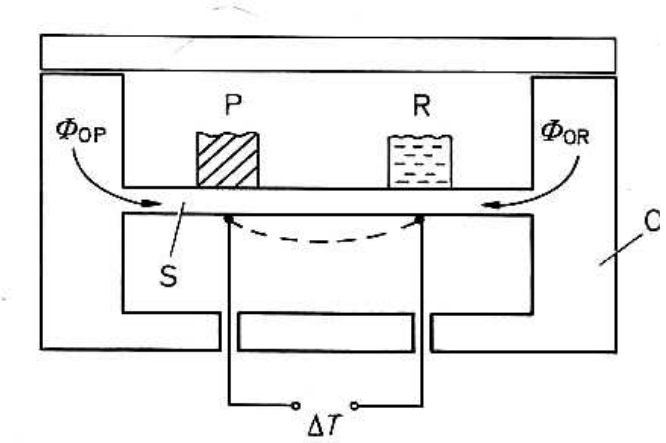

Figure 5.14 Measured difference in heat flow between sample and reference while they are being heated: Differential Scanning Calorimetry.

The different thermal events observed in at DSC plot are glass transition, crystallization, melting point and curing (Figure 5.15). Differential scanning calorimetry can be used to measure a number of characteristic properties of a sample. Using this technique it is possible to observe fusion and crystallization events as well as glass transition temperatures T_g. DSC can also be used to study oxidation, as well as other chemical reactions (Skoog et al., 1998; Dean, 1995; Pungor, 1995; O'Neill, 1964).

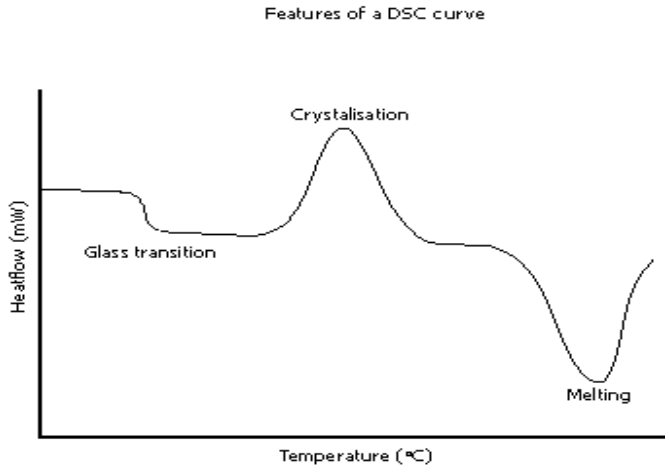

Figure 5.15 Typical thermogram plots DSC.

Glass transitions may occur as the temperature of an amorphous solid is increased. These transitions appear as a step in the baseline of the recorded DSC signal. This is due to the sample undergoing a change in heat capacity; no formal phase change occurs (Dean, 1995; Skoog et al., 1998). DSC measures endothermic and exothermic transitions as a function of temperature:

- Endothermic heat flows into a sample as a result of either heat capacity (heating) or some endothermic process (glass transition, melting, evaporation, etc.).
- Exothermic heat flows out of the sample as a result of either heat capacity (cooling) or some exothermic process (crystallization, curing, oxidation, etc.).

As the temperature increases, an amorphous solid will become less viscous. At some point the molecules may obtain enough freedom of motion to spontaneously arrange themselves into a crystalline form. This is known as the crystallization temperature (T_c). This transition from amorphous solid to crystalline solid is an exothermic process, and results in a peak in the DSC signal. As the temperature increases the sample eventually reaches its melting temperature (T_m). The melting process results in an endothermic peak in the DSC curve. The ability to determine transition temperatures and enthalpies makes DSC a valuable tool in producing phase diagrams for various chemical systems (Dean, 1995)

Di Gioia and Guilbert (1999) used modulated-DSC to study the zein plasticization by water, glycerol, and octanoic acid plasticizers. Increasing plasticizer concentration decreased T_g. A study carried out on thermal gelation of whey proteins (Fitzsimons et al., 2007) revealed

the existence of an endothermic peak that reflects the slow formation of intermolecular bonds (aggregation). The denaturation of proteins has been extensively studied by differential scanning calorimetry (DSC), where denaturation is observed as an endothermic peak (Privalov and Khechinashvili, 1974). The glass transition temperature (Tg) has been the main studied parameter to understand the mechanical properties of gluten proteins (Kalichevsky and Blanshard, 1992). The glass transition of glutenin and its depression due to water plasticization were observed from studies using thermal and mechanical behaviours of the glutenin fraction by DSC and mechanical spectroscopy (Cocero and Kokini, 1991). Other authors confirmed this statement (Kalichevsky et al., 1993).

5.2.2 Thermogravimetric analysis or Thermal Gravimetric Analysis (TGA)

Thermogravimetric analysis is a type of measurement that is performed on samples to determine changes in weight in relation to change in temperature. Such analysis relies on a high degree of precision in three measurements: weight, temperature, and temperature change. As many weight loss curves look similar, the weight loss curve may require transformation before results may be interpreted. A derivative weight loss curve can be used to show the point at which weight loss is most apparent. Again, interpretation is limited without further modifications and deconvolution of the overlapping peaks may be required.

TGA is commonly employed in research and testing to determine characteristics of materials such as polymers, to determine degradation temperatures, absorbed moisture content of materials, the level of inorganic and organic components in materials, decomposition points of explosives, and solvent residues. The analyzer usually consists of a high-precision balance with a pan (generally platinum) loaded with the sample. The pan is placed in a small electrically heated oven with a thermocouple to accurately measure the temperature. The atmosphere may be purged with an inert gas to prevent oxidation or other undesired reactions. A computer is used to control the instrument.

Analysis is carried out by raising the temperature gradually and plotting weight (percentage) against temperature. The temperature in many testing methods routinely reaches 1000°C or greater, but the oven is so greatly insulated that an operator would not be aware of any change in temperature even if standing directly in front of the device. After the data are obtained, curve smoothing and other operations may be done such as to find the exact points of inflection.

5.2.3 Dynamic Mechanical Thermal Analysis

Dynamic Mechanical Thermal analysis determines changes in sample properties resulting from changes in five experimental variables: temperature, time, frequency, force, and strain. The DMTA uses samples that can be in bulk solid, film, fiber, gel, or viscous liquid form. Interchangeable fixtures are employed to allow for the measuring of different properties, including and perform: modulus, stress relaxation, glass transitions, and softening points, etc..

Regarding DMTA tests, viscoelastic materials typically exist in two distinct states. They exhibit the properties of a glass (high modulus) at low temperatures and those of a rubber (low modulus) at higher temperatures (eventually, they also may flow if theirs melting point is exceeded). By scanning the temperature during a DMTA experiment this change of state, the glass transition or alpha relaxation, can be observed. In these tests, the storage modulus *E*' (elastic response) and loss modulus *E*'' (viscous response) of polymers are measured as a function of temperature or time as the polymer is deformed under an oscillatory load (stress) at a controlled (isothermal or programmed) temperature in a specified atmosphere.

Under an oscillating force, $F(\omega) = F_0 \sin(2\pi\omega t)$ where F_0 is the amplitude of the force, ω is the frequency and *t* is the time in the inverse units of F_0, gives rise to a dynamic stress, $\sigma^*(\omega) = F(\omega)/A = \sigma_0 \sin(2\pi\omega t)$, where A is the sample's cross sectional area. The resulting strain, $\varepsilon^* = L(\omega)/L_0$, for a viscoelastic material will display an in-phase component and an out of phase component, $\varepsilon^* = \varepsilon' \sin(2\pi\omega t) + \varepsilon'' \cos(2\pi\omega t)$. More typically, the strain is the independent parameter, $\varepsilon^* = \varepsilon_0 \sin(2\pi\omega t)$ and the stress is a complex response, since the material response is often a function of the maximum strain, ε_0. The complex modulus can be calculed as, $|E^*|^2 = |E'|^2 + |E''|^2$, the loss tangent as, $E''/E' = \tan(\delta)$.

Moreover, DMTA is capable of detecting glass transitions when, due to the breadth of the transition or the small change in heat capacity, it is not possible to detect such transitions by DSC (Cuq et al., 1997). Thus, during measurement of the moduli (E', E") and tan δ of a polymer at a chosen oscillatory frequency over a sufficiently wide range of temperature, the effect of the polymer's glass transition can be clearly observed. The glass transition is detected as a sudden and considerable (several decades) change in the elastic modulus and an attendant peak in the tan δ curve. The temperature, T_g , at which this peak appears, is known

as mechanical glass transition temperature, and its value depends on the selected oscillatory frequency.

DMTA was used to study the thermoplastic properties of fish myofibrillar proteins. Significant changes in storage modulus (E´), loss modulus (E´´) and tan δ were observed between 215 and 250ºC and were associated with the glass transition of the dry protein. Similar T_g values have been reported for collagen (200ºC, measured by DSC) and gelatin (210ºC, measured by DSC), while lower T_g values characterize corn zein (139ºC, measured by DMTA), casein (144ºC, measured by DMTA), and wheat gluten (160 to 162ºC, measured by DMTA). The differences in T_g values can be attributed to structure, molecular weight and organization, and intermolecular interactions in the different proteins (Cuq et al., 1997).

5.3 Water absorption behaviour

The water absorption property of a material is very important in food packaging and controlled release applications. Permeability depends basically on the hydrophilicity, the microstructure and the motion of the protein chains of the material. For instance, hydrophilic material will repel non-polar molecules and vice versa. Starch materials are rather hydrophilic, whereas protein materials are neither hydrophilic nor hydrophobic. Proteins provide a moderate resistance towards both polar and non-polar substances. To modify hydrophobicity and thereby water resistance, different plasticizers and modified agent have been used (Gillgren and Stading; 2008)

According to Torres (1994), the microstructure of a material influences its permeability; so that cavities inside the material may increase the absorption. Ghanbarzadeh et al., (2007) found that unplasticized zein material had both a structure with a higher concentration of cavities and voids and higher water vapor permeability (WVP) than plasticized films. In fact, any molecule can more easily push its way through a material with high chain segment mobility than through a more static one. Again, plasticization involves a compromise between flexibility and high barrier properties. The moisture content of a plastic is intimately related to such properties as electrical insulation resistance, dielectric losses, mechanical strength, appearance, and dimensions.

The effect upon these properties of a change in moisture content due to water absorption depends largely on the type of exposure (by immersion in water or by exposure to high humidity), shape of the part, and inherent properties of the plastic. With non-

homogeneous materials, such as laminated forms, the rate of water absorption may be widely different through each edge and surface. Even for other homogeneous materials, it may be slightly greater through cut edges than through molded surfaces. Consequently, attempts to correlate water absorption with the surface area must generally be limited to closely related materials and to similarly shaped specimens. For materials of widely varying density, relation between water-absorption values on a volume as well as a weight basis may need to be considered.

III. MATERIALS AND METHODS

1. Materials

1.1 Proteins

Three different protein sources have been used in this research: wheat gluten, rice and potato proteins.

a. Wheat gluten was provided by Riba S.A. (Spain). Gluten protein isolate (WG) composition was 83 wt.%, lipids 1.5–2 wt.%, starch 10 wt.% and ashes 0.7–0.8 wt.%. Its moisture content was 8.0 wt.% on dry basis. Gliadin crude from wheat gluten was provided by Sigma-Aldrich S.A. (Spain)

b. Rice protein was provided by Ferrer Alimentación S.A. (Spain). The content of rice protein isolate (R) was 79 wt.%, lipids 5.0 wt.%, carbohydrates 16 wt.% and ashes 2.0 wt.%. Its moisture content was 12 wt.% on dry basis.

c. Potato protein was provided by Ferrer Alimentación S.A. (Spain). Potato protein isolate (P) is composed of 82 wt.%, lipids 1.0 wt.%, and ashes 0.5 wt.%. Its moisture content was 10 wt.% on dry basis.

1.2 Plasticizers

Two different plasticizers were used in this research: glycerol (G) and polyethyleneglycol (PEG) with different molecular weight.

a. Glycerol was the main plasticizer used to preparation of different bioplastics. It was provided by Prolabo S.A. (Spain).

b. Polyethyleneglycol of different molecular weight (200, 600, 4000 and 8000 g/mol) were used to investigate the effect of plasticizers on gluten based bioplastics. It was provided by Panreac S.A (Spain).

1.3 Active and antimicrobial agents

a. Potasium Chloride was used as active agent embedded in the biopolymer matrix. It was provided by Panreac Química, S.A. (Spain).
b. Essential oils and their active agents were provided by Sigma- Aldrich (U.S.A) and Destilerías Muñoz Gálvez, S.A. (Murcia, Spain). Some properties of antimicrobials used in this study are shown in Table 1.1. Essential oils and their active agents assessed in this study were selected for their antimicrobial properties previously reported for pharmaceutical, food and packaging applications (Coma, 2008; Cava et al., 2007; López et al., 2007; Rojas-Graü et al., 2007; Cutter, 2006; Seydim and Sarikus, 2006; Burt, 2004; Devlieghere et al., 2004; Lopez-Rubio et al., 2004; Friedman et al., 2004, Burt and Reinders, 2003; Quintavalla and Vincini, 2002; Hao et al., 1998; Lis-Balchin et al., 1997; Nelson, 1997).

Table 1.1 Properties of essential oil and their antimicrobial (or active) agents.

Biocide	**Antimicrobial agent**	**Boiling point (ºC)**	**Melting point (ºC)**	**Density (g/cm^3)**
Cinnamon oil	Eugenol/cinamaldehyde	249	-	1.025
Oregano oil	Carvacrol, thymol	-	-	0.920
Red thyme oil	Thymol	190		0.916
White thyme oil	Thymol	-	-	0.917
Clove oil	Eugenol	-	-	10.462
Rosemary oil	Pinene, cineol, alcanfor	176	-	0.908
Peppermint oil	Mentol	206	-	0.900
Bergamot oil	Citral, limonene, linalool	-	-	0.877
Orange oil	Citral, limonene, linalool	177	-	0.843
Lemongrass oil	Citral, limonene, linalool	-	-	0.894
Lemon oil	Citral, limonene, linalool	177	-	0.852
Carvacrol (98%)		243		0.910
Cinamaldehyde (≥ 99%)		248	-	1.049

Biocide	Antimicrobial agent	Boiling point (ºC)	Melting point (ºC)	Density (g/cm^3)
Eugenol (Natural≥ 98%)		-	12	1.064
Limonene (97%)		176	-	0.843
Linalool (97%)		196	-	0.861
Citral (95%)		220	-	0.888
Thymol (≥ 99%)		-	49	0.965

1.4 Modifying agents

The modifying agents used in this research were formic acid, octanoic acid, candelilla wax and citric acid. They were of analytical grade and obtained from Panreac Química, S.A., (Spain).

2. Formulation of bioplastics

The effect of different proteins and glycerol content on the final properties of the bioplastics is reported in chapter VI.1 of Results and Discussion. The formulations studied there are shown in Table 2.1.

Table 2.1 Formulation of protein based bioplastics studied in Chapter VI.1.

Sample number	Sample name	Type of protein	Protein (wt.%)	Glycerol (wt.%)
1	WG/G	Wheat Gluten	67	33
2	WG/G	Wheat Gluten	60	40
3	R/G	Rice	67	33
4	R/G	Rice	57	43
5	P/G	Potato	67	33
6	P/G	Potato	57	43

In Chapter VI.2, the effect of formulation and mixing process at high temperature is assessed. In addition, a specific formulation wheat gluten/potato based bioplastics (1:1) was mixed at 80°C and then it was extruded with different temperature profiles. The plasticizer

used is glycerol (G) in at fixed 40 wt.%. The protein concentration is fixed at 60 wt.%. The formulations studied there are shown in Table 2.2.

Table 2.2 Formulation of protein based bioplastics studied in Chapter VI.2.

Sample number	Sample name	Type of protein	Protein Ratio (wt/wt)
1	WG/R/G	Wheat gluten/Rice	3:1
2	WG/R/G	Wheat gluten/Rice	1:1
3	WG/R/G	Wheat gluten/Rice	1:3
4	WG/P/G	Wheat gluten/Potato	3:1
5	WG/P/G	Wheat gluten/Potato	2:1
6	WG/P/G	Wheat gluten/Potato	2:1
7	WG/P/G	Wheat gluten/Potato	1:1

In Chapter VI.3 the effect of plasticizers on the rheological properties, water absorption and controlled release behavior is studied. The protein used is wheat gluten (WG) in at fixed 67 wt. %. The formulations for such gluten based bioplastics are shown in Table 2.3.

Table 2.3 Formulations of gluten based bioplastics of controlled release studied in Chapter VI.3.

Sample number	Sample name	Glycerol (wt.%)	Water (wt.%)	PEG 200 (wt.%)	PEG 600 (wt.%)	PEG 4000 (wt.%)	PEG 8000 (wt.%)	Active agent (3.5 wt. %)	Modifying agent (3 wt. %)
1	WG/Wt	-	33	-	-	-	-	-	-
2	WG/G/Wt	20.0	13	-	-	-	-	-	-
3	WG/G/Wt/KCl	16.5	13	-	-	-	-	KCl	-
4	WG/G/Wt/KCl/Citric	16.5	10	-	-	-	-	KCl	Citric acid
5	WG/PEG200/Wt/KCl	-	13	16.5	-	-	-	KCl	-
6	WG/PEG600/Wt/KCl	-	13	-	16.5	-	-	KCl	-
7	WG/PEG4000/Wt/KCl	-	13	-	-	16.5	-	KCl	-
8	WG/PEG8000/Wt/KCl	-	13	-	-	-	16.5	KCl	-
9	WG/PEG4000/Wt/KCl/Citric	-	10	-	-	16.5	-	KCl	Citric acid

Sample number	Sample name	Glycerol (wt.%)	Water (wt.%)	PEG 200 (wt.%)	PEG 600 (wt.%)	PEG 4000 (wt.%)	PEG 8000 (wt.%)	Active agent (3.5 wt. %)	Modifying agent (3 wt. %)
10	WG/PEG4000/Wt /KCl/ Formic	-	10	-	-	16.5	-	KCl	Formic acid
12	WG/PEG4000/Wt /KCl/ Octanoic	-	10	-	-	16.5	-	KCl	Octanoic acid
13	WG/PEG4000/Wt /KCl/Wax	-	10	-	-	16.5	-	KCl	Wax

The aim of the Chapter VI.4 was design a new protein based bioplastic with antimicrobial activity for potential application in food packaging. Thus, in the first part of this chapter 18 different antimicrobial agents (essential oils and active agents gathered in Table 1.1) were incorporated in wheat gluten based bioplastics and determine their inhibitory effect against selected food pathogens. In the second part, four specific antimicrobial agent were selected to studied the effect of the concentration into wheat gluten based bioplastics. Different protein formulations in combination with four specific antimicrobial agent were studied in the third section. The formulations for such bioactive gluten based bioplastics are shown in Table 2.4.

Table 2.4 Formulations of bioactive gluten based bioplastics studied in Chapter VI.4.

Sample number	Type of Protein	Protein (wt.%)	Glycerol (wt.%)	Antimicrobial agent	Active agent (wt. %)
1	Wheat Gluten	67	23	Red thyme	10
2	Wheat Gluten	67	23	Cinnamon	10
3	Wheat Gluten	67	23	Clove	10
4	Wheat Gluten	67	23	Peppermint	10
5	Wheat Gluten	67	23	Bergamot	10
6	Wheat Gluten	67	23	Rosemary	10
7	Wheat Gluten	67	23	White thyme	10
8	Wheat Gluten	67	23	Lemon	10
9	Wheat Gluten	67	23	Carvacrol	10
10	Wheat Gluten	67	23	Cinnamaldehyde	10
11	Wheat Gluten	67	23	Oregano	10
12	Wheat Gluten	60	30	Orange	10
13	Wheat Gluten	60	30	Lemongrass	10
14	Wheat Gluten	60	30	Citral	10

Sample number	Type of Protein	Protein (wt.%)	Glycerol (wt.%)	Antimicrobial agent	Active agent (wt. %)
15	Wheat Gluten	60	30	Limonene	10
16	Wheat Gluten	60	30	Linalool	10
17	Wheat Gluten	60	30	Thymol	10
18	Wheat Gluten	60	30	Eugenol	10
19	Wheat Gluten	67	28	Cinnamon	5
20	Wheat Gluten	67	32	Cinnamon	1
21	Wheat Gluten	67	28	Cinnamaldehyde	5
22	Wheat Gluten	67	32	Cinnamaldehyde	1
23	Wheat Gluten	67	28	Clove	5
24	Wheat Gluten	67	32	Clove	1
25	Wheat Gluten	67	28	White thyme	5
26	Wheat Gluten	67	32	White thyme	1
27	WheatGluten/Rice protein 1:1	60	30	Cinnamaldehyde	10
28	WheatGluten/Rice protein 1:1	60	30	Clove	10
29	WheatGluten/Rice protein 1:1	60	30	Cinnamon	10
30	WheatGluten/Rice protein 1:1	60	30	Thymol	10
31	WheatGluten/Potato protein 1:1	60	30	Cinnamaldehyde	10
32	WheatGluten/Potato protein 1:1	60	30	Cinnamon	10
33	Potato / Egg white protein (EW) 1:1	60	30	Cinnamaldehyde	10
34	Potato/Egg white protein (EW) 1:1	60	30	Cinnamom	10
35	WheatGluten/Potato protein 1:1	60	30	Thymol	10
36	WheatGluten/Potato protein 1:1	60	35	Thymol	5
37	WheatGluten/Potato protein 1:1	60	39	Thymol	1

3. Processing of protein based bioplastics

3.1 Mixing process

The bioplastic compounds were mixed in a torque-rheometer (Polylab, Haake, Germany) as that shown in Figure 3.1. It enables the batch mixing of many highly viscous substances and consists of a kneading tool fitted with two counter-rotating rollers, turning with different angular velocities (ratio 3:2).

Figure 3.1 Rheocord torque rheometer (Polylab, Haake, Germany).

Protein powder, plasticizers, active agents and modifying agents were directly fed to the mixing chamber before starting the mixing tests. Both torque and temperature were continuously recorded during the mixing process. The mixing process was always carried out at 50 r.p.m. (Jerez at al., 2005a).

Figure 3.2 Rheomix600p (Polylab, Haake, Germany).

The blends were manufactured in two types of batch mixers: Rheomix 600p and 3000p. Rheomix600p (Figure 3.2) was used when the blend was mixed at room temperature. This mixing chamber can be considered adiabatic, i.e. it was not cooled or heated. Its volume (69 cm^3) was filled with approximately 56 g of sample, corresponding to 85% filling ratio. On the other hand, Rheomix3000p (Figure 2.3) can be electrically heated to obtain a constant mixing temperature, i.e. processing conditions can be considered nearly isothermals. The mixing chamber volume (310 cm^3) was filled with approximately 256 g of sample. The

temperature of the mixing chamber was regulated at 80ºC. This temperature was below the temperature at which the protein may undergo thermal denaturation.

Figure 3.3 Rheomix3000p (Polylab, Haake, Germany).

3.2 Thermomoulding process

Compression-moulded biomaterials were prepared by compressing the blend obtained after the mixing process at 100 bar gauge pressure for 10 min, obtaining 50x10x3 mm^3 specimens (Jerez et al., 2005b) or disks of 25 mm diameter and 1.5 mm gap. The press used to carry out this process was developed in our laboratory and consisted of two electrical heated plates, with electronic temperature control, and a hydraulic pressure system (Figure 3.4). The compression-moulding process was carried out at three different temperatures 90, 120, and 140 ºC for wheat gluten based bioplastics and wheat gluten/rice and potato protein blends. And at 90, 100, 120, 140, 160 and 180ºC, for potato and rice based bioplastics. Theses temperatures were above the highest temperature reached during the mixing process.

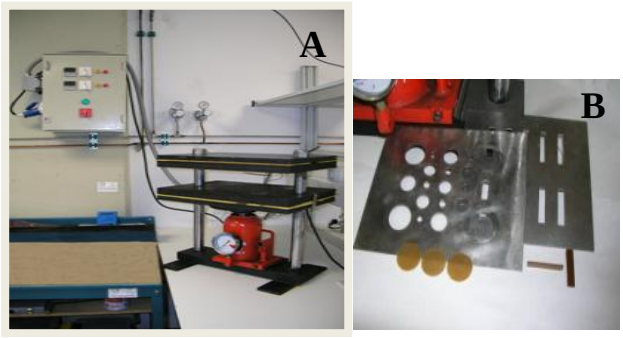

Figure 3.4 Hot-plate hydraulic press for compression-moulding (A) and moulds (B).

3.3 Extrusion

Gluten and potato proteins (ratio 1:1) were pre-mixed with the plasticizer selecting a plasticizer/protein ratio of 0.6 in the torque rheometer at 80ºC (see mixing process above). The blend obtained after the mixing process was transferred to the extruder Rheomex CTW100p (Haake, Germany) (Figure 3.5), which is a conical co-rotating twin screw extruder with a barrel diameter of 25 mm. The extruder barrel consisted of three temperature zones 380 mm long, each zone was equipped with an independent temperature control based on resistive heater. Extruder set-up was equipped with an electrically heated ribbon-shaped die at the exit. This die has pressure and temperature sensors and provides ribbons with dimensions of 50x1 mm^2.

*Figure 3.5 Rheomex CTW100p – ribbon Die (*Polylab, Haake, Germany).

Table 3.1. Extrusion parameters.

Item	Sample name	Temperature profile (°C)	Screw speed (r.p.m)
1	P1	80, 100, 120, 140	30
2	P2	100, 120, 140 ,160	30
3	P3	100, 120, 140, 150	30
4	P1	80, 100, 120, 140	50
5	P2	100, 120, 140 ,160	50
6	P3	100, 120, 140, 150	50
7	P2	100, 120, 140 ,160	70

The temperature zones for blending of gluten/potato and glycerol were maintained at three temperature profiles and the extruder was operated at three screw speeds as shown in Table 3.1. In all cases, the first three temperatures are related to the barrels and the last one is the temperature at the die. The mixing torque and pressure curve were recorded during this process. The extrudate was later struck with a pneumatic die-cutter (ATS Faar, S.p.A, Italy) into rectangular 1-mm-thick specimens.

4. Rheological measurements

4.1 Viscoelastic behaviour

Dynamic rheological properties of the blends were determined using a controlled strain rheometer ARES (Rheometrics Sci., Piscataway, USA), as shown in Figure 4.1, using a serrated parallel-plate geometry (25 mm diameter). In all cases the gap between plates was 1.0-1.4 mm. The blend was placed between plates and the test was started after the blend had rested for 10 min. All tests were performed at least twice.

Temperature sweep test, from 25 to 170°C, were conducted at constant angular frequency (6.28 rad/s) and strain (0.1%) at a heating rate of 2°C/min. Mechanical spectra were recorded from 100 to 0.05 rad/s in oscillatory shear, at constant temperatures of 25, 50, 75, 90 and 120ºC. Strain sweep tests at 6.28 rad/s were carried out in order to obtain the linear viscoelastic region of the material.

Figure 4.1 The ARES rheometer (Rheometrics Sci., Piscataway, USA).

4.2 Viscosity

The viscosity of the different blends was measured immediately after mixing in a capillary rheometer (Rheocap S20, Thermo-Haake, Germany) as shown in Figure 4.2. Viscous flow measurements of plasticized gluten blends were performed at three different wall temperatures (60, 90, and 120ºC). Viscous flow tests for WG/G/Wt, WG/G/Wt/KCl, and WG/G/Wt/KCl/Citric were carried out at 60ºC. In addition, the wheat gluten/rice and potato protein blends at a ratio of 1:1 viscous flow measurements were performed at 90ºC.

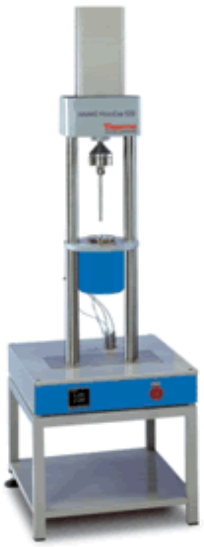

Figure 4.2 Capillary rheometer (Rheocap S20, Thermo-Haake, Germany).

Apparent shear rates ranged from 10 to 1000s^{-1}. A capillary die (1 mm radius) and tubes with L/D=20 and L/D= 30 ratio were used. For each condition, pressure drop against time was monitored. The apparent wall shear stress was corrected for entrance and exit pressure losses, using Bagley's and Weissenberg–Rabinowitch correction to obtain the true wall shear stress.

4.3 Thermomechanical properties

Dynamic Mechanical Thermal Analysis (DMTA) experiments were carried out using a Seiko DMS 6100 (Seiko Instruments, Japan), as shown in Figure 4.3. The specimen had rectangular shape of 50x10x3 mm^3. A double cantilever bending test was performed according to the ASTM standard method D5023–01 (ASTM, 2001a) with a temperature ramp from 30 to 170ºC at a heating rate of 2ºC/min. All experiments were conducted at constant

frequency (1 Hz) and strain within the linear viscoelastic region. During analysis, the storage modulus (E´), the loss modulus (E") and loss tangent, tan (δ), were recorded and plotted versus temperature. Each sample was analyzed at least twice.

Figure 4.3 DMS 6100 (Seiko Instruments, Japan).

5. Thermal, molecular and microstructural characterization

5.1 Differential scan analysis

DSC analysis was performed on plasticized protein samples, in order to determine the compatibility between protein, plasticizers and modifying agent, and to observe changes in their thermal denaturation and glass transition temperatures.

Figure 5.1 DSC analyser Q100 (TA Instruments, USA).

DSC experiments were performed with a Q100 (TA Instruments, USA), using 10 to 20 mg samples, in hermetic aluminum pans, at a heating rate of 5ºC/min. The sample was purged with a nitrogen flow of 50 ml/min. The calorimeter is shown in Figure 5.1.

5.2 Thermogravimetric analysis

The volatility of antimicrobial agents was studied by termogravimetric analysis, using a Q50 (TA Instruments, USA) as shown in Figure 5.2. The measurement was carried out at a heating rate of 10ºC/min.

A thermo-gravimetric study, recording weight loss vs. Temperature curves (TG) and calculating time derivative of the weight loss (DTG) curves, was also performed on raw materials (wheat gluten, gliadin and glycerol) and wheat gluten based bioplastics containing 33 and 40 wt.% glycerol. Pyrolysis and combustion tests, between 40ºC and 600ºC, were carried out on 5-10 mg samples under nitrogen and air atmosphere, respectively. Three heating temperature ramps (5, 10 and 20ºC/min) were selected.

Figure 5.2 TGA Q50 (TA Instruments, USA).

In addition, bioplastic moisture concentration was gravimetrically determined by heating samples of bioplastics in a ventilated oven at 110ºC for 24h. For both wheat gluten based bioplastics containing 33 and 40 wt.% glycerol, the calculated moisture content was 10 wt. %. Once moisture presence was confirmed, for sake of comparison, a new material (dry-WG/G containing 33 wt.%) was obtained by dehydrating bioplastic wheat gluten based bioplastics containing 33 wt.% in desiccators at room temperature.

5.3 Sodium dodecyl sulphate-polyacrylamide gel electrophoresis (SDS PAGE)

Characterization of the molecular properties of P/G, R/G, WG/P/G and WG/R/G was performed by sodium dodecyl sulphate-polyacrylamide gel electrophoresis (SDS PAGE) under reducing conditions as described by Da Silva and Taylor (2004), but using a 4-12% acrylamide gradient gel prepared as described by Byaryhanga et al., (2005). The reducing agent used was 2-Mercaptoethanol, which further denatures the proteins by reducing disulfide linkages, thus overcoming some forms of tertiary protein folding, and breaking up quaternary protein structure (oligomeric subunits).

6. Water absorption test

Water absorption measurements were based on ASTM standard method D570-81 (ASTM, 2001). A bioplastic sample was dried in an oven, at 50ºC, for 24 h, and cooled in a desiccator before weighting. Fifty milligrams of every sample were submerged in 50 ml distilled water for a constant period of time (24h). Water on the surface of the samples was removed, and the samples were weighted again. In order to check the weight of water-soluble residuals, samples with water were dried at 90ºC, for 24 h, and then weighted. The water absorption (Ab) was calculated as follows:

$$Ab = \frac{\left(W_1 - W_0 + W_{sol}\right)}{W_0} x100 \qquad [2.1]$$

where W_1, W_0 and W_{Sol} are the weights of the specimen containing water, the dried specimen, and water-soluble residuals, respectively.

7. Controlled release tests

The dynamic tests for the determination of the active components releasing rate, from a bioplastic sample, were carried out with a conductimeter (Inolab cond level 1, Germany). Each test was performed at least 2 days. A fixed amount of the bioplastic was placed in a container with 50 ml of a solution of sodium azide (0.0776 M). The releasing rate was evaluated as the amount (wt. %) of KCl released after an elapsed time with reference to the initial concentration of this component.

8. Microbiological analysis of protein based bioplastics with antimicrobial agents

The antimicrobial activity of the bioactive agents and the bioactive materials was performed in Petri dishes, where the appropriate solidified agar culture medium was inoculated with a solution of one of the microorganisms studied: *Aspergillus niger* (fungus-mold), *Candida kefir (fungus-yeast), Bacillus cereus (a gram-positive bacteria) and Escherichia coli* (*a gram-negative bacteria).* Portions of bioplastic were placed either on the agar substrate or under the lid (inside) of the petri dish, so that the microbial inhibition was assessed in contact with the culture medium (by biocide release and diffusion) and developing an antimicrobial atmosphere (by biocide release and evaporation). Then, the plates were incubated at 37ºC for 24h in the appropriate incubation chamber. The inhibition of each tested microorganism by each of the tested materials was calculated by measuring the inhibition zone. The minimum inhibitory concentration, MIC, marks the concentration above which no growth is observed by comparison with the control. The method is quantitative if the diameter of the clear zones around the biocides and bioplastics are measured. The area of the whole zone was then calculated subtracted from the piece to the area no colonized around the piece of bioplastic, this difference in area was reported as the zone of inhibition. These tests were in charge of external laboratories of microbiology.

IV. RESULTS AND DISCUSSION

1. Rheological behaviour, physical properties and microstructure of protein-based bioplastics

Bioplastics deriving from plant proteins are becoming an increasingly popular source of raw material for plastic products since they are not only biodegradable but they are also made from renewable resources such as polysaccharides, lipids and proteins (Song and Zheng, 2008; Wirsenius et al., 2004; Irissin-Mangata et al., 2001). However, in order to be suitable for many applications, such as packaging, these bioplastics require improved mechanical and water absorption properties. Wheat gluten is a good example of a protein which has been investigated for its thermoplastic properties. However, this protein is also highly hygroscopic, which renders it inappropriate for this type of application. For this reason, the first part of this chapter considers potato and rice proteins as a new source for the production of bioplastics. To this end, the processing of these proteins with glycerol as plasticizer is compared with wheat gluten based bioplastics. In addition, the effect of glycerol concentration on both rice and potato protein based bioplastics is studied. The resulting bioplastic is characterized in terms of thermo-mechanic properties, flow (viscosity), thermal behaviour (Differential Scan Calorimetry DSC), water absorption and molecular properties. The formulations for such protein based bioplastics are shown in Table 2.1 in Materials and Methods.

The second part of this chapter details how experimental thermogravimetric curves, obtained in a nitrogen atmosphere, were modelled through autocatalytic kinetic equations (based on the Prout-Tompkins model) and so-called pseudo-components. A pseudo-component is a fraction that thermally degrades as a unity but is nevertheless not a pure substance. In addition, the material composition and the role of the plasticizer were analysed by comparing the degradation profiles of the gluten protein, plasticizer and different gluten-based bioplastics.

1.1 Thermoplastic processing of protein-based bioplastics

The manufacture of bioplastics requires a suitable mixing of all the components during the thermoplastic processing in order to obtain a blend with desirable characteristics. This means that the development of torque and temperature are important parameters for describing and characterizing the resultant blend according to the formulation studied.

Wheat gluten based bioplastics

Figure 1.1.1 shows the evolution of torque and temperature during the mixing process at 50 r.p.m., for wheat gluten based bioplastic with two plasticizer concentrations (33 and 40 wt.%). Both blends show a torque evolution with three distinct regions. In the first region, also known as the induction region, there is no significant increase in torque, and the duration of the induction region increases with increased glycerol concentration. In the second region, the torque undergoes an exponential increase with mixing time up to a maximum value. Finally, in the last region, an apparent torque decay is observed (Jerez et al., 2005a). Table 1.1.1 shows that the maximum value of the torque (the torque overshoot) is reached after 62 min mixing for the sample with 40 wt.% glycerol and 22 min for the sample with 33 wt.% glycerol, showing lower values for torque and time with lower glycerol content, which also gave rise to an increase in the slope of this region.

Plasticizer concentration also affects the Specific Mechanical Energy (SME) required to obtain a material with suitable mechanical properties. Hence, Table 1.1.1 also shows the SME values for the bioplastic samples studied, which were calculated as follows (Redl et al., 1999 a,b):

$$SME = \frac{\Omega}{m} \int_0^{tmix} M(t)\partial(t) \qquad [1.1.1]$$

where Ω (in rad/s) is the mixing speed, m (in g) the sample mass, M(t) (in N·m) the torque, and t_{mix} (in s) the mixing time.

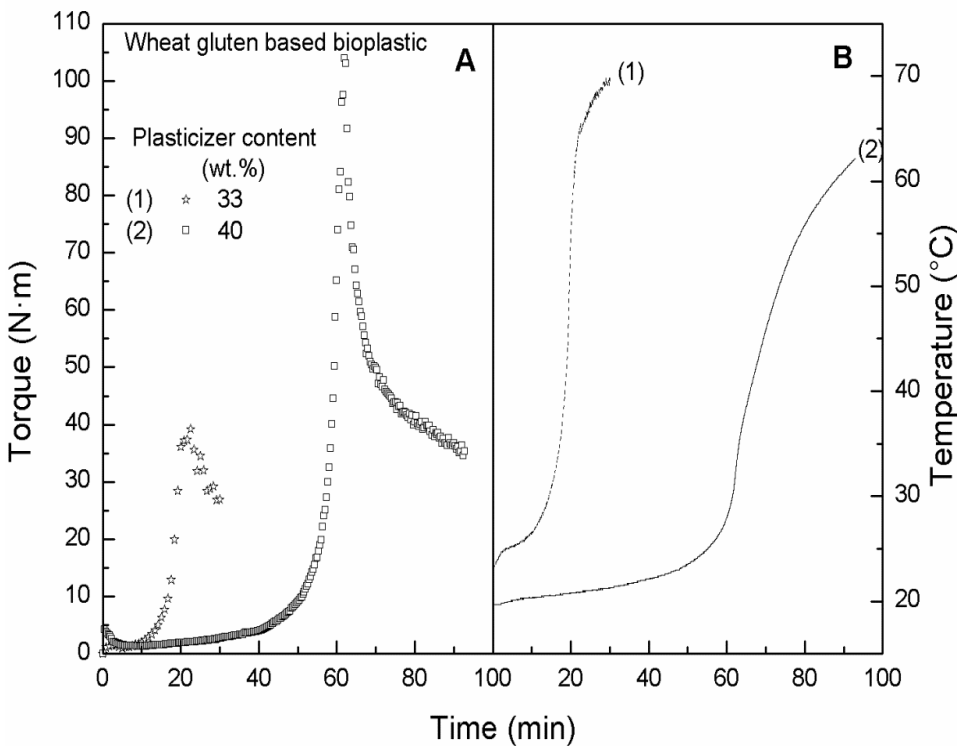

Figure 1.1.1 Torque (A) and temperature (B)profiles recorded during the mixing process for wheat gluten-based bioplastic.

As mentioned above in respect of mixing time, the occurrence of a torque overshoot suggests a dramatic alteration in the gluten structure upon mixing. The final torque decay is associated with a change in consistency from a powder/plasticizer dispersion to a cohesive and elastic material (Redl et al., 1999b). Thus, the time needed to reach a balanced torque depends on the ability of the constituents to interact and, therefore, also on the selected plasticizer (Pommet et al., 2003). Consequently, for the sake of comparison, t_{mix} was always taken as 1.5 t_{peak}.

Table 1.1.1. Specific Mechanical Energy (SME), elapsed time at the overshoot (t_{peak}), and maximum temperature (T_{max}) reached during the mixing process.

Sample name	Glycerol (wt.%)	t_{peak} (min)	T_{max} (ºC)	SME (kJ/kg)
WG/G	33	21.9	74.6	2647
WG/G	40	62.0	62.0	11018

Figure 1.1.1B shows the evolution of temperature during the mixing process for the different systems studied. The temperature curves for wheat gluten based bioplastic with two plasticizer concentrations (33 and 40 wt.%) show an induction period, characterised by a slight increase in temperature. After this region, the temperature undergoes an exponential

increase, and this slope decreases with glycerol content. Consequently, the temperature reached at the peak of torque becomes lower as plasticizer content increases. Furthermore, the final observed torque decay coincides with a slight increase in temperature. Some authors have suggested that the molecular network of the plasticized gluten undergoes an exothermic dissociation and unfolding of macromolecules, which recombine and crosslink through specific linkages (Jerez. et al., 2007; Redl et al., 2003; Redl et al., 1999b; Mitchell et al., 1994).

The viscosities of the samples were measured in order to better understand and predict how the blends will flow under extrusion and other thermomechanical treatments. Figure 1.1.2 presents the viscous flow curves at 90ºC for wheat gluten based bioplastic with two plasticizer concentrations (33 and 40 wt.%), collected just after the mixing process (without any further thermomechanical treatments). These formulations were compared with a commercial synthetic polymer (low density polyethylene, LDPE). As expected, an increase in glycerol content leads to an overall decrease in sample viscosity. The power-law model fits the shear-thinning behaviour observed very well:

$$\eta = \kappa \cdot \dot{\gamma}^{n-1} \qquad [1.1.2]$$

where *k* is the consistency index, and *n* is the flow index. Table 1.1.2 presents the values of these parameters at 90ºC for wheat gluten blends with different glycerol concentration. As can be observed, a remarkable increase in the consistency index is found as glycerol content is decreased. The plasticizer increased the protein mobility which led to a decrease in the viscosity. However, an increase in the flow index is noticed as glycerol content is higher. According to Gontard et al., (1993) glycerol is a relatively small hydrophilic molecule and could easily be inserted between protein chains to form hydrogen bonds with the amide groups of the gluten proteins. Therefore, the plasticizer reduces the intermolecular forces and increases the mobility of polymeric chains, thereby improving the flexibility and the extensibility of the film (Gontard et al., 1993; Irissin-Mangata et al., 2001). This result is interesting and allows the consideration of thermoplastic formation processes such as extrusion for wheat gluten based materials, which would avoid blushing and thermal degradation (Irissin-Mangata et al., 2001; Redl et al., 1999b).

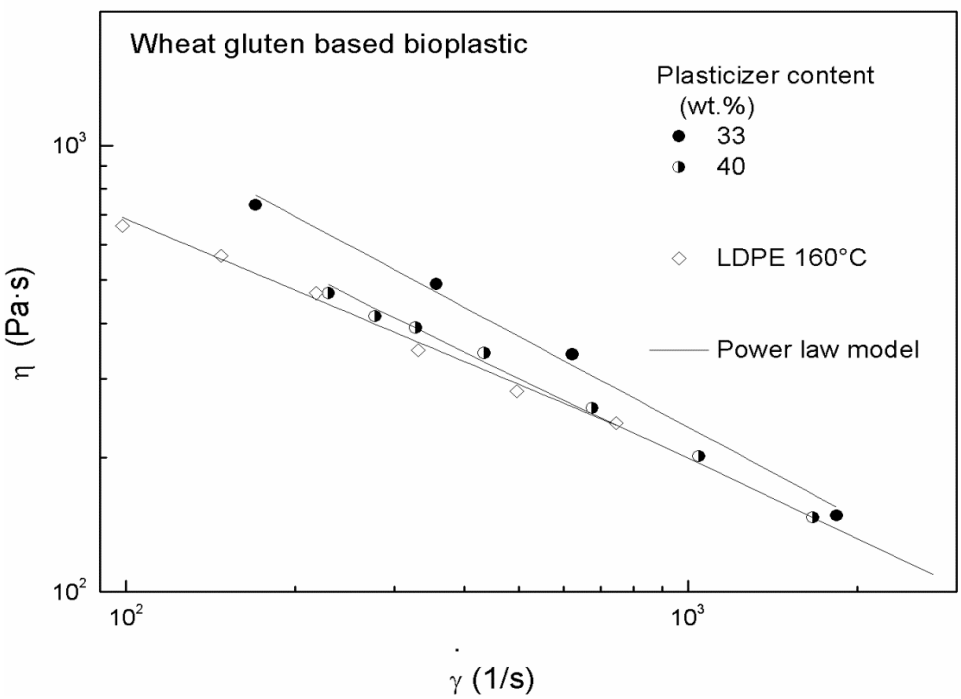

Figure 1.1.2 Viscous flow curves at 90ºC for wheat gluten based bioplastic.

Table 1.1.2. Influence of temperature and composition on the consistency (k) and flow (n) indexes of the different blends studied.

Sample name	**Glycerol (wt.%)**	**Parameters of Power-low model**	
		k (Pa·s^n)	**n**
WG/G	33	20361	0.36
WG/G	40	12557	0.40
LDPE at 160ºC	-	7846	0.47

The viscous behaviour of well-known low density polyethylene (LDPE), processed under typical extrusion conditions at 160ºC, and a shear rate window between 100-300 s^{-1} was compared with both formulation of wheat gluten based bioplastics. This showed that at 90ºC the blend with higher glycerol content exhibited similar viscous behaviour compared to low density polyethylene. However, the blend with lower glycerol content displayed higher viscosity than low density polyethylene. Both bioplastics showed higher values in the consistency index (*k*) and lower values in the flow index (*n*) than LDPE. This fact might open a window for potential industrial applications of these new materials, such as low density polyethylene.

The torque and temperature profiles recorded during the process of mixing the rice protein with different glycerol concentration are shown in Figure 1.1.3. A decrease in torque down to zero was displayed for all rice protein blends, which became even more evident as the glycerol content increased. Moreover, the temperature variation during the mixing process for these samples did not register a continuous increase, as might be expected, rather it remained more or less constant during the mixing process, staying below 19ºC throughout (Figure 1.1.3B). The mixing curves and torque values obtained for the rice protein samples were significantly different to those obtained for wheat gluten blends. Many studies have demonstrated that, although the polymeric protein components undergo a strong interaction with the amino acids in rice, the length of the polymers are shorter than in wheat gluten and as a consequence rice protein blends have lower elasticity than wheat gluten blends (Oszvald et al., 2007; Gujral and Rosell, 2004; Sivaramakrishnan et al., 2004).

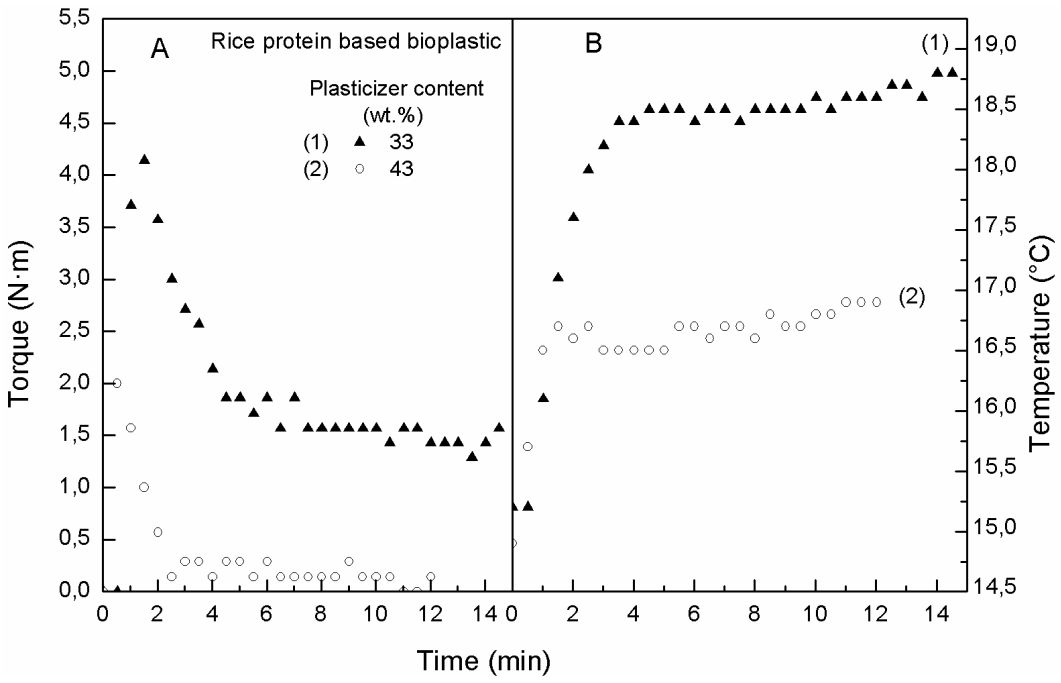

Figure 1.1.3 Evolution of torque (A) and temperature (B) during the mixing process for rice protein-based bioplastic with varying glycerol content.

In contrast, the evolution of torque and temperature during the mixing process for the potato protein blends with varying glycerol content is shown in Figure 1.1.4. This shows that the torque values were slightly higher than for the rice protein blends. However, there was not

a significant increase as compared to the wheat gluten blends. Moreover, these could be compared to the induction region during the mixing of wheat gluten plasticized with glycerol (Figure 1.1.1).

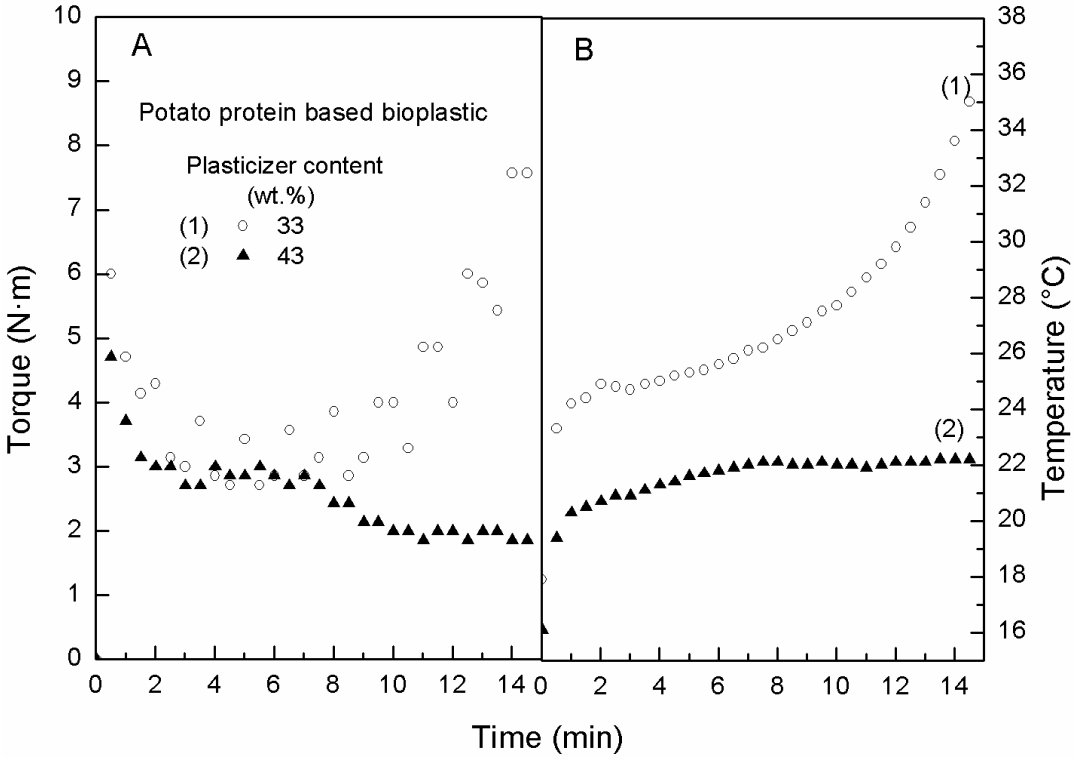

Figure 1.1.4 Evolution of torque (A) and temperature (B) during the mixing process for potato protein based bioplastic with varying glycerol content.

Figure 1.1.4B shows the temperature profile for potato protein blends with varying glycerol content. A constant lower temperature (< 22ºC) obtained during the mixing of blends with 43 wt.% glycerol due to the almost total absence of mechanical energy dissipation. Nevertheless, an increase in temperature of up to 36ºC during the processing of the blend with 33 wt.% glycerol is observed. This temperature can be considered very low when compared with the temperature reached for wheat gluten samples, which might suggest a low thermal dissipation of energy during mixing, probably due to a low interaction between the potato protein and glycerol.

The absence of a torque overshoot for both proteins and a non-exothermic protein reaction, together suggest a low protein structure development during mixing and also poor mixing of the protein and plasticizer. This is probably associated with the low molecular weight of both proteins as compared to, for example, wheat gluten (Oszvald et al., 2008). Hence, it was necessary to apply a post-thermal treatment in order to improve the interaction

between the protein and plasticizer. Also, almost identical behaviour for both protein blends was observed in the temperature variation during the mixing process. This is advantageous as it avoids temperature denaturation or modification of the protein, which in some cases could cause problems. The temperature rose for both proteins during the processing but never exceeded 36ºC, far removed from the denaturation temperature for native rice protein reported to be close to 80ºC (Gorinstein et al., 1996).

Similarly, data relating to thermal denaturation of native potato protein located its unfolding between 55-75ºC, considerably higher than 36ºC (Van Koningsveld, G.A, 2001). Unfortunately, it was impossible to calculate the specific mechanical energy (SME) for either the rice protein blends or the potato protein blends due to their low torque values and the absence of a maximum value for torque; hence, it was not possible to effect a comparison with wheat gluten blends. In addition, the flow behaviour for these blends was not possible to monitor due to the macro phase separation of the plasticizers and protein during the measurements. It may therefore be difficult to extrude those dough-like materials.

1.2 Thermomechanical behaviour of protein based bioplastics

Rice protein based bioplastics

The evolution of the complex modulus and tan δ with temperature as a function of the thermosetting temperature for rice protein based bioplastic with 33 wt.% glycerol is shown in Figure 1.2.1. A decrease in the complex modulus (E*) with temperature is observed. First, E* suffered a change in the slope, which occurs at a range of temperature between 74 and 106°C. After this, samples exhibited different behaviour depending on the thermosetting temperature. In this sense, E* enters a plateau region for samples thermoset below 140°C, and this event tended to appear at higher temperatures as the thermosetting temperature increased. Also, this plateau region was less evident as thermosetting temperature increased, and at the end of the plateau the complex modulus decreased. On the other hand, for samples thermoset at 160 and 180°C, there was no plateau region and instead a continuous decrease in the complex modulus with temperature was observed.

Figure 1.2.1B shows the evolution of tan δ with temperature for rice protein based bioplastic with 33 wt.% glycerol at different thermosetting temperatures. As a result, a maximum in tan δ at a temperature close to 60–75°C was found. Also, a decrease in tan δ

values is observed as thermosetting temperature increased. This maximum in tan δ could be associated with the glass transition of the plasticized protein (Lim et al., 1999). In addition, a minimum in tan δ at a temperature close to 150-160ºC was found.

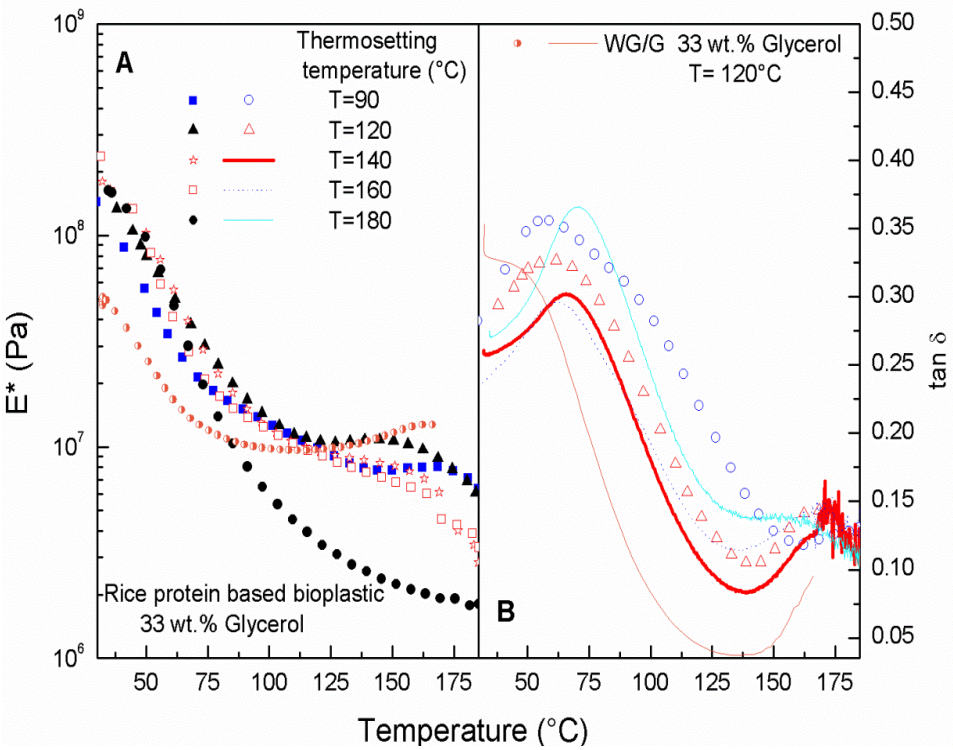

Figure 1.2.1 Dynamic mechanical thermal analysis results, complex modulus (A) and tan δ (B) for rice protein based bioplastic with 33 wt.% glycerol at different thermosetting temperatures.

The influence of rice protein on the development of the bioplastic network structure was compared to the structure development in wheat gluten bioplastic with 33 wt.% glycerol and thermoset at 120°C, as shown in Figure 1.2.1. Wheat gluten plasticized with glycerol (henceforth WG/G) was selected as the benchmark because its viscoelastic properties have been widely studied. According to Jerez et al., 2005, the evolution of the viscoelastic functions for a WG/G sample showed three regions as temperature increased. First, E* decreased to a plateau region (from 20 to 80°C) and a maximum in tan δ around 30°C. Second, a plateau region appeared from 100 to 160°C. Finally, above 160°C, a decrease in the E* was observed and a minimum in tan δ occurs above 125°C. The rice protein samples displayed E* values greater than the benchmarked sample up to the first region (from 20 to 80°C), but beyond 80°C, the reference sample exhibited about the same value at the plateau region. The maximum peak in loss tangent for the rice protein samples was reached at higher temperature (around 50°C) than the reference. Although the minimum in loss tangent was at

about the same temperature as compared with the benchmarked sample, the values in tan δ were significantly higher for rice protein samples than for the WG/G sample.

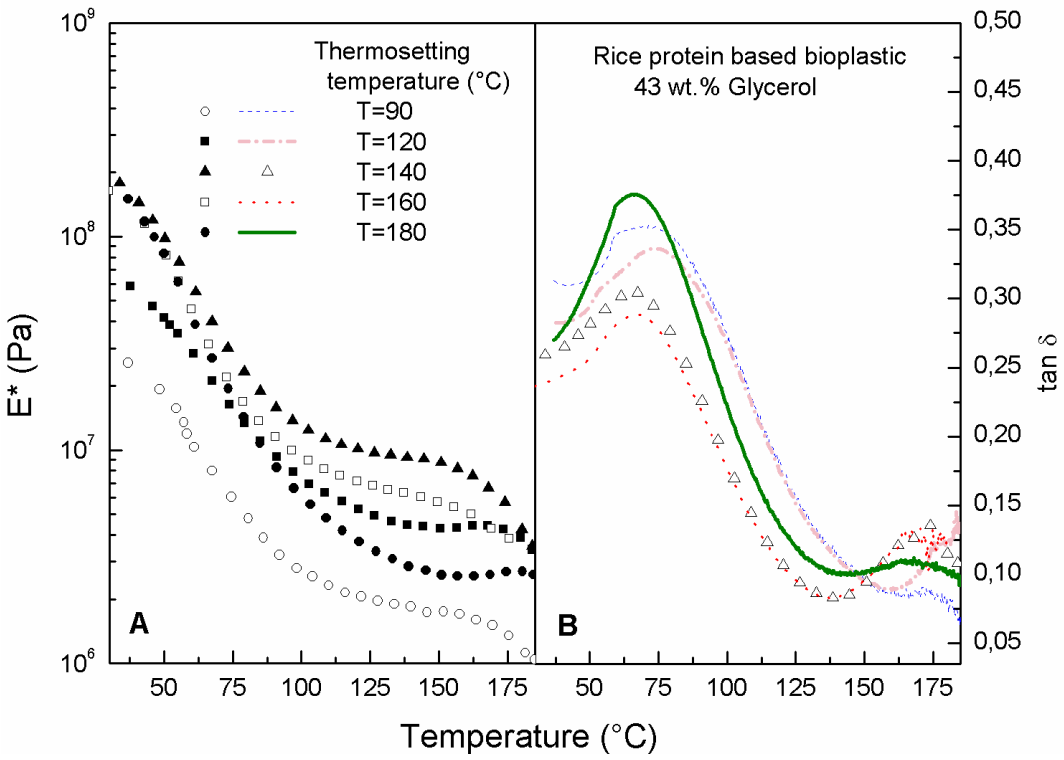

Figure 1.2.2 Dynamic mechanical thermal analysis results for the complex modulus E (A) and tan δ (B) for rice protein based bioplastic with 43 wt.% glycerol at different thermosetting temperatures.*

Figure 1.2.2 shows the changes in complex modulus and loss tangent with temperature for rice protein based bioplastic with 43 wt.% glycerol, submitted to different thermomoulding temperatures. The complex modulus of the rice protein bioplastics decreased with temperature in the same way as rice protein blends with 33 wt.% glycerol, and also exhibited a change in the slope in E*, which occurred at temperatures around 100°C. Moreover, after the change in the slope in the complex modulus, samples thermoset at 120 and 180°C tended to display a plateau region, whereas a gradual decrease in the slope of the complex modulus was observed for the sample thermoset at 160°C. A maximum of loss tangent at lower temperatures appeared as the thermosetting temperature increased. The samples also became more elastic (lower loss tangent) as the thermosetting temperature increased, except for the sample thermoset at 180°C (Figure 1.2.2B). An increase in the complex modulus, between 30 and 75ºC, was observed as the thermosetting temperature increased (from 90 to 140°C). However, an increase in the thermomoulding temperature from 160 to 180°C led to a decrease in E*. This behaviour could suggest an optimum temperature

interval for the rearrangement and alignment of the protein network, in this way helping to improve the protein-plasticizer interaction and giving more flexibility to the material.

Therefore, the viscoelastic properties of rice-based bioplastics were affected by glycerol content and thermomoulding temperature treatment. We identified two groups of behaviour, one group with rice protein samples thermoset at temperature below 140°C and the second with samples thermoset at temperature above 140°C. For samples in the first group, it was observed that an increase in glycerol concentration led to a decrease in E* and glass transition temperature, although the values at the maximum peak in tan δ were not affected. At the same time, an increase in the thermomoulding temperature led to a slight increase in E*, which was most evident in the sample with the highest glycerol content. In addition, the glass transition temperature occurred at a range of temperatures between 60-70°C, while a slight decrease in the values at the maximum peak in tan δ was observed. The rice protein samples for the second group, by contrast, showed a significant decrease in E*, coupled with an almost constant glass transition temperature and a slight increase in the values at the maximum peak in tan δ. The complex modulus and glass transition temperatures for these samples did not vary with glycerol concentration and thermomoulding temperature. According to Jerez et al., 2005a, an increase in the thermosetting temperature for the wheat gluten sample normally led to an increase in both E* and the maximum peak in tan δ, which contrasts with the effect of thermosetting above, albeit non-significant, on E* and tan δ for rice protein-based bioplastic. These samples also showed a higher viscoelastic modulus than wheat gluten based bioplastic.

Potato protein based bioplastics

Figure 1.2.3 shows the evolution of the complex modulus and tan δ with temperature as a function of the thermosetting temperature for potato protein based bioplastic with 33 wt.% glycerol. The complex modulus of the potato protein based bioplastic decreased with temperature as expected. Moreover, a change in the slope in E* was observed. This event occurred within a temperature range of 102-109°C for samples thermoset at temperatures higher than 120°C, whilst a change in the slope in E* at 75°C was observed for the sample thermoset at 90°C. The minimum value in the loss tangent, which might be related to the denaturation/rearrangement temperature, appeared at progressively higher temperatures as the temperature of the thermosetting increased (from 159°C for the sample thermoset at 90°C to 176°C for the sample thermoset at 180°C).

The influence of potato protein on the development of the bioplastic network structure was compared to the structure developed in wheat gluten bioplastic with 33 wt.% glycerol after thermosetting at 120°C, as shown in Figure 1.2.3. The benchmark (i.e, the wheat gluten sample) showed E* values lower than the potato protein samples across almost the whole range of temperatures studied. In addition, the maximum in loss tangent for the potato protein samples always appeared at a higher temperature (90ºC) than the benchmark (30ºC). Furthermore, like the rice protein samples, the minimum value in loss tangent for potato protein-based bioplastics appeared at higher temperatures (see Figure 1.2.1). These values are higher for potato protein bioplastics than for wheat gluten and rice systems, which may be related to more structured systems with higher complex modulus. There were slight increases in E* values in the transition region to glassy behaviour with thermosetting temperature.

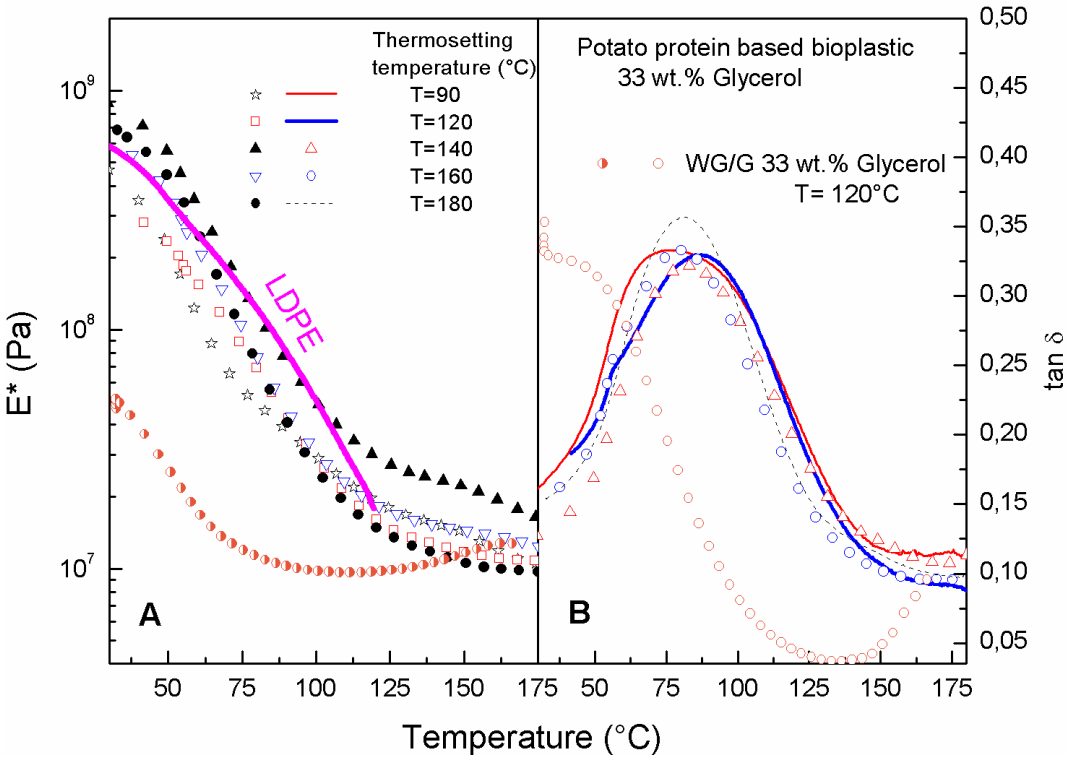

Figure 1.2.3 Dynamic mechanical thermal analysis results, complex modulus, E (A) and tan δ (B) for potato protein based bioplastic with 33 wt.% glycerol at different thermosetting temperatures.*

Figure 1.2.4 shows the evolution of complex modulus and loss tangent with temperature for potato-protein based bioplastic with 43 wt.% glycerol. The complex modulus of the potato protein bioplastic decreased with temperature and showed a change in the slope in E* at a temperature range of 108 to 117°C. A gradual decrease in the slope of the complex modulus was also observed. In addition, an increase in thermosetting temperature first led to a

slight increase in complex modulus values in the glassy region although it then led to a decrease at T >140°C. A maximum peak in tan δ around 80ºC for samples with 43 wt.% was found, excepting the sample thermoset at 90°C (with a peak in tan δ at 96 ºC).

The viscoelastic properties of potato protein-based bioplastic were affected by glycerol content and thermomoulding temperature treatment. Compared to wheat gluten and rice protein bioplastics, potato protein-based bioplastics had a complex modulus value close to 10^9 Pa and did not seem to be too affected by plasticizer concentration or thermosetting treatment.

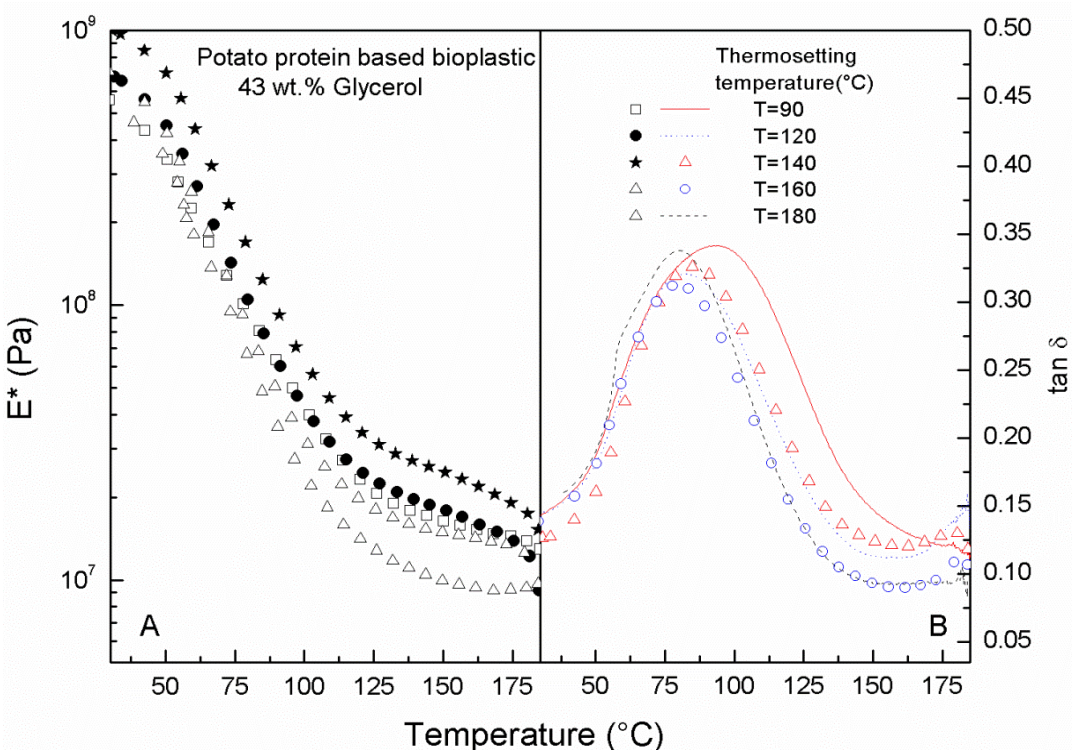

Figure 1.2.4 Dynamic mechanical thermal analysis results showing the complex modulus E (A) and tan δ (B) for potato protein based bioplastic with 43 wt.% glycerol at different thermosetting temperatures.*

Also, the tan δ peak for potato protein samples were located about 30ºC higher than the maximum reached for wheat gluten-based bioplastic. This is indicative of a more structured material, with a higher degree of crosslinking. This would mean that lower protein concentration and lower thermosetting temperatures can be used for potato protein bioplastic leading to complex modulus values similar to those found for LDPE (Figure 1.2.3).

1.3 Thermal behaviour of protein-based bioplastics

The thermograms obtained by differential scanning calorimetry (DSC) of both the rice and potato protein bioplastics, after thermosetting at 120ºC, can be observed in Figure 1.3.1. As may be seen, the rice protein bioplastics showed an endothermic peak located at ~138ºC, whereas the potato protein exhibited a higher peak located at ~150ºC. Previous studies into the thermal denaturation of native rice and potato protein found that potato protein unfolded between 55-75ºC and rice protein around 79-82ºC (Van Koningsveld, 2001; Gorinstein et al., 1996). This strongly suggests that, during the thermoulding temperature treatment, the polypeptide chains in both proteins was rearranged, in this way altering the denaturation temperature. It also demonstrates the high thermal resistance of both proteins in comparison with wheat gluten. Likewise, the minimum in tan δ was found at a temperature close to 150-160ºC for potato protein blends, which is also likely to be related to the denaturation/rearrangement temperature of the bioplastics molecules (Figure 1.2.3 -1.2.4).

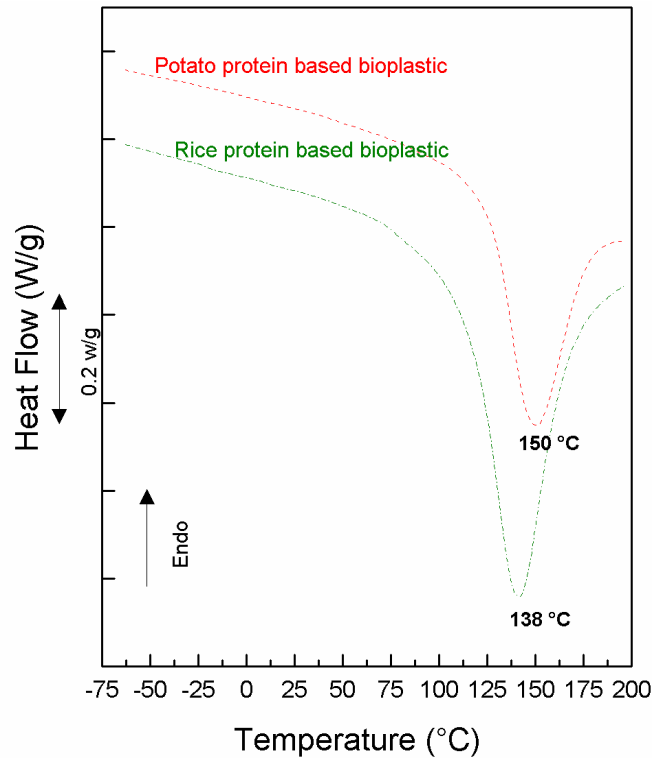

Figure 1.3.1 DSC thermograms for rice and potato protein plasticized with glycerol and thermoset at 120ºC.

This thermal event might be related to the structural unfolding of both protein molecules in the blend, indicating that the potato protein blend is more resistant to high

temperatures than the rice protein/glycerol blend since the event occurred at a higher temperature. However, for the rice protein/glycerol blend, this thermal event occurs within a narrower temperature range than the potato protein blend which means that requires more energy to break the hydrogen bonds and increased hydrophobic interaction (Wright et al., 1977; Privalov and Khechinasvili, 1974). It is worth noting such endothermic events coincide with the aforementioned optimum thermosetting temperatures, at which the highest moduli (and elastic character) were obtained.

1.4 Water absorption properties of protein based bioplastics

Water absorption in bioplastics is an important aspect in relation to various industrial applications, such as active food packaging, moisture absorbents (e.g. hygienic products, agriculture, horticulture, etc.), drug-delivery systems and water-blocking tapes (Zhang et al., 2006).

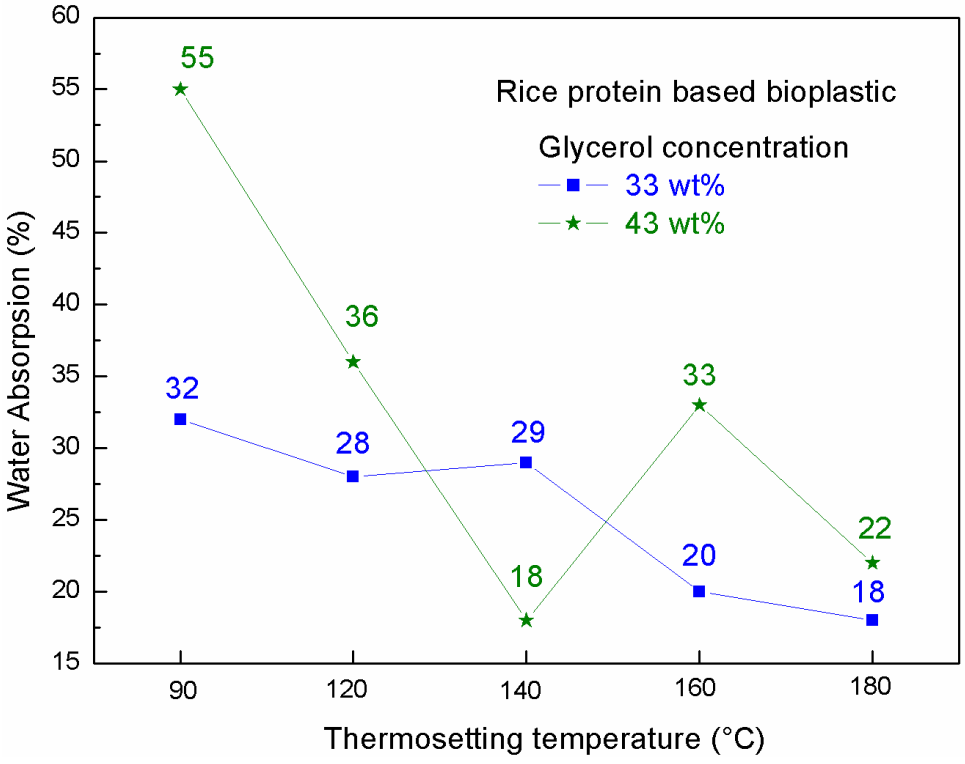

Figure 1.4.1 Water absorption for rice protein bioplastics plasticized with different glycerol concentrations, at different thermosetting temperatures.

Figure 1.4.1 shows the water absorption values for rice protein-based bioplastics manufactured at different thermosetting temperatures and to different formulations. The

observed water absorption values for rice protein based bioplastics with 33 wt.% glycerol showed a continuous decrease with increasing thermosetting temperature, from 90 to 180ºC. Thus, samples thermoset above 160ºC exhibited the lowest water absorption, about 20%. Conversely, at 43 wt.% glycerol content, absorption tended to decrease with higher thermosetting temperatures until these reached 140ºC – registering the lowest absorption – after which it increased to around 33 wt.%.

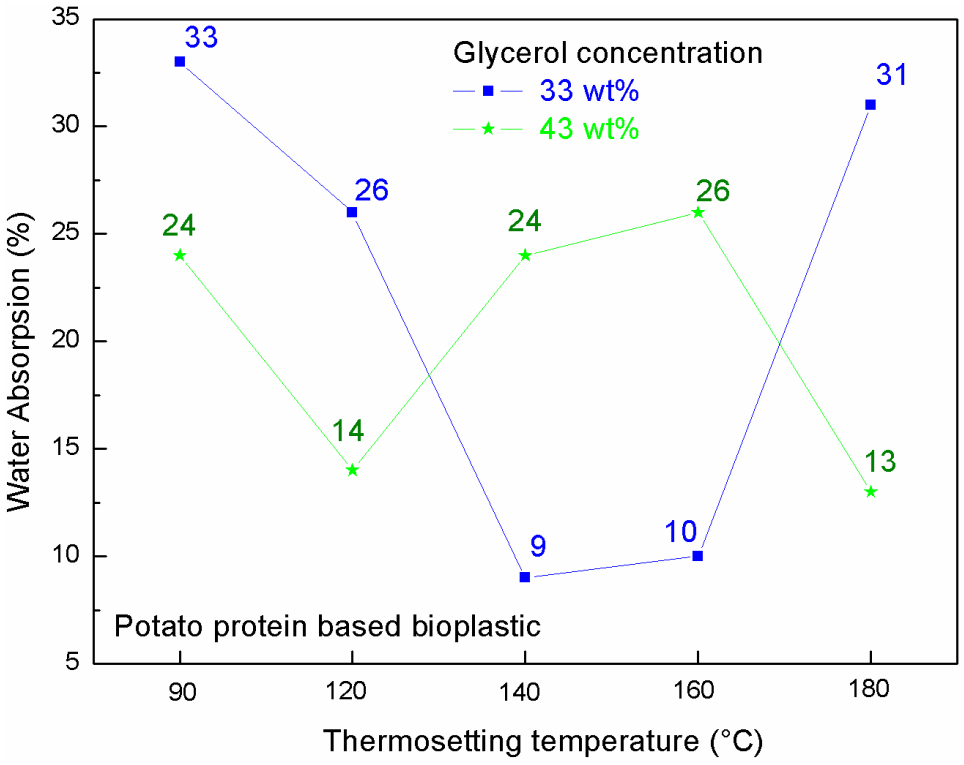

Figure 1.4.2 Water absorption potato protein plasticized with different glycerol concentrations, at different thermosetting temperatures.

Figure 1.4.2 shows the water absorption values for potato protein-based bioplastics manufactured at different thermosetting temperatures and different glycerol concentrations. The water absorption values at 33 wt.% concentration registered the lowest value (9 wt.%) absorption at a thermosetting of 140ºC, after which sample gave higher values with increased thermosetting temperatures. These results are entirely consistent with the higher values in the complex modulus observed at these thermosetting temperatures showing how E* increases as water absorption decreases (Jerez et al., 2007). By contrast, potato protein-based bioplastics with 43 wt.% glycerol did not show a clear trend with thermosetting temperature. This blend exhibited the minimum value in water absorption with the sample thermoset at 180°C (13 wt.%)

As described above, the type of protein used and thermomechanical treatment can lead to protein denaturation and, therefore, to an increase in the degree of crosslinking between molecules (Buonocore et al., 2003). In general, protein denaturation results in an increase of hydrophobicity, due to exposure of hydrophobic groups that are folded inside the intact native protein molecule (Mine, 1997). However, this fact did not occur in all cases due to the presence of hydrophobic single proteins in rice. Both proteins exhibited water absorption values lower than 50 wt.%, these values are low compared to those obtained for wheat gluten blend (Jerez et al., 2007).

Comparing the absorption properties which bring rice and potato protein to the final material, the potato protein based bioplastic showed the lowest water absorption as well as a narrow water absorption range compared to rice protein-based bioplastics.

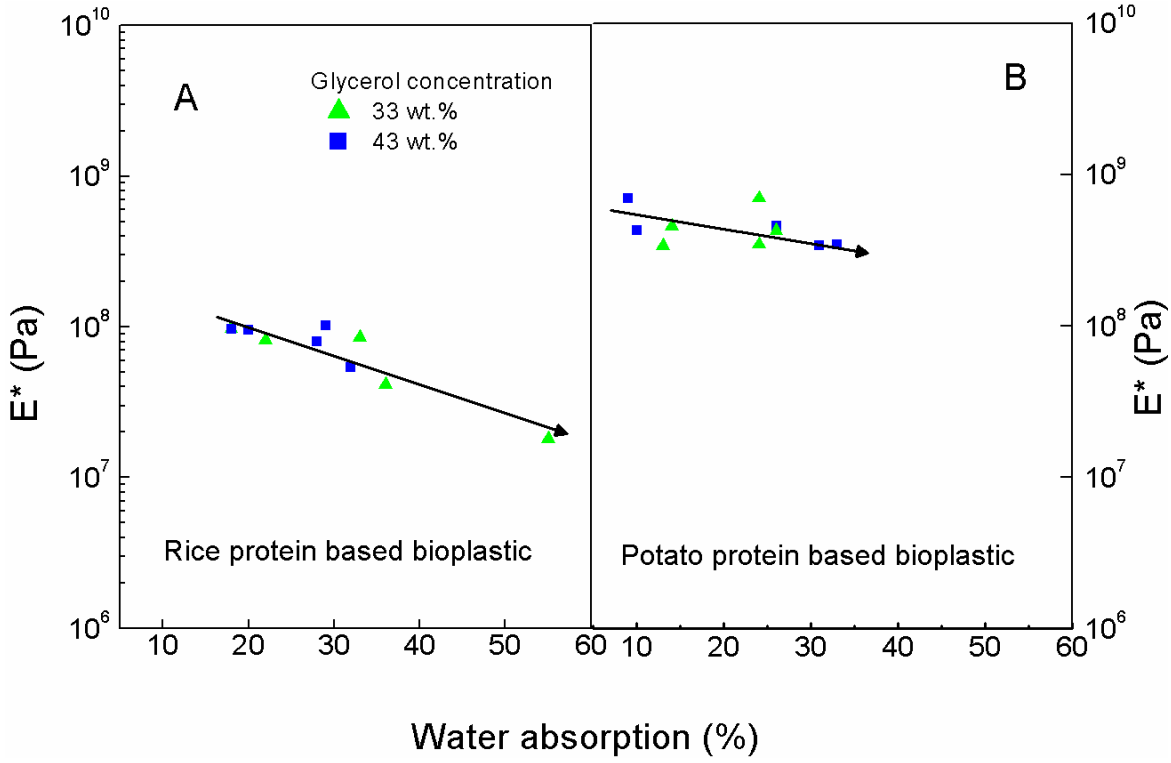

Figure 1.4.3 Relationship between the elastic modulus at 50°C and bioplastic water absorption.

The value of the complex modulus at 50°C can be used to reveal information about the degree of crosslinking (Zheng et al., 2002). With this in mind, such value was used to correlate/associate the modulus values at 50ºC with water absorption (Figure 1.4.3). A similar trend was found for both proteins and for different thermosetting treatments, in which, water absorption increased as the modulus decreased, which is an expected behaviour. This trend

was more significant for rice protein bioplastic as compared to the potato protein based bioplastic.

1.5 Molecular weight distribution of the proteins

In the manufacture of protein-based bioplastics, it is important to understand the composition of the protein and its characteristics, and also how the protein might behave under processing conditions. Understanding these factors is a means of predicting and accounting for possible interactions or reactions between proteins, and the effect of the plasticizers and other components of bioplastics.

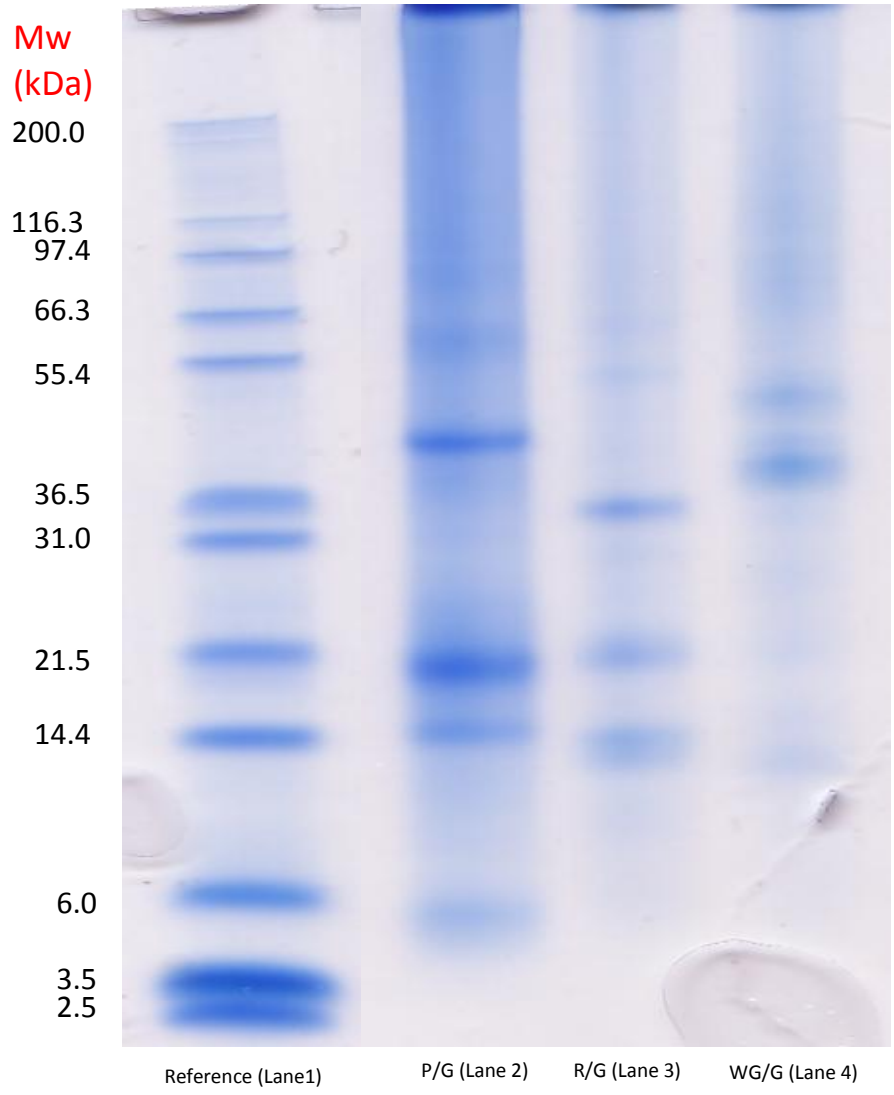

Figure 1.5.1 SDS-PAGE for wheat gluten, rice and potato protein based bioplastics, under reducing conditions. Lane 1: reference, lane 2: potato protein/glycerol(P/G), lane 3: rice protein/glycerol(R/G) and lane 4: wheat gluten/glycerol (WG/G) under reducing conditions.

The molecular weight distribution of wheat gluten, rice and potato protein bioplastics was performed by sodium dodecyl sulphate-polyacrylamide gel electrophoresis (SDS PAGE) under reducing conditions as shown in Figure 1.5.1. The results obtained were compared with a protein standard consisting of 12 protein bands in the range of 2.5 – 200 kDa. This reference (Lane 1) allows accurate molecular weight estimation of the protein sample over a wide molecular weight range.

SDS PAGE under reducing conditions (Figure 1.5.1) showed that the gluten protein bioplastic (Lane 4) contained bands at 36, 45 and 52 kDa, which corresponded to the alpha, beta and gamma-gliadins, respectively. This range of molecular weight could be also related to the low molecular weight glutenins (LMW-GS) according to Kasarda et al., (1983), (20-45 kDa) which, in our case, might be overlapping. Both proteins tend to be rich in asparagine, glutamine, arginine or proline, serine, methionine and isoleucine (Masci et al., 1995; Lew et al., 1992).

In rice protein-based bioplastic (Lane 3), one large band at 14 kDa can be distinguished. Ogawa (1987) found that rice protein consists of three polypeptide subunits with apparent molecular weight distributions of 10, 13 and 16 kDa. The reason why three bands cannot be found in our sample may be that they are so close that they could not be distinguished from each other. Previous studies have mentioned that 13 and 16kDa are cysteine rich (the sulphur amino acid) (Hibino et al., 1989; Ogawa et al., 1987), which means that this protein might tend to interact and aggregate under thermal conditions. Moreover, rice glutelin is extremely insoluble in water because of its hydrophobic, hydrogen and disulfide bonding (Hamada, 1996; Juliano, 1985). In addition to the rice protein sample characterization, this sample exhibited one band at 21 kDa close to the band (25 kDa) cited by many authors for rice albumins which have a wide range of molecular weights (Houston and Mohammed, 1970). However, according to Juliano (1972) the major component of the glutelin is located at 18–20 kDa and is thus located close to the band we found.

The potato protein-based bioplastic (Lane 2) contained a group of proteins at 6, 16, 21 and 45 kDa. The first three bands mentioned might be identified by protease inhibitors. A characteristic of this protein is that it is small, cysteine rich (comprising a large number of disulphide bridges) and heat-resistant (Pouvreau et al., 2005a,b; Van Koningsveld G.A., 2001). This fact might promote the aggregation of the protein under thermal conditions and may explain the highest values of E* and Tg. The 45 kDa band might be identified as patatin which is a hydrophobic protein (Park, 1983). In addition, two weak bands at high molecular

weights 54 and 66kDa were found. These types of oligomers represent about 12wt.% of the protein present (Pouvreau et al., 2001) and consist of proteins such as lectin (Allen et al., 1996).

As a result, among others, glutelin in the rice protein, and the protease inhibitors and patatin in potato protein, may play an important role in both viscoelastic behaviour and water absorption properties due to the characteristics mentioned above.

1.6 Thermal degradation and the role of plasticizers in gluten-based bioplastics

Thermogravimetric analysis, TG, is a powerful tool to monitor the thermal degradation of biopolymers under inert (pyrolysis) or oxidative (combustion) atmospheres (Barneto et al., 2009). TG analysis has been applied to study the thermal degradation of soy-based bioplastics (Swain et al., 2005; Das et al., 2008; Nanda et al., 2007). Swain et al., (2005) distinguished five stages in the TG combustion curve obtained from soy protein. According to these authors, the first stage (up to around 237ºC) was attributed to elimination of water and the dissociation of the quaternary structure of proteins. The following two stages (from 243 to 382ºC and between 388 and 583ºC) are related to the cleavage of different bond types such as covalent bonds between peptides and S-S, O-N, and O-O linkages of protein molecules, respectively. The fourth stage (between 589 and 710ºC) is associated to protein decomposition with volatiles formation and finally, beyond 710ºC only char remains. Using different kinetic models, for each stage, these authors determine the kinetic parameters (pre-exponential factor and activation energy) that better fit the experimental data. As for biodegradable plastics based on glycerol-plasticized wheat gluten, Sun et al., (2007) qualitatively described their combustion and distinguish four stages: A) the first two stages are is related to the elimination of water (below 200ºC) and glycerol (from 200 to 290ºC); the third one (between 290 and 340ºC) and the fourth (above 340ºC) are related with the cleavage of different bonds; covalent peptide bonds in the amino acids residues, or S-S, O-N, and O-O linkages from protein molecules.

Previous TG studies have not provided quantitative discussions about the effect of the gluten-glycerol-based bioplastic formulation or a simulation of the pyrolysis of this type of materials. With the aim of achieving a further insight into the thermal degradation of gluten-based bioplastics, a novel kinetic model has been proposed which draws the different release/degradation patterns shown by the material compounds. In the present study, experimental thermogravimetric curves, obtained under nitrogen atmosphere, were modelled

through autocatalytic kinetic equations (based on Prout-Tompkins model) and the so-called pseudo-components. A pseudo-component is a fraction that thermally degrades as a unity but, nevertheless, it is not a pure substance. In addition, material composition and the role of the plasticizer have been analysed by comparing the degradation profiles of gluten protein, plasticizer and different gluten-based bioplastics.

1.6.1 Thermogravimetric analysis of wheat gluten based bioplastics

Figure 1.6.1 compares the thermal degradation of gluten and two bioplastics with different glycerol contents (33 and 40 wt.%) under inert and oxidative atmospheres. As we can see, from room temperature to 450ºC (volatilization zone) the degradations profiles of gluten and bioplastics are slightly affected by air presence. However, at higher temperatures (oxidation zone) apparent differences are observed between them, related to the combustion of carbonaceous residues (char).

Regarding bioplastic materials, the experimental weight loss rate curves (DTG), obtained under nitrogen atmosphere, show at least four thermal events, labelled as peaks P1 to P4 (Figure 1.6.1A). Among them, peaks P3 and P4 (located at 230 and 309ºC) are the most relevant ones and strongly affected by bioplastic composition. Instead, gluten volatilization is characterised by three main weight loss peaks (labelled as P1, P2 and P4 in Figure 1.6.1A). Additionally for all samples, a peak P5, associated to char oxidation, only appears under air atmosphere.

Table 1.6.1, which gathers some characteristic parameters calculated from TG and DTG curves under nitrogen atmosphere, has been used to compare the effect of the material composition on the degradation profiles of bioplastics with 33 and 40 wt.% glycerol. Initially, Table 1.6.1 shows that both bioplastics undergo similar weight losses up to 600ºC for pyrolysis, $ML_{max} \approx 85$ wt. %. However, the height of peaks P3 and P4 seems to be strongly affected by the bioplastic formulation (see parameter v_{max} in Table 1.6.1). Thus, bioplastic with 33 wt.% exhibits a peak P3 lower than P4, whereas both peaks have similar height in bioplastic with 40 wt.% glycerol (Figure 1.6.1 and Table 1.6.1). As a result, a higher glycerol concentration leads to an increase in peak 3, whereas peak 4 becomes smaller. This fact points out the different nature of those bioplastic compounds responsible for the degradation of peaks P3 and P4.

According to Sun et al., 2007, the first (P1) and second (P2) peaks (located close to 80 and 160ºC, respectively) of the thermal degradation of gluten may be associated to the loss of free and bonded water respectively, whereas the fourth (P4) peak (close 320ºC) would be related to the proteins volatilization. Likewise, according to experimental data shown in Figure 1.6.2A, glycerol volatilization starts close 100ºC and progressively increases up to the highest weight loss rate close to 237ºC. This result suggests occurrence of peak P3 is mainly related to the glycerol used as bioplastic plasticiser.

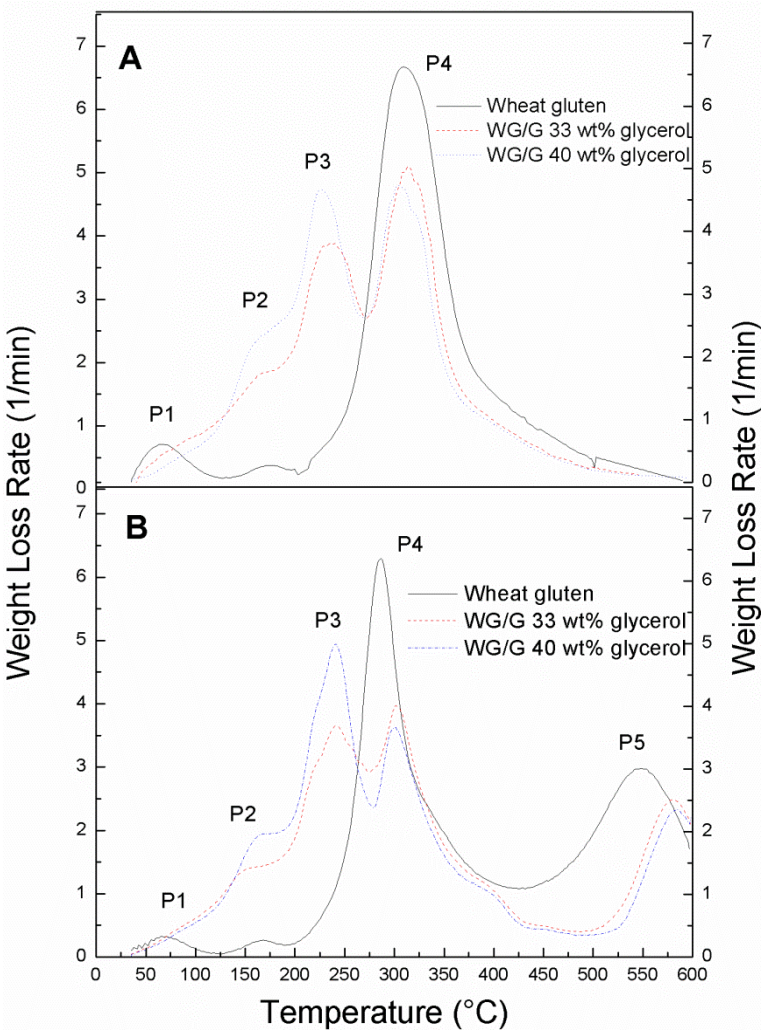

Figure 1.6.1 Thermal degradation of gluten and two bioplastics (33 and 40 wt.% glycerol): A) under inert atmosphere, B) under air atmosphere.

Table 1.6.1 Thermal degradation parameters for two bioplastics with different gluten/glycerol ratio (subscripts 3 and 4 refer to P3 and P4 peaks in Figure 2, respectively).

Bioplastics WG/G		**ML_{max} (g/100g)**	**T_{max3} (ºC)**	**v_{max3} (min^{-1})**	**T_{max4} (ºC)**	**v_{max4} (min^{-1})**
33wt.%. glycerol	pyrolysis	84.3	233	3.8	309	5.1
	combustion	99.0	243	3.6	304	3.9
40wt.%. glycerol	pyrolysis	85.9	230	4.6	308	4.7
	combustion	98.9	243	4.9	303	3.6

These assumptions are supported by a subsequently bioplastic drying. Figure 1.6.2B compares the pyrolysis of two bioplastics: WG/G and dry-WG/G with 33 wt.% glycerol, moist and dry, respectively. As may be seen, the height of peak P4 increases due to the higher protein concentration of the dehydrated bioplastic (dry-WG/G with 33 wt.% glycerol), whereas peaks P1 to P3 decrease after the water loss. Accordingly, it is apparent that P1 arises from the loss of free water and P3 from the glycerol volatilization at high temperature. However, in moist bioplastics, the peak P2 (close 160ºC) is related to both the loss of bonded water and the loss of volatilized glycerol at low temperature (at 160ºC the glycerol volatilization is close 6 wt.%, see Figure 1.6.2A). These results are in good agreement with those obtained by Chen et al., (2005) for soy-protein-based materials, who suggested the weight loss below 150ºC may be attributed to evaporation of absorbed water, weight loss between 150 and 290ºC is due to glycerol evaporation and, finally, protein degradation would take place above 290ºC.

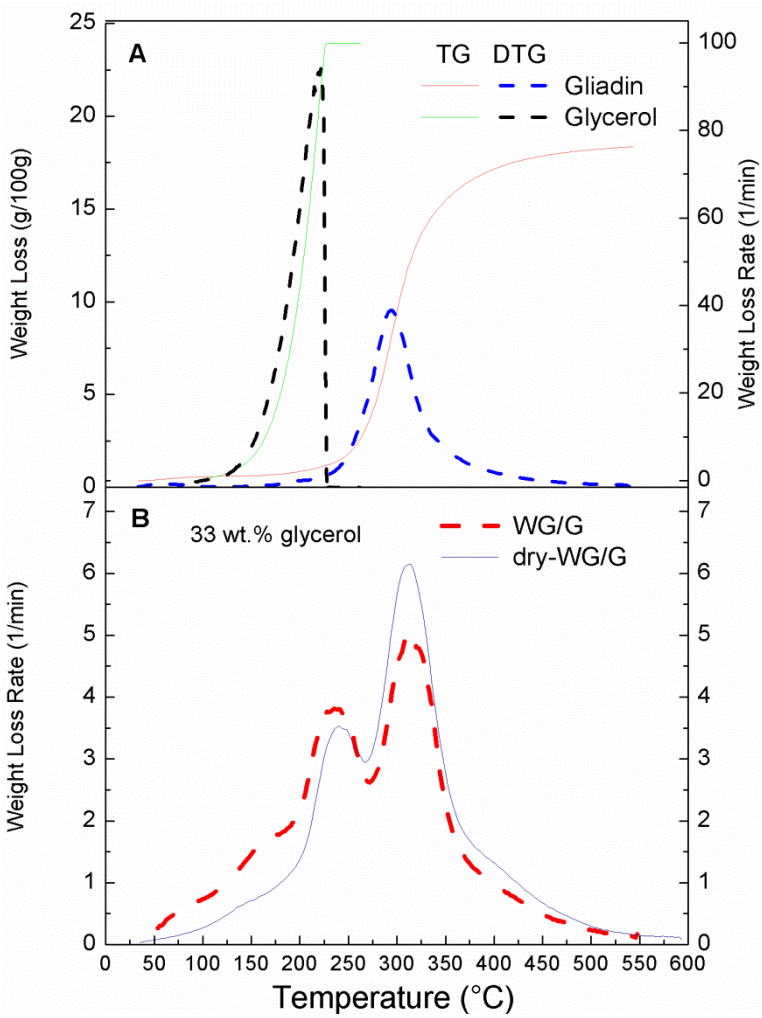

Figure 1.6.2 Glycerol and gliadin volatilization (A) and pyrolysis of two bioplastics with different moisture (B).

Furthermore, the volatilization environment affects the protein degradation (peak P4). As seen in Figure 1.6.1B, for gluten and bioplastics degradations, the oxygen presence makes sharper peak P4 and shifts it to lower temperature. This effect is more evident for gluten isolate (the peak P4 is shifted from 304 to 282ºC) than for bioplastics (e.g. for WG/G with 33 wt.% glycerol the peak P4 is shifted from 308 to 300ºC). Gluten isolate is a complex blend that mainly contains residual starch and the gluten proteins: glutenin and gliadin. As commented above, both proteins present different molecular conformation and polymerisation degree so that different degradation paths should be expected during their pyrolysis or combustion. According to Figure 1.6.2A, under nitrogen atmosphere, pure gliadin reaches the highest weight loss rate at 315ºC (using 10ºC/min as heating rate), yielding 25 % char. Regarding the other 75% volatiles, about 90 % of them are lost below 400ºC. It is expected

that monomeric gliadin degrades at lower temperature than polymeric glutenin, so that the long tail found at high temperature seems to be related polymeric glutenin. In addition, Peak 4 should also arise from the residual starch degradation that typically gives a sharp peak close to 300ºC, which is shifted to low temperature by oxygen presence (Barneto et al., 2010). As a result, the observed shifting of P4 in presence of air would be mainly related to residual starch and gliadin degradations.

1.6.2 Thermogravimetric model

As previously seen, wheat gluten thermal degradation occurs through different stages, which are related to the main gluten isolate compounds (mainly gliadin and glutenin proteins and residual starch) and material natural moisture. Similarly, DTG curves of the glycerol-gluten-based bioplastic pyrolysis have shown several peaks related to bioplastic formulation: water (P1); water/glycerol bioplastics (P2 and P3); and gluten proteins and starch (P4).

In order to simulate experimental TGA data, the gluten and bioplastics degradations have been modelled on the basis of the simplified processes shown in Figure 1.6.3. Under inert atmosphere, protein related pseudo-components (S_i) undergo volatilization that yield light volatiles (V_{i1}) and char (R_i), which remains in thermobalance. Under air environment, char previously obtained oxidises, yielding new volatiles (V_{i2}) and ash (A). On this regard, some assumptions have been made for sake of simplicity: i) although starch pyrolysis typically yields char, considering its residual concentration this will be considered negligible, and therefore, only protein pseudo-components (Glu and Glia) yield char; and ii) the weight loss detected by thermobalance is the sum of independent pseudo-component degradations and, therefore, samples are considered as the sum of all pseudo-components.

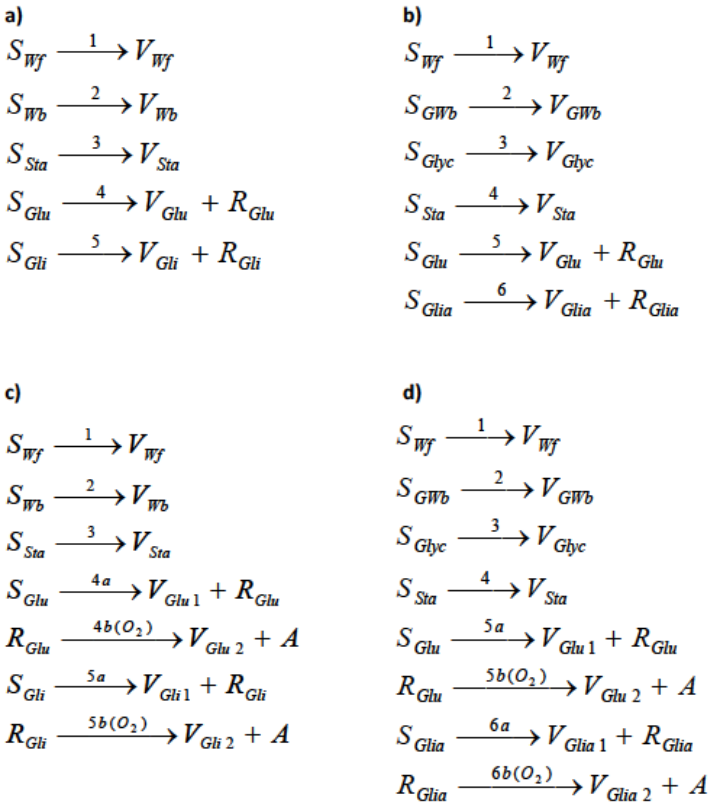

Figure 1.6.3 Simplified schemes for gluten pyrolysis (a), bioplastic pyrolysis (b), gluten combustion (c), and bioplastic combustion (d)

As for gluten isolate, five pseudo-components were proposed: S_{Wf} (free water), S_{Wb} (bonded water), S_{Sta} (residual starch), S_{Glu} (glutenin) and S_{Glia} (gliadin). For bioplastics, six pseudo-components were proposed: S_{Wf} (free water), S_{GWb} (moist glycerol that volatilizes at low temperature), S_{Glyc} (glycerol that volatilizes at high temperature), S_{Sta} (residual starch), S_{Glu} (glutenin) and S_{Glia} (gliadin).

The thermal degradation of pseudo-components has been simulated by means a nucleation model based on the Prout-Tompkims equation (Prout and Tompkins, 1944 and 1946). According to this, the reaction rate depends on both non-reacted and reacted fractions. In this work, a modified Prout-Tompkims differential equation, used by Burnham et al., (1996), has been used to describe the evolution of the reaction conversion (α_i):

$$\frac{d\alpha_i}{dt} = k_i(1-\alpha_i)^n(s+\alpha_i{}^m) \qquad [1.6.1]$$

where the reaction order (n) and the nucleation order (m) affect non-reacted and reacted fractions, respectively. The factor s, usually assumed as 0.01 (Burnham et al, 1996), is a constant that assures coherent values for reaction rate when conversion is close to extreme values of 0 or 1. The kinetic constant (k_i) is expressed by the Arrhenius law [$k_i=k_{0i}\exp(E_i/RT)$], where k_{0i} is the pre-exponential factor and E_i the activation energy. Equation 1.6.1 turns into classical nth-order kinetic equation if the nucleation order is zero. When the importance of the autocatalysis increases (high heating rate and oxidative atmosphere), the nucleation order also increases (Barneto et al., 2009). This fact affects the DTG curve, turning broad peaks into sharp peaks which are inconsistent with the nth-order model.

Table 1.6.2 Abbreviations used for parameters of the kinetic model.

Gluten pseudo-components	**Gluten-glycerl based bioplastics pseudo-components**	**Kinetics parameters**
W_f : free water	W_f : free water	k : Kinetic constant
W_b : bonded water	GW_b : bonded water and glycerol that volatilises at low temperature	k_0 : pre-exponential factor
Sta : residual starch	Sta : residual starch	E : activation energy
Glia : gliadin	Glia : gliadin	n : reaction order
Glu : Glutenin	Glu : Glutenin	m : nucleation order
	Glyc : glycerol	V_i : volatile weight
		$V_{\infty i}$: volatile weight at infinite time
		∞: reaction conversion

Using the volatile weight (V_i) obtained from each pseudo-component, Equation 1.6.1 can be expressed as follows:

$$\frac{dV_i}{dt} = k_i V_{\infty i}(1-\frac{V_i}{V_{\infty i}})^{n_i}[s+(\frac{V_i}{V_{\infty i}})^m] \qquad [1.6.2]$$

where α_i is replaced by $V_i/V_{\infty i}$ and $V_{\infty i}$ is the volatile weight at infinite time. As a consequence, it is necessary to determine five parameters for each component: pre-exponential factor, activation energy, reaction order, nucleation order, and mass of volatiles at infinite time.

Integration and optimization of the kinetic equations were carried out using the Runge-Kutta and Gauss-Newton methods, respectively. The objective function to be minimized is:

$$OF = \sum_{i=1}^{n} \left(\frac{dm_{\exp}}{dt} - \frac{dm_{cal}}{dt} \right)^2 \qquad [1.6.3]$$

where $\frac{dm_{\exp}}{dt}$ and $\frac{dm_{cal}}{dt}$ are, in that order, the experimental and calculated weight loss rates for the n points of each experiment. The model validity was tested by calculating the variation coefficient (*VC*):

$$VC(\%) = \frac{\sqrt{OF/(N-P)}}{\frac{d\overline{m}_{\exp}}{dt}} 100 \qquad [1.6.4]$$

where *N* and *P* are the number of data points and parameters fitted, respectively; and $\frac{d\overline{m}_{\exp}}{dt}$ is the average of the experimental mass loss rates. Tables 1.6.3 and 1.6.4 show the calculated kinetic parameters that characterise pyrolysis and combustion of gluten isolate and bioplastics at three heating rates.

1.6.3 Thermal degradation of gluten isolate

Therefore, this model proposes the thermal degradation of wheat gluten through its main compounds (starch, gliadin, glutenin and material natural moisture) by means of five pseudo-components labelled as W_f, W_b, Sta, Glia and Glu, which respectively represent free water, bonded water, residual starch, gliadin and glutenin proteins. It should be noticed that pseudo-component are not pure substances, but fractions that thermally degrades in a characteristic way (i.e. temperature range). As may be deduced from scheme a) in Figure 1.6.3, during pyrolysis the pseudo-components W_f and W_b completely volatise, as a result of a simple process of dehydration. The pseudo-component Sta, it is assumed, that completely volatilises. And, finally, pseudo-components Gli and Glu produce volatiles and carbonaceous residues (char), which remains in the thermobalance. Additionally, Scheme c) in Figure 1.6.3 depicts the combustion model for gluten, which, besides previous volatilization, also includes char oxidation for Glia and Glu pseudo-components.

Table 1.6.3 shows calculated kinetic parameters that characterise the thermal degradation of gluten at three heating rates (average values). As a whole, we can observe that kinetic parameters which characterise the volatilization of the pseudo-components in air atmosphere (first step of the combustion) are similar to those obtained from pyrolysis. Figure 1.6.4 shows the good agreement between experimental and calculated DTG curves, and the degradation profile simulated for each pseudo-component. According to the model, in both atmospheres, the highest weight loss rates of free and bonded water are reached close to 70 and 168ºC, estimating the gluten moist content as 3.5 wt. %, where about 2.1 wt. % appears as free water (W_f) and 1.4 wt. % as bonded water (W_b). Furthermore, the development of bonds between water and the protein matrix shifts the activation energy values for the water release from 36 kJ/mol to 60 kJ/mol (see Table 1.6.3).

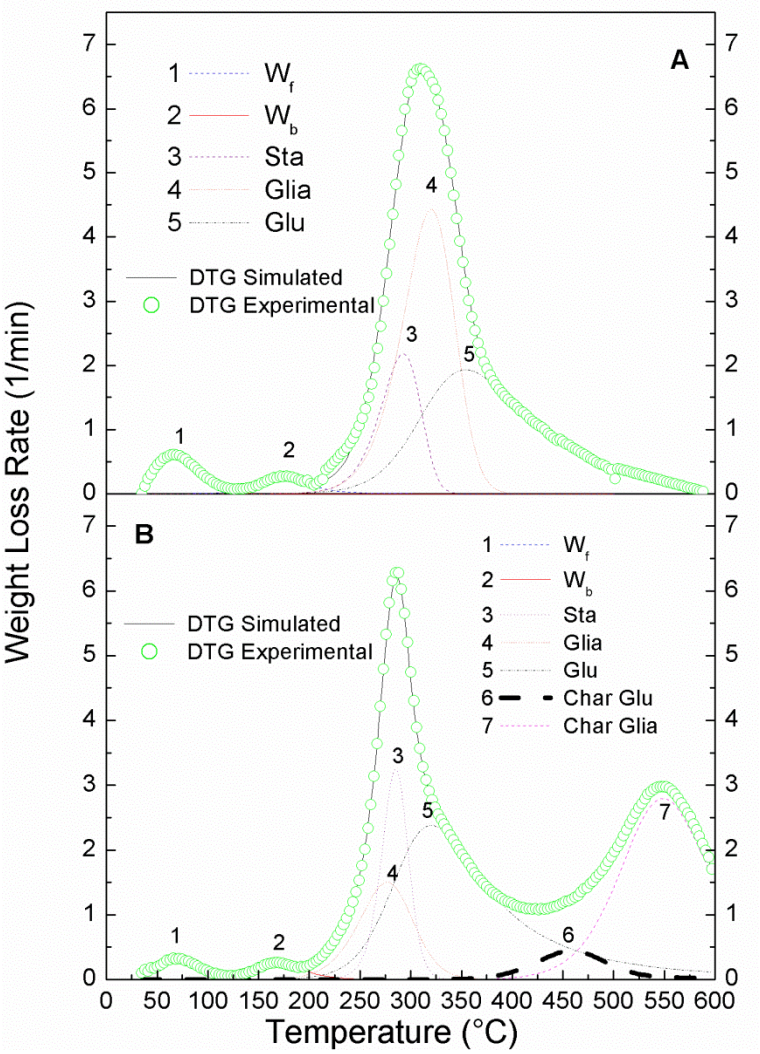

Figure 1.6.4 Simulation of the thermal degradation of gluten: a) under inert atmosphere, b) under air atmosphere.

Volatilization of residual starch takes place according to a first order kinetic with activation energy 131-136 kJ/mol. As occurs for cellulose (Barneto et al., 2010), under air, starch peak is shifted to low temperature (i.e. from 293 to 273ºC, using 5ºC/min as heating rate) and nucleation order increases from 0.02 to 0.49. Oxygen presence also produces significant changes in protein fraction.

Gliadin drastically reduces its volatilization from 29 to 10 %, promoting the char formation under air. The broad glutenin peak (reaction order close to 3) is shifted to lower temperature, about 48 ºC (from 355 to 307ºC, using 5ºC/min as heating rate) and gliadin peak becomes smaller (reaction order close to 1) and is shifted from 320 to 277ºC, i.e. 33ºC in the same direction. Moreover, activation energy values for both proteins decrease about 5 kJ/mol.

Table 1.6.3 Kinetic parameters for the thermal degradation of the gluten pseudo-components (average value and standard deviation).

		W_f	W_b	*Sta*	*Glia*	*Glu*	Char Glia	Char Glu
Pyrolysis	**Ln k_o (s^{-1})**	8.2±0.4	11±1	26±3	18.7±0.4	7.5±0.1	-	-
	E_{act} (kJmol^{-1})	36±2	61±6	135±2	116±1	66±2	-	-
	n	1.7±0.5	1.6±0.1	1.1±0.1	1.1±0.1	2.9±0.1	-	-
	m	0.3±0.2	0.3±0.2	0.02±0.02	0.02±0.02	0.4±0.1	-	-
	V_∞ (%)	2.1±0.5	1.4±0.2	10.9±0.5	29.1±0.5	32.2±0.3	-	-
Combustion	**Ln k_o (s^{-1})**	7.9±0.1	11.7±0.1	24±1	19.4±0.1	7.3±0.1	19.55	19.55
	E_{act} (kJmol^{-1})	36±1	60±1	131±1	111±1	61±3	169±1	148±1
	n	1.2±0.2	1.7±0.1	1.2±0.1	1.4±0.1	3.0±0.1	2.0±0.1	1.5±0.1
	m	0.2±0.1	0.5±0.1	0.49±0.05	0.01±0.01	0.5±0.1	0.1±0.1	0.1±0.1
	V_∞ (%)	2.1±0.5	1.4±0.1	10.9±0.4	10.2±0.3	34.7±0.1	33.0±0.5	4.3±0.1

On the other hand, gluten composition can be estimated from kinetic data obtained under oxidative environment. Adding the weight of volatiles obtained from each pseudo-component in both volatilization and char oxidation, gluten composition calculated as: 2.1 wt. % free water, 1.4 wt. % bonded water, 10.9 wt. % residual starch, 43.2 wt. % gliadin and 39.0 wt. % glutenin. According to Sun et al., (2007) the protein content in the wheat gluten is close to 75 wt. %, where 40-50 wt. % is gliadin and 35-45 wt. % is glutenin. Likewise, Pallos et al., (2006) affirm the amounts of gliadin and glutenin in vital wheat gluten are approximately

equal. Furthermore, calculated residual starch is in good agreement with that indicated in the experimental section, about 10 wt. % residual starch.

1.6.4 Thermal degradation of gluten-glycerol based bioplastics

As shown in Figure 1.6.3, the thermal degradation of bioplastics has been modelled by means of six pseudo-components: free water (W_f), bonded water and glycerol that volatilizes at low temperature (GW_b), glycerol (Glyc), residual starch (Sta), gliadin (Glia), and glutenin (Glu). As for the plasticiser, the main difference with gluten isolate is related to the bonded water, because a part of glycerol volatilizes in the same temperature interval.

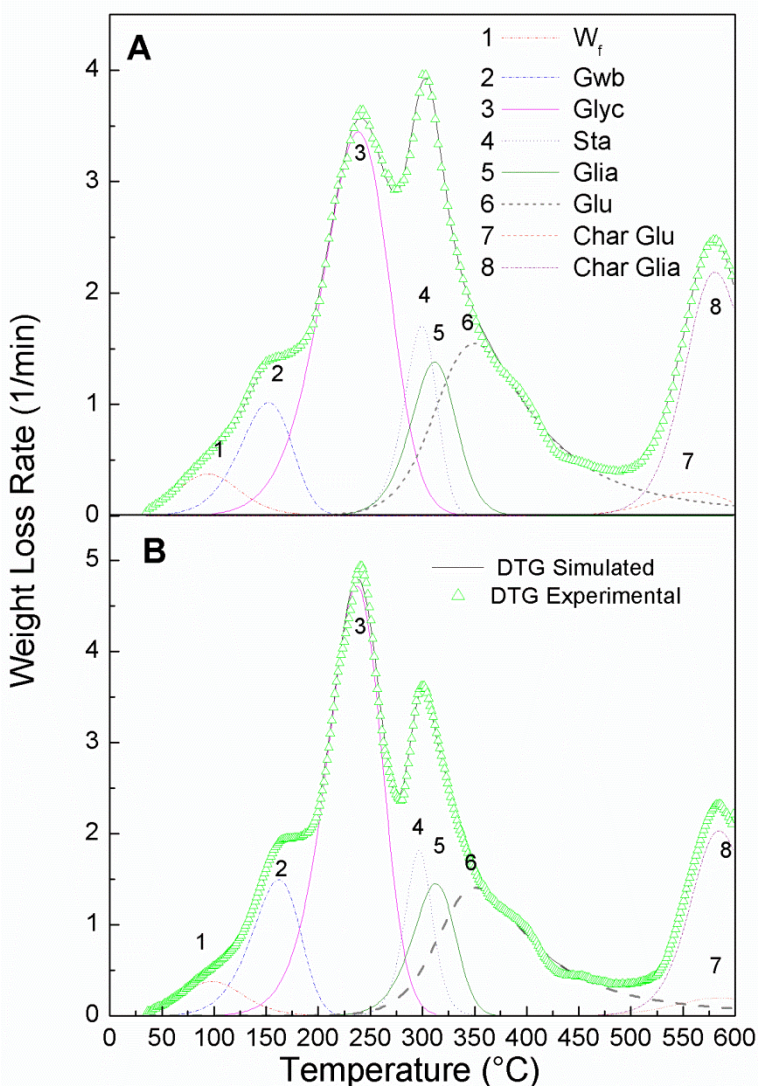

Figure 1.6.5 Combustion simulation of two bioplastics with different glycerol content: A) WG/G with 33 wt.% glycerol, B) WG/G with 40 wt.% glycerol.

The interaction with the protein matrix causes that glycerol volatilization is more complex, being necessary two pseudo-components to represent its degradation. As seen for gluten, pyrolysis model of bioplastics (scheme "b)" in Figure 1.6.3) assumes that pseudo-components based on water, glycerol and starch fully volatilizes, and only gliadin and glutenin proteins yield char. Finally, char obtained from gluten proteins oxidizes under air environment (scheme d) in Figure 1.6.3).

Table 1.6.4 Kinetic parameters that describes the thermal degradation of three bioplastics (dry-WG/G and WG/G with 33 wt.%; WG/G with 40wt.%) under inert and oxidative environments.

		W_f	GW_b	*Glyc*	*Sta*	*Glia*	*Glu*	*Char Glia*	*Char Glu*
WG/G with 33 wt.% glycerol; nitrogen	**Ln k_o (s^{-1})**	8.1	11.3	11.2	24.2	18.5	7.9	-	
	E_{act} (kJmol^{-1})	39	58	69	135	114	68	-	
	n	1.8	1.0	1.0	1.1	1.0	2.6	-	
	m	0.2	0.01	0.01	0.2	0.2	0.4	-	
	V_∞ (wt. %)	4.3	6.8	27.4	7.1	18.6	21.0	-	
Dry-WG/G with 33 wt.% glycerol; nitrogen	**Ln k_o (s^{-1})**	8.4	12.0	11.0	23.6	18.4	7.9	-	
	E_{act} (kJmol^{-1})	43	62	68	133	113	69	-	
	n	1.0	1.0	1.3	1.1	1.2	2.6	-	
	m	0.1	0.01	0.3	0.3	0.4	0.4	-	
	V_∞ (wt. %)	1.1	4.5	23.8	8.8	22.2	24.2	-	
WG/G with 33 wt.% glycerol; air	**Ln k_o (s^{-1})**	7.8	11.3	11.1	24.1	19.0	7.1	19.6	19.6
	E_{act} (kJmol^{-1})	39	57	69	135	115	63	172	171
	n	1.5	1.1	1.2	1.2	1.3	2.8	2.0	1.4
	m	0.1	0.05	0.01	0.3	0.3	0.5	0.4	0.04
	V_∞ (wt. %)	3.9	6.6	28.5	6.9	7.9	22.4	19.3	2.2
WG/G with 40 wt.% glycerol; air	**Ln k_o (s^{-1})**	7.8	12.0	11.3	23.8	19.7	7.2	19.6	19.6
	E_{act} (kJmol^{-1})	40	61	69	131	118	63	173	176

		W_f	GW_b	*Glyc*	*Sta*	*Glia*	*Glu*	*Char Glia*	*Char Glu*
	n	1.5	1.1	1.1	1.3	1.1	2.9	2.0	1.6
	m	0.1	0.1	0.2	0.5	0.2	0.5	0.5	0.01
	V_∞ **(wt. %)**	3.3	8.9	32.3	6.4	7.7	19.7	17.2	2.3

Table 1.6.4 shows kinetic parameters calculated for all studied bioplastics. As may be observed in Figure 1.6.5, the model describes fairly well the bioplastic thermal decomposition, under air atmosphere, irrespective of its formulation. As expected, an increase in glycerol/gluten ratio leads to a higher amount of the pseudo-components GW_b (from 6.6 to 8.9 wt.%) and Gly (from 28.5 to 32.3 wt.%). In addition, the increase glycerol/gluten ratio is also accompanied by a shifting of the GW_b peak to a higher temperature, from 151 to 161ºC, and by a higher the activation energy from 57 to 61 kJ/mol. These facts agree with a GW_b pseudo-component relatively enriched in glycerol.

1.7 The role of plasticizers in glycerol-based bioplastics

Aiming to a further insight in the plasticiser (water and glycerol) behaviour during bioplastic thermal decomposition, Figure 1.6.6 compares the DTG profiles under nitrogen for two bioplastics with different moisture contents. In addition, this figure includes calculated degradation profiles of pseudo-components.

According to the simulations of dry-WG/G and WG/G with 33 wt.% glycerol samples (Table 1.6.4), water absorption increases the height of peaks P1, P2 and P3, changing pseudo-components: a) W_f from 1.1 to 4.3 wt.%; b) GW_b from 4.5 to 6.8 wt %; and c) Glyc from 23.8 to 27.4 %.

As a result, free water increases 3.2 wt.%, bonded water increases 2.3 wt.% and the water in P3 also increases 3.6 wt.%. Adding these quantities and considering the residual moisture in dry bioplastic (1.1 wt.%), the estimated water content in the bioplastic is 10.2 wt.%, a value that agrees with the experimental moisture obtained for WG/G with 33 wt.% (see Experimental Section). In addition, these results confirm that peak P3 mainly arises from glycerol volatilisation (and some water). Similarly, Peak P2 refers to a water/glycerol blend, where some glycerol evaporates at low temperature and water release would be affected by certain interaction with the protein matrix (Sun et al., 2007). As calculated from gluten DTG

curves, water release undergoes a significant delay in its temperature range, taking place between 60 and 200ºC (e.g. see pseudo-components W_f and W_b in Figure 1.6.4).

Likewise, glycerol volatilisation profile is strongly altered by both the water content and interaction with the protein matrix, as may be deduced from simulation shown in inset of Figure 1.6.6B. These simulated curves were obtained using the kinetic parameters calculated for pseudo-components GW_b and Glyc. As may be seen, close to 150ºC, the volatilization of glycerol and bonded-water take place simultaneously, leading to a shoulder in DTG curves, more apparent in the moist bioplastic (WG/G 33 wt.% glycerol).

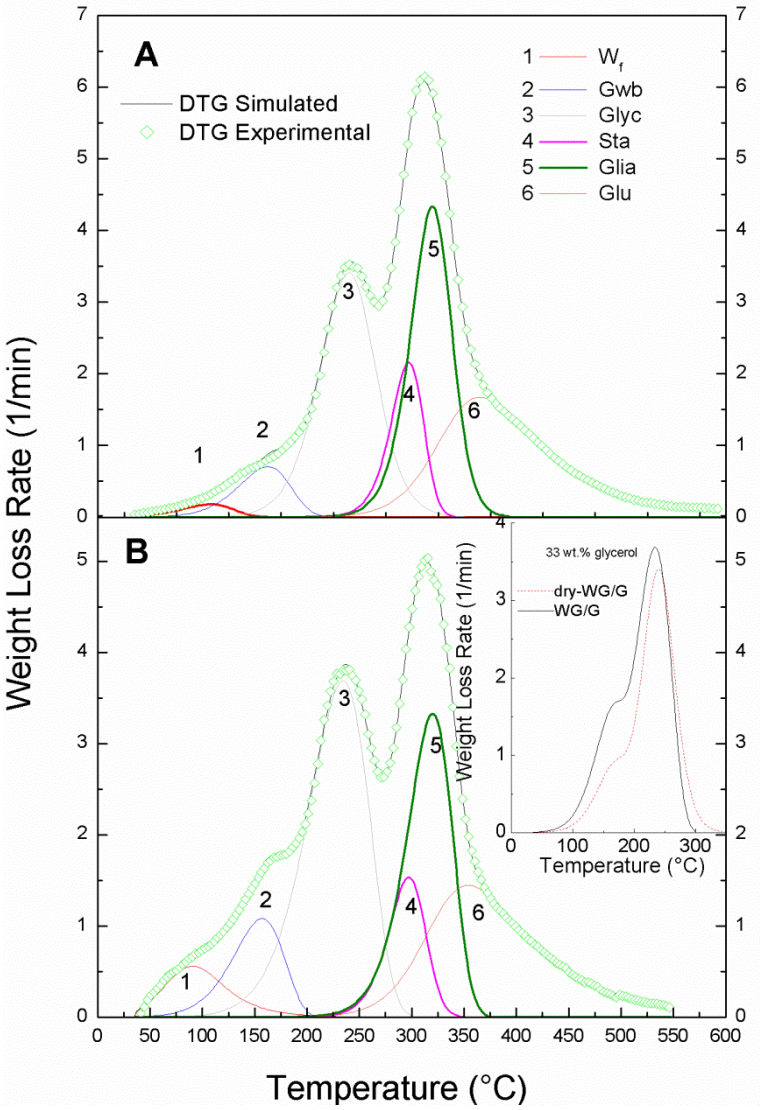

Figure 1.6.6 *Simulation of the thermal degradation of a gluten-glycerol based bioplastic under inert atmosphere (pyrolysis): A) dry bioplastic (33 wt.% glycerol), B) moist bioplastic (33 wt.% glycerol). Inset: Simulation of the plasticiser release from the protein matrix.*

On the other hand, instead of the sudden drop observed in the pure glycerol DTG curve above 240ºC (Figure 1.6.2A), the protein matrix seems to hinder the glycerol release, which is delayed about 50ºC and shows an apparent volatilisation tail up to 300ºC (see bioplastic dry-WG/G with 33 wt.%, inset of Figure 1.6.6). A fact pointing out that glycerol plays relevant plasticizing roles in the protein matrix through diverse physicochemical interactions (hydrogen bonds, hydrophobic, etc.). However, such interactions seem to be influence by bioplastic moisture. Thus, it should be noticed that the presence of water promotes glycerol weight loss, shifting its peak from 240ºC for the dry bioplastic to 230ºC for the moist bioplastic WG/G with 33 wt.% glycerol (Figure 1.6.6).

Estimation of bioplastic composition from thermogravimetry analysis

As previously seen for gluten isolate, bioplastic composition can be estimated using the weight loss calculated for each pseudo-component during its volatilization and char oxidation (Table 1.6.4). Accordingly, data shown in Table 1.6.5 have been obtained in dry and ash free basis and assuming, for dry bioplastics, that pseudo-component WG_b is pure glycerol (and, therefore, without water). As may be seen, there is a good agreement between calculated and the actual bioplastic composition (see experimental section), e.g. estimated plasticiser concentration was for dry-WG/G with 33 wt.% about 32.2 wt.% glycerol and for dry-WG/G with 40 wt.% bioplastic 39.6 wt.% glycerol.

Table 1.6.5 Bioplastics composition based on pseudo-components (dry and ash free basis).

dry-Bioplastic	***GW_b* (wt.%)**	***Glyc* (wt.%)**	***Sta* (wt.%)**	***Glia* (wt.%)**	***Glu* (wt.%)**
33 wt.% glycerol	6.5	25.7	8.0	31.2	28.5
40 wt.%glycerol	8.8	30.8	7.5	27.6	25.3

2. Effect of formulation and processing of protein-based bioplastics

According to the results obtained in chapter 1, it was concluded that potato and rice proteins were good raw materials for producing bioplastics. These new materials might be attractive for the plastics industry, especially in view of the similarity of their properties to LDPE and their low water absorption compared to starch and other proteins (e.g., wheat gluten and zein). However, we believe that incorporating wheat gluten into rice and potato protein based bioplastics is beneficial for the flexibility of the resulting material. This new material would display characteristics of both proteins, that is, the flexibility and thermomouldability of wheat gluten alongside the desirable water absorption properties of rice and/or potato proteins. In this study the plasticizer used was glycerol, (G) which was fixed at 40 wt.%, with the protein concentration accounting for the remaining 60 wt.%. Thus, the first part of this chapter deals with blends of rice protein and wheat gluten thermomechanically mixed at different ratios, whilst the second part concerns potato protein and wheat gluten, mixed at different ratios but processed at 80°C and thermoset at 120°C. Finally, a specific formulation was mixed at 80°C and was then extruded with different temperature profiles. The formulations for such protein based bioplastics are shown in Table 2.2 in Materials and Methods.

2.1 Thermomechanical processing of wheat gluten/rice protein-based bioplastics

Thermoplastic processing

Figure 2.1.1 shows the evolution of torque and temperature for different ratios of wheat gluten/rice protein blends, plasticized with 40 wt.% of glycerol over the course of the mixing process, carried out at 50 r.p.m. As mentioned above in respect of the mixing process of proteins and plasticizer, the occurrence of a torque overshoot until a maximum peak of torque is reached suggests a dramatic evolution of the protein structure upon mixing. This behaviour can be considered typical of wheat gluten, as described in the first chapter and also by Jerez et al., 2005a. Blends with wheat gluten/rice protein ratios of 1:0, 3:1 and 1:1 showed

a torque evolution with three different regions as described in chapter 1 for the processing of the wheat gluten blend. An increase in the induction region can be observed as rice protein concentration increased. This means that samples with higher concentrations of rice protein take longer to reach the maximum value of the torque. However, there was no distinguishable peak for torque for the sample with wheat gluten/rice protein ratio of 1:1. In this case, after the induction region the torque profile was characterized by a continuous increase, and then a tendency towards steady state values of torque.

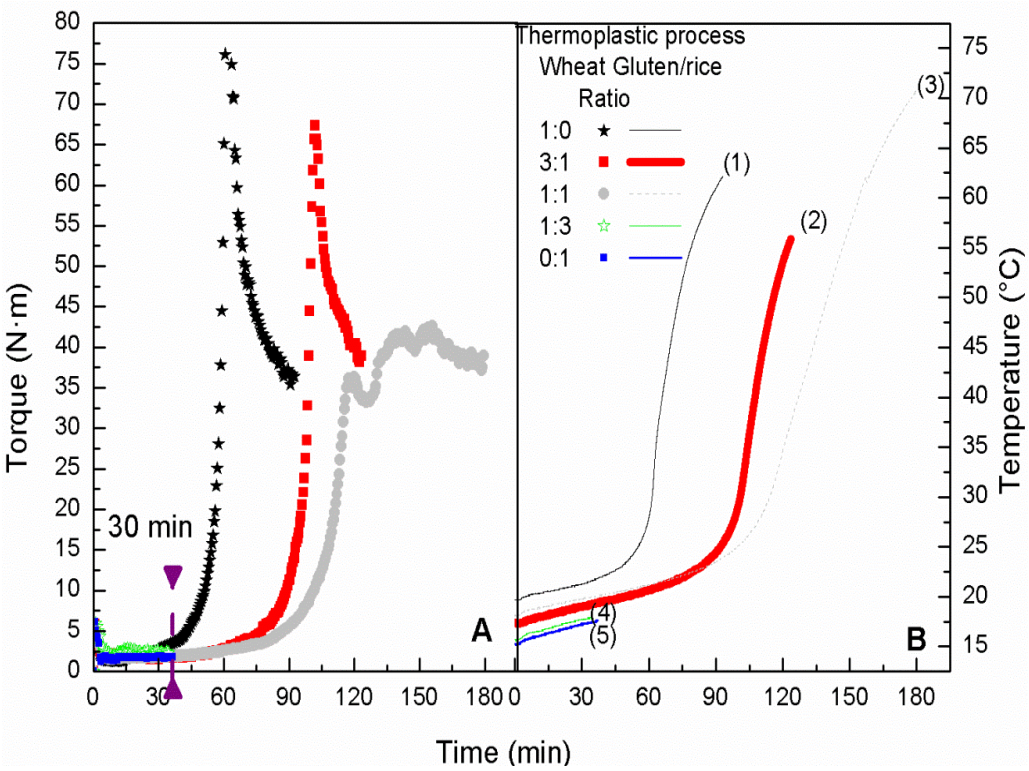

Figure 2.1.1 Evolution of torque (A) and temperature (B) during the mixing process for wheat gluten/rice protein at different ratios.

A decrease in the peak torque value can be observed as rice protein concentration increases. This decrease is probably due to the short amino acids present in rice protein which would lower the elasticity in the blend (Oszvald et al., 2007; Gujral and Rosell, 2004; Sivaramakrishnan et al., 2004).

The temperature profile for blends with wheat gluten/rice protein ratios of 1:0, 3:1 and 1:1 was characterized by two regions of increase, the first slight and the second exponential (Figure 2.1.1B). This behaviour corresponds to the evolution of torque values mentioned above.

The mixing time t_{mix} for blends with wheat gluten/rice protein ratios of 1:0, 3:1 and 1:1 was estimated throughout as 1.5 t_{peak}. Figure 2.1.1 and Table 2.1.1 show that the maximum value of torque (the torque overshoot) is reached after more than 60 min mixing for all these blends. This is longer than the mixing time for wheat gluten or rice protein, and might be due to the low, and slow, interaction of both proteins with the plasticizer; especially the rice protein. Hence, it is likely to take longer to reach the maximum peak as rice protein content increases in the blends, rendering the process unsuitable for industrial applications as it would incur a waste of time and energy. To mimic industrial processing, the mixing process of samples with wheat gluten/rice protein ratios of 1:3 and 0:1 was stopped after about 30 min when samples still were in the induction region (Figure 2.1.1A). Consequently it was necessary to apply a post-treatment to get a final material with suitable properties. The temperature evolution of these samples displayed a non-increase, which corresponds to the non-increase in torque during the mixing process (Figure 2.1.1B).

Table 2.1.1 Specific Mechanical Energy (SME), elapsed time at the overshoot (t_{peak}), and maximum temperature (T_{max}) reached during the mixing process.

Bioplastics (40 wt.% plasticizer)	**Wheat Gluten:Rice protein**	**t_{peak} (min)**	**T_{max} (ºC)**	**SME (kJ/kg)**
WG/G	1:0	62	62	11018
WG/R/G	3:1	102	55	8993
WG/R/G	1:1	153	70	16939

Similarly, the protein ratio also affected the specific mechanical energy (SME) required to obtain a material with suitable mechanical properties, and this data, calculated according to Equation 1.1.1, chapter 1, is likewise included in Table 2.1.1 for the three blends. A significant increase in SME values is observed for sample with a ratio of 1:1 compared to the blend with a ratio of 1:0. By contrast, a decrease in SME values for the sample with a ratio of 3:1 was observed.

In addition, the flow of the blends under extrusion was studied. Figure 2.1.2 presents the viscous flow curve at 90ºC for the wheat gluten/rice protein blend at a ratio of 1:1, collected immediately after the mixing process. A significant influence of rice protein can be observed on the blend due to a decrease in sample viscosity compared to the wheat gluten blend.

The power law model fits the shear-thinning behaviour observed well (see Equation 1.1.2 in chapter 1). Table 2.2.2 presents the values of the parameters at 90ºC for the wheat gluten/rice protein 1:1 blend. As can be observed, a remarkable decrease in the consistency index, and an increase in flow index, are found when rice protein was added to the blend. In addition, these results showed that the viscosity at 90ºC of WG/R/G was significantly lower than the viscosity of low density polyethylene processing at 160ºC.

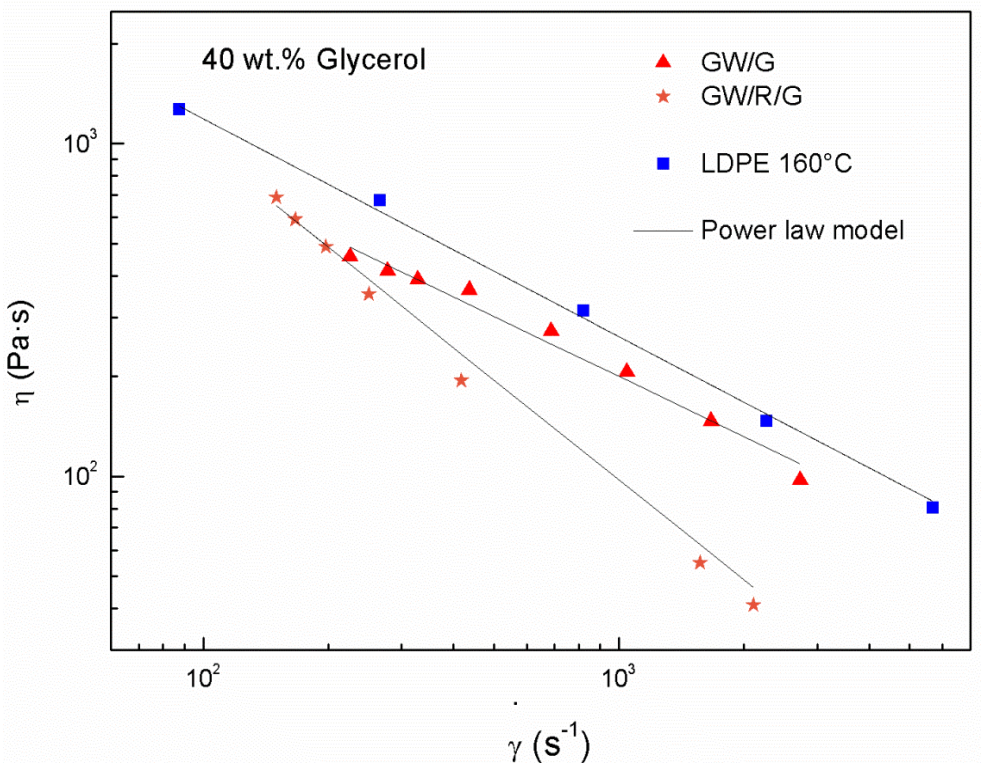

Figure 2.1.2 Viscous flow curves at 90ºC for wheat gluten/rice protein 1:1 ratio.

Table 2.2.2 Influence of protein composition on the power law parameters, consistency (k) and flow index (n) for the different blends studied.

Composition	**Parameters of Power-low model**	
	***k* (*Pa·s^n*)**	***n***
WG/G	12557	0.40
WG/R/G	97286	0.04
LDPE at 160 ºC	7846	0.47

Thermomechanical properties

Figure 2.1.3 shows the behaviour of two viscoelastic functions (E* and tan δ) with temperature for wheat gluten/rice protein samples at a ratio of 3:1, obtained by the mixing process and thermomoulded at three different temperatures. The results for these blends demonstrated that an increase in thermosetting temperature generally led to an increase in the complex modulus, this being more evident when the thermosetting temperature was raised from 90 to 120ºC. E* decreased to a minimum at 110ºC and then underwent a remarkable increase for samples thermoset below 120ºC. This increase was more evident for samples thermoset at 90ºC with similar E* values to the glassy region ($E^*=10^6$ Pa at 160ºC). This phenomenon may be related to an incomplete protein denaturation during its preceding thermomechanical processing. Finally, above 160ºC, a decrease in the slope of E* growth was noticed and a minimum in tan δ took place at 150ºC for samples thermoset at temperature below 120ºC.

It is worth mentioning that this behaviour is characteristic of wheat gluten-based bioplastic with 33 wt.% glycerol as shown in the first chapter (Figure 1.2.1). By contrast, E* values did not show any significant increase for the sample thermoset at 140ºC. In this case, E* decreased to a plateau region such that after 90ºC the modulus remained constant with temperature. Further, bioplastics moulded at 140ºC did not show a remaining thermosetting potential (see Figure 2.1.3). Indeed, greater protein thermal denaturation is expected in bioplastics thermoset at 140ºC, leading to more structured systems with higher values for the linear viscoelastic functions. There was no evidence of a maximum for tan δ with temperature; however, a decrease in the values of tan δ and a decrease in the temperature of the minimum for tan δ as thermosetting temperature increased was observed.

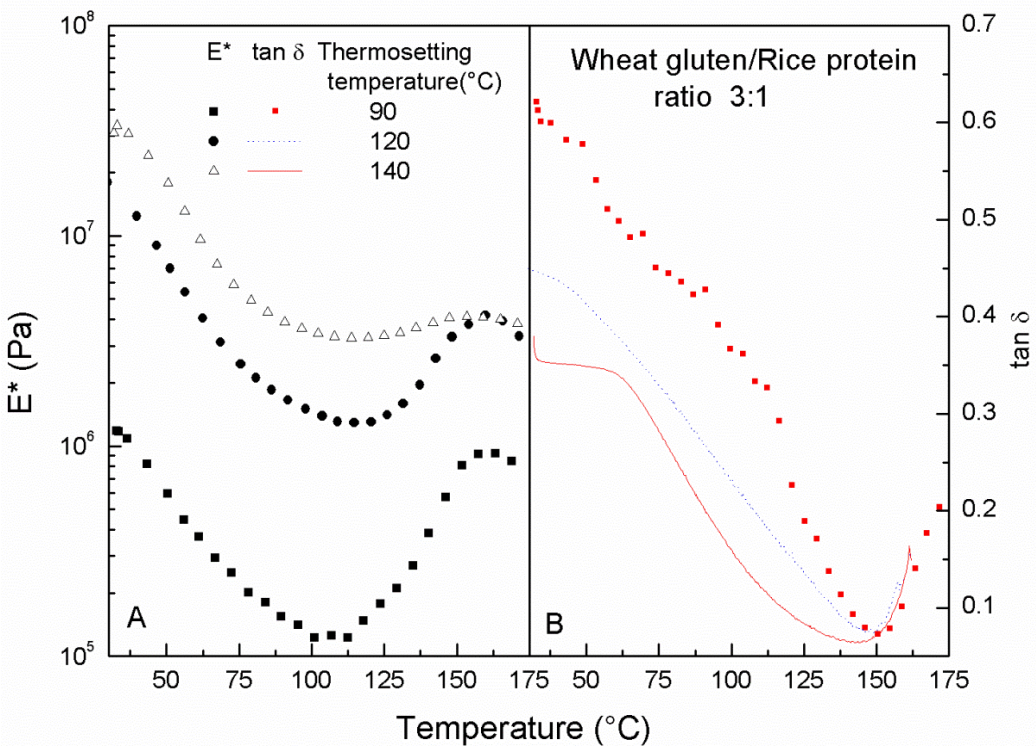

Figure 2.1.3 Dynamic mechanical thermal analysis results, complex modulus (A) and tan δ (B) for wheat gluten/rice protein samples with a ratio of 3:1 obtained by the mixing process after thermomoulding at three different temperatures.

Figure 2.1.4 shows DMTA scans from 30 to 180ºC for wheat gluten/rice protein 1:1 blends, as a function of thermosetting temperature. An increase in the moulding temperature induced a significant increase in the complex modulus compared to the same blends with a ratio of 3:1 thermoset at 90ºC. A non-significant difference in the evolution of the complex modulus was observed for samples thermoset at 120ºC compared to those at 140ºC. In this case, all samples described a decrease in the complex modulus from the glassy region to the plateau region. This plateau region was wider when the thermosetting temperature was increased. After the plateau region, the sample thermoset at 90ºC exhibited a remarkable increase in the viscoelastic modulus with temperature up to a maximum of around 150°C, and finally, a decrease in the slope of the modulus was observed. In the same way, samples thermoset at 120 and 140ºC showed similar behaviour until the end of the plateau region. Thus, samples thermoset at 120 and 140°C underwent an increase in the complex modulus, at higher temperatures (close to 160°C) and then also showed a decrease in the modulus with temperature.

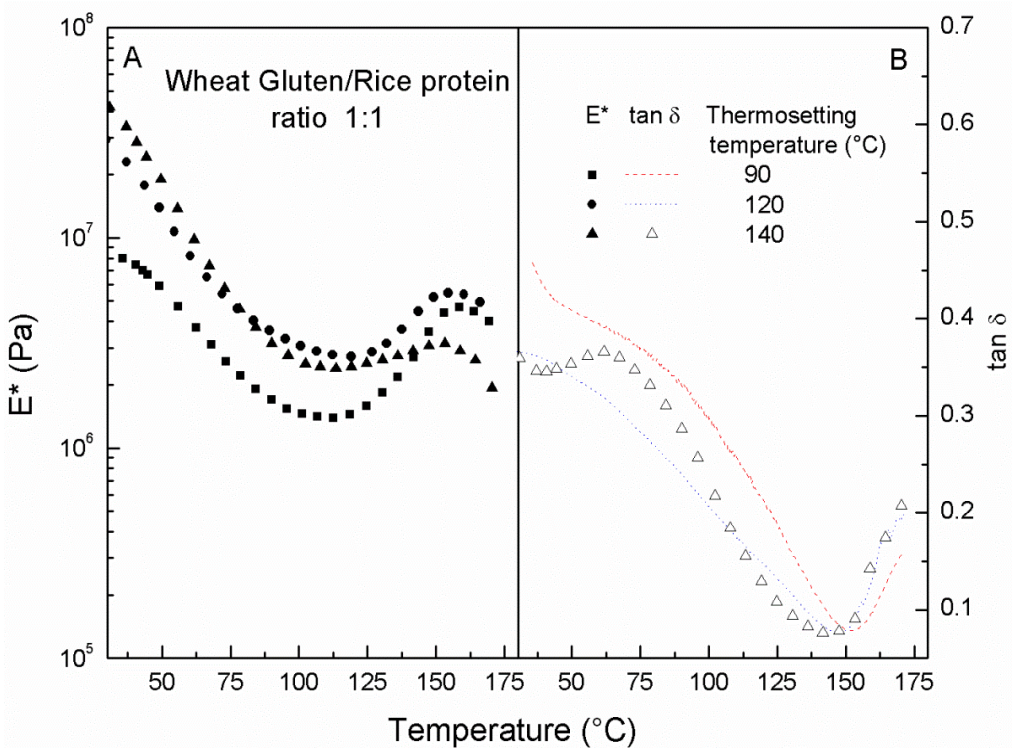

Figure 2.1.4 Dynamic mechanical thermal analysis, complex modulus (A) and tan δ (B) for wheat gluten/rice protein samples with a ratio of 3:1 obtained by the mixing process and then thermomoulded at three different temperatures.

Figure 2.1.4B shows the evolution of tan δ with temperature for the wheat gluten/rice protein blends with a ratio of 1:1. There was no evidence of a maximum in tan δ with temperature for sample thermoset at temperature below 120°C, but a maximum in tan δ located at 60°C for the sample themoset at 140°C was found. Also evident was a decrease in the minimum of tan δ as thermosetting temperature increased. This behaviour was also found for the 3:1 wheat gluten/rice protein blends.

Figure 2.1.5 shows DMTA scans from 30 to 180ºC for wheat gluten/rice protein blends with a ratio of 1:3 in terms of thermosetting temperature. An increase in this temperature led to a significant increase in the complex modulus, more evident in samples thermoset at 90 and 120ºC. All samples underwent a decrease in the complex modulus from the glassy region to a minimum at 120ºC, at which point each sample exhibited different behaviour. The samples thermoset at 120 and 90ºC showed an increase in the complex modulus as temperature increased. However, these samples had different complex modulus values in the glassy region, with the sample thermoset at 90ºC being lower (below 10^7 Pa). This sample displayed almost no difference between the complex modulus values in the glassy region and the minimum, which exhibited a value above 10^6 Pa. This could be evidence of a low

thermosetting potential for this sample. Furthermore, the sample thermoset at 120ºC exhibited complex modulus values close to those of the one thermoset at 140ºC. On the other hand, samples thermoset at 140ºC showed a plateau region after the minimum in the complex modulus until the temperature reached 160ºC, after which the modulus decreased slightly.

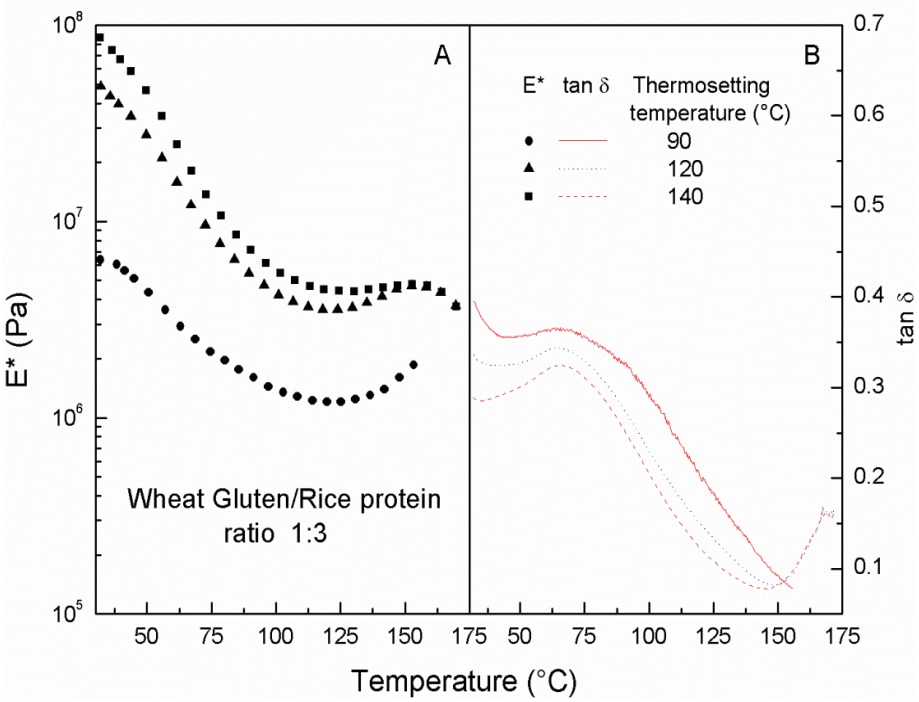

Figure 2.1.5 Dynamic mechanical thermal analysis results: complex modulus (A) and tan δ (B) for wheat gluten/rice protein samples with a ratio of 1:3 obtained by the mixing process after thermomoulding at three different temperatures.

The evolution of tan δ with temperature for the wheat gluten/rice protein blend (1:3 ratio) is shown in Figure 2.1.5B. A maximum for tan δ at a temperature close to 70°C was observed, as well as a minimum at a temperature around 150-160ºC. Also notable, was that the minimum tan δ occurred at lower temperatures as the thermosetting temperature increased.

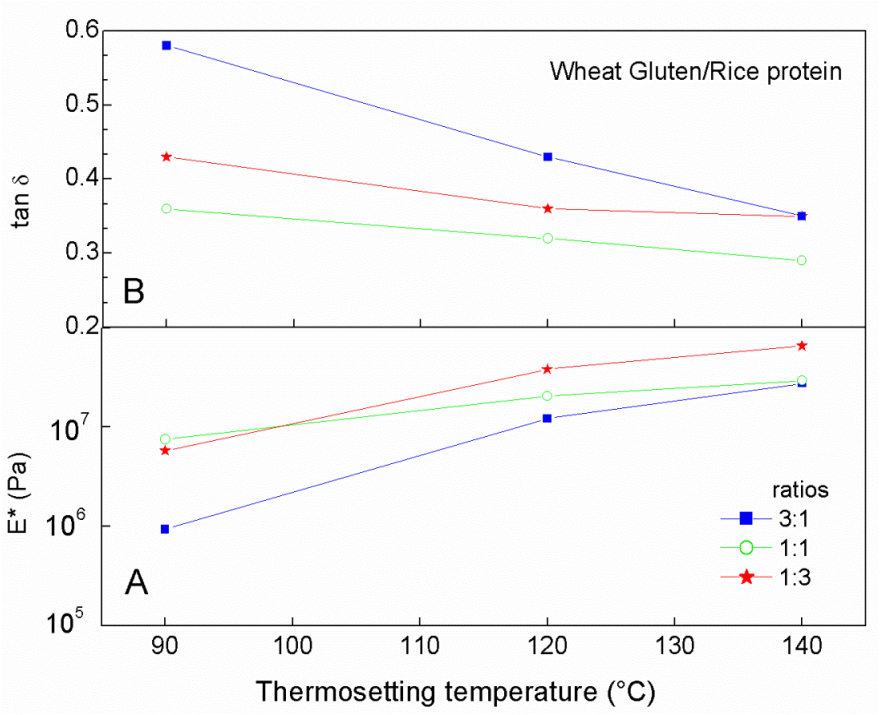

Figure 2.1.6 Effect of protein ratio and thermosetting processing on the complex modulus (A) and tan δ values (B) for wheat gluten/rice protein samples.

The influence of different protein ratios on the viscoelastic properties of both proteins (wheat gluten and rice protein) is shown in Figure 2.1.6. The corresponding values of complex modulus (A) and the tan δ (B) at 40°C were chosen for the sake of comparison. All samples exhibited an increase in the complex modulus as thermoulding temperature increased, although this increase was not significant beyond themosetting temperatures of 120°C. As expected, E* increased for samples with higher rice protein content. In addition, the complex modulus for samples with the same proportion of wheat gluten and rice protein was barely affected by the thermomoulding temperature. On the other hand, tan δ values at 40°C decreased as thermosetting temperature increased. Also, an increase in the rice protein content led to an increase in tan δ values. As expected, samples with high wheat gluten content showed more wheat gluten behaviour and vice versa.

Figure 2.1.7 shows the DSC thermogram for wheat gluten/rice protein blend with a ratio of 1:1 thermoset at 120ºC. The thermograms showed an endothermic peak located at ~130ºC, some 8ºC lower than that obtained for the rice protein blend. The denaturation of protein in the wheat gluten/rice protein blend occurred within a wide temperature range, and therefore the low energy necessary for this transition suggests a higher degree of denaturation for the wheat gluten/rice protein blend than for the rice protein blend.

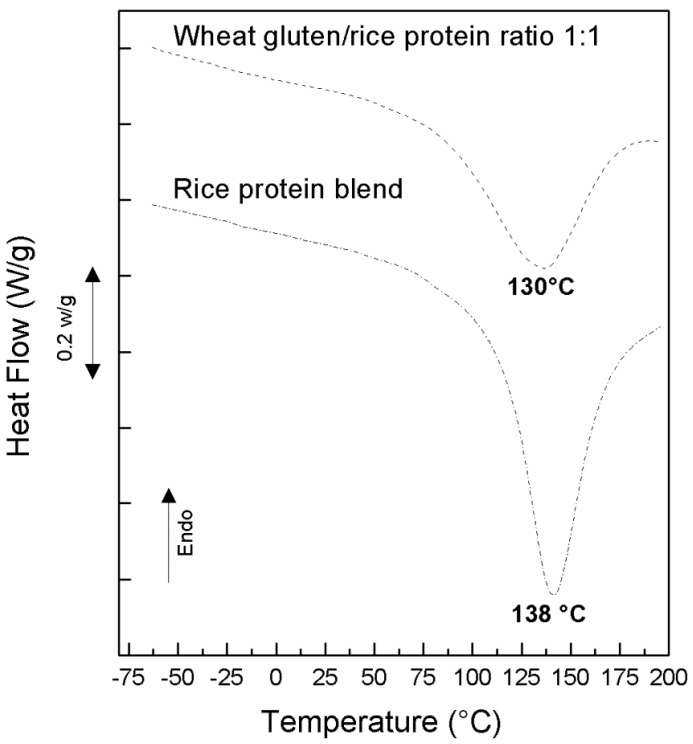

Figure 2.1.7 DSC thermograms for different bioplastics thermoset at 120ºC.

Water absorption properties and molecular weight distribution characterization

Figure 2.1.8 shows the water absorption values for wheat gluten/rice protein-based bioplastic manufactured with different ratios and under different thermo-moulding conditions. A general observation for all the samples is that the water absorption values decreased as rice protein content increased. This behaviour correlates with the high complex modulus values found for the rice protein samples (Figure 2.1.6), such that higher values of the complex modulus led to lower water absorption.

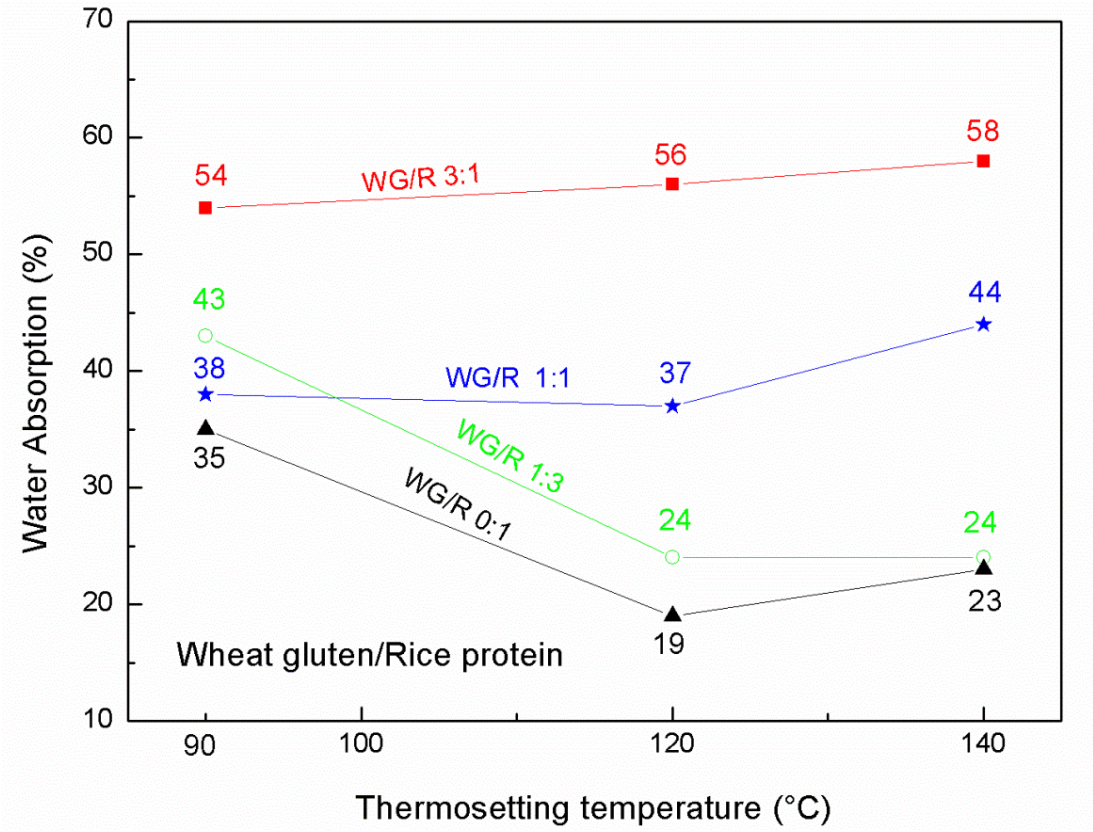

Figure 2.1.8 Water absorption for wheat gluten/rice protein blends (WG/R) at different protein ratios, after different thermosetting temperatures.

In the case of all samples, water absorption was affected by thermosetting temperature [to varying degrees]. The samples with a wheat gluten to rice protein ratio of 1:3 (24 wt.%) showed identical water absorption values when thermoset at 120 and 140ºC, the lowest amongst the samples, while samples with a ratio of 1:1 (~37 wt.%) showed a non-significant difference when thermoset at 90 and 120ºC. The highest water absorption value for these samples was at a thermosetting of 140ºC (44 wt.%). The samples with highest content of wheat gluten showed no significant changes in water absorption with thermosetting temperature, and exhibited the highest values of water absorption across the whole range of thermosetting temperatures studied.

As mentioned above, the combination of both proteins (rice protein and wheat gluten) exhibited properties of each. Figure 2.1.9 shows the results of the characterization of the molecular weight of individual proteins and peptides in the 1:1 wheat gluten/rice protein blend thermoset at 120ºC, which was performed by sodium dodecyl sulphate-polyacrylamide gel electrophoresis (SDS PAGE) under reducing conditions. The figure shows that wheat gluten/rice protein-based bioplastic (lane 1) presented the same bands for both proteins (wheat

gluten and rice protein). The three bands indentified as gliadins and glutenins showed evidence of wheat gluten (lane 3) while the three bands indentified as glutelin and albumins exhibited evidence of rice protein in the blend (lane 2). This result demonstrates that the blend might combine characteristics and behaviour of both proteins.

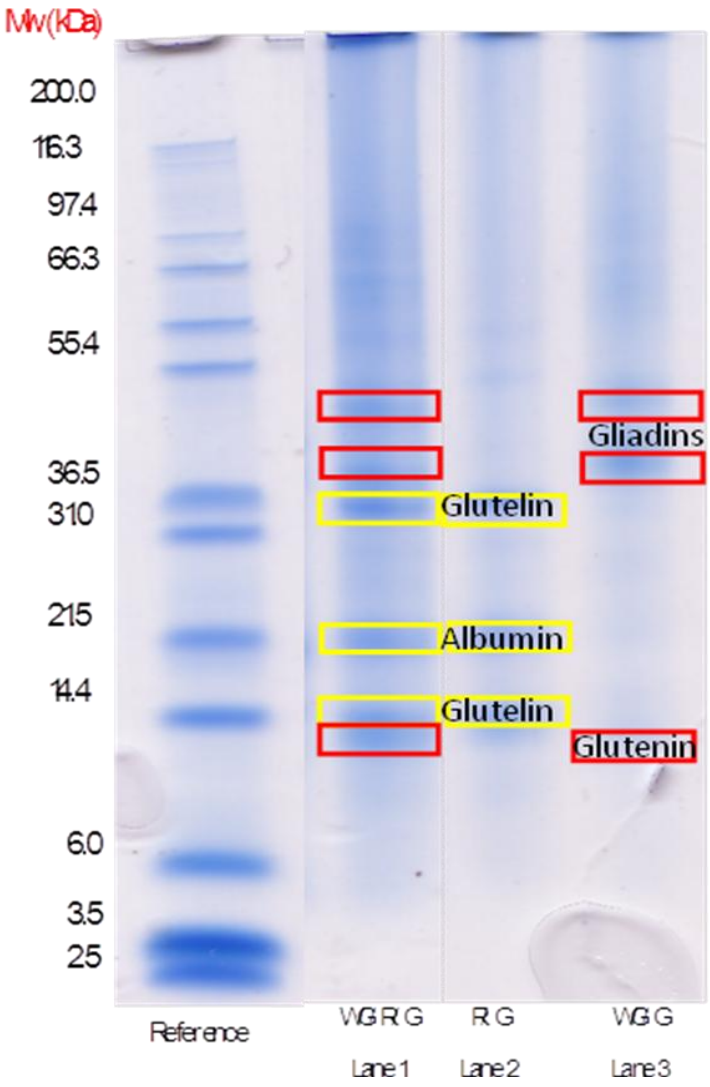

Figure 2.1.9. SDS-PAGE for wheat gluten/rice protein/glycerol (lane 1), rice protein/glycerol (lane 2) and wheat gluten/glycerol (lane 3) under reducing conditions.

2.2 Thermomechanical processing of wheat gluten/potato protein based bioplastics

Thermoplastic processing at high temperature

Figure 2.2.1 shows the evolution of torque for different ratios of wheat gluten/potato protein bioplastic plasticized with 40 wt.% of glycerol during the process of mixing at 50

r.p.m. The blends showed different torque evolution according to the formulation. As can be observed, wheat gluten/potato protein in 1:1 ratio processed at room temperature presented low torque values; however, when the same blend was processed at 80°C, a considerable increase in the torque values was observed (from 5 to 40 N·m).

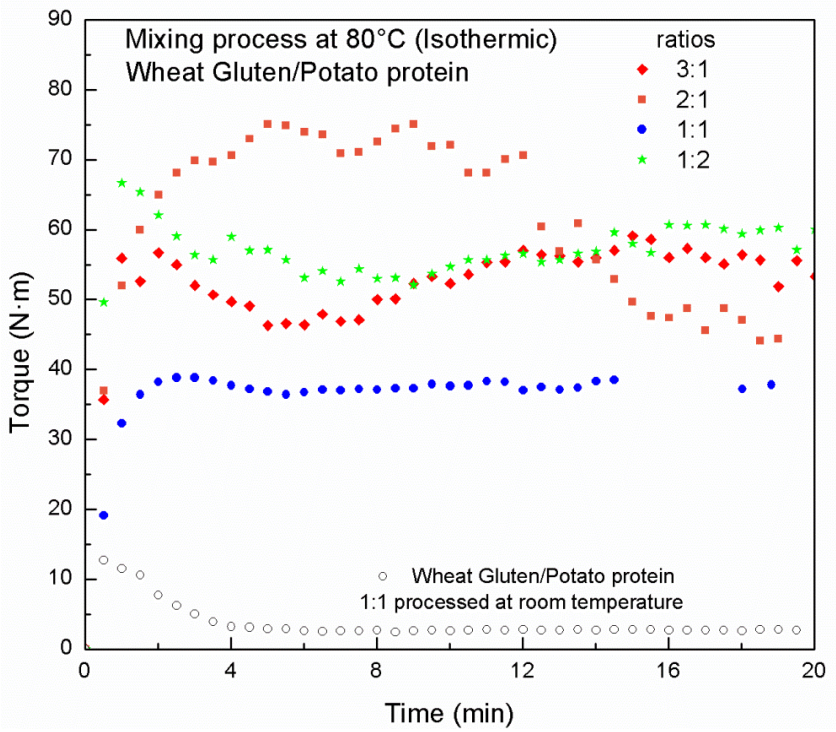

Figure 2.2.1 Evolution of torque during the mixing process at 80ºC in isothemic conditions for wheat gluten/potato protein blends at different protein ratios.

The torque profile for blends of at least 50% wheat gluten content presented two regions, the first exhibiting an instantaneous increase in torque and the second constant values. On the other hand, the torque profile for the sample with the highest potato protein content exhibited an increase in torque with mixing time up to a maximum value (at 6 min), which was higher than that for samples containing less potato protein. Finally, a torque decay was observed.

Table 2.2.3 shows the Specific Mechanical Energy (SME) required during the mixing process. For the sake of comparison, t_{mix} was set to 15 minutes, due to the absence of an evident maximum value of torque for all samples. This parameter was calculated for the bioplastic samples studied as it was mention in Equation 1.1.1 (chapter 1).

Table 2.2.3 Specific Mechanical Energy (SME), expended during the mixing process.

Bioplastics 40 wt.% plasticizer	**Wheat gluten: potato protein ratios**	**$T_{processing}$ (ºC)**	**SME (kJ/kg)**
Wheat gluten	1:0	25	11018
WG/P/G	3:1	80	4118
WG/P/G	2:1	80	5281
WG/P/G	1:1	80	2909
WG/P/G	1:2	80	4510
WG/P/G	1:1	25	403

The SME values for all samples were affected by the protein ratio, in the same way that it affected the torque profile. It can be observed that the addition of potato protein to the formulation significantly reduced the SME values compared to wheat gluten-based bioplastic. Thus, the highest SME value occurred with the sample with a wheat gluten/potato protein ratio of 2:1, whilst the lowest value was found for the sample with both proteins in equal ratio. Meanwhile, the wheat gluten/potato protein ratios of 3:1 and 1:2 showed similar values for SME. The mixing process at 80ºC also affected the SME values, such that an increase in mixing temperature led to a significant increase in SME.

Figure 2.2.2 presents the viscous flow curves for the wheat gluten/potato protein blend (in 1:1 ratio), collected just after the mixing process. A significant increase in the viscosity of the sample can be observed in comparison with the wheat gluten-based blend. Indeed, the viscosity of this new material was even higher than that of low density polyethylene (LDPE) at 160ºC. This behaviour is related to hydrophobic protein interaction, which is more prevalent in potato protein than in wheat gluten and rice protein.

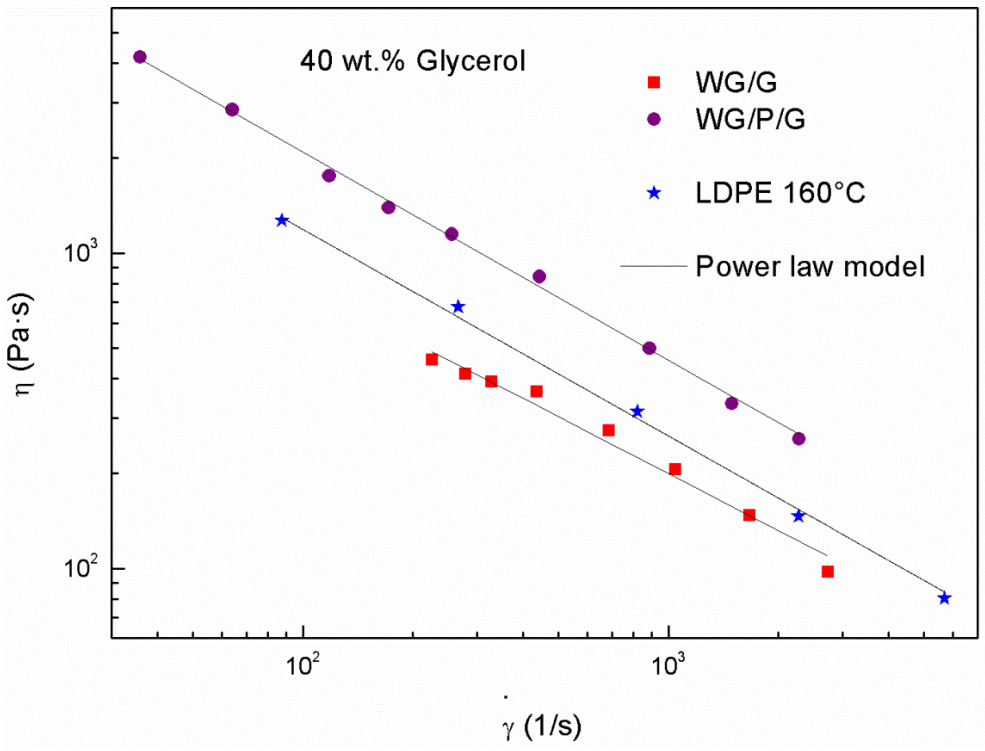

Figure 2.2.2 Viscous flow curves at 90ºC for wheat gluten/potato protein in a ratio of 1:1.

Table 2.2.4 Influence of protein composition on the consistency (k) and flow index (n) of blends studied.

Composition	**Parameters of Power-law model**	
	***k* (*Pa·s^n*)**	***n***
WG/G	12557	0.40
WG/P/G	43821	0.33
LDPE at 160 ºC	7846	0.47

The power law model fits the observed shear-thinning behaviour fairly well (Equation 1.1.2 in chapter 1). Table 2.2.4 presents the values of the model parameters for the 1:1 wheat gluten/rice protein blend. As can be observed, a remarkable increase in the consistency index and a decrease in the flow index were found when potato protein was added to the blend. As compared with low density polyethylene (LDPE) under typical extrusion conditions (160ºC, and a shear rate window between 100-300 s^{-1}), the consistency index of the LDPE was lower and the flow index was higher than the values calculated for the wheat gluten/potato protein blend.

Thermomechanical properties

Figure 2.2.3 shows the behaviour of two viscoelasticity functions (E* and tan δ) with temperature, for different ratios of wheat gluten/potato protein mixed at 80ºC and then thermomoulded at 120ºC. The complex modulus for these blends, which mix both proteins, falls between the E* for potato protein-based and wheat gluten-based bioplastics. They proved to be more thermo-stable than wheat gluten, but returned complex modulus values lower than those for potato protein, as can be seen in Figure 2.3.3.

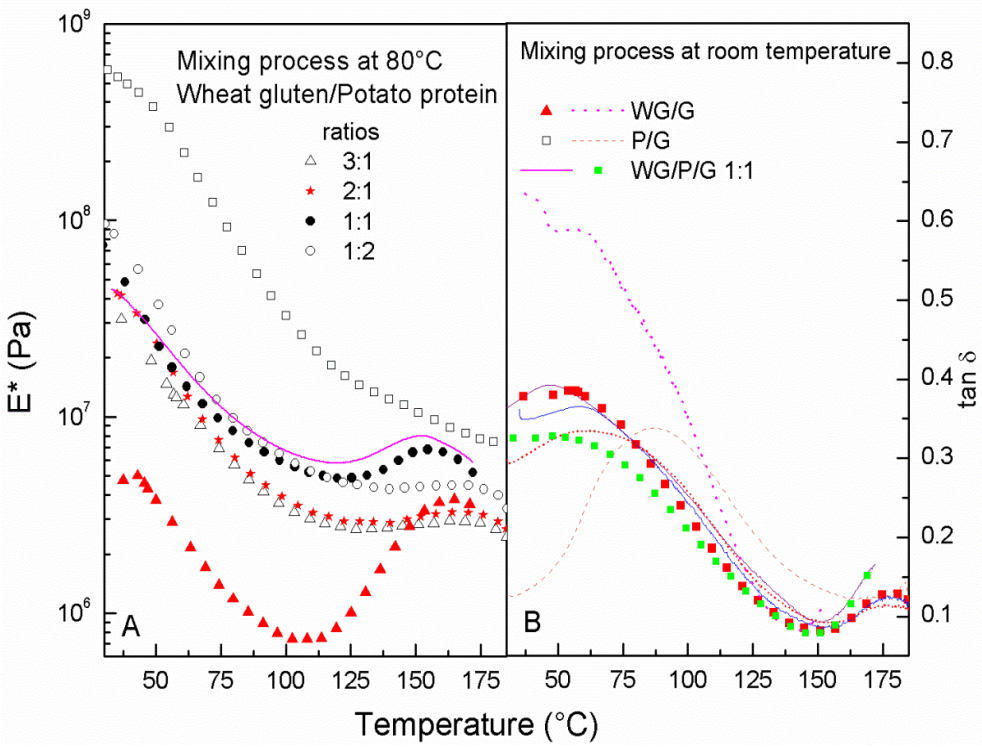

Figure 2.2.3 Dynamic mechanical thermal analysis results, complex modulus (A) and tan δ (B) for wheat gluten/potato protein samples at different protein ratios, mixed at 80°C and thermomoulded at 120°C.

The samples can be classified into two groups, the first, samples with low complex modulus exhibiting a viscoelastic behaviour close to that of wheat gluten, and the second, samples with high complex modulus exhibiting a viscoelastic behaviour close to that of potato protein. Accordingly, the first group includes bioplastics formulated with wheat gluten/potato protein ratios of 3:1 and 2:1. A decrease in E* can be observed for both samples, the with the slope of E* changing close to 100ºC, after which it enters a quite large plateau region from 120 to 180ºC. These samples did not show a clear maximum value for tan δ, although a minimum for both samples was found close to 150ºC (Figure 2.2.3B). The second group

includes bioplastics formulated with ~~a~~ wheat gluten/potato protein ratios of 1:1 and 1:2. The 1:1 blend saw a decrease in E* with temperature until a minimum was reached, after which a slight increase was followed by a renewed decrease. The high temperature during the mixing process did not affect the evolution of the complex modulus with temperature for this sample but it led to a slight decrease in the complex modulus. This means that processing at high temperature might help the interaction between proteins and plasticizer.

Meanwhile, the 1:2 wheat gluten/potato protein sample exhibited an evolution of the complex modulus with temperature similar to samples in the first group, although the complex modulus values were higher in this case. Also, a minimum in tan δ was observed close to 150ºC for this group of samples (Figure 2.2.3B).

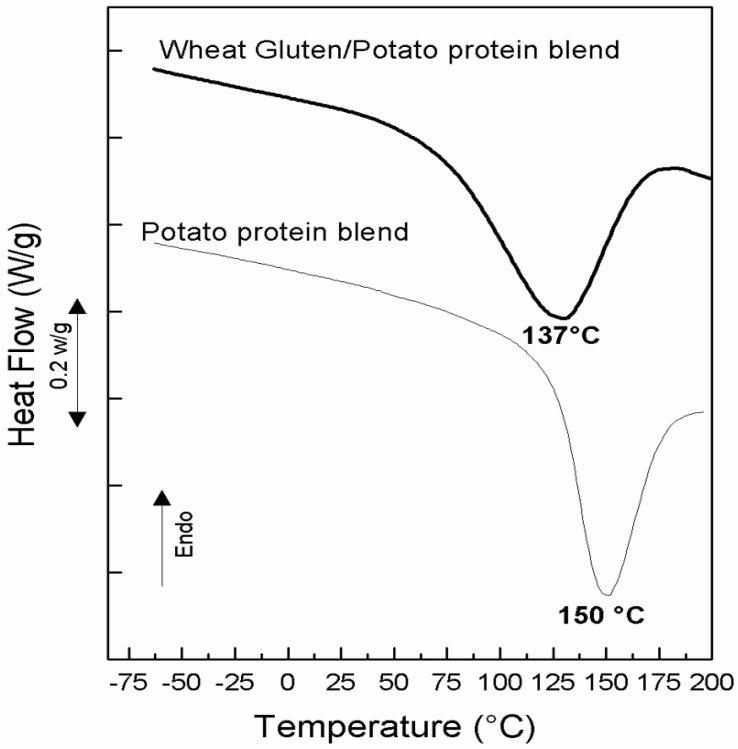

Figure 2.2.4 DSC thermograms for different bioplastics thermoset at 120ºC.

Figure 2.2.4 shows the DSC thermoscans for the 1:1 wheat gluten/potato protein blend, mixed at room temperature and thermoset at 120ºC. The samples showed an endothermic peak located at ~137ºC, which is 13ºC lower than the temperature found for the sample plasticized with potato protein. This decrease of the denaturation temperature might be

due to the presence of wheat gluten in the formulation. In addition, the denaturation of the wheat gluten/potato protein blend occurred within a wider temperature range than potato protein blend.

Water absorption properties and molecular weight distribution characterization

The formulation and thermal history seem to produce significant differences in the types of network formed. Figure 2.2.6 shows the influence of formulation on the water absorption values for wheat gluten/potato protein-based bioplastics at different protein ratios, mixed at 80°C and thermomoulded at 120°C. As can be observed, there was no significant difference for wheat gluten/potato protein samples at ratios of 3:1, 2:1, and 1:2, by process mixing at 80°C. These samples exhibited water absorption values of around 35 wt.%. However, the sample with a ratio of 1:1 presented the lowest water absorption value (23 wt.%).

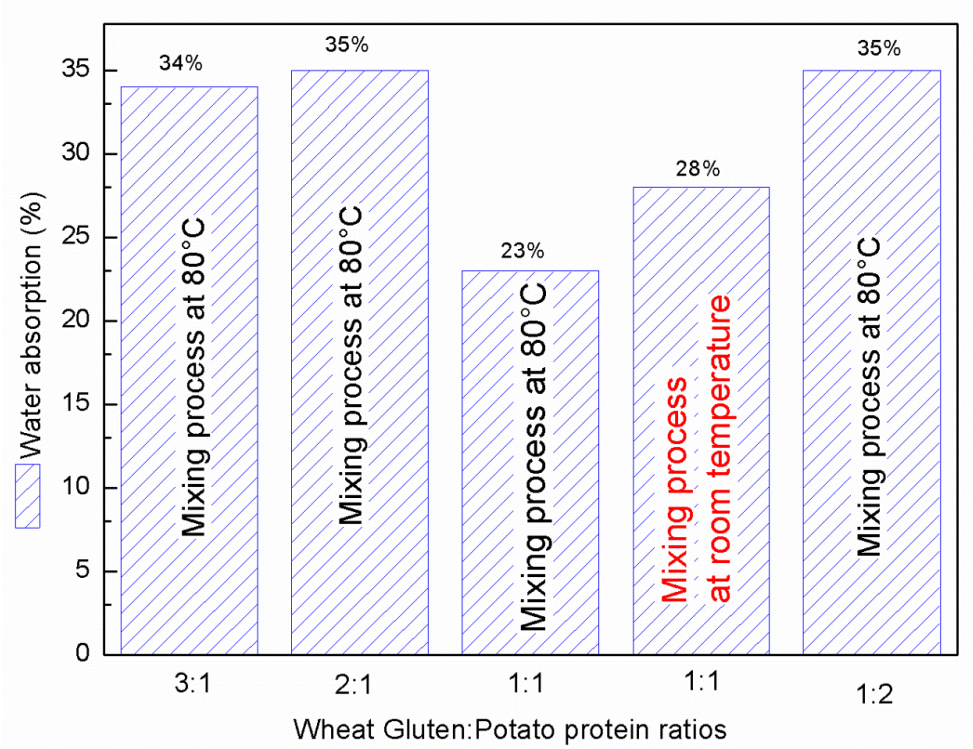

Figure 2.2.6 Water absorption for wheat gluten/potato protein blends at different ratios, mixed at 80°C and thermomoulded at 120°C.

The high temperature during the mixing of the 1:1 wheat gluten/potato protein sample led to a reduction in water absorption from 28 to 25 wt.%. These results suggest that the processing temperature produces significant differences in the type of network formed, most evident in the water absorption behaviour.

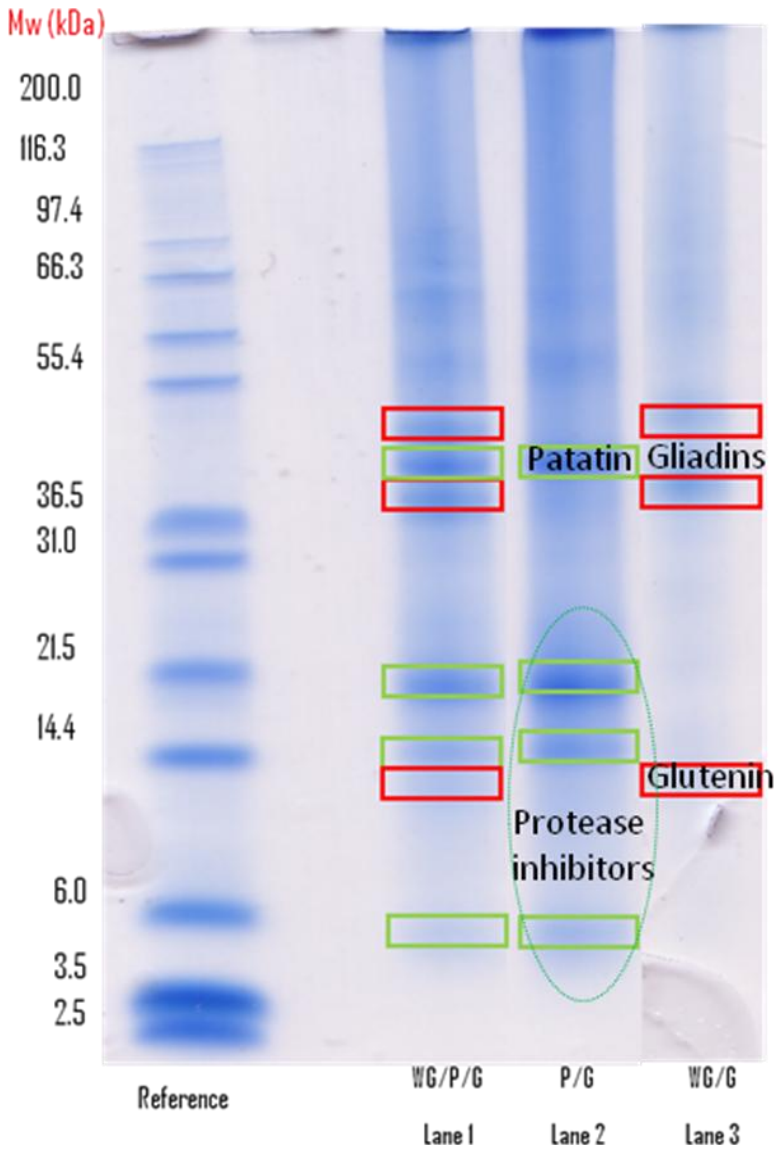

Figure 2.2.7 SDS-PAGE for wheat gluten/potato protein/glycerol (lane 1), potato protein/glycerol (lane 2) and wheat gluten/glycerol (lane 3) under reducing conditions.

Similarly to the combination of rice protein and wheat gluten (Figure 2.1.9), the behaviour of this blend was also governed by the wheat gluten. The characterization of the molecular weight of individual proteins and peptides in this blend was performed by sodium dodecyl sulphate-polyacrylamide gel electrophoresis (SDS PAGE) under reducing conditions; the results are shown in Figure 2.2.7. These results shows that wheat gluten/potato protein-

based bioplastic (lane 1) presented the same bands for both proteins (wheat gluten and potato protein). Three bands of gliadins and glutenins were identified in the blend, as were identified in the wheat gluten-based bioplastic (lane 3), whilst three bands of protease inhibitors and patatin were also identified for the potato protein-based bioplastic (lane 2). The proteins present in potato protein are cysteine rich (the sulphur amino acid) which means that this protein might tend to interact and aggregate under thermal conditions. This might explain the low water absorption values obtained when the sample was processed at a high temperature.

2.3 Extrusion of wheat gluten/potato protein-based bioplastic

Extrusion is an important processing method for thermoplastic materials which is used to produce films, sheets and profiles. During this process, the material is exposed to high temperature, pressure and shear. In the case of protein based materials both temperature and shear induce structural changes such as denaturation and melting. Thus, in this study we consider the ability to process wheat gluten and potato protein together. The resulting physical properties are strongly dependent on the degree of structural change to the proteins involved.

Thermomechanical and water absorption properties

Fig. 2.3.1 shows the evolution of the complex modulus and tan δ with temperature for wheat gluten/potato protein (1:1 ratio) bioplastic obtained by mixing at 80°C and extruded at 30 r.p.m., according to three temperature profiles (see Table 3.1 in Materials and Method). The samples extruded at temperature profiles P_2 and P_3 displayed similar behaviour at high temperature. In both samples, a decreased modulus with temperature and a change in the slope of E* around 100°C were observed. However, an increase in the die temperature in the temperature profile led to an increased modulus at low temperature and a decrease in the temperature where the minimum tan δ was located.

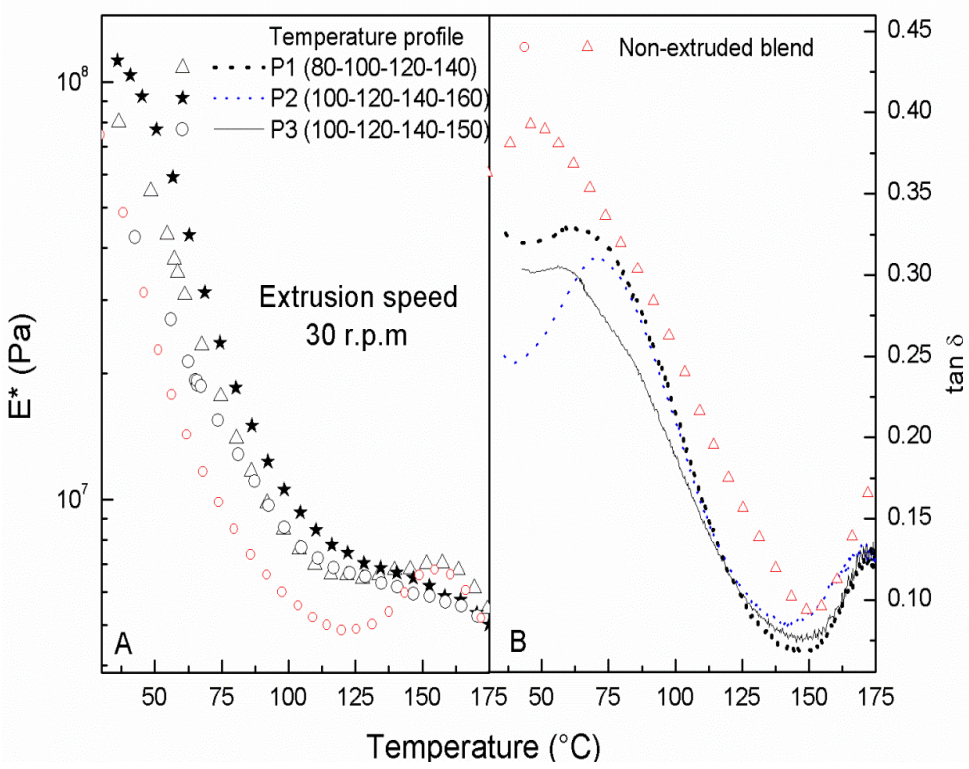

Figure 2.3.1 Dynamic mechanical thermal analysis results, complex modulus (A) and tan δ (B) for three temperature profiles of wheat gluten/potato protein at a ratio of 1:1, obtained by mixing at 80°C followed by extrusion at 30 r.p.m.

The maximum tan δ were located at 80ºC for P_2 and 60ºC for P_1 (see 2.3.1B). The sample extruded at the lower temperature (profile P_1), presented a decrease in the modulus up to 100°C, and then a plateau region up to 150°C, after which E* decreased again with temperature. A general observation is that all temperature profiles led to an increase in both viscoelasticity functions (E* and tan δ) with temperature compared to the non-extruded sample. This can be explained by an increase in the degree of crosslinking due to protein aggregation by the formation of new intermolecular disulphide bonds (Schofield et al., 1983).

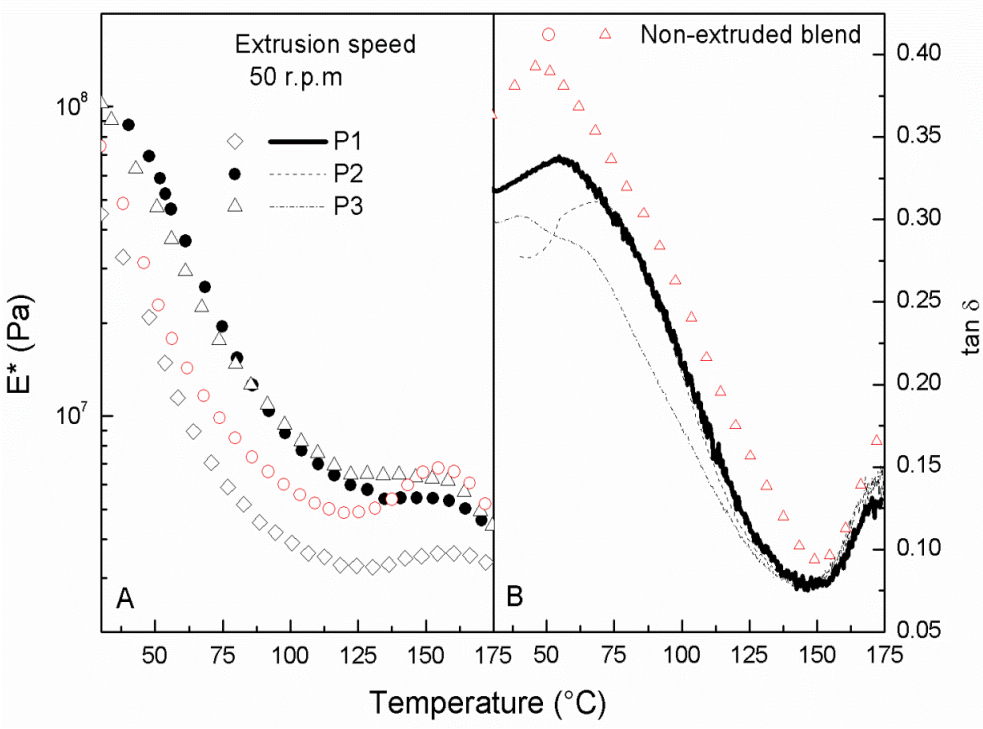

Figure 2.3.2 Dynamic mechanical thermal analysis results, complex modulus (A) and tan δ (B) for different temperature profiles of wheat gluten/potato protein at a ratio of 1:1, obtained by mixing at 80°C followed by extrusion at 50 r.p.m.

Figure 2.3.2 shows the behaviour of E* and tan δ with temperature for different temperature profiles of wheat gluten/potato protein at a ratio of 1:1, obtained by mixing at 80°C and extruding at 50 and 70 r.p.m. In this case, the samples extruded at temperature profiles P_2 and P_3 showed similar behaviour up to 120ºC, suggesting that an increase in the die temperature did not significantly affect the evolution of the viscoelastic modulus until this point and the onset of the plateau region. This region started at 120°C for samples extruded with the P_2 profile and at 130°C for the P_3 profile. This region was larger for samples extruded with P_2 than P_3. In addition, a maximum tan δ at higher temperature was found for samples extruded with the P_3 profile (69°C) than samples extruded with the P_2 profile (42°C). Both samples exhibited higher values for E* than the non-extruded sample. By contrast, a significant decrease in E* and a maximum tan δ at 53°C was observed for the sample extruded at a lower temperature (profile P_1). In this case, the evolution of the complex modulus with temperature was constantly lower than the non-extruded sample and the samples extruded with the P_2 and P_3 profiles.

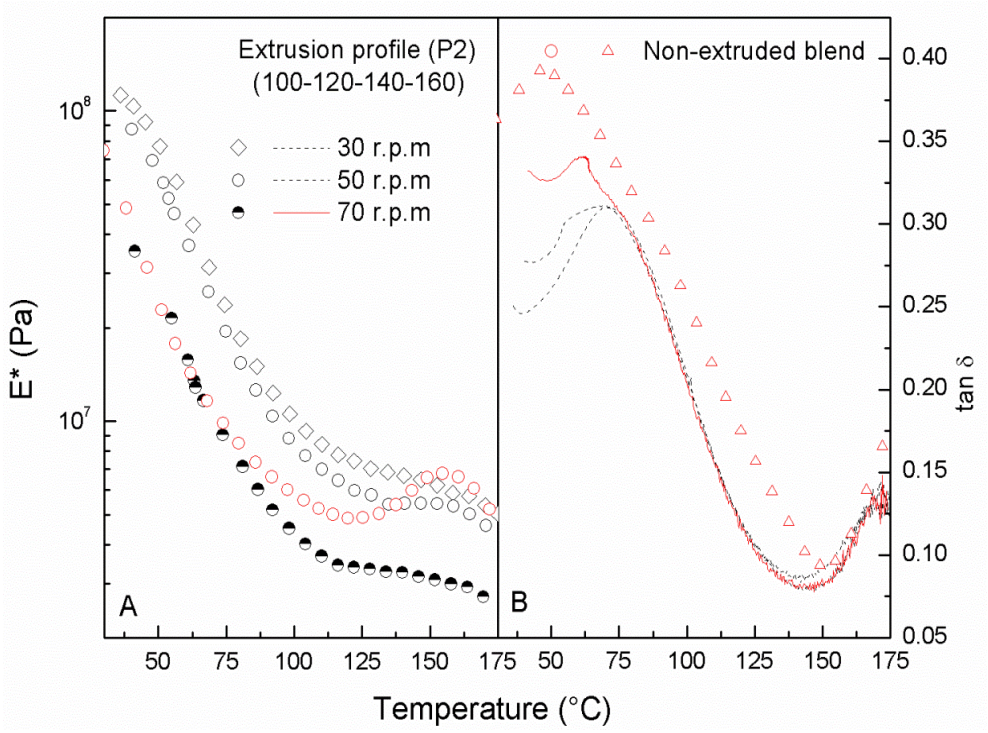

Figure 2.3.3 Dynamic mechanical thermal analysis results, complex modulus (A) and tan δ (B) for wheat gluten/potato protein at a ratio of 1:1, obtained by mixing at 80°C and extruding with P_2 temperature profile and different extrusion speeds.

Figure 2.3.3 shows the evolution of E* and tan δ with temperature for wheat gluten/potato protein at a ratio of 1:1, obtained by mixing at 80°C and extruded with the P2 profile at different extrusion speeds. The evolution of the complex modulus with temperature showed a similar behaviour for all the extrusion speeds studied. In all cases, there was a decrease in E* with temperature, which was followed by a change in the slope of E* around 100°C, and then a plateau region. An increased extrusion speed led to an increase in this plateau region. In addition, an increase in the extrusion speed led to a decrease in E*. The tan δ maximum was located at a higher temperature for samples extruded at low speed (71°C) than for the sample extruded at the highest speed (62°C).

Figure 2.3.4 illustrates the correlation between temperature profile and screw speed during the extrusion process and the effect on the complex modulus at 40°C (A) glass transition temperature (B), and corresponding values of the tan δ maximum (C) for wheat gluten/potato protein blends. A decrease in the complex modulus at 40°C was observed as screw speed increased for samples extruded with the temperature profiles P_1 and P_2. By contrast, for samples extruded at P_3, an increase in the complex modulus was observed when the screw speed during the extrusion process was increased. In addition, the tan δ peak

temperature decreased as screw speed increased for the samples extruded with the temperature profiles P_1, P_2 and P_3. There were non-significant changes in the corresponding tan δ values, except for samples extruded at P_1 (50 r.p.m.) and P_2 (70 r.p.m) which had higher values, meaning that these samples were less elastic.

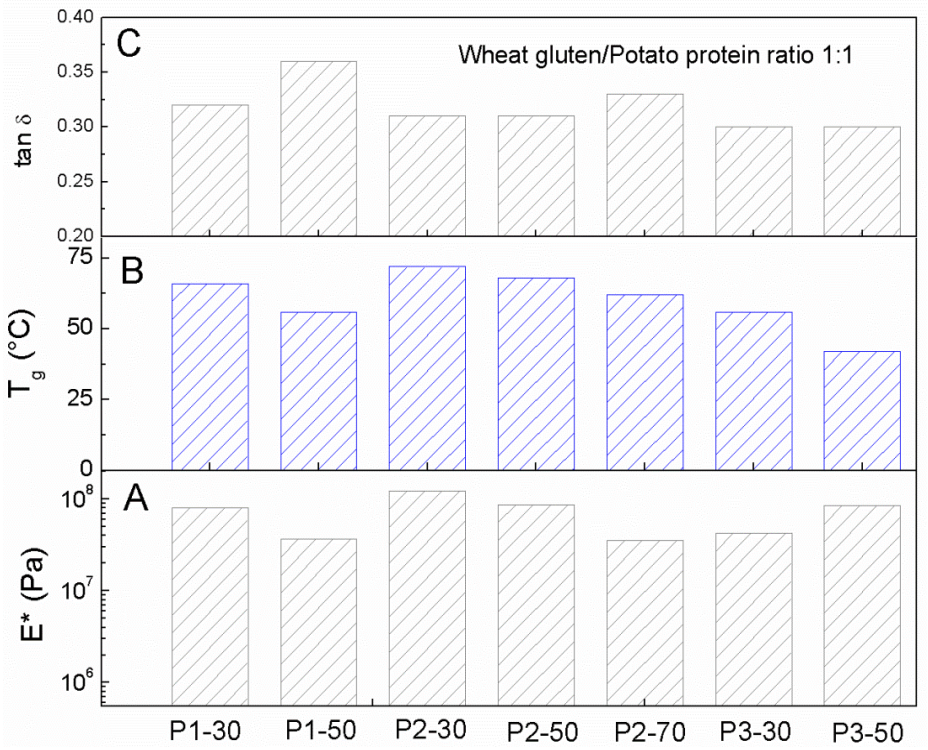

Figure 2.3.4 Correlation between temperature profile and screw speed during the extrusion process and the effect on the complex modulus at 40°C (A) glass transition temperature (B) and corresponding values of the tan δ maximum (C) for wheat gluten/potato protein at a ratio of 1:1.

Water absorption properties

Figure 2.3.5 shows the influence of the extrusion process on water absorption properties for wheat gluten/potato protein at a ratio of 1:1, obtained by mixing at 80°C, followed by an extrusion process at different temperature profiles and screw speeds. It can be seen that the extrusion process did not improve the water absorption properties of the samples. Only samples extruded at P_3 (50 r.p.m.) and P_1 (30 r.p.m.) absorbed less water than the non-extruded sample.

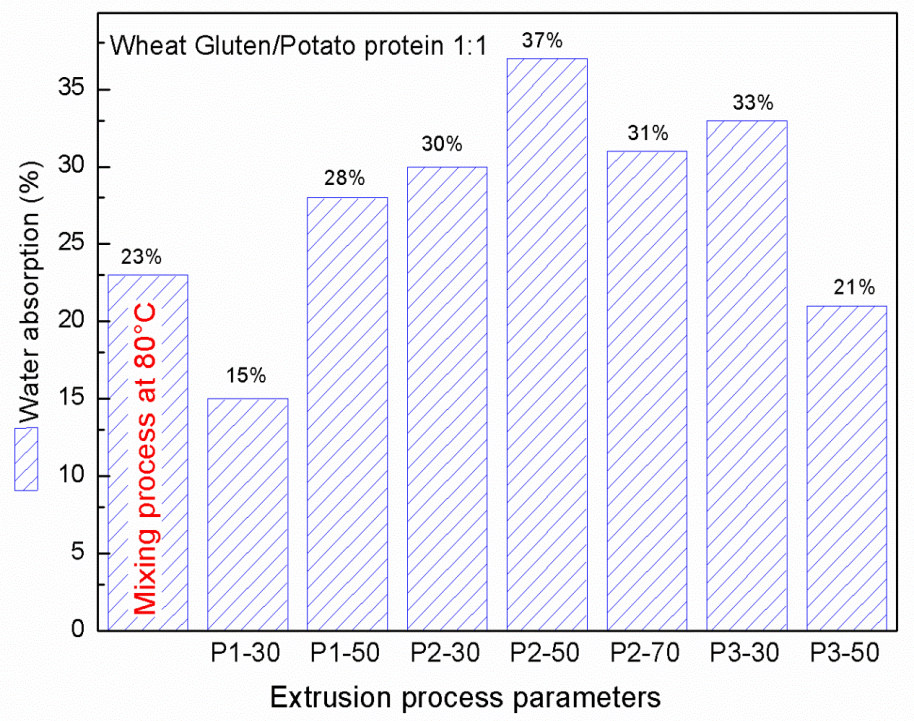

Figure 2.3.5 Water absorption for wheat gluten/potato protein at a ratio of 1:1, obtained by mixing at 80°C followed by extrusion under different conditions.

The best result was the sample extruded with P_1 (30 r.p.m.). In this case, the sample was extruded through four zones with a gradual increase in temperature. The temperature in the first zone was the same that used during the mixing process (80°C). The subsequent zones were thus: 2^{nd} (100°C), 3^{rd} (100°C) and finally 4^{th} zone (120°C). Consequently, we believe that both proteins (potato protein and wheat gluten) need a slow increase in temperature and a slow screw speed to achieve a re-arrangement of the protein structure in order to improve both viscoelastic and water absorption properties simultaneously.

3. Development of new controlled-release materials based wheat gluten

The controlled release of active agents and water absorption in biopolymer systems have received considerable attention in recent years, due to their significant applications in the fields of biomedical, pharmaceutical, environmental and agricultural engineering (Castro et al., 2008; Buchholz and Graham, 1998). The aim of this chapter is to report the development of new controlled-release bioplastics based on wheat gluten. This chapter is composed of three parts. The first one is about controlled-release matrices based on glycerol, water, wheat gluten and an "active agent", KCl (source of potassium chloride in agriculture). The characterisation focused on the effect that formulation, processing, and further thermal treatments exerted on the thermomechanical properties, physico-chemical characteristics and rheological behaviour of the bioplastics obtained. KCl release from the bioplastic into water was regulated by adding citric acid to a specific formulation. The second part is about the use of less hygroscopic plasticizers as a way of modifying bioplastic release/swelling properties. Initially bioplastics formulated with polyethylene glycol (PEG), water and wheat gluten were manufactured in order to determine the effect of varying PEG molecular weight. Secondly, the addition of different types of modifying agents, on a specific formulation, was assessed to enhance the controlled release of the "active agent", KCl. Dynamic mechanical thermal analysis (DMTA), differential scanning calorimetry analysis (DSC), release and water absorption tests were carried out in order to study the influence of these variables. Finally, the third part of this chapter focuses on the thermomoulding process of blends plasticized with varying PEG molecular weight and its effect on their thermomechanical properties as well as degree of water swelling and KCl controlled-release kinetics. In this chapter, the protein used is wheat gluten (WG) at a fixed concentration of 67 wt. %. The formulations for such gluten-based bioplastics are shown in Table 2.3 in Materials and Methods.

3.1 Rheological behaviour and physical properties of controlled-release bioplastics based on wheat gluten

3.1.1 Thermoplastic processing of wheat gluten-based bioplastics

The evolution of torque and temperature during this mixing process, at 50 r.p.m., for the different systems studied are shown in Figure 3.1.1, which depends on the system studied. Three different regions WG/G blend, plasticized with 33 wt.% of glycerol is observed. The first region, where no significant increase in torque is observed, also known as induction region; the second region, where torque undergoes an exponential increase with mixing time up to a maximum value; and the last region, where an apparent torque decay is observed (Jerez et al., 2005a).

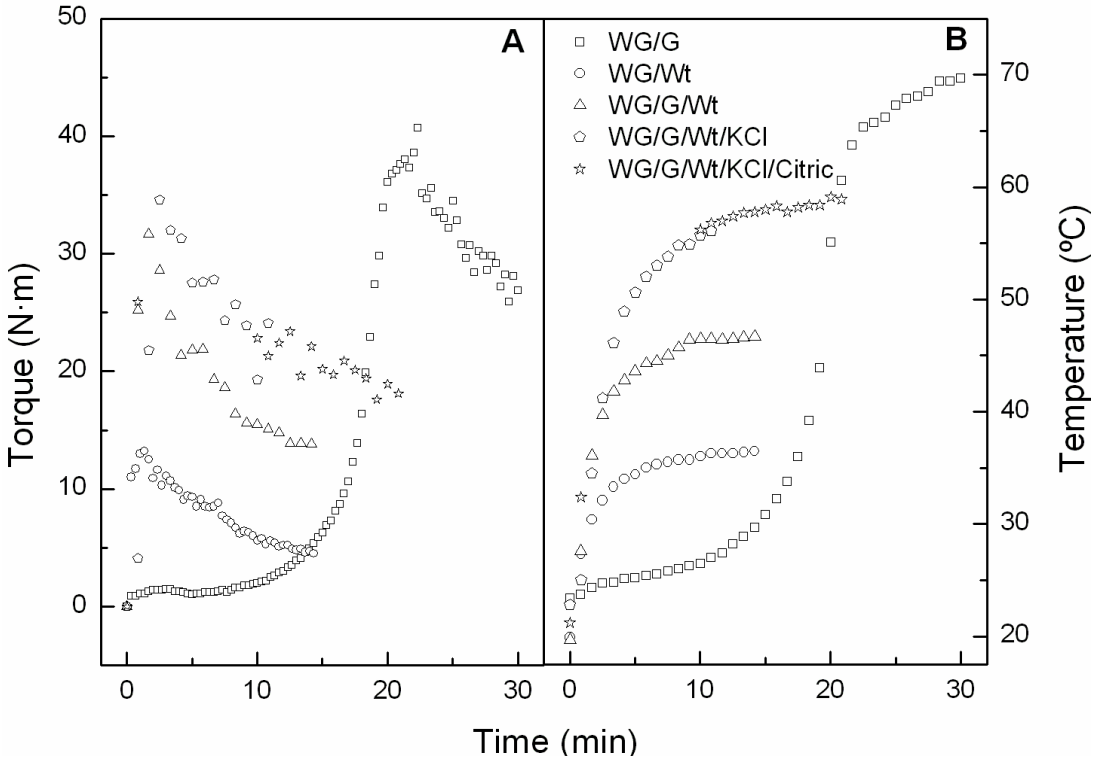

Figure 3.1.1. Evolution of torque (A) and temperature (B) during the mixing process of different bioplastics.

On the contrary, samples containing water (Wt) in their formulation (See Table 2.3 in Materials and Methods) only present two regions, characterized by an instantaneous increase in torque, up to a maximum value, and then a continuous decay down to steady state values. Table 3.1.1 shows that the maximum value of torque is reached after as long as 22 min mixing for WG/G blend. On the contrary, blends containing water as plasticizer reached the maximum much faster, after only 2-3 min.

Similarly, the plasticizer also affects the specific mechanical energy (SME) required to obtain a material with suitable mechanical properties. Table 3.1.1 presents the SME values calculated by Equation 1.1.1 (chapter 1). As previously mentioned for the mixing time the occurrence of a transient torque peak suggests an evolution of the gluten structure upon mixing and the final torque decay is associated with a change in consistency from a powder/plasticizer dispersion to a cohesive and elastic material (Redl et al., 1999a; Redl et al., 2003). Thus, the time needed to reach an equilibrium torque depends on the ability of the constituents to interact and therefore, on the selected plasticizer (Pommet et al., 2003). The mixing time, t_{mix} was calculated as previously, as 1.5 T_{peak} for the sake of comparison in all cases.

Table 3.1.1. Specific Mechanical Energy (SME), time for the torque maximum (t_{peak}) and maximum temperature (T_{max}) reached during mixing process.

Bioplastics	**T_{peak} (min)**	**T_{max} (ºC)**	**SME**
WG/G	21.9	74.6	2647
WG/Wt	1.3	36.4	151
WG/G/Wt	1.6	47.3	289
WG/G/Wt /KCl	2.2	56.6	361
WG/G/Wt/KCl/Citric	2.2	58.8	467

As can be seen in Table 3.1.1, water addition led to a dramatic decrease in SME. Moreover, citric acid and KCl additions only led to slight increases in torque (Figure 3.1.1 and Table 3.1), as a consequence of the lower water content.

Figure 3.1.1B shows the evolution of temperature during the mixing process for the different systems studied. The temperature curves for all the blends containing water are characterised by an instantaneous exponential increase, while the curve for the WG/G blend shows an induction period up to 30ºC, above this value temperature underwent the same remarkable increase. This region has been related to the rearrangement of the protein molecules. Some authors have suggested that the plasticized molecular network of gluten undergoes an exothermic dissociation and unfolding of the macromolecules, which recombine and crosslink through specific linkages (Redl et al., 1999b; Redl et al., 2003; Mitchell et al., 1994; Jerez. et al., 2007). It is apparent that the final temperature of the blend after processing increases as water content decreases in the blend, ranging from 36 to 75ºC (Table 3.1.1).

3.1.2 Rheological behaviour of the release matrices

Figure 3.1.2 shows the mechanical spectrum, at 75ºC, for WG/G and WG/G/Wt/KCl blends previously thermoset at three temperatures (90, 120 and 140ºC), and at constant gauge pressure (100 bar).

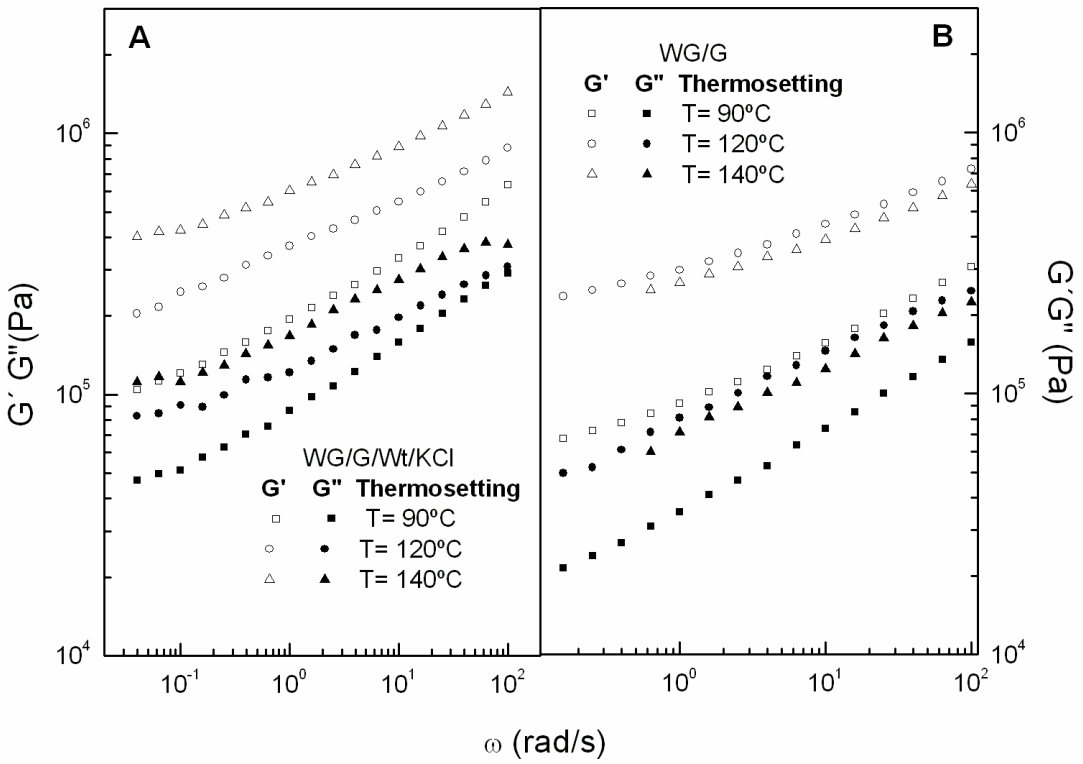

Figure 3.1.2 Frequency dependence of the linear viscoelasticity functions for biplastics containing KCl (A) and without added active agent (B), processed at different temperatures.

All samples display mechanical spectra typical of entangled/crosslinked, highly structured systems. Consequently, elastic characteristics are predominant, with values of the storage modulus, G´, much higher than the loss modulus, G", in the whole frequency range studied. As expected from previous results, an increase in the moulding temperature yielded a continuous increase in both modulus values (Figure 3.1.2). However, the addition of water and KCl led to materials with higher viscoelastic moduli than those containing only glycerol as plasticizer. This fact suggests an enhancement in the material microstructure (Gennadios et al., 1996).

Likewise, controlled-release matrices, containing water and KCl, showed different flow behaviour at 60ºC, as me be deduced from Figure 3.1.3 for some of the different blends studied (please see Table 2.3 of Materials and Methods, for the detailed composition).

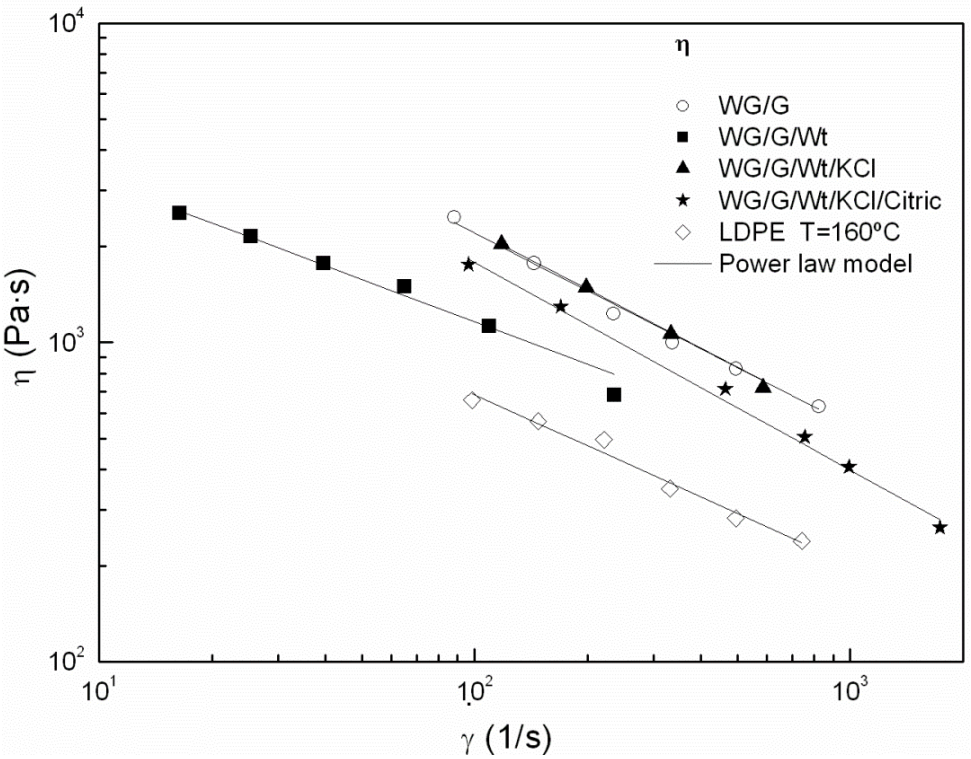

Figure 3.1.3 Influence of blend composition on the viscous flow behaviour of WG/G/Wt, WG/G//Wt/KCl and WG/G/Wt/KCl/citric blends, at 60ºC.

Table 3.1.2 Influence of temperature and composition on the consistency (k) and flow (n) indexes.

Compositions	**Measurement Temperature (ºC)**	**Parameters of Power-law model**	
		k (Pa·s^n)	**n**
WG/G	60	35075	0.40
WG/G/Wt	60	8893	0.55
WG/G/Wt/KCl	60	37207	0.40
WG/G/Wt/KCl/Citric	60	35310	0.35
LDPE	160	7846	0.47

As seen in Figure 3.1.2, blends containing water in their formulation displayed lower viscosity than WG/G samples, although the presence of KCl produced a slight increase in blend consistency. On the other hand, the addition of citric acid to the blend yielded a decrease in viscosity, showing a more pronounced shear thinning behaviour and, therefore,

lower values of the flow index, *n*, (Table 3.1.2). This may be explained by the reducing ability of citric acid to affect strong chemical interactions within gluten, weakening S-S bonds among gluten molecules and favouring slippage among them, which result in the acidic lysis of gluten in the presence of acid citric (Jiugao et al., 2005). Previous studies have shown that the use of citric as plasticizer increases extensibility, decreases mechanical resistance and modifies material hydrophilicity (Pommet et al., 2005).

3.1.3 Thermomechanical behaviour of controlled-release matrices

Typical DMTA scans (from 30 to 160ºC) for WG/G/Wt/KCl and WG/G/Wt/ KCl/acid blends submitted to different thermo-setting temperatures (between 60 and 140ºC) are shown in Figure 3.1.4. As can be observed, for all the thermo-setting temperatures studied, a decrease in the complex modulus E* (up to temperatures around 90ºC, see Figure 3.1.4A), and a maximum in tan δ (at temperatures around 60-70ºC, see Figure 3.1.4B) always occured. These results indicate a change in the microstructural characteristics of the sample (Figure 3.1.4B), typical for a glass transition temperature of the plasticized gluten proteins (Jerez et al., 2007). In our case, tan δ was always lower than 1, which corresponds to a highly elastic microstructure.

The results obtained for WG/G/Wt/KCl blends demonstrate that an increase in thermosetting temperature generally led to an increase in the complex modulus; more important when thermosetting temperature was raised from 90 to 120ºC. On the other hand, the loss tangent maximum appeared at higher temperatures. These results are in good agreement with those obtained after compression moulding at 60 and 90ºC, which showed a remaining thermosetting potential above 100ºC, leading to a remarkable increase in E* with increasing temperature (Figure 3.1.4A). This behaviour may be related to the incomplete protein denaturation during its previous thermomechanical processing. On the contrary, E* values do not significantly increase for WG/G/Wt/KCl blends submitted to thermomechanical processing above 120ºC. These results are also in good agreement with those obtained from DSC measurement (Figure 3.1.5). So, WG/G/Wt/KCl samples showed an endothermic peak located at 141ºC, which has been related to the thermal denaturation of the gluten protein (Jerez et al., 2005a). As a consequence, bioplastics moulded at temperatures close to this (i.e 120 and 140ºC) did not show any remaining thermosetting potential (Figure 3.1.4). Moreover, a higher thermal denaturation is expected in bioplastics thermoset at 120 and 140ºC, leading to more structured systems with higher values of the linear viscoelasticity functions.

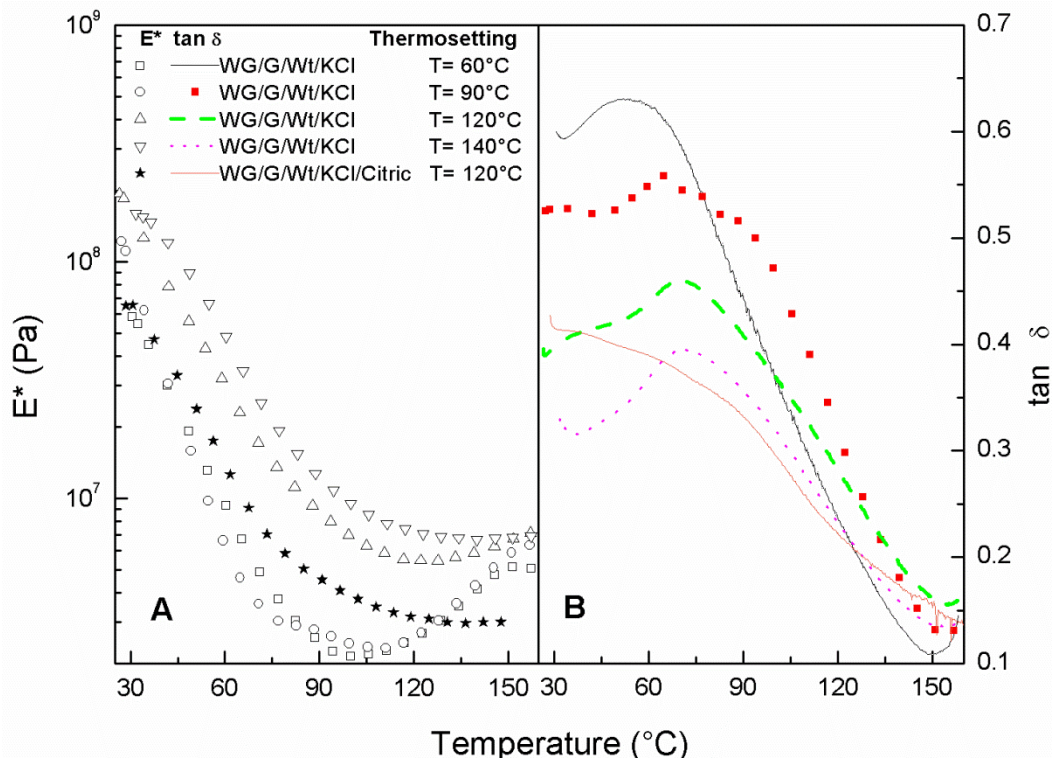

Figure 3.1.4 Dynamic mechanical thermal analysis results, complex modulus (A) and tan δ (B) for selected blends, after different thermosetting temperatures.

Furthermore, the tan δ temperature curves can be used to reveal information concerning molecular and/or segmental scale motions in polymers (Zheng et al., 2002) and the maximum of tan δ has previously been associated to the glass transition temperature (T_g) of the plasticized proteins (Figure 3.1.4B) (Jerez et al., 2007). The higher values of T_g found as thermosetting temperature increases could therefore be explained by the presence of a significant incidence of polymer–polymer interactions, both hydrogen bonding and covalent interactions (Pouplin et al., 1999).

However, the addition of the citric acid yields a decrease in the glass transition temperature of the gluten-based bioplastics (Figure 3.1.4B). Thus, when citric acid was added to the blend, a dramatic change in the complex modulus values was observed, with much lower E* values for this blend (see Figure 3.1.4A). Furthermore, DSC measurements performed on the sample just after mixing showed a thermal denaturation/rearrangement temperature at 129ºC significantly lower than that found in WG/G/Wt/KCl samples (Figure 3.1.5).

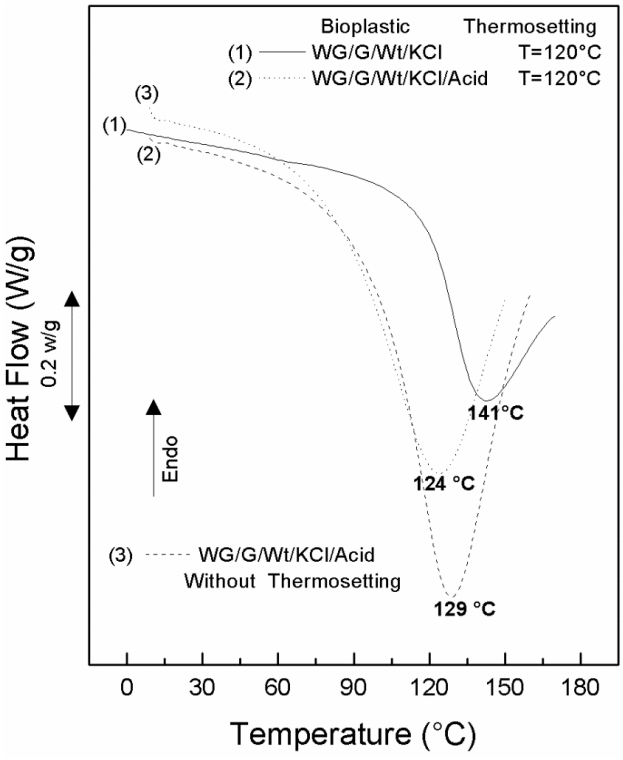

Figure 3.1.5 DSC thermograms for WG/G/Wt/KCl and WG/G/Wt/KCl/citric blends, after thermosetting at 120ºC and without thermal treatment.

Thus, the endothermic event decreases up to 14ºC after thermosetting at 120ºC. As a result, it is not expected to found a remaining thermosetting potential in samples thermo-moulded at 120ºC (Figure 3.1.4A). The lower values of E* might be explained by the reduced crosslinking density (Gontard and Ring, 1996), and the replacement of hydrophobic interactions by protein–plasticizer interactions (Kalichevsky et al., 1992). A change, that seems to be promoted by the addition of a reducing agent (citric acid) and increased by the thermomechanical treatment (thermoset at 120ºC).

3.1.4 KCl release and water absorption

Previous results have pointed out that both processing conditions and bioplastic formulation may lead to materials with a wide range of mechanical responses and, therefore microstructures. As a result, different swelling and release capabilities should be expected. Figures 3.1.6 and 3.1.7 show, respectively, the kinetics of KCl release and water-absorption values for samples with different thermomechanical treatments and formulations. A sigmoidal model fits fairly well the KCl release results obtained:

$$\frac{M - M_\infty}{M_0 - M_\infty} = \frac{1}{1 + \left[t / t_{1/2}\right]^P} \qquad [3.1.1]$$

where M_0, M and M_∞ denote the concentration (wt. %) of KCl initially released, after a time t, and for very long time, respectively; $t_{½}$ is the time for 50% KCl release, and P is a parameter related to the rate of release. Table 3.1.3 shows the values of these parameters.

Table 3.1.3 Effect of thermosetting temperature and citric acid content on the release parameters from equation [3.1.1], for the different blends studied.

Composition	Conditions Temperature (ºC)	Water pH	Parameter			
			M_0	M_∞	$t_{½}$	P
WG/G/Wt/KCl	90	7.45-5.88	2.45	99.60	55.40	0.90
WG/G/Wt/KCl	120	7.45-5.88	7.00	92.53	95.00	0.85
WG/G/Wt/KCl	140	7.45-5.88	13.92	90.00	100.00	0.98
WG/G/Wt/KCl /Citric	120	7.11–5.90	0	98.90	149.73	1.16
WG/G/Wt/KCl	120	5.75-5.62	0	100.00	69.52	1.26

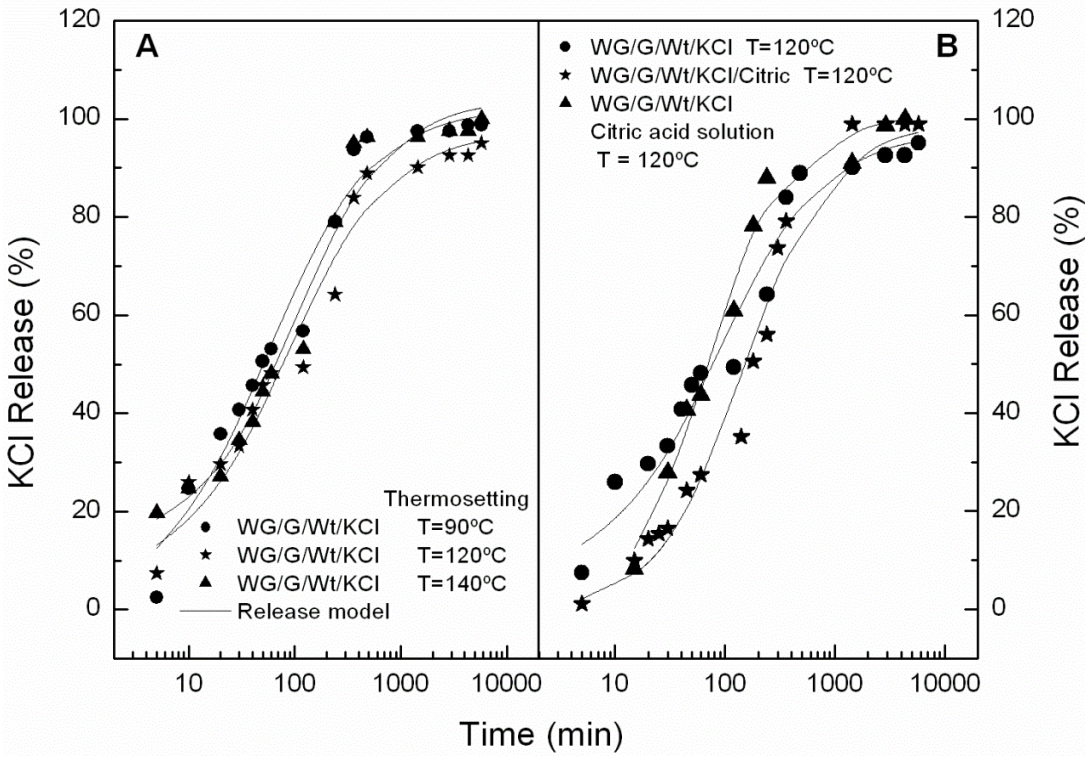

Figure 3.1.6 KCl release behaviour of WG/G/Wt/KCl and WG/G/Wt/KCl/citric blends processed at different temperatures.

The effect of thermosetting temperature on KCl release can be deduced from Figure 3.1.6A and Table 3.1.3. Thus, it can be observed that WG/G/Wt/KCl samples show an increase in $t_{1/2}$ as thermosetting temperature increases. Furthermore, a higher thermosetting temperature leads to a higher instantaneous release concentration (M_0) and to a lower final concentration in the water (M_∞).

Figure 3.1.7 shows water absorption values after 24 h, for the samples submitted to different thermomechanical treatments. As can be observed, the water absorption values decrease as thermosetting temperature increases. This result may be explained taking into account that the swelling ratio of a polymeric matrix decreases as the degree of crosslinking increases (Zheng et al., 2002; Buonocore et al., 2003).

As described above, bioplastic thermomechanical treatment leads to an aggregation of gluten or protein denaturation and, therefore, to an increase in the degree of crosslinking between molecules (Figures 3.1.4 and 3.1.5). Moreover, it is known that, as the degree of polymer crosslinking decreases, the available free space for active agent diffusion increases, and the rate of active agent release also increases (Bachtsi and Kiparissides, 1996; Buonocore et al., 2003). On the contrary, an increase in the degree of polymer crosslinking due to material thermosetting temperature decreases the available free space for active agent diffusion, which results in a decrease in active agent release rates (Figure 3.1.6A).

However, this microstructural interpretation cannot explain the results found in the bioplastic containing citric acid (Figure 3.1.6 B and 3.1.7). Citric addition led to a remarkable decrease in release rate of the active agent (Figure 3.1.6 B), because $t_{½}$ increases from 90 to 150 minutes (Tables 3.3). This is an unexpected result, taking into account, the remarkable increase in swelling ratio found by citric addition, from 84 to 164 wt.% (Figure 3.1.7). The new microstructure formed within the protein matrices did not show any instantaneous release of KCl (M_0) and was able to diffuse up to 99% of KCl. In addition, these results are not related to the water pH, as previously pointed out by other authors (Juigao et al., 2005; Vallejo et al., 2005). Thus, the release test was also carried out in a citric acid solution of pH= 5.6, and using the sample WG/G/Wt/KCl thermoset at 120ºC (Table 3.3 and 3.1.6 A). As may be found in Figure 3.1.6 B, release test performed at pH=5.6 shows a $t_{½}$ value close to that found at pH=7.7 (70 and 95 min respectively), but much lower than that found in protein matrices containing citric acid (Table 3.3). As a result, both the decrease in release rate and

the increase in swelling ratio may be related to the microstructure changes found by citric acid addition.

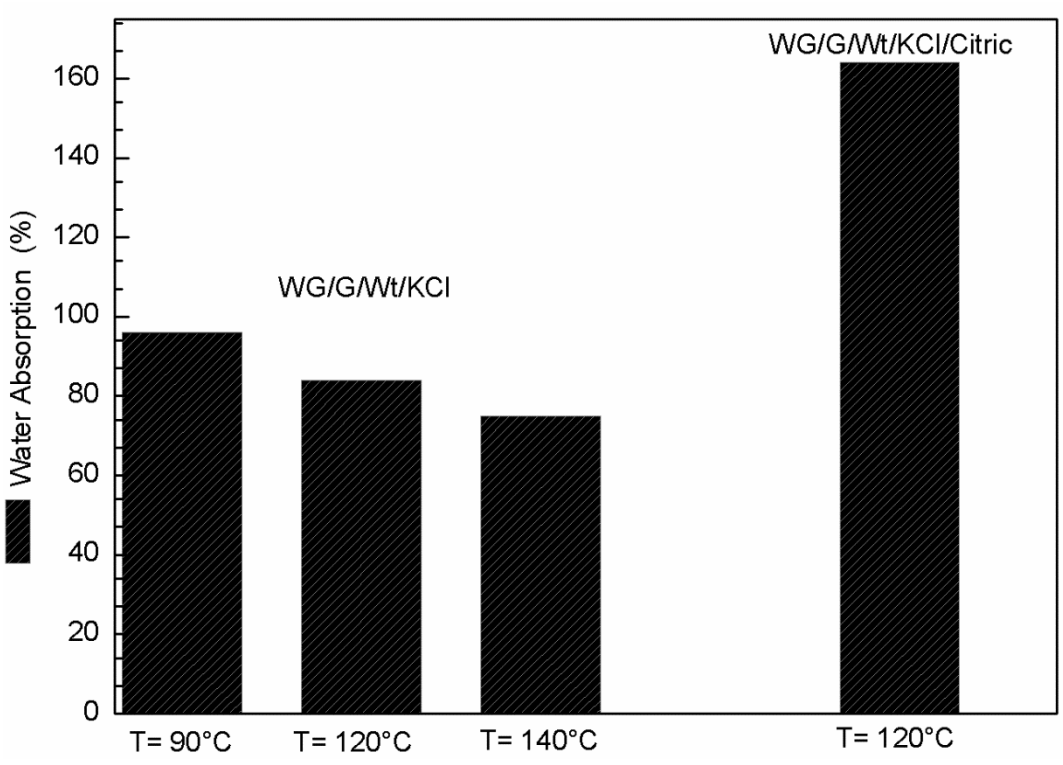

Figure 3.1.7 Water absorption of WG/G/Wt/KCl and WG/G/Wt/KCl/citric blends processed at different temperatures.

Previous results have shown that citric acid leads to an important decrease in the crosslinking degree of the protein network (Figure 3.1.4 and 3.1.5), which may explain the dramatic increase in swelling ratio by the raise of available free spaces within the protein matrix. However, the observed slow release of KCl seems to be related to the increases in hydrophilic bonds (due to the breakdown of *S-S* bond into *S-H*). Under such conditions, the presence of a polar plasticizer may affect hydrogen bonds and, therefore, increase the compatibility between protein molecular and the salt solution (i.e. glycerol, water, citric acid and KCl). As a result, the relative affinity of the plasticizer to the polymer matrices is found to be significant, affecting the release patterns in both the slope and the shape of the release curves (Siepmann et al., 2008). A low protein-plasticizer affinity (sample WG/G/Wt/KCl at 120ºC) leads to a fast leaching out of the plasticizer from polymeric matrices with high instantaneous release concentration, M_0, and high concentration of the residual (W_{sol}/W_o , see Equation 3.1.1), close to 25%. On the contrary, a high protein-plasticizer affinity (sample WG/G/Wt/KCl/Citric) leads to M_0 values close to zero and lower concentration of the residual

(W_{sol}/W_o , see Equation 3.1.1), about 19.4 %. This fact points to the plasticizer acting as a carrier of the active agent during its leaching out of the matrix.

3.2 Effect of plasticizers and modifying agents on the rheological and controlled-release properties of wheat gluten-based bioplastic

3.2.1 Influence of the plasticizer molecular weight

Thermoplastic processing

Torque and temperature profiles recorded during the process of mixing of the protein and plasticizers, such as water/glycerol and water/polyethylene glycols (each PEG having different molecular weight) are shown in Figure 3.2.1. In all cases, torque evolution presented two regions which were characterized by an instantaneous increase in torque up to a maximum value followed by a continuous decay towards a steady state value. Similarly, two different temperature zones are also found during the mixing process (inset, Figure 3.2.1).

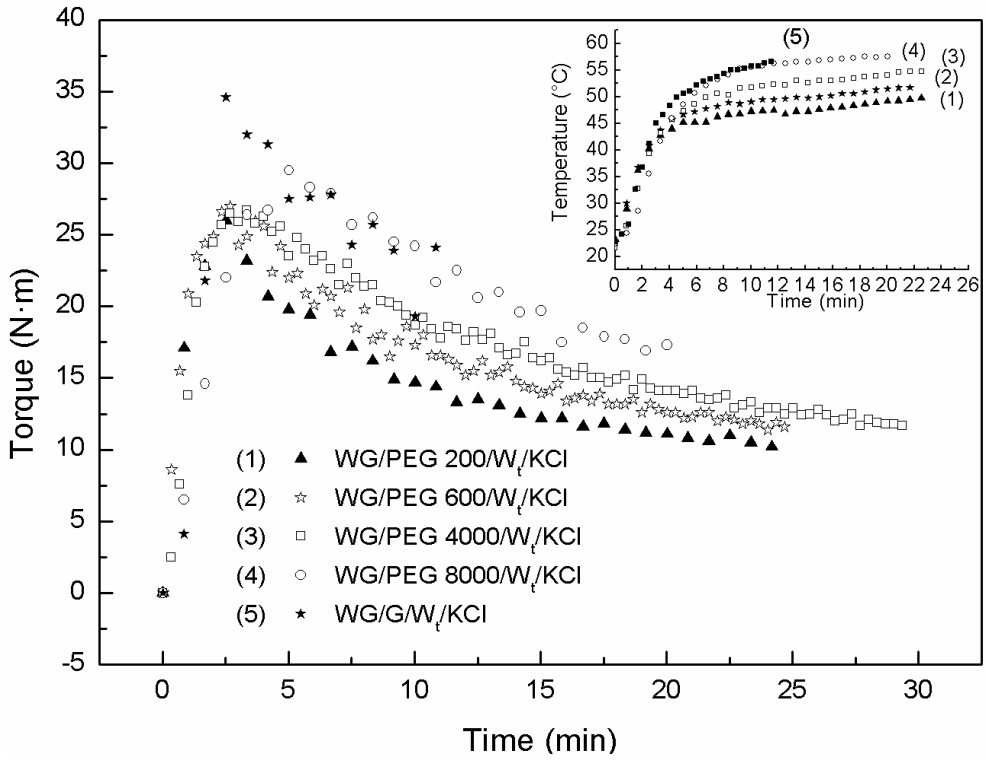

Figure 3.2.1. Evolution of torque and temperature during the mixing process of gluten-based bioplastics with different plasticizers.

As may be observed, temperature showed a remarkable increase up to 45-55ºC and evolved to a plateau once the torque overshoot was exceeded. Accordingly, mixing

temperature did not exceed plasticizer boiling points and was low enough to prevent severe protein aggregation or thermal degradation (Zarate et al., 2011).

Table 3.2.1 shows that torque overshoot appears after 2-3 min mixing (t_{peak}) for samples containing PEG 200, PEG 600 and PEG 4000. In contrast, the mixture containing PEG 8000 exhibited the overshoot later, t_{peak}≈6 min. Furthermore, compared to the reference system (i.e. water/glycerol as plasticizer), PEG addition tended to shift t_{peak} towards higher values. It is worth noting that the occurrence of a torque overshoot suggests a dramatic evolution of a gluten structure during mixing and, followed by the final torque decay, is associated with a change in consistency from a powder/plasticizer dispersion to a cohesive and viscoelastic material (Redl et al., 1999a). Thus, the time needed for the torque overshoot (and, eventually, to achieve a balanced value) depends on the ability of the constituents to interact all together and is necessarily affected by the selected plasticizer (Pommet et al., 2003) Therefore, the observed delay in t_{peak} would suggest a higher incompatibility between the protein matrix and the plasticizer, PEG, which is more apparent as its molecular weight increases.

Table 3.2.1. Specific Mechanical Energy (SME), time for the maximum torque (t_{peak}) and maximum temperature (T_{max}) reached during mixing process.

Bioplastics	**t_{peak} (min)**	**T_{max} (ºC)**	**SME (kJ/kg)**
WG/G/ W_t /KCl	2.20	58.8	289.00
WG/PEG 200/ W_t /KCl	2.57	51.97	414.50
WG/PEG 600/ W_t /KCl	2.13	49.82	376.72
WG/PEG 4000/ W_t /KCl	2.85	55.13	481.20
WG/PEG 8000/ W_t /KCl	5.50	57.53	1073.48
WG/PEG 4000/ W_t /KCl/Wax	3.03	58.64	120.80
WG/PEG 4000/ W_t /KCl/CA	2.22	53.54	515.74
WG/PEG 4000/ W_t /KCl/FA	4.31	63.54	173.98
WG/PEG 4000/ W_t /KCl/OA	4.05	73.22	695.33

In the same way, the plasticizer also affects the specific mechanical energy (SME) required to obtain a material with suitable mechanical properties. Thus, Table 3.2.1 shows the SME values calculated by Equation 1.1.1. As may be seen, samples formulated with polyethylene glycol required a higher SME than the reference sample containing glycerol. In addition, SME values increased with the PEG molecular weight for the different bioplastics.

Figure 3.2.2 shows DMTA scans from 30 to 160ºC performed on WG/PEG/Wt/KCl bioplastics as a function of PEG molecular weight. Compared to the reference system, PEG addition led to an increase in the complex modulus values at temperatures below 80ºC. Likewise, a similar effect was found among bioplastics containing PEG as the molecular weight increased from PEG 200 to PEG 4000 (Figure 3.2.2 A).

Bioplastics containing either glycerol or PEG200 presented the well-known glass transition from the glassy to rubbery, with a peak in tan δ close to 70ºC (Jerez et al., 2005a). Furthermore, these samples showed a remaining thermosetting potential above 130ºC, undergoing a remarkable increase in E* with temperature (Figure 3.2.2A), and exhibiting a minimum in loss tangent close to 155ºC (Figure 3.2.2B). Such a thermosetting process is related to the incomplete protein denaturation during its previous thermomechanical manufacture, as may be deduced from DSC scans conducted on the sample plasticized with glycerol, which had an endothermic peak located at ca. 140ºC (see curve 1 in Figure 3.2.3A).

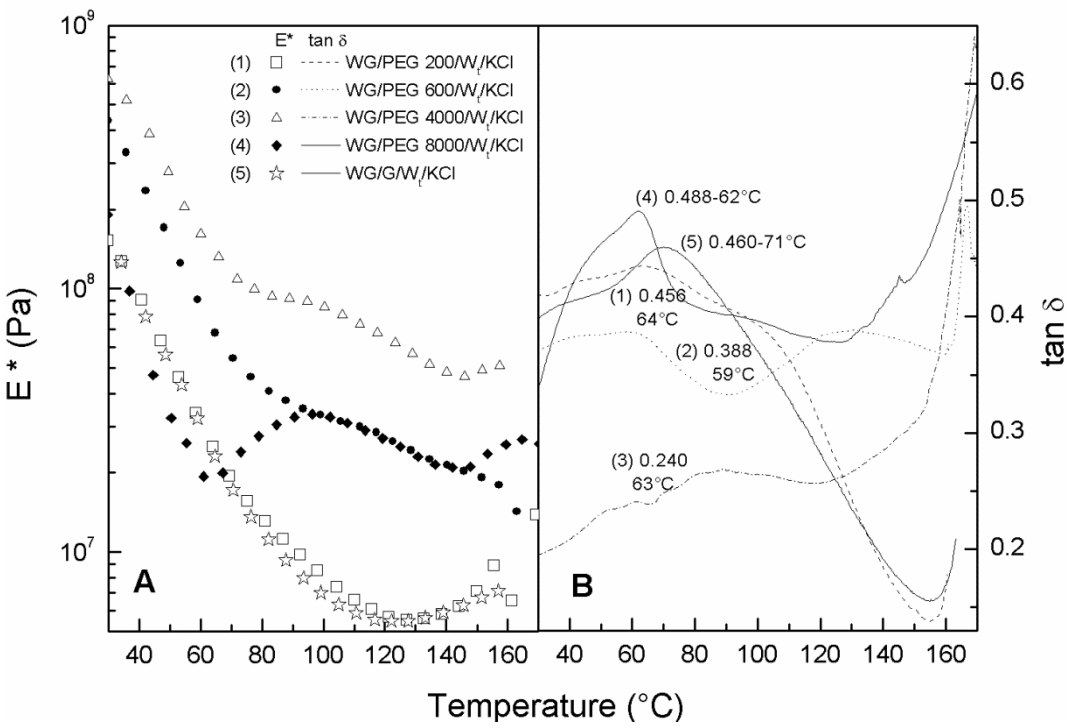

Figure 3.2.2 Dynamic mechanical thermal analysis results, complex modulus and loss tangent for selected blends, after thermoset at 120ºC.

However, tan δ profiles apparently change for blends containing PEG600, PEG4000 and PEG8000, i.e. these systems do not show the minimum at 155ºC (Figure 3.2.2B). This viscoelastic behaviour suggests the development of a different microstruture induced by the higher molecular weight PEGs, which also agrees with the less evident and broader denaturation thermal event shown in Figure 3.2.3A for PEG 4000 and 8000. Also, this result seems to be related to the progressive decline (or flattening) in the slope of E*, observed above 80ºC, for PEG 600 and PEG 4000 blends.

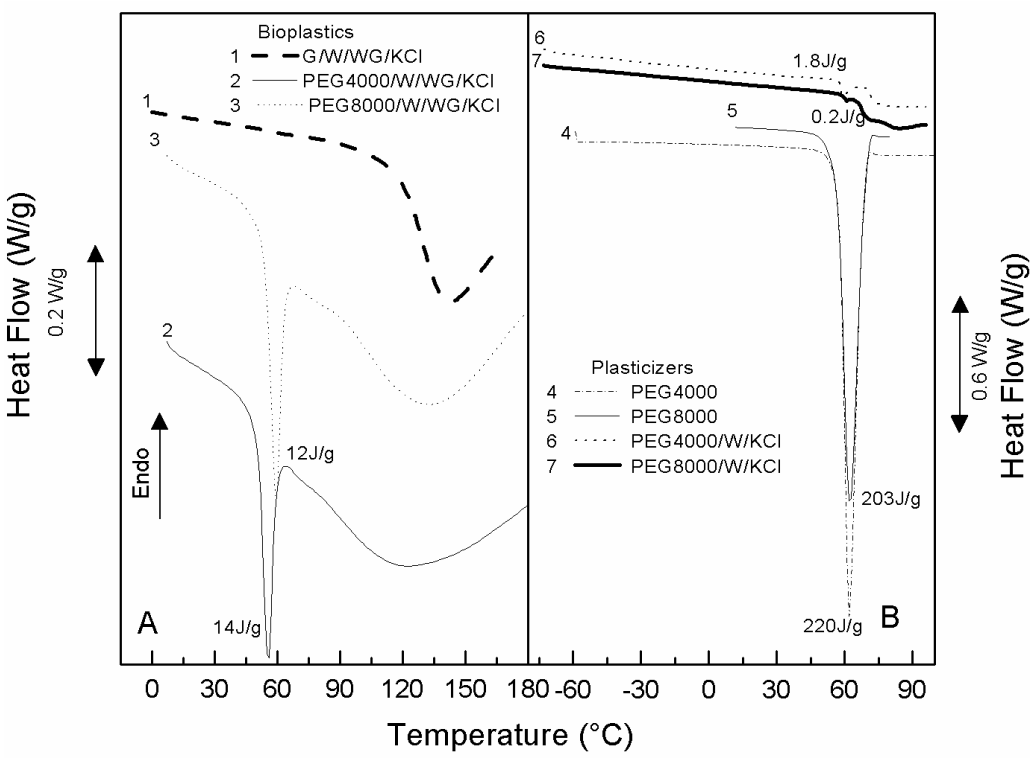

Figure 3.2.3 DSC thermograms for selected blends, after thermoset at 120ºC (A) and plasticizers (B).

Moreover, the bioplastic formulated with PEG8000 exhibits an unexpected increase in the complex modulus as temperature rises from 60 to 100ºC. Such complex viscoelastic behaviour has been reported elsewhere for other materials based on polylactic acid, PLA (Gonzalez-Gutierrez et al, 2010), suggesting the existence of a mixture of compounds with different thermomechanical responses. Such PLA-based bioplastics show a sharp decrease in E* at about 70ºC (glass transition temperature of the polylactic matrix), causing a rubbery plateau until 90ºC. At this point, cold crystallization occurred, yielding a rapid increase in the complex modulus afterwards, which was followed by a final decay starting at 110ºC, corresponding to the onset of melting. In this case, the presence of two incompatible phases

induces the rearrangement of the polymeric chains, which eventually turns out in an improvement of the visoelastic response (i.e. E* increases as temperature does).

It is worth mentioning that the sample containing PEG 8000 shows values of E* lower than those obtained for the bioplastic formulated with glycerol between 30 and 60ºC and, above this temperatures, the bioplastic also shows the above commented improvement of the viscoelastic response. In the same way, the appearance of a new molten phase, above 60ºC, seems to be related to this fact. As shown in Figure 3.2.3A, an additional endothermic peak is found close to 60ºC in the bioplastic, which can be clearly identified with the melting point of the pure crystalline plasticizer (PEG4000 and 8000) (see curves 4 and 5 in Figure 3.2.3B). This new molten PEG phase, characterized by a lower polar character, would induce the subsequent rearrangement of the polar groups of the protein chains, which would result in the observed increase in E* between 60 and 100ºC.

Likewise, this additional thermal event (and the complex rheological response) may evidence a certain incompatibility between the protein matrix and those PEGs with high molecular weight. Moreover, such an endothermic peak is not present in the PEG/water/KCl solutions actually used as plasticizers (curves 6 and 7 in Figure 3.2.3B), which would mean that water and PEG play different plasticizing roles in the bioplastic, according to their affinity. It is well known that water easily establishes hydrogen bonds with proteins. Instead, PEG, with less hydroxyl groups per molecule, would present lower affinity with the polymeric network as molecular weight is higher. Eventually, this seems to lead to an apparent phase separation (confirmed by the endothermic peak found at 60ºC in the bioplastic), similar results were obtained elsewhere (Cao et al., 2009, Turhan et al., 2001). On these grounds, the existence of a macroscopic phase separation was visually confirmed in the bioplastic plasticized with PEG 8000 (likely, yielding a significant decrease in the complex modulus values, see Figure 3.2.2A).

KCl controlled release and bioplastic water absorption

The effect of plasticizer molecular weight on the degree of water swelling and KCl controlled-release kinetics was studied on blends containing 16.5 wt.% of the different plasticizers (Figure 3.2.4 and Table 3.5). A sigmoidal model fitted the KCl release behaviour found fairly well (Equation 3.1.1). Table 3.2.2 shows the values of these parameters.

On the whole, with the exception of PEG8000, glycerol replacement by PEG brings about a lower release of KCl (Figure 3.2.4). Thus, the highest amount of active agent finally released, M_∞, is close to 70%, which is much lower than that reached by the bioplastic containing glycerol, with about 95% KCl released (Table 3.2.2). Among bioplastics containing polyethylene glycol, release rate (or parameter P) increases as the molecular weight does (i.e. PEG addition would result in a worse ability to control KCl release). Conversely, water absorption of materials plasticized with PEG increases with the plasticizer molecular weight (up to 191 wt.% for PEG4000).

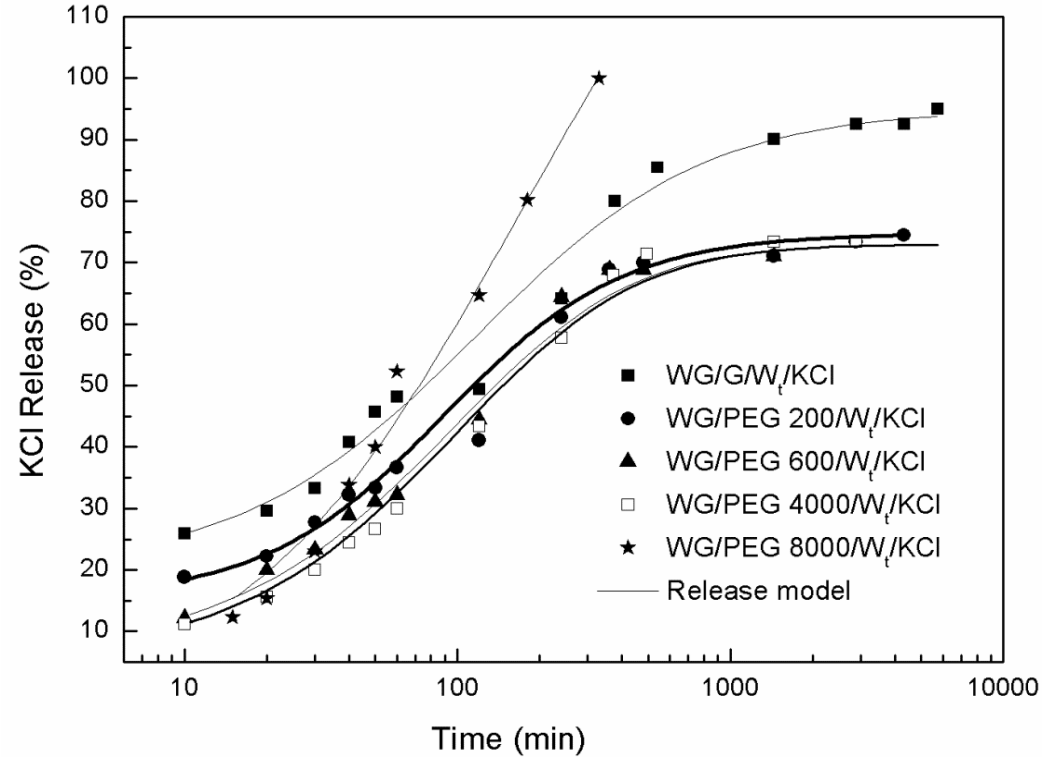

Figure 3.2.4 KCl release behaviour of gluten-based bioplastics with different plasticizers after thermoset at 120ºC.

On the other hand, bioplastic formulated with PEG 8000 exhibits a different behaviour, raising bioplastic release rate (with the shortest $t_{1/2}$ and the highest slope, P) and the KCl concentration finally released (up to100%) and lowering material water uptake, Ab (Table 3.2.2). This result is consistent with the above discussed incompatibility between PEG 8000 and the protein matrix. Thus, up to PEG 4000 a decrease in attractive forces between protein chains, an increase in free volume and segmental motions would be expected (Turhan and Sahbaz, 2004), leading to a higher water uptake which would reduce the effective osmotic pressure within the swollen polymeric matrix. On the contrary, the observed macroscopic

phase separation for PEG8000 would hinder such processes (i.e. leading to lower water absorption and a higher release rate due to a higher effective osmotic pressure).

Table 3.2.2. Effect of PEG molecular weight and modifying agents on the release parameters from Equation 3.1.1 and water absorption values for the different blends studied.

Composition	Water pH	Parameter				Water Absorption
		M_0	M_∞	$t_{½}$	P	Ab (%)
WG/G/ W_t /KCl	7.45-5.88	20.00	95.00	114.00	1.02	84
WG/PEG 200/ W_t /KCl	7.45-5.88	15.40	74.77	88.80	1.33	99
WG/PEG 600/ W_t /KCl	7.45-5.88	11.99	72.28	86.50	1.49	132
WG/PEG 4000/ W_t /KCl	7.45-5.88	11.83	75.65	110.22	1.57	191
WG/PEG 8000/ W_t /KCl	7.11–5.90	8.20	100.0	74.00	1.64	125
WG/PEG 4000/ W_t /KCl/W	7.64-6.87	10.00	87.67	96.10	1.39	102
WG/PEG 4000/ W_t /KCl/CA	7.57-5.88	10.00	88.21	111.83	1.02	148
WG/PEG 4000/ W_t /KCl/FA	7.67-6.01	9.79	92.25	81.89	1.25	174
WG/PEG 4000/ W_t /KCl/OA	7.52-7.14	28.00	100.00	25.42	3.10	96

3.2.2 Effect of modifying agents on a selected formulation (PEG 4000)

According to the results presented so far, the bioplastic containing PEG4000 showed optimal flexural, release and swelling properties and was therefore chosen for further studies of modification by agents such as citric acid (CA), formic acid (FA), octanoic acid (OA) and candelilla wax (Wax).

As seen in Figure 3.2.5, mixing torque and temperature curves recorded with the modifying agents are qualitatively similar to those shown in Figure 3.2.1, showing the same mixing regions described above. However, Table 3.2.1 shows that modifier addition gave rise to t_{peak} values higher than that found for the sample without modifiers. Calculated Specific Mechanic Energy (SME) was significantly lower for blends with candelilla wax and formic acid and higher for the blend with octanoic acid. Furthermore, it is worth noting that citric acid addition led to the highest torque value at the peak, as well as the highest mixing temperature (73ºC). In this sense, gluten de-aggregates during mixing due to shear (Redl et al., 1999a; Weegels et al., 1995), and can also aggregate if the temperature is higher than 60ºC

(Redl et al., 1999a; Kokini et al., 1994). This led to remarkable physical changes in the blend and, eventually, in the final bioplastic.

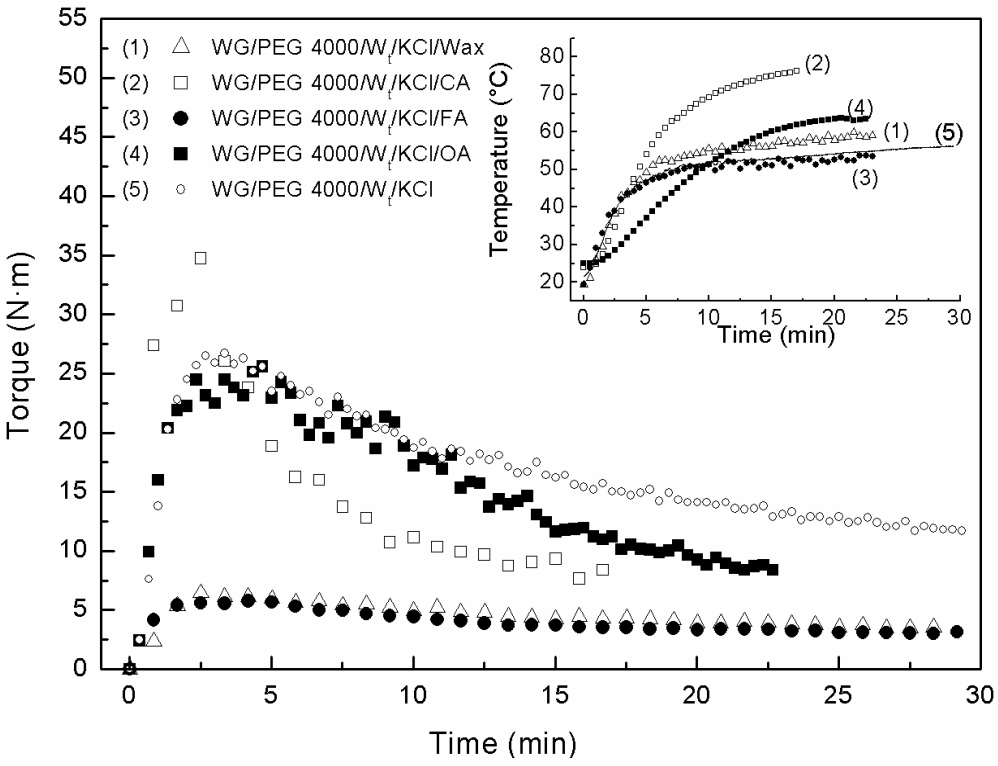

Figure 3.2.5. Evolution of torque and temperature during the mixing process of gluten-based bioplastics with PEG 4000 and modifing agents (citric, formic and octanoic acid, and wax).

As seen in Figure 3.2.6, the sample containing citric acid showed values of E* higher than those found for the other modifiers. Nevertheless, compared to the reference system (WG/PEG4000/Wt/KCl), all modifying agents led to lower values of E* (more noticeable for the formic acid). Moreover, the development of a plateau in E* at about 90ºC suggested certain loss of compatibility between the plasticizer and the polymer matrix (Figure 3.2.6). As may be observed, wheat gluten-based bioplastics showed a rapid decrease in E* up to 60°C, coinciding with a maximum in the loss tangent, and at this point E* tended to reach a plateau or started increasing up to 100ºC. This effect was more apparent for those systems containing carboxylic acids (particularly for formic acid).

Compared to the reference system, the lower values of E* found might be explained by a reduced crosslinking density (Gontard and Ring, 1996) and the replacement of hydrophobic interactions by protein–plasticizer interaction (Kalichevsky et al., 1992). Thus,

the acidic environment provided by the resulting plasticizers might prevent aggregation of gluten protein (Pommet et al., 2005). As a consequence, such protein-plasticizer interactions seemed to be mainly due to the water/carboxylic acid fraction, which further contributed to reduce the PEG4000 compatibility. Moreover, the loss of compatibility, also evidenced by the above-mentioned thermal transitions observed for PEG4000 (Figure 3.2.3), turns out to be more noticeable in the presence of the weakest protein matrix developed by the formic acid (Figure 3.2.6). Finally, for the system containing wax, the lower values of E* would be related to the non-polar character of this additive (highly incompatible with the other polar bioplastic compounds), which would lead to a macroscopic phase separation similar to that previously found for the blend with PEG8000.

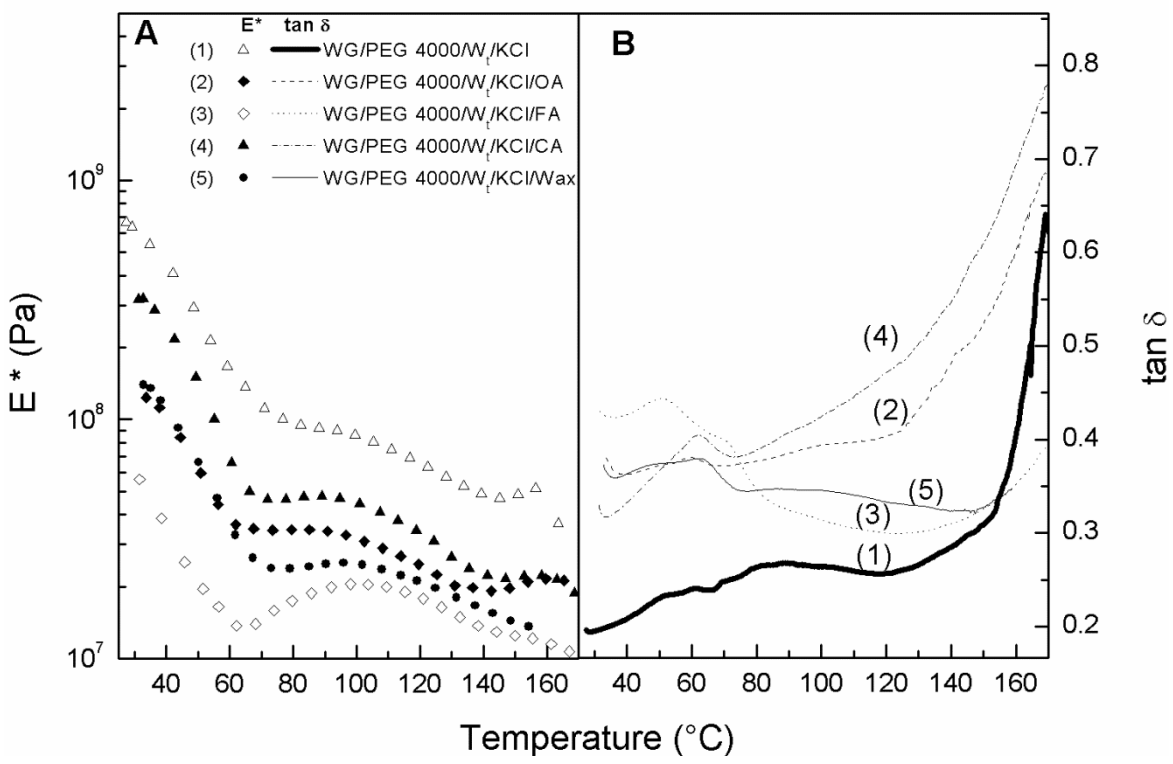

Figure 3.2.6. Dynamic mechanical thermal analysis results, complex modulus and loss tangent for selected blends, after thermoset at 120ºC.

Figure 3.2.7 and Table 3.2.2 show the effect of the different modifying agents studied on the KCl release behaviour and water absorption capacity of gluten-based bioplastics, respectively. Compared to the reference system, the addition of modifying agents generally led to a higher amount of KCl finally released (M_∞) and reduced water absorption (although, it is less evident for the system containing formic acid). As seen in Figure 3.2.7, release patterns strongly depend on the selected additive. Compared to the reference system, wax and

formic and octanoic acids bring about faster release rates (i.e. shorter $t_{1/2}$ values and relatively high slopes, P). This result turns out to be even more evident for octanoic acid. Although this acid strongly reduces bioplastic water uptake (Table 3.2.2), initially hindering the diffusion of KCl, its hydrophobic nature also leads to a polymer matrix with low affinity with the polar salt, which lastly results in the fastest release rate observed (P=3.10). By contrast, citric acid seems to enhance bioplastic properties, displaying release kinetics with a lower P (same value as that shown by bioplastic containing glycerol) and releasing more KCl than the reference system (M_∞≈88 and 74%, respectively), although water uptake capacity is slightly reduced.

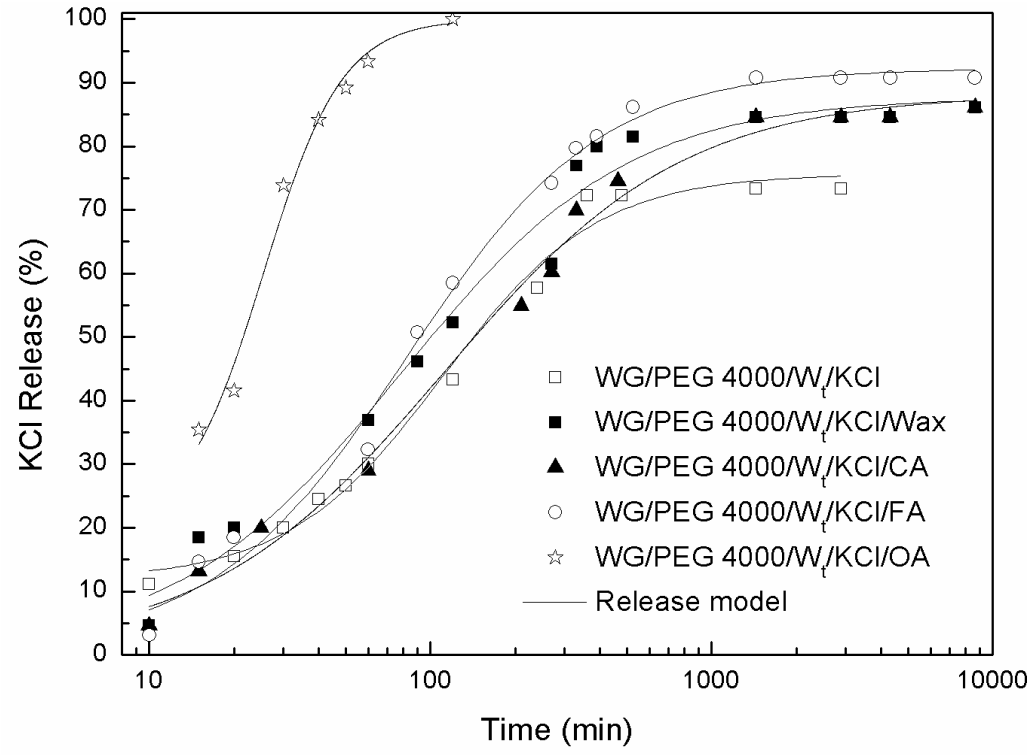

Figure 3.2.7. KCl release behaviour of gluten-based bioplastics with PEG 4000 plasticizer and modifing agents.

Compared to the reference system (WG/PEG4000/Wt/KCl) and the other modifiers, citric acid seemed to impart the most suitable balance between an enhanced protein/salt affinity and material mechanical properties (with slightly lower modulus than the reference system), yielding slower release patterns, higher KCL leaching capacity and suitable water uptake.

3.3 Effect of thermomoulding process on the rheological and controlled-release properties of gluten-based bioplastics plasticized with varying PEG molecular weight

3.3.1 Thermomechanical behaviour of controlled-release matrices plasticized with varying PEG molecular weight

Polyethylene glycol 200

DMTA scans from 30 to 160°C performed on WG/PEG200/Wt/KCl bioplastics as a function of thermosetting temperature are shown in Figure 3.3.1. It can be observed an increase in the complex modulus values as thermomoulding temperature rises. Furthermore, E* curves show a minimum that appears later (from 90 to 130ºC), and with higher modulus values, as thermosetting temperature is raised from 60 to 140°C.

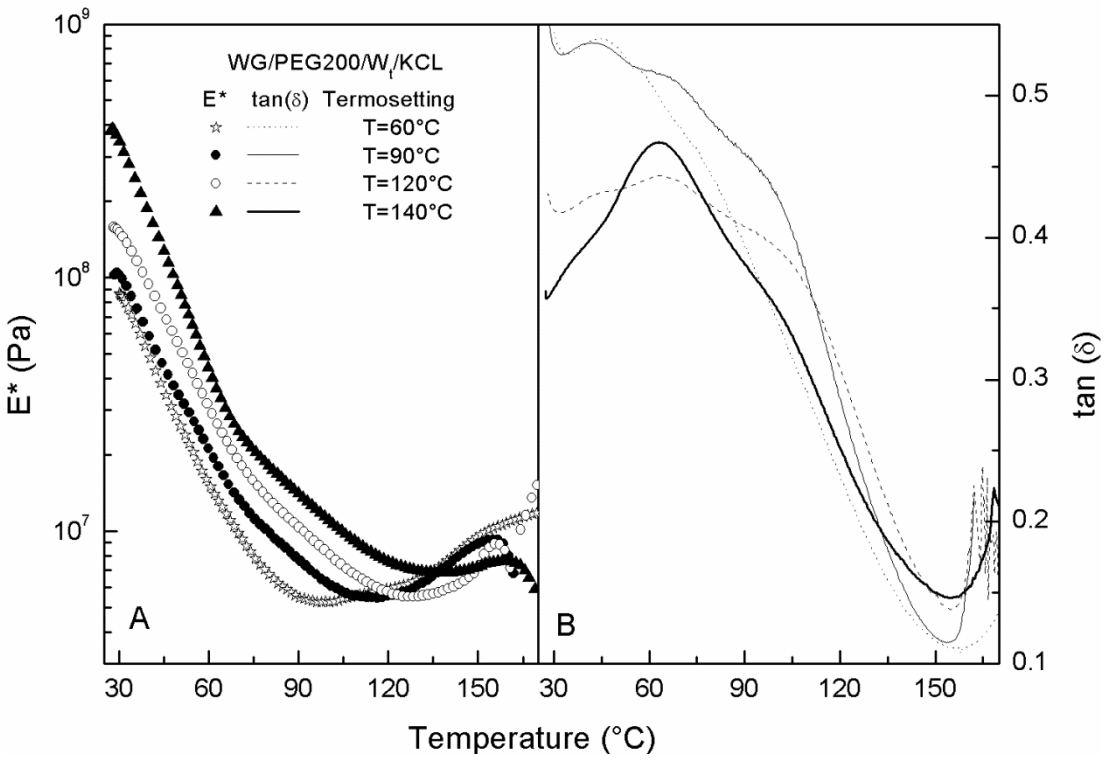

Figure 3.3.1. DMTA results for a selected blend plasticized with PEG 200 after being subjected to different thermosetting temperatures.

Likewise, the maximum in tan δ shifted from 43°C for samples thermoset below 90°C to 67ºC for samples thermomoulded above 120°C (Figure 3.3.1B). Interestingly, this values are lower than the temperature found for wheat gluten plasticized with glycerol (Jerez et al., 2005a), which could mean that PEG 200 induce a different structure in the blends. Finally,

after the minimum in E*, samples underwent a remarkable increase in E* with temperature (Figure 3.2.1A) and exhibited a minimum in loss tangent close to 155°C (Figure 3.2.1B).

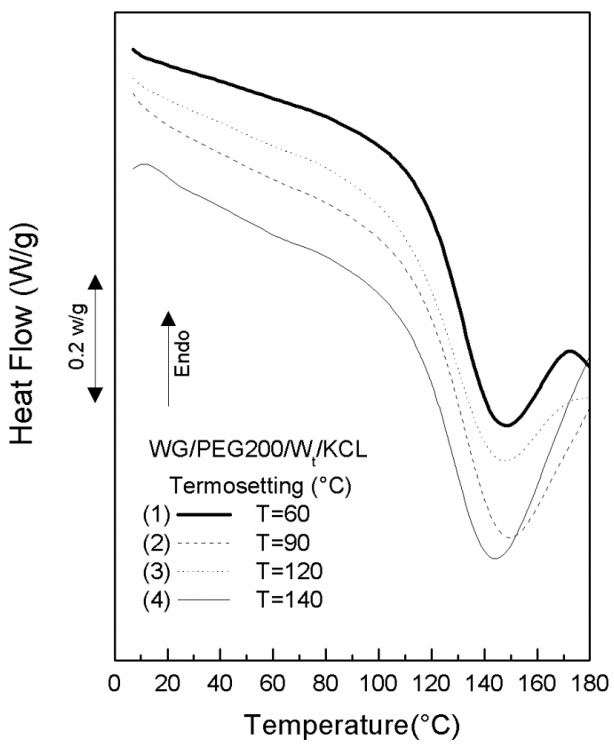

Figure 3.3.2. DSC thermograms for a selected blend plasticized with PEG 200, after being subjected to different thermosetting temperatures.

Such a remaining thermosetting potential seems to be related to the incomplete protein denaturation during its previous thermomechanical manufacture, as might be deduced from DSC scans conducted on the samples, which had an endothermic peak located at ca. 140°C (Figure 3.3.2). Then, it is expected further protein thermal denaturation at temperatures close to this value (140°C), leading to more structured systems with higher values of the linear viscoelastic functions. That was the reason why bioplastics thermomoulded at 140°C hardly show remaining thermosetting potentials (see Figure 3.3.1).

Polyethylene glycol 600

Figure 3.3.3 shows DMTA scans from 30 to 160°C performed on WG/PEG600/Wt/KCl bioplastics as a function of thermosetting temperature. An increase in thermomoulding temperature led to higher complex modulus values, which is more evident for samples thermoset at temperatures above 90°C.

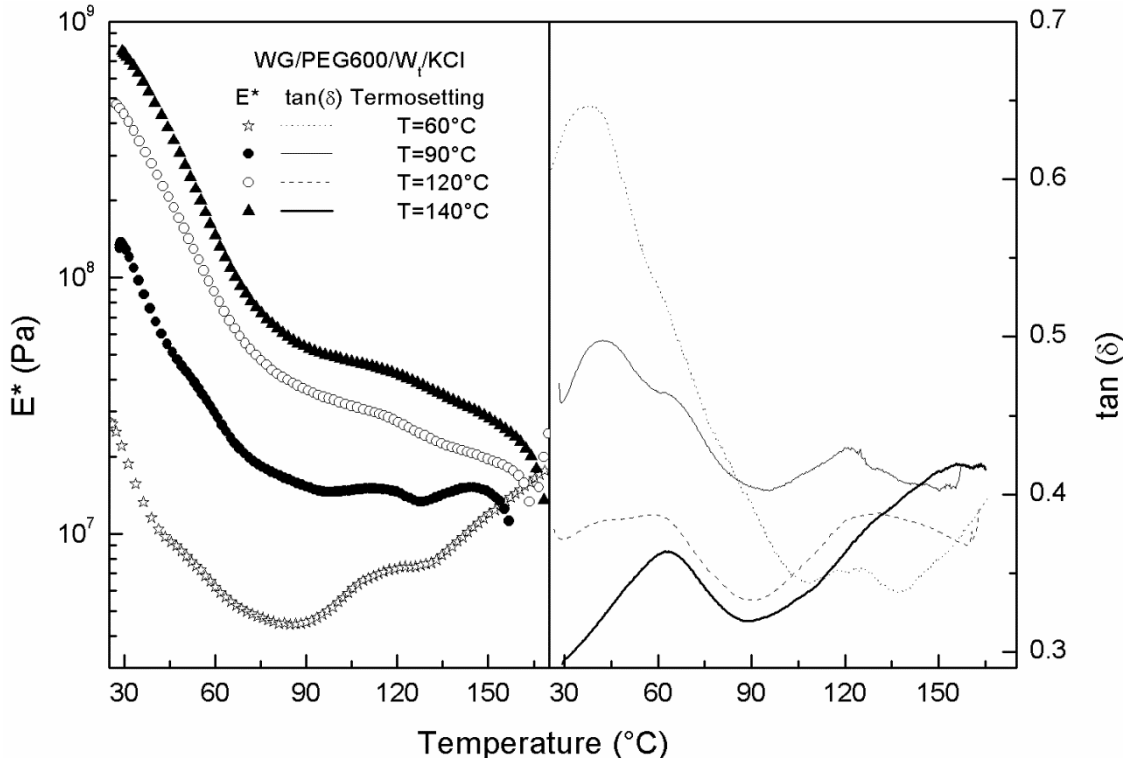

Figure 3.3.3 DMTA results for a selected blend plasticized with PEG 600 after being subjected to different thermosetting temperatures.

Sample thermoset 60°C showed a decreased in E* with temperature up to a minimum closed to 80°C, and exhibeted similar behaviour to bioplastics containing PEG 200 and glycerol thermoset a 60°C. Then, an apparent increase in E* is observed with temperature up to the same E* values found for higher moulding temperatures (close to $2 \cdot 10^7$ Pa). Conversely, samples thermoset above 90°C did not show remaining thermosetting potentials.

A clear change in the tan δ profiles, more evident for samples thermoset at temperature lower than 90°C, was observed (Figure 3.3.3B), with a peak in tan δ close to 40°C. In addition, a significant decrease in tan δ values at this maximum is found as thermosetting temperature increased. It seems that higher thermosetting temperature led to more elastic blends (Figure 3.3.3B). Also, a minimum around 90°C followed by an increase in tan δ for samples thermoset above 90°C is observed. As previously mentioned, this viscoelastic behaviour seems to be related to the lower slope of E* (or flattening), observed above 80 ºC in those samples thermoset above 90°C.

Polyethylene glycol 4000

Figure 3.3.4 shows DMTA scans from 30 to 160°C performed on WG/PEG4000/Wt/KCl bioplastics as a function of thermosetting temperature. Again, higher thermosetting temperatures led to higher values of the complex modulus. However, compared to glycerol-plasticized bioplastics, an early increase in the complex modulus is observed in Figure 3.3.4 between 60 and 100ºC. As seen above, samples thermoset at low temperature (e.g. 60 and 90ºC) exhibit a certain remaining thermosetting potential, which would contribute to such increase.

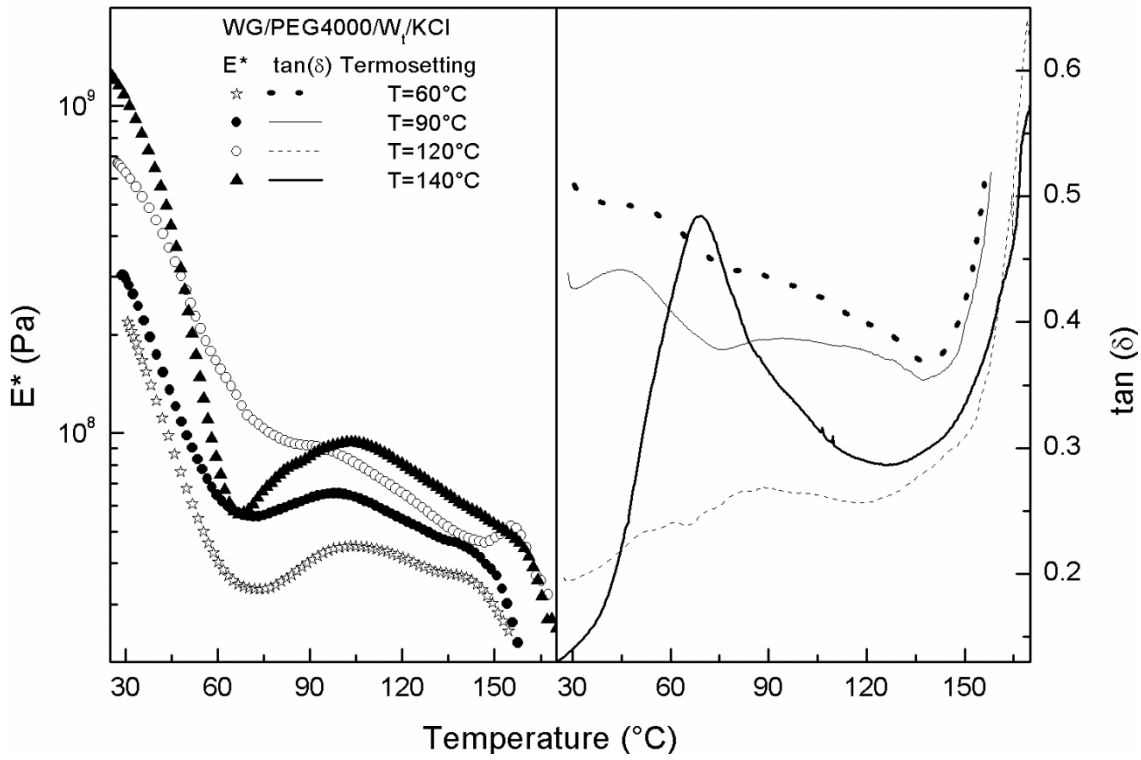

Figure 3.3.4 DMTA results for a selected blend plasticized with PEG 4000 after being subjected to different thermosetting temperatures.

However, sample thermoset at 140ºC showed an apparent minimum close to 60ºC with low values of E*. This event seems to be associated to a pronounce peak in tan δ around 60°C followed by a decay in their corresponding tan δ values (Figure 3.3.4B). As discussed above, a new molten PEG phase, characterized by a lower polar character, would induce the subsequent rearrangement of the polar groups of the protein chains, which would result in the observed increase in E* between 60 and 100ºC.

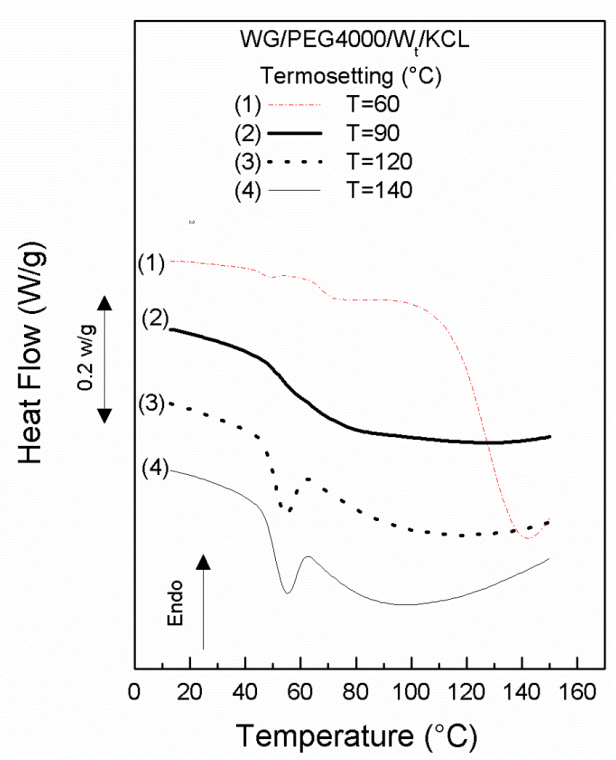

Figure 3.3.5 DSC thermograms for selected blend plasticized with PEG 4000 after being subjected to different thermosetting temperatures.

This assumption seems to be confirmed by means of DSC scans conducted on bioplastics with PEG4000 thermoset at different temperatures (Figure 3.3.5). The thermogram showed a glass transition event at 60°C for samples thermoset at low temperature (below 90°C). In addition, an endothermic peak is found closed to 150°C, which would be related to aggregation of the protein. Interestingly, an endothermic peak is found close to 60ºC in bioplastics thermoset above 120°C, which could be identified as the melting point of the pure crystalline plasticizer (PEG4000). This peak became more apparent as thermosetting temperature increased. As discussed before, this thermal event may evidence a higher incompatibility between the protein matrix and the plasticizer (PEG4000) as thermosetting temperature increases. As a result, the thermal treatment applied on the samples leads to an apparent phase separation (Yuan et al., 2001).

3.3.2 KCl controlled release and bioplastic water absorption

As seen in the last section, glycerol replacement by PEG led to a slower release of KCl and a higher water absorption for system plasticized by PEG4000 and thermoset at 120 ºC. This section focuses on the effect that thermosetting processing exerts on blends plasticized

with varying PEG molecular weight. In this sense, Figures 3.3.6 and 3.3.7 show KCl release and water absorption properties of such systems. The KCl release behaviour has been fitted to a signomoidal model by the equation 3.1.1 and Table 3.3.1 gathers the calculated values for parameters M_0 and M_∞ which respectively refer to the concentrations (wt. %) of KCl initially and finally released by the bioplastic. In addition, parameters such as the time for 50% KCl release ($t_{½}$) and the rate of release (P) are shown in Table 3.3.1 .

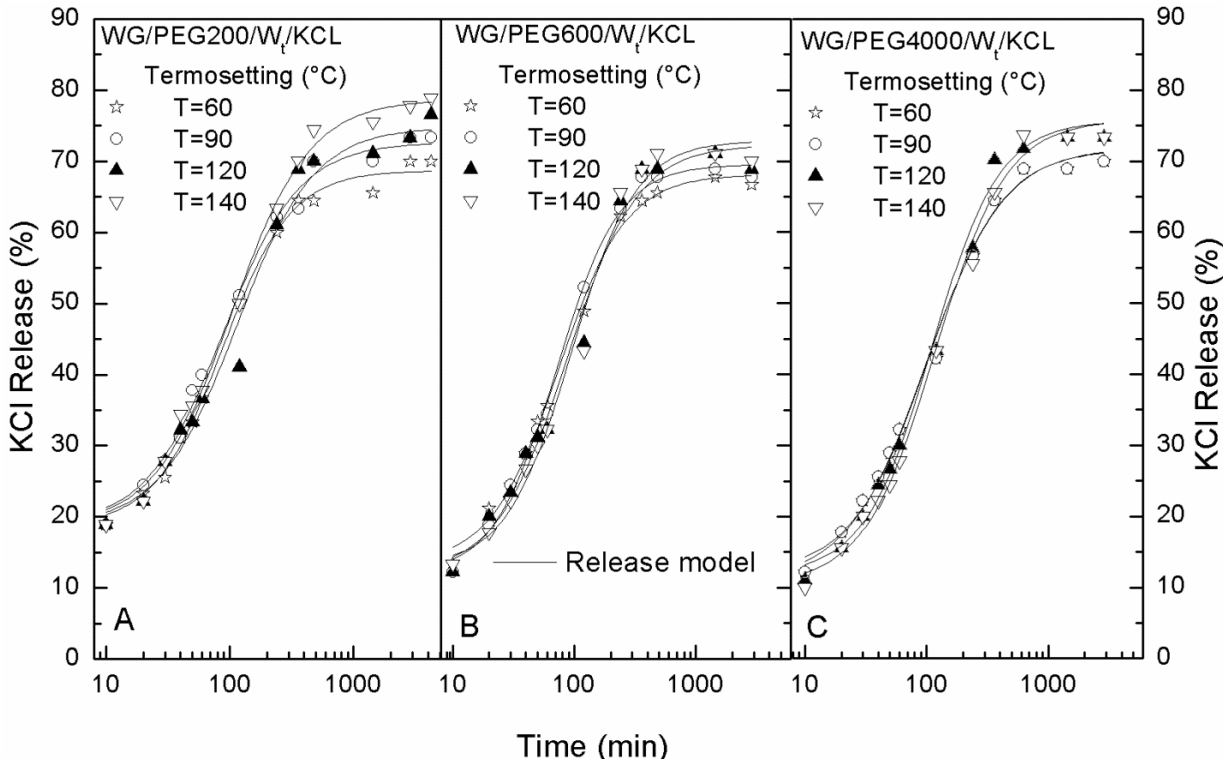

Figure 3.3.6 KCl release behaviour for selected blend plasticized with PEG 200(A), PEG600(B) and PEG 4000 (C) after different thermosetting temperatures.

Table 3.3.1 shows that a decrease in the rate of release (*P*) and an increase in $t_{1/2}$ takes place as thermosetting temperature is higher, for bioplastics plasticized by PEG200. On the other hand, samples formulated with PEG600 and PEG 4000 (Figures 3.3.6B and C) exhibited an increase in both $t_{1/2}$ and *P* as thermosetting temperature is higher (Table 3.3.1).

As may be seen, major differences among moulding temperatures appear at the longest release times (Figure 3.3.6). In all cases, an increase in the thermomoulding temperature slightly lowers the values of M_0 but, conversely, the thermal treatment raises the final concentration of KCl released (M_∞). A similar behaviour for bioplastics plasticized with

glycerol is also found, although in this case the release of KCl was slower (Tables 3.2.2 and 3.3.1).

Table 3.3.1. Effect of thermosetting temperature on the release parameters from equation [3.1.1], for gluten-based bioplastics plasticized with varying PEG molecular weight

Composition	Conditions Temperature (°C)	Parameter			
		M_o	M_∞	$t_{½}$	P
WG/PEG200/Wt/KCl	60	18.50	68.50	75.16	1.55
WG/PEG200/Wt/KCl	90	16.50	72.45	75.47	1.38
WG/PEG200/Wt/KCl	120	15.40	74.77	88.80	1.33
WG/PEG200/Wt/KCl	140	14.50	78.85	85.45	1.27
WG/PEG600/Wt/KCl	60	11.00	68.50	69.78	1.44
WG/PEG600/Wt/KCl	90	9.00	70.82	70.12	1.46
WG/PEG600/Wt/KCl	120	11.99	72.28	86.50	1.49
WG/PEG600/Wt/KCl	140	10.38	73.13	87.54	1.52
WG/PEG4000/Wt/KCl	60	11.00	71.87	98.78	1.34
WG/PEG4000/Wt/KCl	90	12.00	71.68	101.57	1.39
WG/PEG4000/Wt/KCl	120	11.83	75.65	110.22	1.57
WG/PEG4000/Wt/KCl	140	10.00	75.00	112.27	1.58

Finally, Figure 3.3.7 shows the water absorption capability of bioplastics containing polyethylene glycol as a function of thermosetting temperature. As may be seen, water absorption tends to increases as moulding temperature does, a result more apparent for the highest molecular weight (PEG 4000).

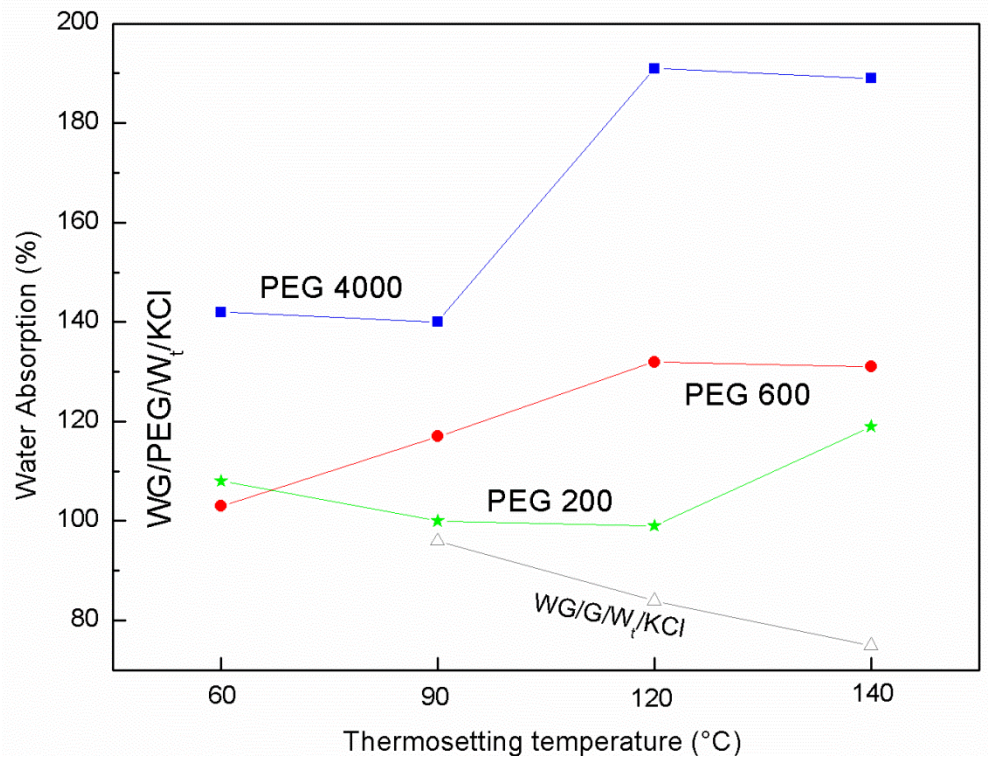

Figure 3.3.7 Water absorption for wheat gluten plasticized with varying PEG molecular weight processed at different temperatures.

4. Protein-based bioplastics with antimicrobial activity for potential application in food packaging

Antimicrobial packaging is a promising and rapidly emerging technology in which antimicrobials, such as essential oils, as well as their individual chemical constituent agents, are incorporated into, or coated onto, food packaging materials to prolong the self-life of the packed food, usually by extending the lag phase and reducing the growth rate of microorganisms (Han JH, 2000; Nakatsu et al., 2000; Suppakul et al., 2003). To this end, the first part of this chapter concerns the incorporation of 18 such antimicrobial agents into wheat gluten-based bioplastics, and the measurement of their inhibitory effect against selected food pathogens for several applications. In the second part, four specific antimicrobial agent were selected for a study into the effect of the concentration on wheat gluten-based bioplastics. Different protein formulations in combination with four specific antimicrobial agents were

studied in the third section. Finally, a study was made of the effect of cinnamaldehyde and different concentrations of thymol on the thermomechanical characteristics, antimicrobial activity and water absorption properties of samples of potato protein and wheat gluten bioplastic, which had been processed at 80°C, and thermoset at 120°C.

4.1 Effect of the incorporation of antimicrobial agents into wheat gluten based bioplastics

Despite of the broad application of protein-based bioplastics, there is nothing in the literature regarding the use of natural antimicrobial agents (essential oil and their antimicrobial agents) in bioplastics, whether manufactured by mixing, extrusion or thermomoulding. In this section, the inhibitory effect of eighteen antimicrobial agents against four selected food pathogens is evaluated. The study includes antimicrobial agent and protein interaction during processing, and the influence on the viscoelastic and water absorption properties. The formulations for such bioactive gluten-based bioplastics are shown in Table 2.4 in Materials and Methods. The antimicrobial concentration is fixed at 10 wt.%.

Thermoplastic processing

As demonstrated in previous results, the manufacture of bioplastics requires complete mixing of all the components during the thermoplastic processing. The blends in this study contained 10 wt.% antimicrobial agent, 23 wt.% glycerol and 67 wt.% wheat gluten. Two blends, one containing red thyme and the other oregano essential oil were selected as examples to describe the evolution of torque and temperature during mixing process, the results of which are shown in Figure 4.1.1. As can be seen, the evolution of torque exhibited different regions depending on the antimicrobial agent. In the first region, a non-significant increase in torque can be seen. Then, a significant increase in torque up to a maximum value is observed in the second region. Finally, a torque decay is obtained. The sample containing red thyme produced three regions during mixing, while, the sample containing oregano produced only two. The temperature evolution also displays different zones during the mixing process, which are related to the torque regions (Figure 4.1.1B).

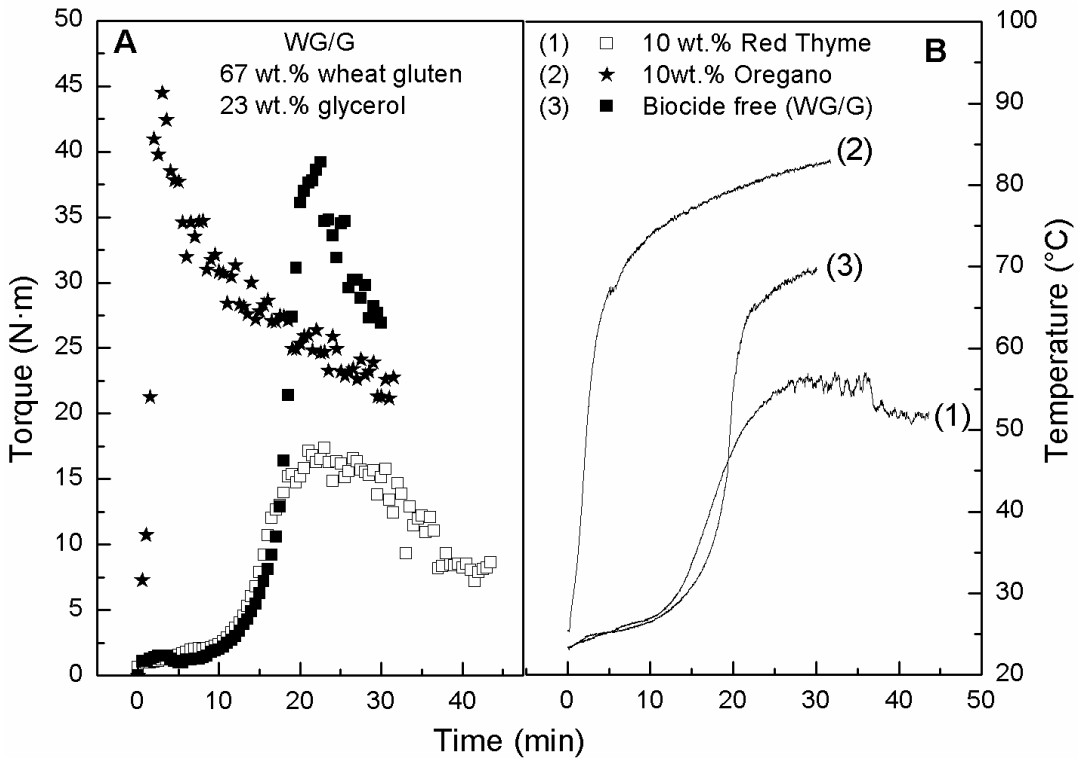

Figure 4.1.1 Evolution of torque and temperature during the mixing process for blends containing 10 wt.% oregano and red thyme, 23 wt.% glycerol and 67 wt.% wheat gluten.

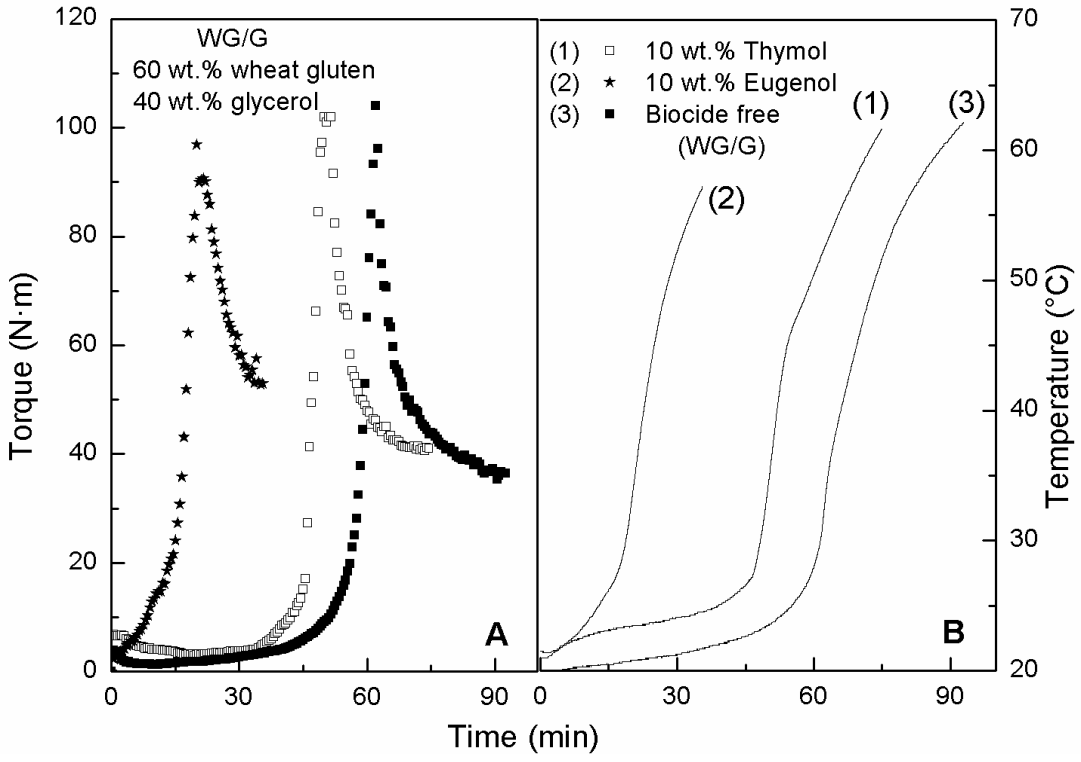

Figure 4.1.2 Evolution of torque and temperature during the mixing process for blends containing 10 wt.% thymol and eugenol, 30 wt.% glycerol and 60 wt.% wheat gluten.

The sample containing red thyme reached a lower maximum torque value than the sample without the antimicrobial agent, but this peak was reached in the same time for both (Fig. 4.1.1). Meanwhile, the sample containing oregano reached a maximum in less time than the sample without the antimicrobial agent, although the difference in the torque values at the maximum for both samples was not significant.

A further seven antimicrobial agents were tested as additives to wheat gluten-based bioplastic, in all cases with a higher glycerol content, as shown in Table 2.4 in Material and Methods. These blends contained 10 wt.% antimicrobial agent, 30 wt.% glycerol and 60 wt.% wheat gluten. It is worth mentioning that these blends exhibited higher maximum torque values and took longer to reach this peak than the two samples mentioned above due to the high glycerol concentration in the blends. As an example, two of the seven blends, those containing thymol and eugenol, have been selected to describe the evolution of torque and temperature during the mixing process. The evolution of torque and temperature also exhibited different regions depending on the antimicrobial agent, as shown in Figure 4.1.2. Thus, the sample containing thymol produced three regions during mixing, while, the sample containing eugenol only produced two. The temperature evolution also displayed different zones during the mixing process, which relate to the torque regions (Figure 4.1.2B). In both cases, there was a non-significant difference at the maximum torque value. Although the sample containing eugenol reached this maximum in less time than the sample containing thymol and the sample without any antimicrobial agent.

The plasticizer and antimicrobial agent both affect the parameters governing the mixing process. These parameters include specific mechanical energy (SME), temperature and time taken to reach maximum torque. The SME values for the bioplastics studied were calculated using to Equation 1.1.1, chapter 1. The mixing time t_{mix} was always estimated as 1.5 t_{peak} for the sake of comparison. Table 4.1.1 gathers the mixing process parameters for 18 formulations of bioplastic containing 10 wt.% antimicrobial agents, wheat gluten and glycerol.

Table 4.1.1. Processing parameters for protein-based bioplastics with antimicrobial agents

Sample number	Glycerol (wt.%)	Antimicrobial agent (10 wt.%)	Mixing process parameters			Volatility at 100ºC (wt.%)
			T_{max} (ºC)	t_{max} (min)	SME (KJ/Kg)	
	33	none	75	21.9	2647	-
1	23	Red thyme	51	26.0	2026.6	30
2	23	Cinnamon	60	20.5	2539.5	6
3	23	Clove	72	17.4	2439.3	3
4	23	Peppermint	52	15.4	1257.2	17
5	23	Bergamot	45	14.8	1162.6	34
6	23	Rosemary	47	6.3	375.8	54
7	23	White thyme	53	22.9	1849.5	23
8	23	Lemon	40	6.5	384.8	47
9	23	Carvacrol	88	3.6	556.8	5
10	23	Cinnamaldehyde	108	6.0	727.0	4
11	23	Oregano	83	3.0	854.5	-
	40	none	62	62.0	11018	-
12	30	Orange	39	30.5	4157.6	20
13	30	Lemongrass	42	26.2	4251.6	4
14	30	Citral	69	33.3	9424.3	3
15	30	Limonene	41	17.5	3472.9	4
16	30	Linalool	40	29.9	10128.2	7
17	30	Thymol	62	50.3	7423.9	1
18	30	Eugenol	57	20.5	4251.6	1

As can be seen, the maximum value of torque is reached at different times depending on glycerol content and type of antimicrobial agent. The samples containing 23 wt.% glycerol divide into two different groups, the first comprising samples which reached maximum torque between 14 and 26 min. and which included samples containing red thyme, cinnamon, clove, bergamot, peppermint and white thyme, and the second comprising samples which reached maximum torque within 6.5 min and which included samples containing rosemary, lemon, carvacrol, oregano and cinnamaldehyde. As this suggests, the samples in the latter group experienced a rapid increase in torque until they reached the maximum, and as a result, they failed to produce a first region during the torque evolution, unlike the samples in the first group, which all did. By contrast, samples containing 30 wt.% glycerol took longer to reach a maximum (in excess of 26 min) than those with lower glycerol content, with the exception of the blend containing limonene, which reached this maximum at 17.5 min.

During the mixing process an interaction between components might trigger an exothermic reaction and cause an increase in the temperature of the blends. In our case, this temperature should be lower than temperature of protein denaturation and antimicrobial agent evaporation. Table 4.1.1 gathers the maximum temperature reached at the end of the mixing process for all blends. These results show that only carvacrol, oregano and cinnamaldehyde reached a temperature close to 100ºC, a temperature sufficient to cause denaturation of the wheat gluten. The volatility of the various antimicrobial agents at 100ºC might give us an idea about of much might have evaporated during the mixing process or thermomechanical treament (Table 4.1.1). The most volatile of the antimicrobial agents was rosemary (54 wt.%) followed by lemon (47 wt.%), bergamot (34 wt.%) and red thyme (30 wt.%). The other antimicrobial agents exhibited values of volatility lower than 30 wt.% . None of the mixtures reached 100ºC during the mixing process, with the exception of cinnamaldehyde, which reached a final temperature in the mixing process of 108ºC, so it is likely that approximately 4% of antimicrobial agent could have been lost during the mixing process (Table 4.1.1).

As can be seen in Table 4.1.1, biocide addition led to a decrease in SME for all blends. In the case of blends with 23 wt.% glycerol, the sample containing lemon exhibited the lowest SME values, followed by carvacrol, whilst in the case of those with 30 wt.% glycerol, the sample containing limonene presented the lowest SME, followed by orange, lemongrass and eugenol.

Antimicrobial activity

The effectiveness in killing microorganisms was tested in two ways: first, by placing the bioplastic on a solid media, and second, by placing the bioplastic on the inside of the lid. The latter may be useful in non-contact food applications. Figures 4.1.3 and 4.1.4 show two examples of microbiological tests in which bioplastics were placed on the inside of the lid for samples containing cinnamon and clove essential oils. In these cases, the volatility of cinnamon and clove have created an antimicrobial atmosphere within the container against two selected bacteria (E.Coli and S.Aureus).

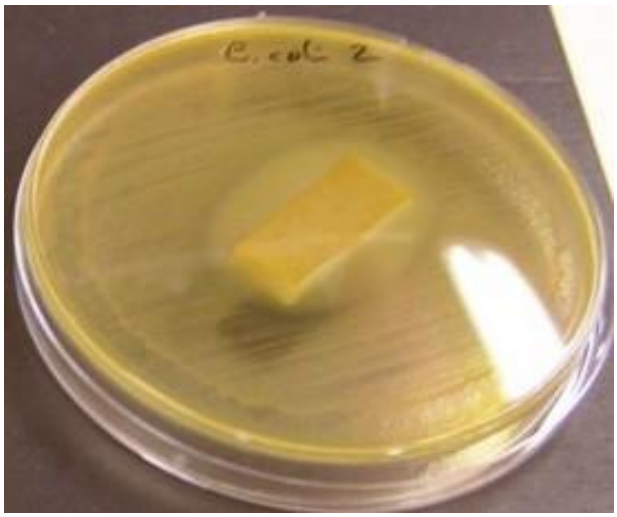

Figure 4.1.3 Microbiological analysis in selected media (E.coli) for wheat gluten/glycerol containing 10 wt.% cinnamon on the inside of the lid.

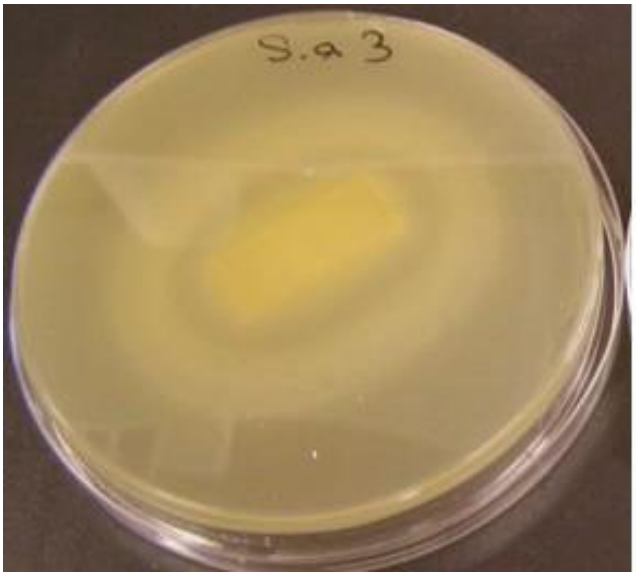

Figure 4.1.4 Microbiological test in selected media (S. Aureus) for wheat gluten/glycerol (WG/G) containing 10 wt.% clove on the inside of the lid.

Figures 4.1.5 and 4.1.6 show two examples of the microbiological analysis when bioplastic containing cinnamaldehyde was placed on a solid media. As can be observed cinnamaldehyde has created a wide inhibition zone around itself against two selected microorganisms (E.coli and A.Niger). This high degree of antimicrobial activity was more evident when compared to samples without antimicrobial agents, Figures 4.1.5A and 4.1.6A, where no antimicrobial activity is observed.

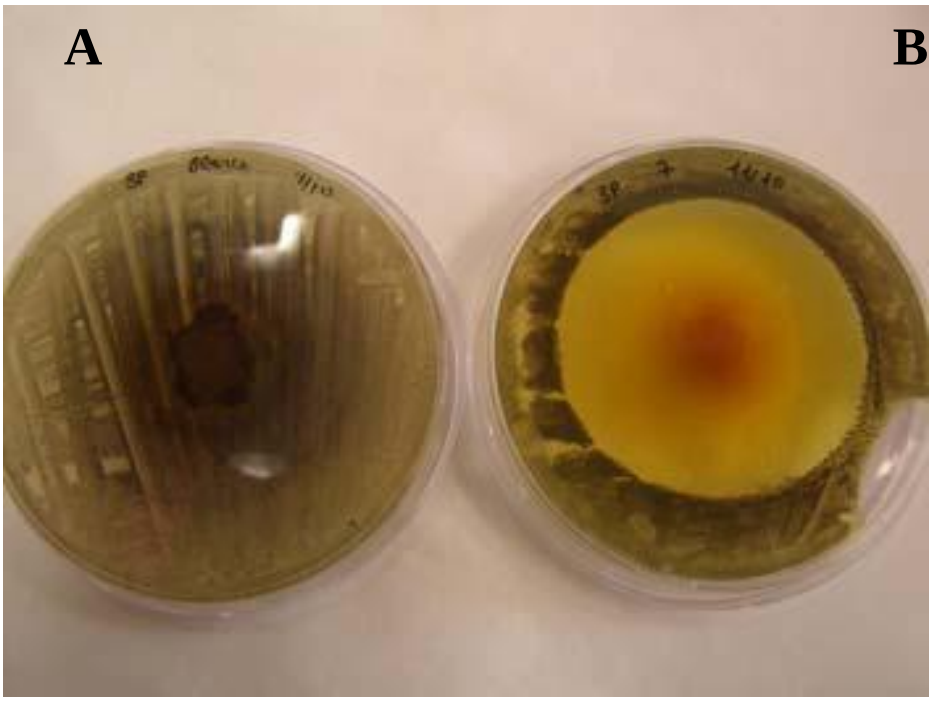

Figure 4.1.5 Microbiological test in selected media (E.coli) for wheat gluten/glycerol (reference) (A), and wheat gluten/glycerol containing 10 wt.% cinnamaldehyde (B).

The antimicrobial effectiveness of the bioactive agents was measured by the inhibition zone assay (Table 4.1.2). The main biological activity and the potential uses of essential oils in the food industry are derived from their capacity to kill microorganisms. In this respect, cinnamon, clove, red and white thyme, carvacrol, cinnamaldehyde, eugenol and thymol at 10 wt.% were effective against all the microorganisms studied. Some authors have reported the antimicrobial activity of eugenol, thymol and carvacrol against bacteria (Periago et al., 2004), yeast (Arora and Kaur, 1999) and fungi (Vazquez et al., 2001).

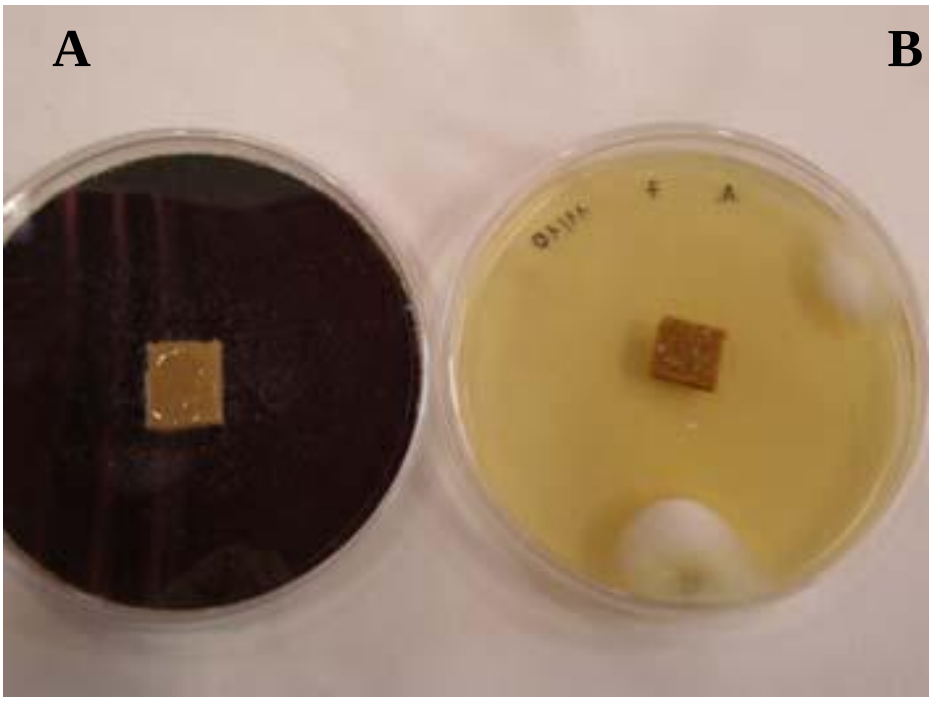

Figure 4.1.6 Microbiological test in selected media (A. Niger) for wheat gluten/glycerol (reference) (A), and wheat gluten/glycerol containing 10 wt.% cinnamaldehyde (B).

Table 4.1.2. Antimicrobial results for bioplastic specimens.

Sample number	**Antimicrobial agent (10 wt.%)**	**E. Coli** (Gran - bacteria)	**S. aureus** (Gran + bacteria)	**C. albicans** (Fungus)	**A.niger** (Fungus)
1	Bergamot	-	-	-	-
2	Cinnamon	++	++	++	+++
3	Clove	++	++	++	+++
4	Pepermint	-	-	-	+
5	Red thyme	+	+	+	+
6	Carvacrol	++	++	++	+++
7	Cinnanaldehyde	+++	+++	+++	+++
8	Lemon	-	-	-	-
9	Rosemary	-	-	-	-
10	White thyme	++	++	++	+++
11	Citral	-	-	+++	+++
12	Lemongrass	-	-	+++	+++
13	Limonene	-	-	-	-
13	Orange	-	-	-	-
14	Eugenol	++	++	++	+++
15	Linalool	-	-	-	-
16	Thymol	+++	+++	+++	+++

Inhibition zone diameter:
+++ (70 mm< d)
++ (70 mm< d >20 mm)
+ (d < 20 mm)
- Without activity

In terms of ability to inhibit growth of the selected microorganisms, the best results were obtained for samples containing cinnamaldehyde, carvacrol, white thyme, thymol, eugenol and linalol. On the other hand, samples containing orange, lemon, bergamot, rosemary and limonene oils were not as effective as the other oils or components tested, whilst citral and lemongrass were effective only for fungi (C. albacans and A. Niger). Citrus essential oils could represent a good candidate for improving the shelf-life and safety of minimally processed fruit. In fact, it is well known that these oils can have a pronounced antimicrobial effect.

Water absorption properties

Previous studies have pointed out that both processing conditions and bioplastic formulation may lead to materials with a wide range of mechanical responses and underlying microstructures (Rouilly et al., 2006; Jerez et al., 2005a, 2007). As a result, different swelling capabilities should be expected. Table 4.1.3 gathers the water absorption values after 24 h for wheat gluten/glycerol blends containing 10 wt.% of the 18 different antimicrobial agents. It can be observed that the addition of peppermint, carvacrol and cinnamaldehyde led to a significant reduction in water absorption for blends containing 23 wt.% glycerol. These values were 54 wt.% for samples with peppermint, 55 wt.% for samples with carvacrol and 56 wt.% for samples with cinnamaldehyde. On the other hand, samples containing bergamot, cinnamon, clove, oregano, white and red thyme all exhibited similar water absorption behaviour which led to a decrease in water absorption to values around 70 wt.%.

Table 4.1.3. Water absorption for protein-based bioplastics with antimicrobial agents

Sample number	**Glycerol (wt.%)**	**Antimicrobial agent (10 wt.%)**	**Water absorption (wt.%)**
1	23	Red thyme	80
2	23	Cinnamon	75
3	23	Clove	75
4	23	Peppermint	54
5	23	Bergamot	71
6	23	Rosemary	93
7	23	White thyme	74
8	23	Lemon	95
9	23	Carvacrol	55
10	23	Cinnamaldehyde	56

Sample number	Glycerol (wt.%)	Antimicrobial agent (10 wt.%)	Water absorption (wt.%)
11	23	Oregano	76
12	30	Orange	89
13	30	Lemongrass	57
14	30	Citral	48
15	30	Limonene	98
16	30	Linalool	90
17	30	Thymol	82
18	30	Eugenol	73

In the case of samples with 30 wt.% glycerol, the sample containing citral exhibited the lowest swelling ratio, 48 wt.%, followed by lemongrass with 57 wt.%. In addition, a decrease in water absorption to 73 wt.% was observed for the sample containing eugenol, and 80 wt.% for thymol. There was no apparent effect on water absorption by the addition of linalool, limonene, lemon and rosemary.

Thermomechanical properties

Different formulations of protein-based bioplastic can produce a very broad range of rheological characteristics. With this in mind, samples were selected and those containing 10 wt.% cinnamon, clove, red thyme, carvacrol, cinnamaldehyde, thyme and eugenol were evaluated for their thermomechanical properties. The selection took into account the previous results with respect to water absorption capacity and antimicrobial activity. Figure 4.1.7 shows typical DMTA scans (from 30 to 160ºC) of wheat gluten/glycerol samples containing 10 wt.% antimicrobial agent, and obtained by moulding at 100 bar and thermosetting at 90ºC. A significant decrease in the complex modulus for samples containing 30 wt.% of glycerol was observed (Figure 4.1.7B), due to the high glycerol concentration in the blend, with a difference of about one decade compared to samples containing 23 wt.% glycerol (Figure 4.1.7A). The evolution of complex modulus for both formulations was quite similar. First, there was a decrease in E* to a minimum value in a temperature range of between 95 and 135ºC. The addition of cinnamon, clove and red thyme led to a increase in E* at this minimum for samples containing 23 wt.% glycerol. This increase was more evident in the sample containing cinnamon (Figure 4.1.7A). By contrast, for samples containing 30 wt.% glycerol, only eugenol led to a significant increase in E* at the minimum (Figure 4.1.7B). Finally, a remarkable increase in E* with temperature can be observed above 135ºC.

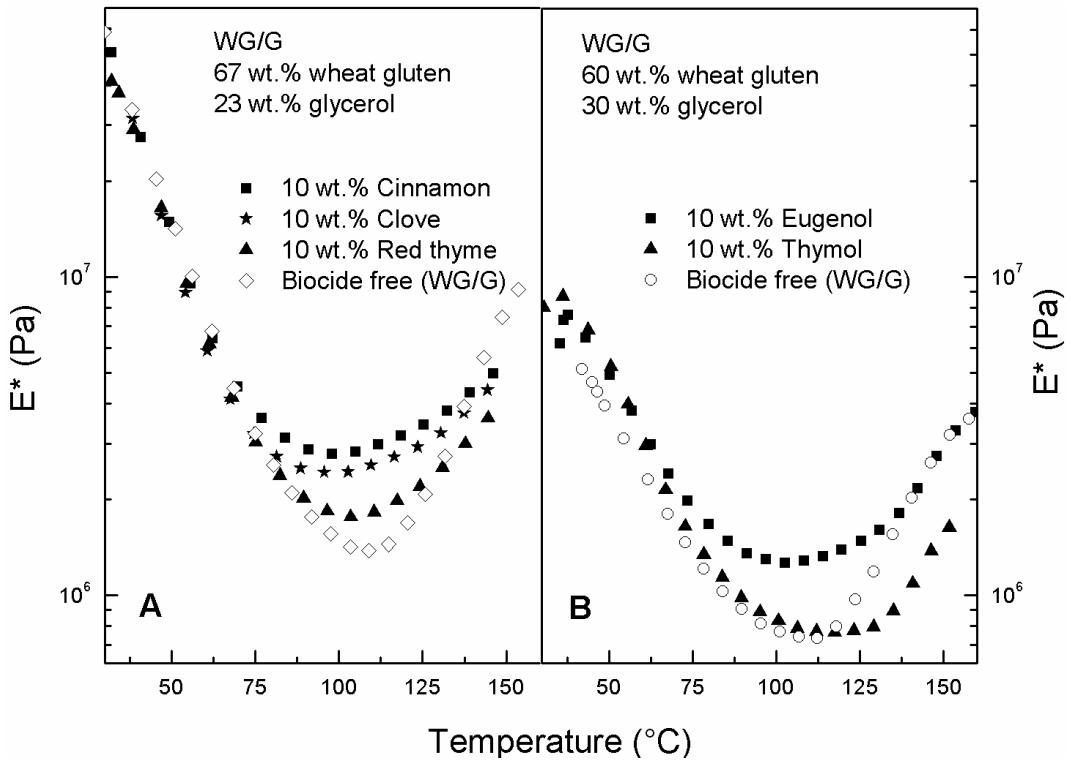

Figure 4.1.7 Dynamic mechanical thermal analysis results, complex modulus (E) for blends containing 10 wt.% cinnamon, clove and red thyme, 23 wt.% glycerol and 67 wt.% wheat gluten (A), and blends containing 10 wt.% eugenol and thymol, 30 wt.% glycerol and 60 wt.% wheat gluten (B).*

Table 4.1.4. Thermomechanical values for wheat gluten-based bioplastic with different antimicrobial agents.

Sample number	**Glycerol (wt.%)**	**Antimicrobial agent (10 wt.%)**	**E* (Pa) at 30ºC**
1	23	Cinnamon	5.07E+07
2	23	Clove	5.96E+07
3	23	Red thyme	4.12E+07
4	23	Oregano	7.97E+07
5	23	Carvacrol	7.49E+07
6	23	Cinnamaldehyde	7.24E+07
7	33	Biocide Free	5.77E+07
8	30	Eugenol	6.20E+06
9	30	Thymol	5.96E+07
10	40	Biocide Free	4.74E+06

Table 4.1.4 shows the complex modulus at 30ºC for wheat gluten-based bioplastics with 10 wt.% of different antimicrobial agents. As can be observed, the complex modulus values at 30ºC seems not to be affected by the addition of cinnamon, clove and red thyme

compared to the sample without an antimicrobial agent. However, a further increase in E* for samples containing carvacrol, cinnamaldehyde and eugenol is observed (Table 4.1.4). In this case, the addition of these antimicrobial agents led to an increase in the crosslinking in the protein, which also correlates with the low water absorption values obtained for these samples.

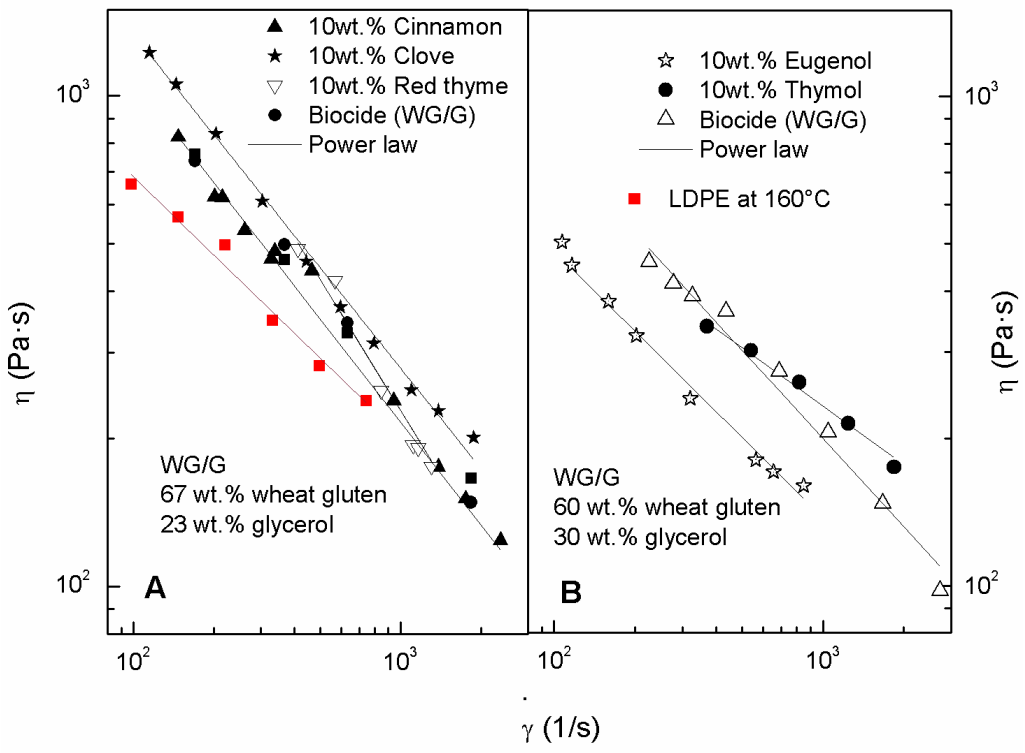

Figure 4.1.8 Influence of blend composition on the viscous flow behaviour, at 90ºC, for blends containing 10 wt.% cinnamon, clove and red thyme, 23 wt.% glycerol and 67 wt.% wheat gluten (A) and blends containing 10 wt.% eugenol and thymol, 30 wt.% glycerol and 60 wt.% wheat gluten (B).

Figure 4.1.8 shows viscous flow curves at 90ºC for wheat gluten/glycerol samples containing 10 wt.% antimicrobial agents, collected just after the mixing process. Two behaviours, depending to the glycerol content, are observed. In the case of samples containing 23 wt.% glycerol, the addition of clove led to a slight increase in viscosity (Figure 4.1.8A). However, there was not a significant difference in the viscosity by the addition of cinnamon and red thyme. The viscosity of these materials was higher than the well-known low density polyethylene (LDPE) at 160ºC.

In the case of samples containing 30 wt.% glycerol, the addition of eugenol led to a decrease in viscosity compared to the sample without an antimicrobial agent. The viscosity of

this material was similar to the low density polyethylene (LDPE) at 160ºC. Meanwhile, a non-significant difference was observed in the viscosity by the addition of thymol compared to sample without an antimicrobial agent. However, a slight increase in the viscosity at higher shear rate is noticed (Figure 4.1.8B).

The power-law model fits the shear-thinning behaviour observed fairly well (Equation 1.1.2 in chapter 1). Table 4.1.5 gathers the values of *k*, the consistency index, and *n*, the flow index, for the different blends studied.

Table 4.1.5. Antimicrobial agent effect on the viscosity parameters for wheat gluten-based bioplastic containing 10 wt.% antimicrobial agent.

Sample number	**Glycerol (wt.%)**	**Antimicrobial agent (10 wt.%)**	**Parameters of Power-low model**	
			***k* ($Pa \cdot s^n$)**	***n***
1	LDPE	Biocide free	7846	0.47
2	33	Biocide free	20361	0.36
3	23	Cinnamon	27134	0.30
4	23	Clove	30617	0.32
5	23	Red thyme	106864	0.11
6	40	Biocide free	12557	0.40
7	30	Eugenol	3588	0.60
8	30	Thymol	5939	0.45

As can be observed in Table 4.1.5, the addition of clove, red thyme and cinnamon led to an increase in the consistency index and a decrease in the flow index for samples containing 23 wt.% glycerol. This behaviour was more evident for the sample containing red thyme. On the other hand, a significant decrease in the consistency index and a decrease in the flow index is observed for samples containing 30 wt.% glycerol by the addition of eugenol and thymol.

4.2 Effect of antimicrobial agents concentration into a wheat gluten based bioplastics

Based on the results of the last section, four specific antimicrobial agents were selected to study how these could affect the viscoelastic and water absorption properties of the bioplastics obtained if incorporated at different concentrations. In this section wheat gluten is used as protein and glycerol as plasticizer. The antimicrobial agents selected were cinnamon, cinamaldehyde, clove and white thyme. These antimicrobial agents were selected mainly for their strong effectiveness against all the microorganisms studied.

Thermoplastic processing

The evolution of torque and temperature during the mixing process for wheat gluten-based bioplastics with three concentrations of cinnamon oil are shown in Figure 4.2.1. All three blends presented a torque evolution with three regions similar to the wheat gluten sample without biocide as described in Chapter 1.

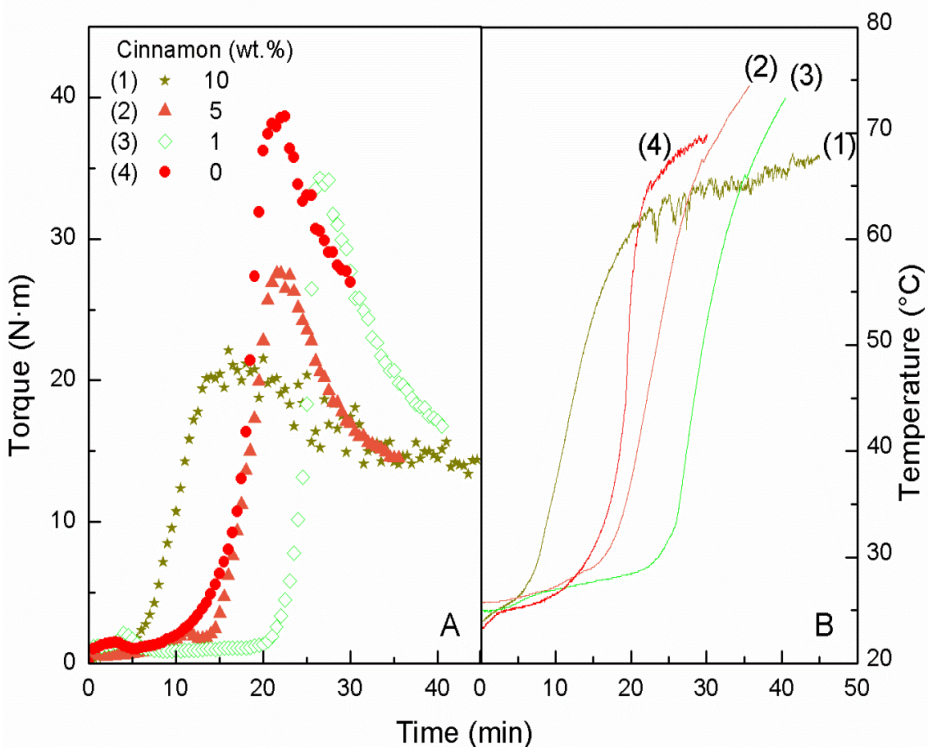

Figure 4.2.1 Evolution of torque and temperature during mixing for wheat gluten-based bioplastic with different concentrations of cinnamon as antimicrobial agent.

It can be observed that an increase in cinnamon oil concentration led to a decrease in the induction region. In this instance, the value of the torque maximum, and the time required

to achieve it, decrease as the cinnamon content increased. In addition, different temperature regions were also found during the mixing process, which were related to the torque regions (Figure 4.2.1B). Consequently, the temperature reached at the peak of torque became lower as the cinnamon oil content decreased. This may related to the lower values of torque observed with higher cinnamon oil content. The final temperature of the mixing process was reached before 74ºC for the blend containing the lowest cinnamon oil concentration.

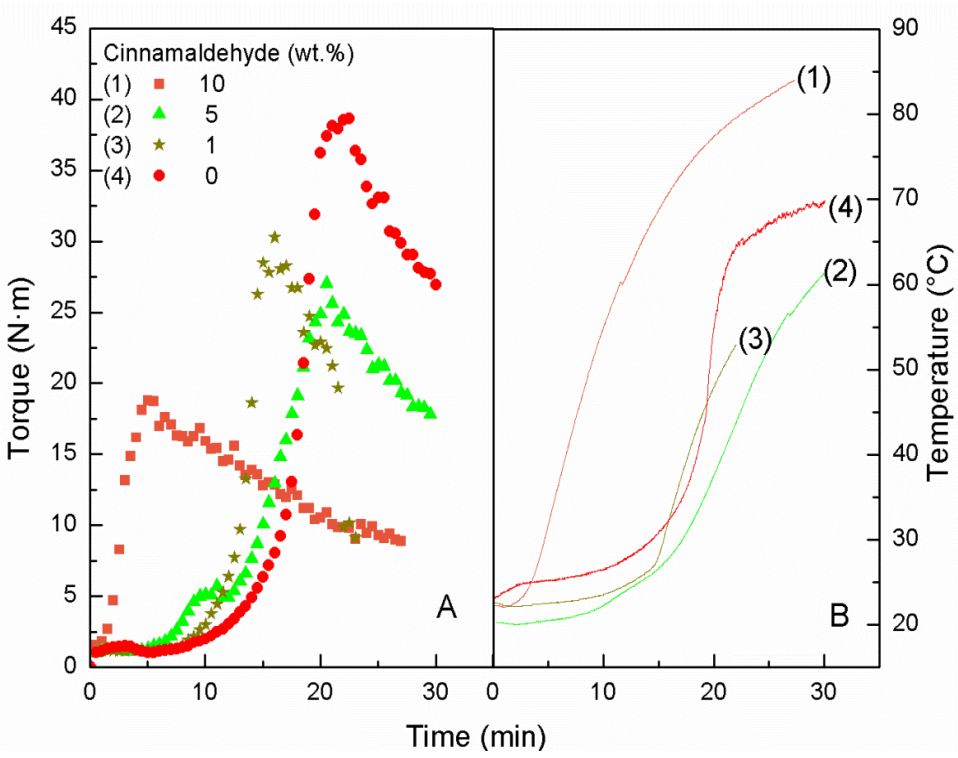

Figure 4.2.2 Evolution of torque and temperature during mixing for wheat gluten-based bioplastic with different concentrations of cinnamaldehyde as antimicrobial agent.

Figure 4.2.2 shows the evolution of torque and temperature during the mixing process for wheat gluten-based bioplastics at three concentrations of cinnamaldehyde. A torque evolution with three regions can be observed for samples containing less than 5 wt.% cinnamaldehyde, similar to the behaviour for the blend without antimicrobial agent. By contrast, the sample containing the highest concentration of cinnamaldehyde (10 wt.%) showed a torque evolution with only two regions. In this case, the torque underwent an exponential increase in mixing time until it reached a maximum value. This maximum torque values became lower as the cinnamaldehyde concentration increased. In addition, the evolution of temperature described different regions related to the torque regions (Figure 4.2.1B). An increase in cinnamaldehyde content led to an increase in the temperature during

mixing (Figure 4.2.2B). The final temperature of the mixing process was reached before 85ºC for the blend containing the highest concentration of cinnamaldehyde. We believe that the α, β unsaturated aldehyde contained in the cinnaldehyde, together with the protein, might produce a high exothermic reaction, thus increasing the temperature and breaking down the protein structure (Balaguer et al., 2011). This phenomenon may explain the decrease of torque as the cinnamaldehyde content increased.

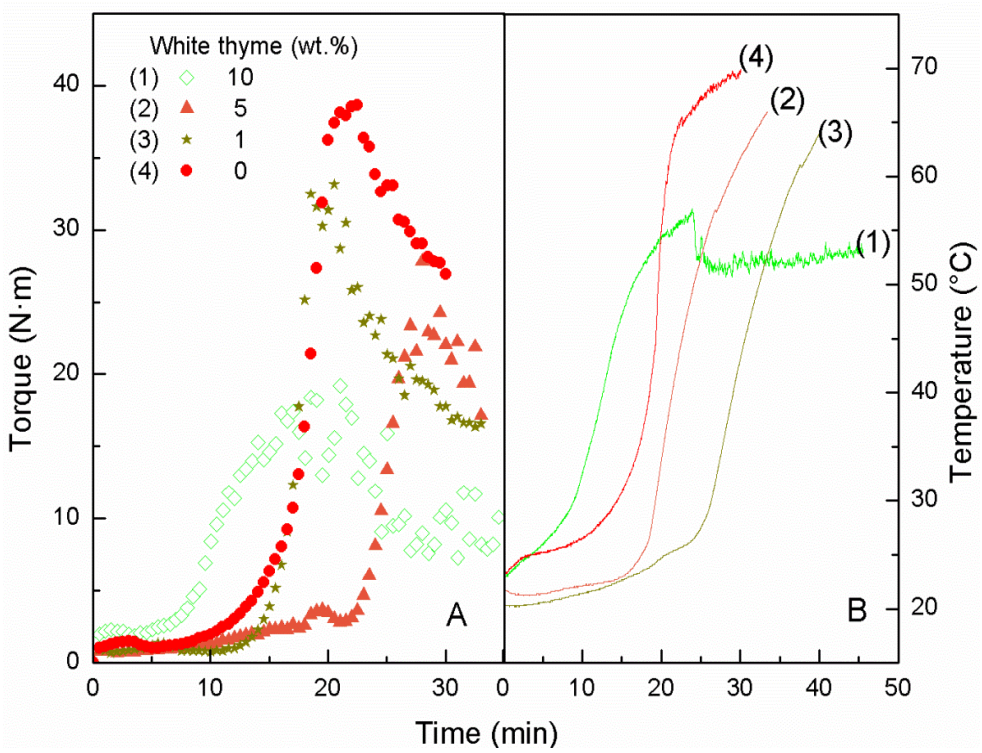

Figure 4.2.3 Evolution of torque and temperature during mixing for wheat gluten-based bioplastic with different concentrations of white thyme as antimicrobial agent.

Figure 4.2.3 shows the evolution of torque and temperature during the mixing process for wheat gluten-based bioplastics at three concentrations of white thyme oil. All samples presented a torque evolution with three regions, like the sample without biocide, although the torque maximum became lower as white thyme concentration increased. In the case of the sample with the highest white thyme content (10 wt.%), a non-distinguished peak was observed. Maximum torque was reached at 20 min for samples with 10 and 1 wt.% while samples with 5 wt.% reached the maximum at 30 min. Different temperature zones were also found during the mixing process, which were related to the torque regions. In all the cases, the

temperature reached (66ºC) was lower than that reached for the sample without an antimicrobial agent (Figure 4.2.3B).

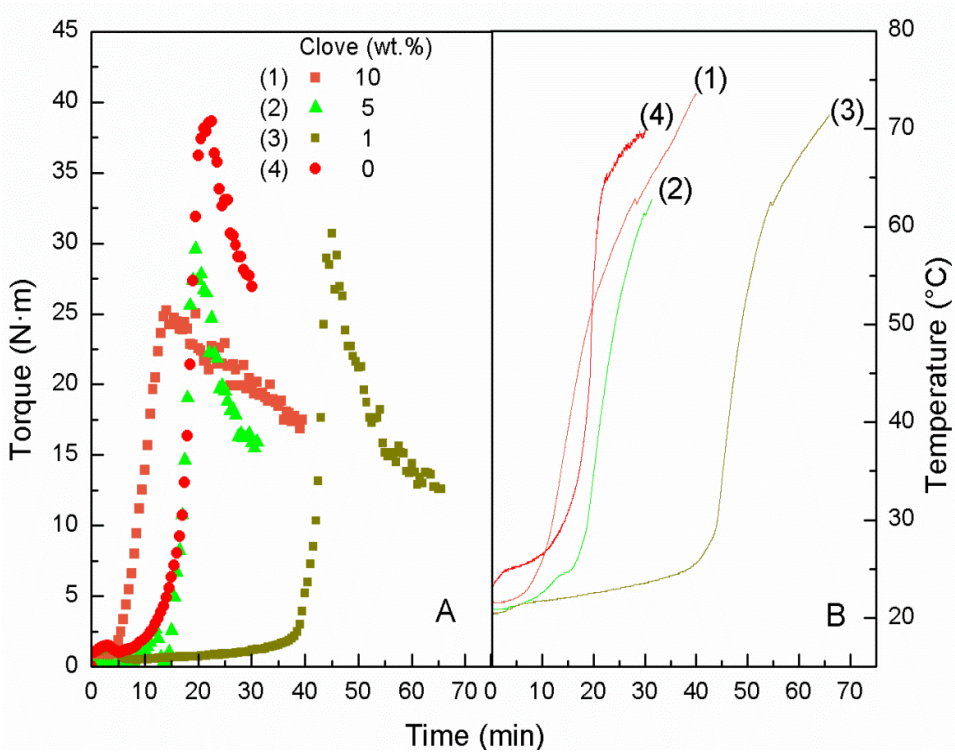

Figure 4.2.4 Evolution of torque and temperature during mixing for wheat gluten-based bioplastics with different concentrations of clove as antimicrobial agent.

Figure 4.2.4 shows the evolution of torque and temperature during the mixing process for wheat gluten-based bioplastics at three concentrations of clove oil. Samples containing 1 and 5 wt.% presented a torque evolution with three regions. The induction region tended to disappear as clove oil concentration increased. As can be observed, the maximum torque and the time required to reach it decreased as clove content increased. This behaviour was also observed for samples with cinnamon oil, which also contains eugenol as a major component. However, the sample with 1 wt.% clove oil took longer to reach a peak in torque (60 min) than the sample with 1 wt.% cinnamon oil (30 min). Different temperature zones were also found during the mixing process, which were related to the torque regions (Figure 4.2.4B). The final temperature of the mixing process was reached before 70ºC for the blends with 1 and 10 wt.% clove oil.

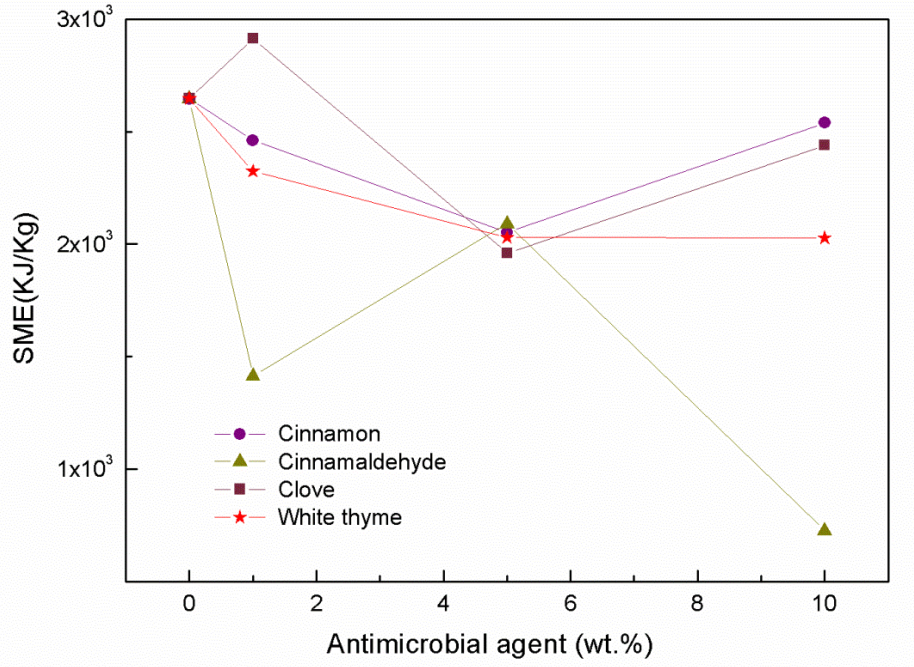

4.2.5 Specific mechanical energy (SME) for wheat gluten-based bioplastics with different concentrations of antimicrobial agent.

The type of biocides and their content also affects the specific mechanical energy (SME) required to obtain a material with suitable mechanical properties. Figure 4.2.5 shows the SME values for samples containing cinnamon, cinnamaldehyde, clove and white thyme at different concentrations. The SME for each sample was calculated with Equation 1.1.1. The addition of an antimicrobial agent in the formulation led to a decrease in SME compared with the sample without biocide, with the exception of the sample with 1 wt.% clove oil, which presented the highest SME values. All samples presented similar SME values at 5 wt.% antimicrobial agent. However, the addition of 1 and 10 wt.% cinnamaldehyde led to a significant decrease in SME, whilst an increase in white thyme concentration led to a decrease in SME.

Figure 4.2.6 presents the viscous flow curves at 90ºC for wheat gluten-based bioplastic with different concentrations of cinnamon (A) and cinnamaldehyde (B), collected just after the mixing process. The addition of cinnamon or cinnamaldehyde led to a decrease in the viscosity compared to the sample without an antimicrobial agent, with the sample containing cinnamon exhibiting lower viscosity than the one containing cinnamaldehyde, although overall, the influence of the antimicrobial agent content in the viscosity of both samples was non-significant.

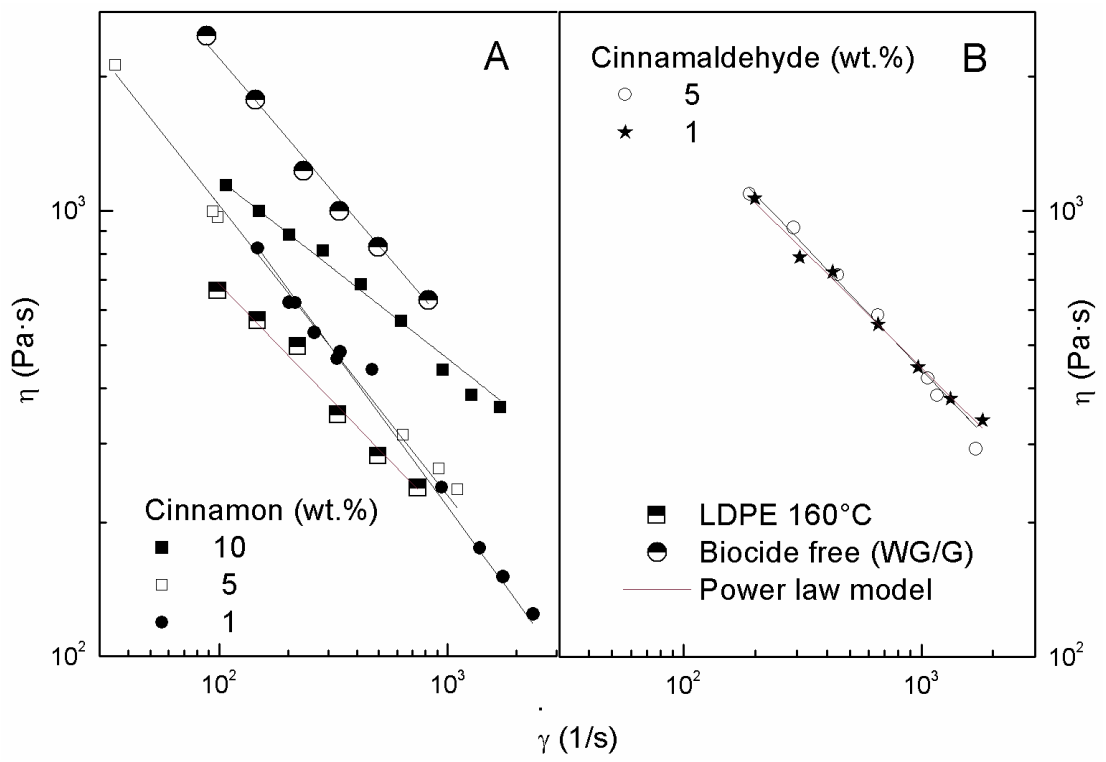

4.2.6 Viscous flow curves at 90ºC for wheat gluten-based bioplastics with different concentrations of cinnamon (A) and cinnamaldehyde (B) as antimicrobial agent.

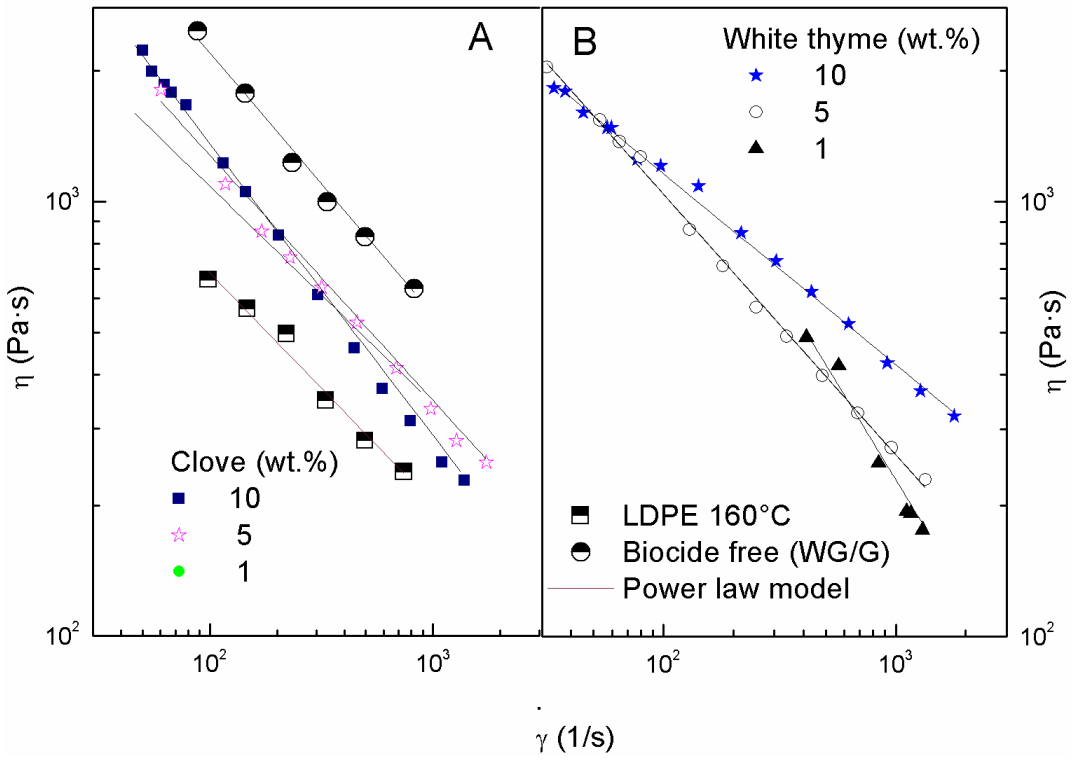

4.2.7 Viscous flow curves at 90ºC for wheat gluten-based bioplastic with different concentrations of clove (A) and white thyme (B) as antimicrobial agent.

Figure 4.2.7 presents the viscous flow curves at 90ºC for wheat gluten-based bioplastics with different concentrations of clove (A) and white thyme (B), collected just after the mixing process. The addition of clove oil led to a decrease in the viscosity compared to the sample without an antimicrobial agent, although in this case the influence was non-significant (Figure 4.2.7A). On the other hand, the addition of white thyme led to a significant increase in viscosity (Figure 4.2.7B).

Table 4.2.1. Antimicrobial agent effect on the viscosity parameters for wheat gluten-based bioplastic at different concentrations of antimicrobial agents.

Sample number	**Antimicrobial agent**	**Concentration (wt.%)**	**Parameters of Power-low model**	
			κ (Pa·s^n)	***n***
1	Biocide free	0	24702	0.33
2	Cinnamon	1	9156	0.56
3	Cinnamon	5	16095	0.43
4	Cinnamon	10	50691	0.21
5	Clove	1	10845	0.50
6	Clove	5	17203	0.43
7	Clove	10	50691	0.21
8	Cinnamaldehyde	1	18189	0.45
9	Cinnamaldehyde	5	18693	0.45
10	White thyme	1	8808	0.56
11	White thyme	5	16512	0.40
12	White thyme	10	50691	0.21

The power-law model fits the observed shear-thinning behaviour well (see Equation 1.1.2). Table 4.2.1 gathers the viscosity parameter for wheat gluten-based bioplastics with four antimicrobial agents at different concentrations. As can be observed, there was an increase in the consistency index and a decrease in the flow index as clove and white thyme concentration increased. However, a non-significant influence of the cinnamaldehyde concentration in the viscosity parameter is observed.

Antimicrobial activity

The antimicrobial effectiveness of cinnamon oil, cinnamaldehyde, clove and white thyme oil at three different concentrations was measured by the inhibition zone assay, the results of which are shown in Table 4.2.2. All of the prepared blends with 10 and 5 wt.% antimicrobial agent exhibited antimicrobial activity against E.Coli, S. Aureus, C. Albicans, and A. Niger, but showed different degrees of inhibition.

Table 4.2.2. Antimicrobial results for wheat gluten-based bioplastic at different concentrations of antimicrobial agent.

Sample number	**Antimicrobial agent**	**Concentration (wt.%)**	**E. Coli** (Gran - bacteria)	**S. aureus** (Gran + bacteria)	**C. albicans** (Fungus)	**A.niger** (Fungus)
1	Cinnamon	10	++	++	++	+++
2	Cinnamon	5	+	+	-	-
3	Cinnamon	1	-	-	-	-
4	Clove	10	++	++	++	+++
5	Clove	5	+	+	++	++
6	Clove	1	-	-	-	-
7	White thyme	10	++	++	++	+++
8	White thyme	5	++	+	++	++
9	White thyme	1	-	-	-	-
10	Cinnamaldehyde	10	+++	+++	+++	+++
11	Cinnamaldehyde	5	++	++	++	++
12	Cinnamaldehyde	1	+	+	-	-

Inhibition zone diameter:
+++ (70 mm< d)
++ (70 mm< d >20 mm)
+ (d < 20 mm)
- Without activity

According to inhibition zone diameter (IZD), the sample with 10 wt.% cinnamaldehyde produced the greatest degree of inhibition against all the microorganisms studied. In general, all the samples at this concentration showed a high degree of antimicrobial activity, although it was most effective against A. Niger. As expected, samples with 5 wt.% antimicrobial agent exhibited lower antimicrobial activity than samples with 10 wt.%. At this concentration, white thyme and clove showed similar behaviour, although cinnamon oil was only effective against the bacteria but neither of the fungi. At 1%, none of the antimicrobial agents was enough to kill the microorganism selected, with the exception of

cinnamaldehyde, which showed at least low effectiveness against both bacteria (E.Coli and S. Aureu).

Thermomechanical properties

Figure 4.2.8 shows the behaviour of the viscoelasticity function (E*) with temperature for wheat gluten-based bioplastic at different concentrations of cinnamon (A) and cinnamaldehyde (B), obtained by mixing and then thermomoulding at 90°C. In both cases, the results demonstrated that an increase in antimicrobial agent generally led to an increase in the complex modulus. It can also be noted that cinnamaldehyde led to higher complex modulus than cinnamon oil. A minimum in the complex modulus E* at around 100ºC was observed for both additives. This minimum occurred at slightly lower temperature than that of the sample without antimicrobial agent, and in both instances was more evident for samples at 10 wt.%. It seems that the protein was thermal-denaturated during the preceding mixing process, where the temperature increased up to 80ºC for both samples.

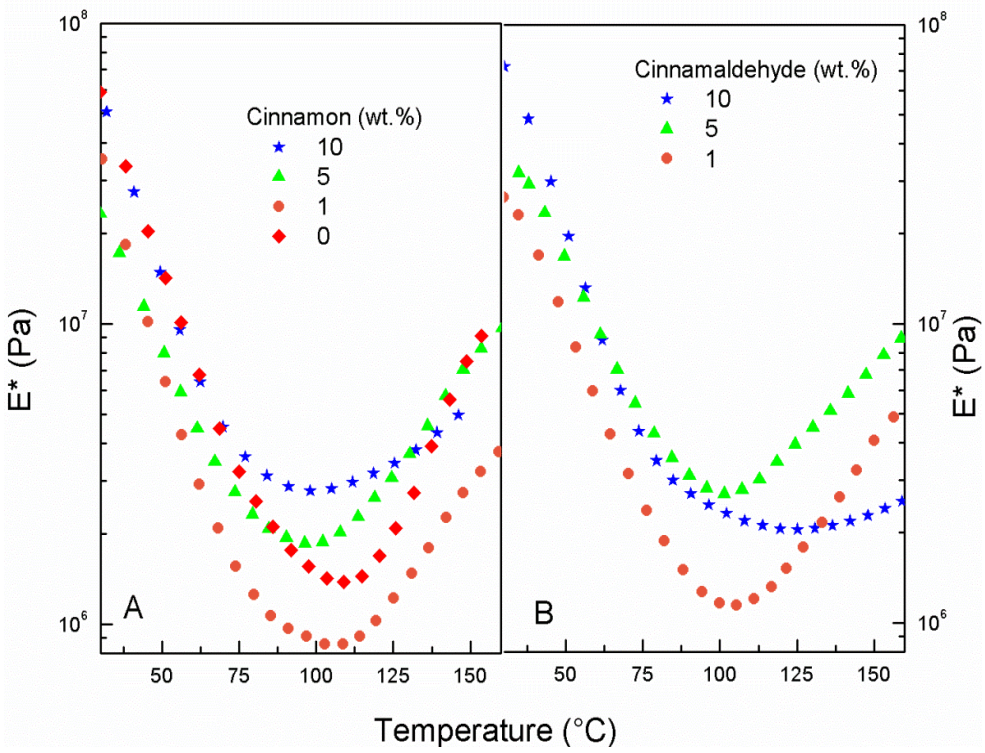

Figure 4.2.8. Dynamic mechanical thermal analysis results, complex modulus (E) for wheat gluten-based bioplastic at different concentrations of cinnamon (A) and cinnamaldehyde (B) as antimicrobial agent.*

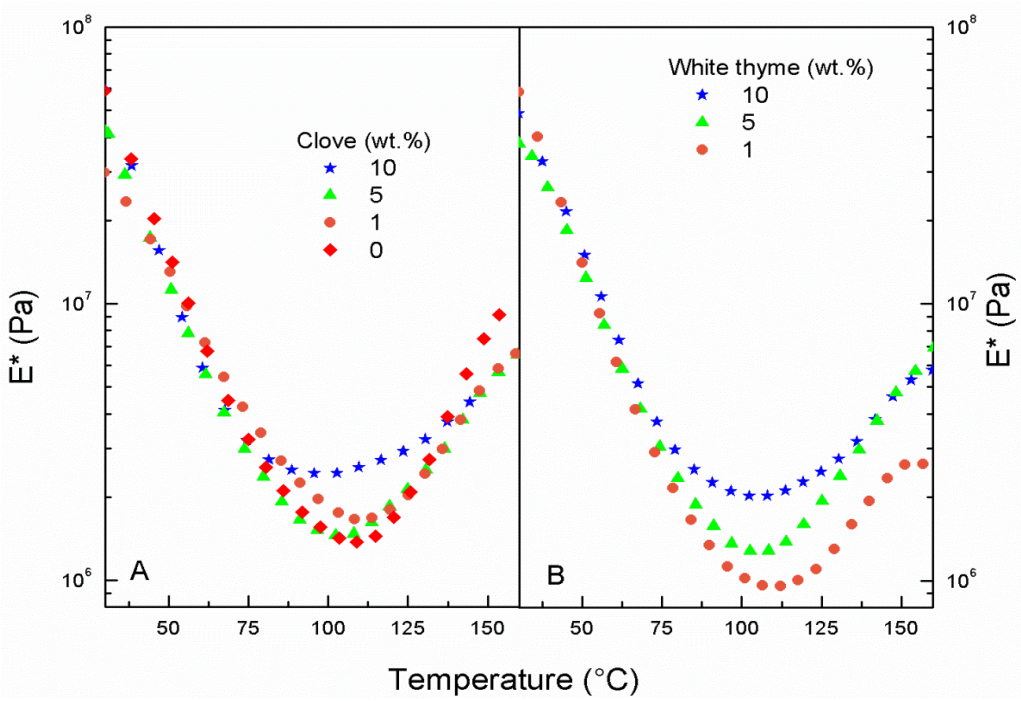

Figure 4.2.9. Dynamic mechanical thermal analysis results, complex modulus (E) for wheat gluten-based bioplastic different concentrations of clove (A) and white thyme (B) as antimicrobial agent.*

Figure 4.2.9 shows the behaviour of the viscoelasticity function (E*) with temperature for wheat gluten-based bioplastic at different concentrations of clove (A) and white thyme (B), mixed and then thermomoulded at 90°C. As can be seen, there were non-significant differences in the complex modulus for samples with 1 and 5 wt.% clove oil compared with the sample without an antimicrobial agent. However, 10 wt.% clove oil led to an increase in the complex modulus. On the other hand, the results for blends with white thyme oil showed that an increase in antimicrobial agent generally led to an increase in the complex modulus.

In general, a certain decrease in the complex modulus was observed at lower temperatures for all samples. This behaviour could be the result of some plasticizing effect caused by the addition of additives to the protein matrix. Nevertheless, an increase in the cinnamaldehyde and clove oil content led to an increase in the complex modulus, whilst an increase in the white thyme oil content led to a decrease in E*.

With respect to tan δ, there were non-significant differences in the tan δ peak values for the samples with cinnamon and clove oil compared with the sample without an antimicrobial agent. A significant increase in the tan δ peak (~60°C) was observed for the sample with cinnamaldehyde. However, this parameter was not affected by the antimicrobial

agent content as the corresponding tan δ peak values decreased as the cinnamaldehyde content increased. By contrast, an increase in white thyme oil content led to a decrease in the maximum tan δ.

Water absorption properties

Figure 4.2.10 shows water absorption values after 24 h for wheat gluten-based bioplastic with different antimicrobial agents obtained by mixing and then thermosetting at 90°C.

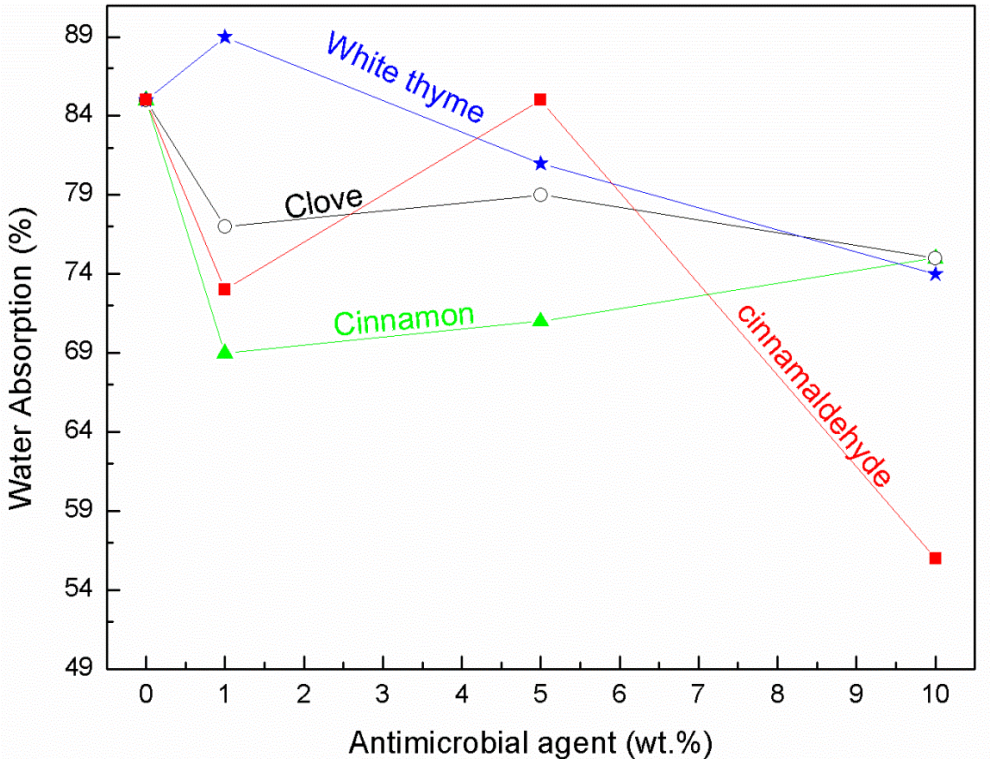

Figure 4.2.10 Water absorption of wheat gluten-based bioplastic at different concentrations of antimicrobial agent.

It can be seen that the addition of the antimicrobial agent led to a decrease in the water absorption, with the exception of the sample with 1 wt.% white thyme oil, which produced the highest values, higher than that for the sample without antimicrobial agent. A decrease in water absorption as white thyme oil content increases can also be observed. This behaviour corresponds to the increase in the complex modulus as the white thyme concentration increases (Figure 4.2.9B). By contrast, an increase in cinnamon oil content led to an increase

in water absorption, despite the increase in the complex modulus observed as cinnamon concentration increases (Figure 4.2.8A). The effect of clove oil concentration on water absorption was non-significant. The minimum values for water absorption occurred with the sample with 10 wt.% cinnamaldehyde. This might be due to the themal-denaturation of the protein during the mixing process as a result of the exothermic reaction between the protein and cinnamaldehyde.

4.3 Effect of antimicrobial agents on different formulations of protein-based bioplastics

Based on the results obtained in Chapter 2, it was concluded that the combination of potato and rice proteins together with wheat gluten were good raw materials for producing bioplastics. These new materials demonstrated the properties of being as flexible and thermomouldable as wheat gluten whilst retaining the good water absorption properties of rice and/or potato proteins. Continuing the investigation into these materials, this section considers different protein formulations in combination with 10 wt.% cinnamon, clove, cinnamaldehyde and white thyme as antimicrobial agent.

Thermoplastic processing

- *Wheat gluten/Rice protein blends with antimicrobial agents.*

Figure 4.3.1 shows the evolution of torque and temperature during the mixing process at 50 r.p.m., for wheat gluten/rice protein blends containing 30 wt.% glycerol, 60 wt.% protein and 10 wt.% antimicrobial agent. The mixing process was halted at 30 min when the samples were still in the induction region, as mentioned in the second chapter. Hence, all experiments were performed under the same processing conditions, with 30 minutes of mixing, such that a post-treatment was necessary to obtain a suitable material.

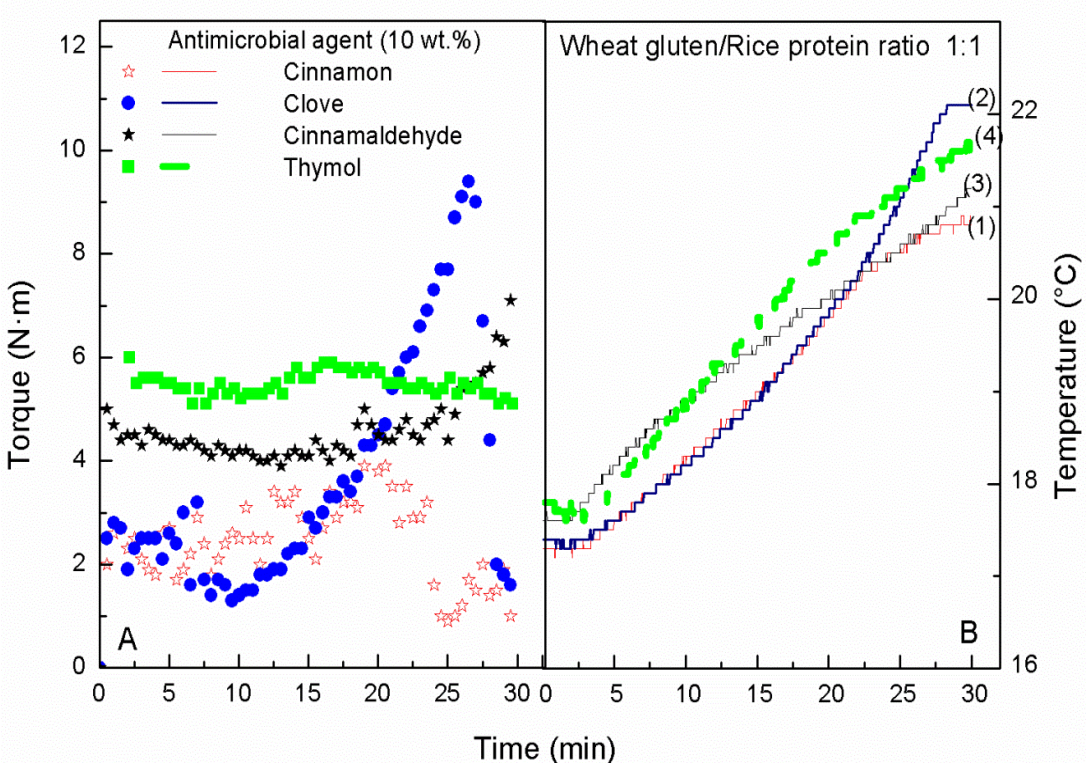

Figure 4.3.1 Evolution of torque (A) and temperature (B) during mixing for wheat gluten/rice protein blends containing 30 wt.% glycerol, 60 wt.% proteins and 10 wt.% antimicrobial agent.

As can be seen, a non-significant increase in torque and temperature during mixing occurred. This behaviour was due to properties of the rice protein, mentioned in section 2.1 of the second chapter. Although torque was low, its evolution during mixing varied according to the antimicrobial agent. Thus, samples with clove and cinnamaldehyde exhibited an induction region, which was of greater duration for samples with cinnamaldehyde (20 min) than for clove (10 min). After that, the torque underwent an increase with mixing time until it reached a maximum value, which was higher for clove. This bioplastic, though not the cinnamaldehyde, also exhibited an apparent torque decay. On the other hand, the sample with cinnamon exhibited the lowest values of torque, with a low maximum at 20 min, after which an apparent torque decay was observed. With respect to thymol, this sample produced higher torque values than the cinnamon, although a non-significant increase in torque during mixing was observed for this sample.

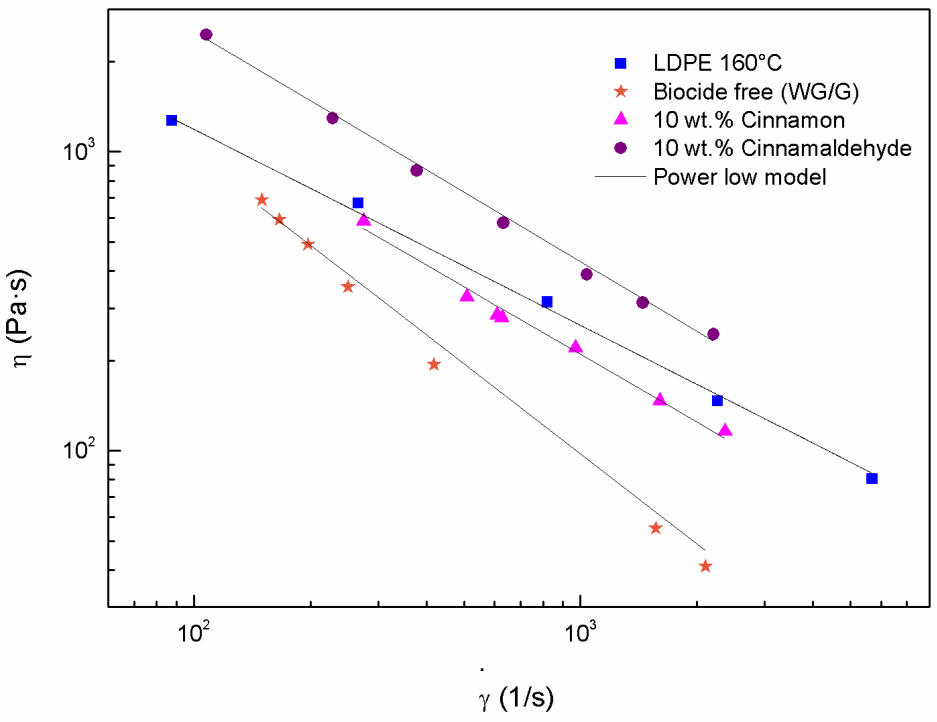

Figure 4.3.2 Viscous flow behaviour at 90ºC for wheat gluten/rice protein blends containing 23 wt.% glycerol and 10 wt.% antimicrobial agent.

Table 4.3.1. Antimicrobial agent effect on the viscosity parameters for wheat gluten/rice protein blends containing 30 wt.% glycerol and 10 wt.% antimicrobial agent.

Sample number	**Antimicrobial agent (10 wt.%)**	**Parameters of Power-law model**	
		***k* (*Pa·s*^{n})**	***n***
1	Biocide free	97286	0.032
2	LDPE	7846	0.47
3	Cinnamon	37435	0.25
4	Cinnamaldehyde	87969	0.23

Figure 4.3.2 presents the viscous flow curves at 90ºC for wheat gluten/rice protein blends with cinnamon and cinnamaldehyde, collected just after the mixing process. A significant increase in viscosity can be noted for both bioplastics compared to the sample without an antimicrobial agent. This increase was more evident for the sample with cinnamaldehyde. The viscosity of this sample was higher than that of the low density polyethylene (LDPE) at 160ºC. The power-law model fits the observed shear-thinning

behaviour well (see Equation 1.1.2). Table 4.3.1 presents the parameters of the power-law model for these blends. It can be observed that both antimicrobial agents led to a decrease in the consistency index and an increase in the flow index compared to the sample without an antimicrobial agent. In addition, these results showed that, for samples with an antimicrobial agent, the consistency index was higher, and the flow index lower, than low density polyethylene processed at 160ºC.

- *Potato-based protein blends with antimicrobial agents.*

Figure 4.3.3 shows the evolution of torque and temperature during the mixing process at 50 r.p.m., for two bioplastic formulations, each containing 30 wt.% glycerol, 60 wt.% protein and 10 wt.% antimicrobial agent. The mixing process for blends was halted during the induction region (30 min for the wheat gluten/potato protein blend and 10 min for the potato/egg white protein (EW) blend) and, subsequently, each protein-based dough was subjected to the post-treatment required to obtain a suitable material.

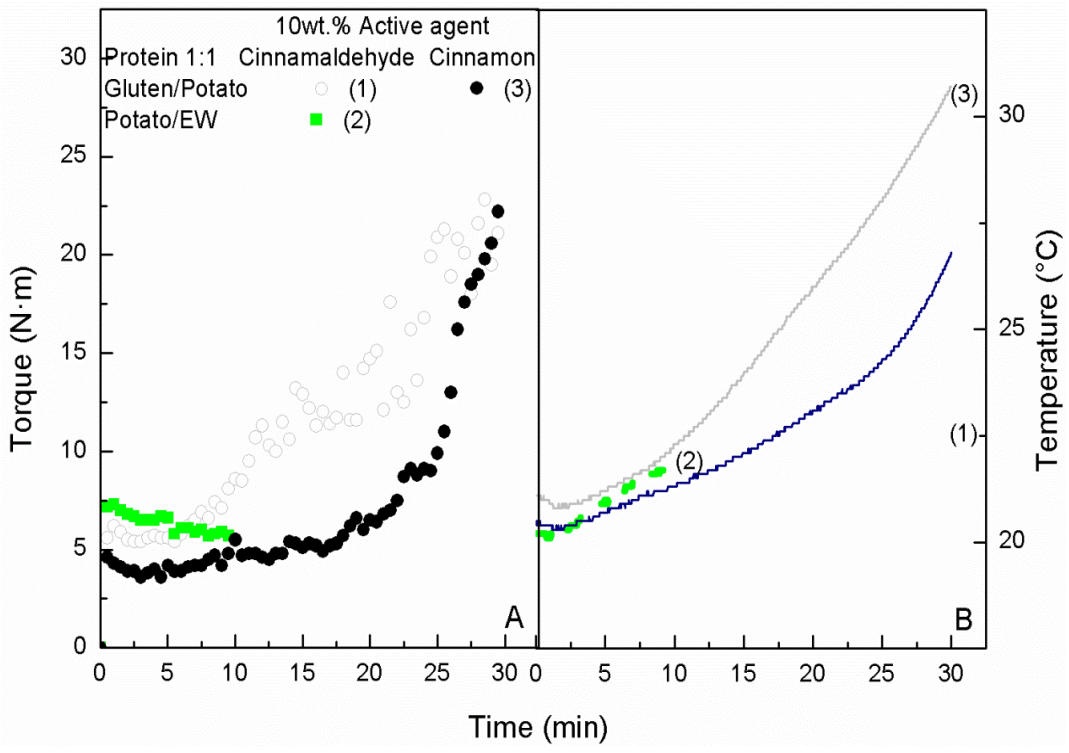

Figure 4.3.3 Evolution of torque (A) and temperature (B) during mixing for protein-based bioplastic containing 30 wt.% glycerol and 10 wt.% antimicrobial agent.

A non-significant change in the evolution of torque for the potato/egg white protein (EW) bioplastic with cinnamaldehyde is evident. On the other hand, an exponential increase to a maximum in torque can be noted for the wheat gluten/potato protein blend. The cinnamon blend, in contrast, maintained a constant torque value for 15 min, after which there was an increase in torque with mixing time until a maximum was reached. Meanwhile, the cinnamaldehyde blend produced an increase in torque after a shorter time (5 min) and also exhibited a slightly higher torque value than the sample with cinnamon.

Figure 4.3.3 B shows the evolution of temperature during the mixing process for the different systems studied. A non-significant increase in the temperature during the mixing process for these blends can be observed. The maximum temperature reached during the mixing was 30°C, which was achieved by the sample with cinnamaldehyde. This behaviour corresponds to the increase in torque mentioned above.

Thermomechanical properties of protein-based bioplastics with antimicrobial agents.

Figure 4.3.4 shows DMTA scans from 30 to 180ºC performed for wheat gluten/rice protein blends with 10 wt.% of different antimicrobial agents. It can be observed that the addition of an antimicrobial agent led to a slight increase in E* and also an increase in the maximum tan δ compared to the sample without an antimicrobial agent. However, a non-significant difference in the evolution of the complex modulus can be observed. Thus, samples with thymol and cinnamaldehyde exhibited the highest E* values at 30°C ($4 \cdot 10^7$ Pa) and a maximum tan δ close to 58ºC. A similar evolution of E* with temperature was obtained for samples with clove and cinnamon. These samples registered an E* measurement at 30°C of around $2 \cdot 10^7$ Pa. A maximum tan δ close to 58ºC was also observed for samples containing cinnamon.

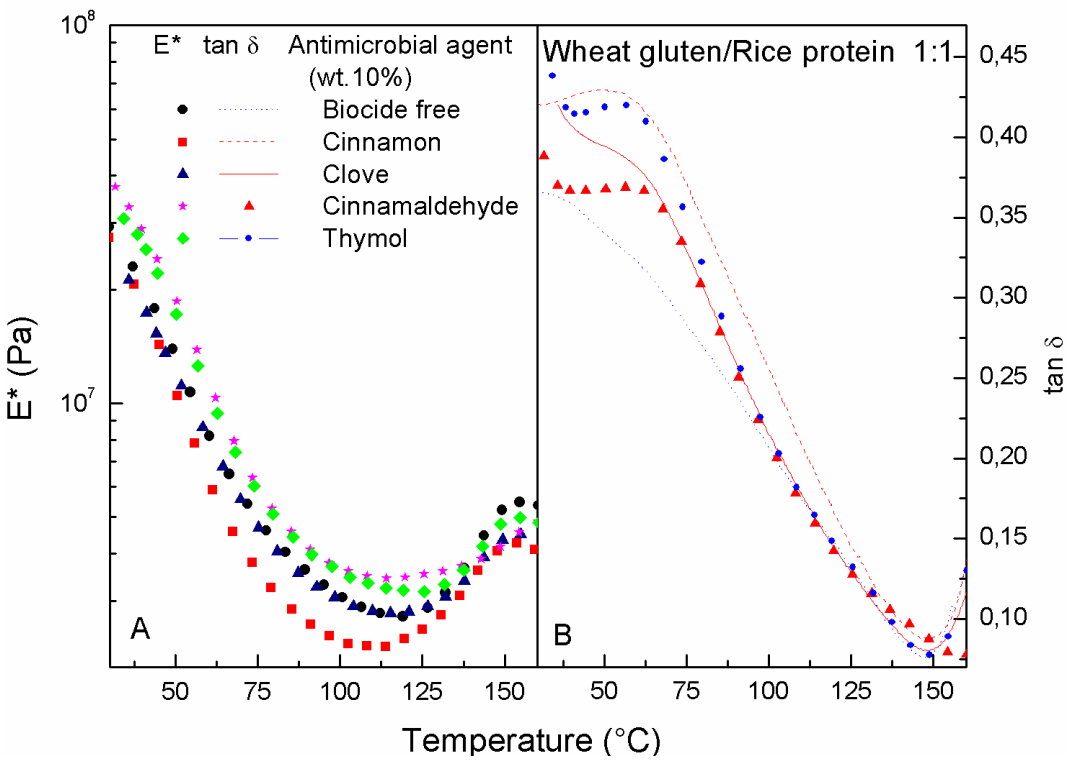

Figure 4.3.4 Dynamic mechanical thermal analysis results, complex modulus (A) and tan δ (B), for protein-based bioplastic containing 30 wt.% glycerol and 10 wt.% antimicrobial agent.

Figure 4.3.5 shows DMTA scans from 30 to 180ºC performed on blends of wheat gluten/potato protein and potato/egg white protein (EW) with 10 wt.% of two antimicrobial agents. A non-significant difference can be observed in the evolution of the complex modulus with temperature for the wheat gluten/potato protein blend compared to the sample without an antimicrobial agent. These samples exhibited E* values close to 10^8 Pa at 30ºC. However, from 100 to 150ºC, a slight increase in E* occurred for samples with cinnamaldehyde. In the case of cinnamon, the modulus entered a plateau region from 100 to 150ºC. It can also be noted that the addition of an antimicrobial agent led to an increase in the tan δ maximum at a temperature close to ~70ºC, compared to the sample without an antimicrobial agent (50ºC). An increase in tan δ values was also observed.

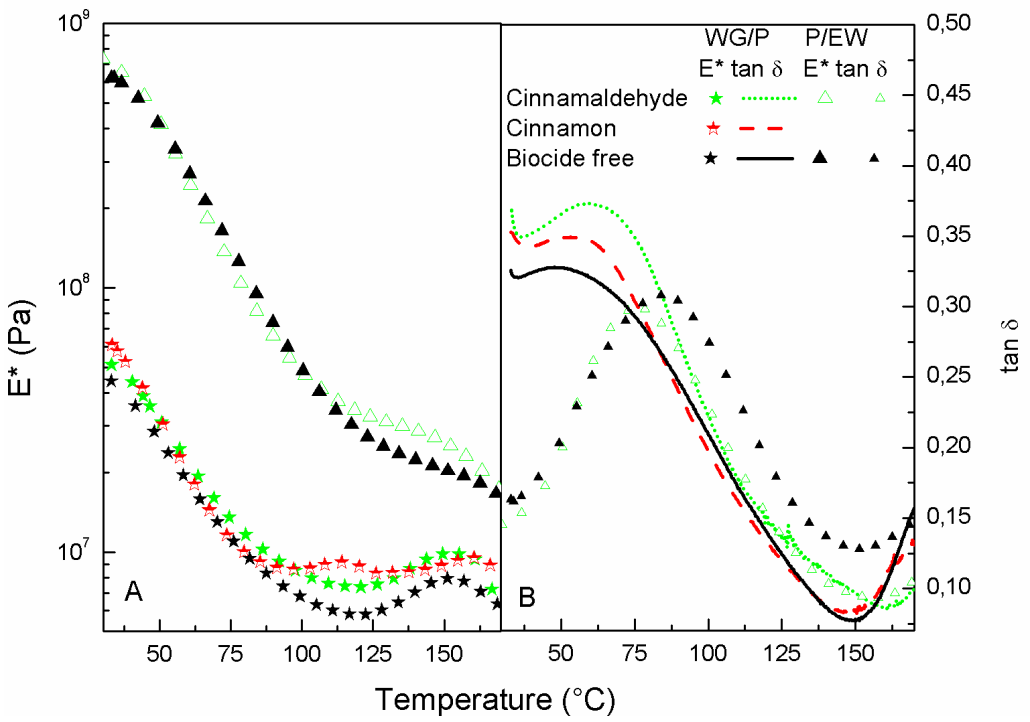

Figure 4.3.5 Dynamic mechanical thermal analysis results, complex modulus (A) and tan δ (B), for protein-based bioplastic containing 30 wt.% glycerol and 10 wt.% antimicrobial agent.

With regard to the potato/egg white protein (EW) blend, a decrease in the complex modulus (E*) with temperature was observed for the sample with cinnamaldehyde (Figure 4.3.5). First, E* suffered a change in the slope, after which a continuous decrease in the complex modulus with temperature was noted. This sample exhibited E* values of around 10^9 Pa at 30ºC, similar to the potato protein-based bioplastic discussed in Chapter 1 (see Figure 1.2.5) and to the sample without an antimicrobial agent, although there was a slight increase in E* from 100 up to 150ºC. The maximum loss tangent appeared at a higher temperature (84 ºC) in comparison with the sample without an antimicrobial agent (around 70ºC).

Water absorption properties of protein based bioplastics with antimicrobial agents.

Figure 4.3.6 shows the water absorption values for different bioplastics with 10 wt.% antimicrobial agents. A general observation was that the addition of cinnamaldehyde led to a significant decrease in the water absorption for all the bioplastics studied. This behaviour was most evident in the potato/egg white protein (EW) blend, which underwent a threefold decrease in comparison with its reference value (the biocide-free bioplastic).

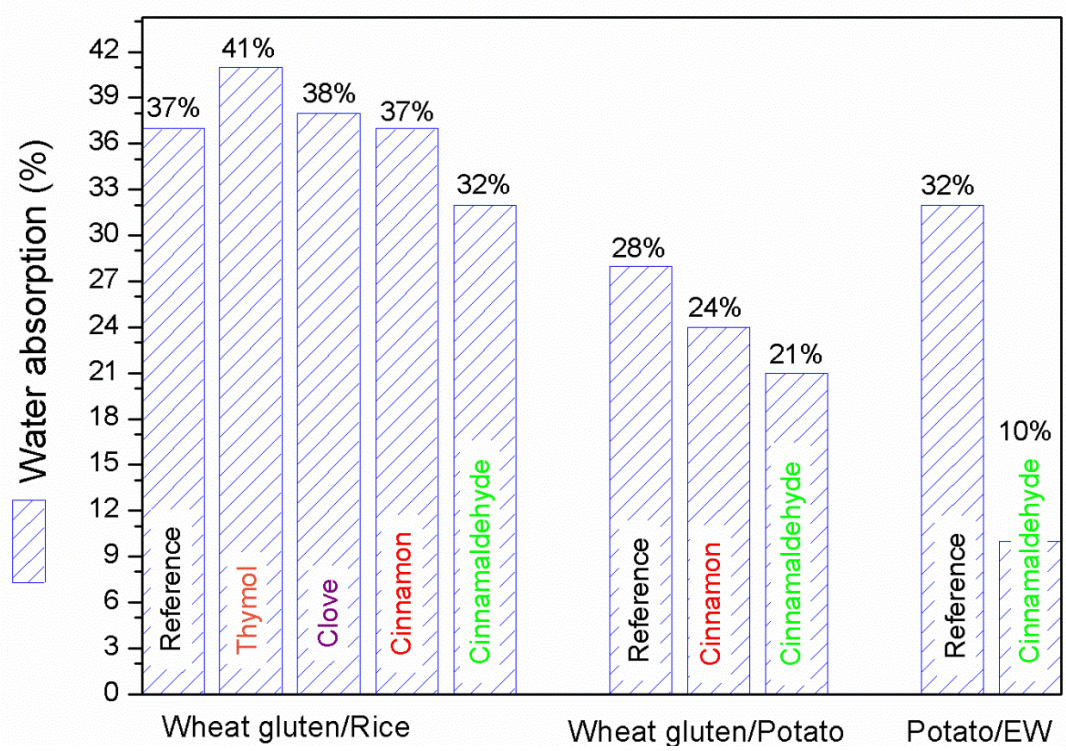

Figure 4.3.6 Water absorption of protein-based bioplastic containing 30 wt.% glycerol and 10 wt.% antimicrobial agent.

In the case of the wheat gluten/rice protein blend, a non-significant difference in water absorption was observed by the addition of cinnamon, and a slight increase by the addition of clove and thymol. However, in the case of the wheat gluten/potato protein blend, a decrease in water absorption was noted in comparison with the reference value.

4.4 Thermomechanical processing of wheat gluten/potato protein-based bioplastics containing antimicrobial agents

Thermal histories seem to produce significant differences in the protein network formed, most evident in the water absorption behaviour, as mentioned in Chapter 2. These new materials might be attractive for the plastics industry. Potato protein and wheat gluten samples incorporating, on the one hand, different concentrations of thymol and, on the other, 10 wt.% cinnamaldehyde were processed at 80°C and then thermoset at 120°C.

Thermoplastic processing at high temperature

Figure 4.4.1 shows the evolution of torque during mixing at 80ºC of wheat gluten/potato protein with 10 wt.% of two antimicrobial agents. The blends showed a torque

evolution with distinct regions depending on the formulation. In the first region, torque underwent an exponential increase with mixing time until it reached a maximum value, which was reached before 2 min mixing. After this, the samples exhibited an apparent torque decay. In the cases of samples with a high thymol content (≥5 wt.%), torque increased until values stabilised at higher values than the maximum in the first region. On the other hand, sample with cinnamaldehyde presented a similar behaviour such as samples with thymol, but in this case, torque undergoes an significant increase. In addition, the maximum value in the torque is reached at 6 min mixing.

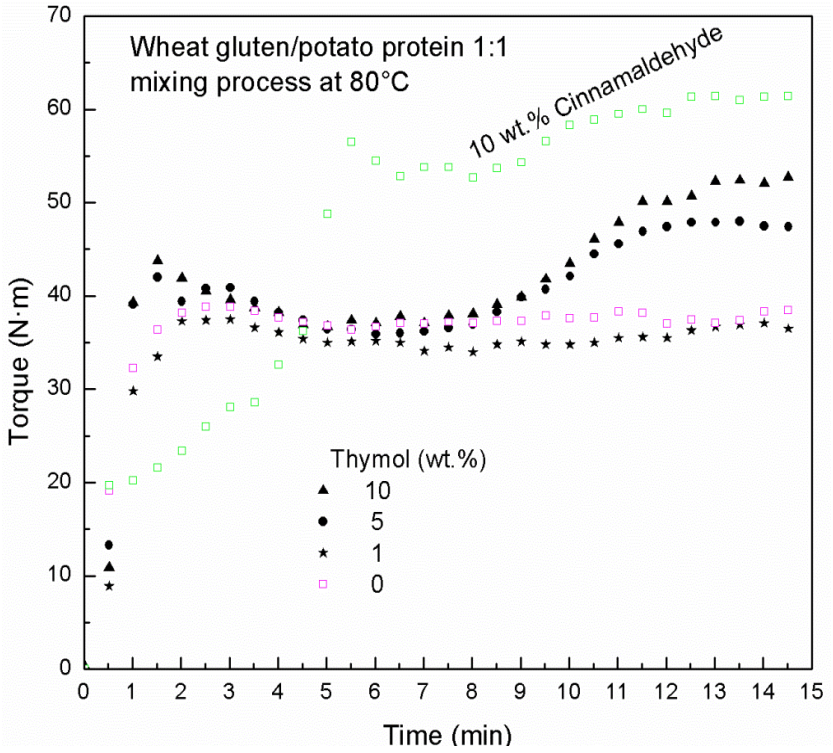

Figure 4.4.1 Evolution of torque during mixing for wheat gluten/potato protein blends with two different antimicrobial agents.

As can be observed, an increase in the thymol concentration led to an increase in SME. There was a non-significant difference in SME calculated for the sample with 1 wt.% thymol compared to the one without an antimicrobial agent. On the other hand, the sample with cinnamaldehyde exhibited the highest SME values (Table 4.4.1).

Table 4.4.1 Specific Mechanical Energy (SME), reached during the mixing process.

Sample number	Glycerol (wt.%)	Antimicrobial agent	Concentration (wt.%)	SME (kJ/kg)
1	30	Cinnamaldehyde	10	2647
2	30	Thymol	10	2026
3	35	Thymol	5	2539
4	39	Thymol	1	2439
5	40	Biocide free	0	1257

Figure 4.5.2 shows the viscous flow curves at 90ºC for wheat gluten/potato protein blends with 10 wt.% of two antimicrobial agents. Samples were collected just after the mixing process. Two behaviours can be observed depending on the antimicrobial agent. Thus, the addition of cinnamon led to a decrease in viscosity compared to the sample without an antimicrobial agent, while, cinnamaldehyde led to an increase in viscosity. The viscosity of these materials was higher than that of the well-known low density polyethylene (LDPE) at 160ºC.

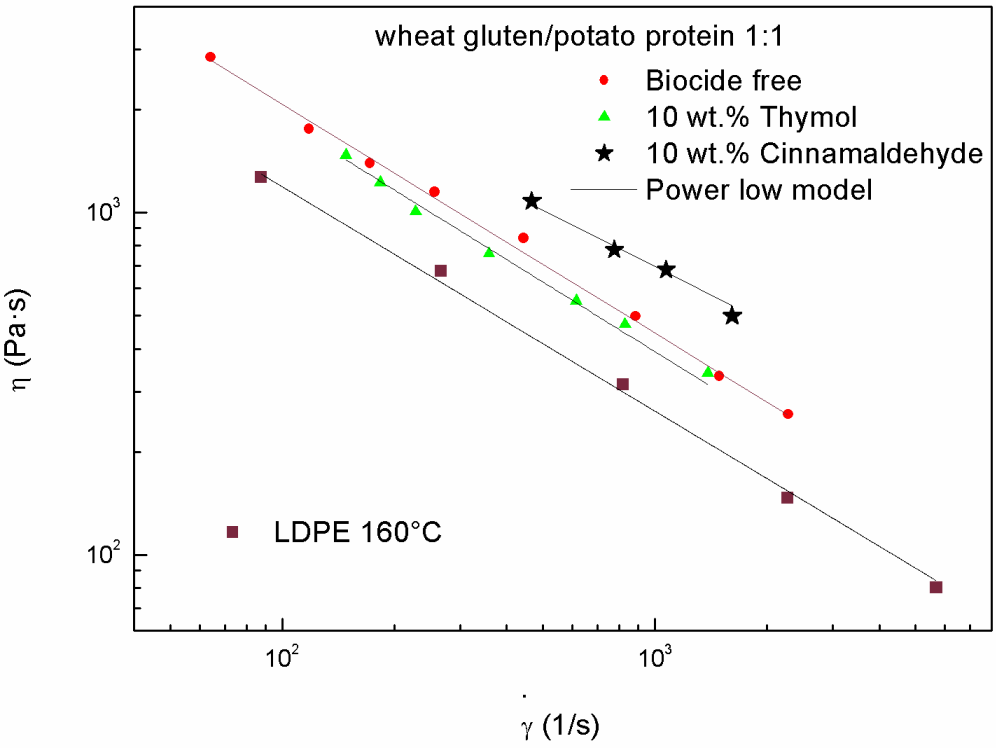

Figure 4.4.2 Viscous flow curves for wheat gluten/potato protein blends with two different antimicrobial agents at 90ºC.

The power-law model fits the observed shear-thinning behaviour well (Equation 1.1.2). Table 4.4.2 gathers the values of these parameters for wheat gluten/potato protein blends with 10 wt.% of two antimicrobial agents. A remarkable increase in the consistency index and a slight decrease in the flow index can be observed for the sample with thymol compared to the sample without an antimicrobial agent. However, a significant decrease in the consistency index is observed only for the sample with cinnalmaldehyde. The aldehyde groups present in both cinnaldehyde and cinnamon could have produced crosslinking or aggregation of the protein which might have increased the viscosity of the blend (Balaguer et al., 2011).

Table 4.4.2 Influence of protein composition on the consistency (k) and flow (n) indexes of the different blends studied.

Sample number	**Antimicrobial agent (10 wt.%)**	**Parameters of Power-low model**	
		k ***(Pa·s^n)***	***n***
1	Biocide free	43821	0.33
2	LDPE	7846	0.47
3	Cinnamaldehyde	31007	0.32
4	Thymol	41537	0.45

Thermomechanical and water absorption properties

Figure 4.4.3 shows the behaviour of two viscoelastic functions (E* and tan δ) with temperature, for wheat gluten/potato protein with thymol at different concentrations and cinnamaldehyde at 10 wt.%, obtained by mixing at 80°C and thermosetting at 120ºC. It can be observed that the addition of thymol led to a decrease in E*, while, cinnaladehyde led to a significant increase in E* compared to the sample without an antimicrobial agent. In both cases, the maximum tan δ was reached at a higher temperature for samples with thymol (~59ºC) and cinnamaldehyde (65ºC) than for the sample without an antimicrobial agent

(~50ºC). A non-significant difference was found in the complex modulus values at 30ºC (about $6 \cdot 10^7$ Pa) for samples with thymol compared to the sample without an antimicrobial agent. Thus, the modulus decreased to a minimum at 120°C. This was followed by a slight increase up to 160°C, and finally a decrease in E*. A significant decrease in E* from 80 to 140°C was observed for samples with thymol compared to the sample without an antimicrobial agent. A maximum in tan δ close to 59ºC for the samples containing thymol was noted.

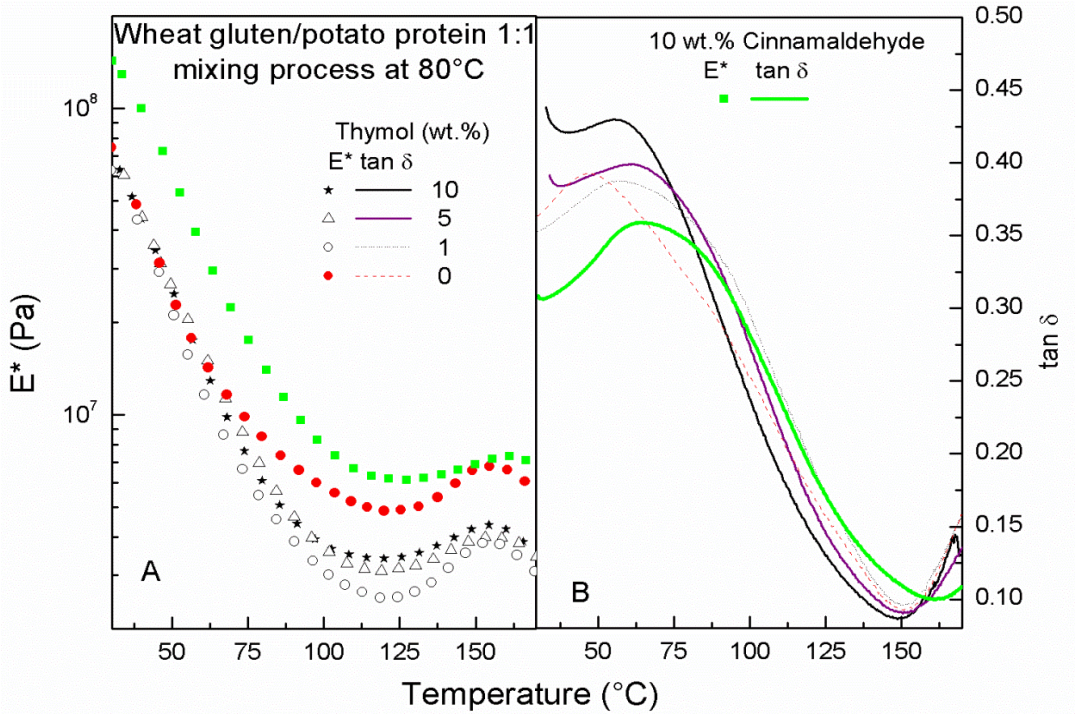

Figure 4.4.3 Dynamic mechanical thermal analysis results, complex modulus (A) and tan δ (B) for wheat gluten/potato protein blends with two different antimicrobial agents, mixed at 80°C and thermomoulded at 120°C.

On the other hand, the sample with 10 wt.% cinnamaldehyde showed a significant increase in E* (above 10^8 Pa) and a maximum in tan δ close to 65ºC. In this case, E* underwent a decrease to a minimum at 110°C. Then, E* entered a fairly long plateau region up to 160ºC. This sample was more thermally stable at lower temperatures than the sample with 10 wt.% thymol and the sample without an antimicrobial agent. The addition of cinnamaldehyde probably led to an increase in crosslinking in the protein (Balaguer et al., 2011), while, thymol, together with glycerol, could have played the role of plasticizer because of the similarities in the structure of glycerol and phenolic derivatives (both of them having -OH groups), thus leading to a decrease in the crosslinking of the protein.

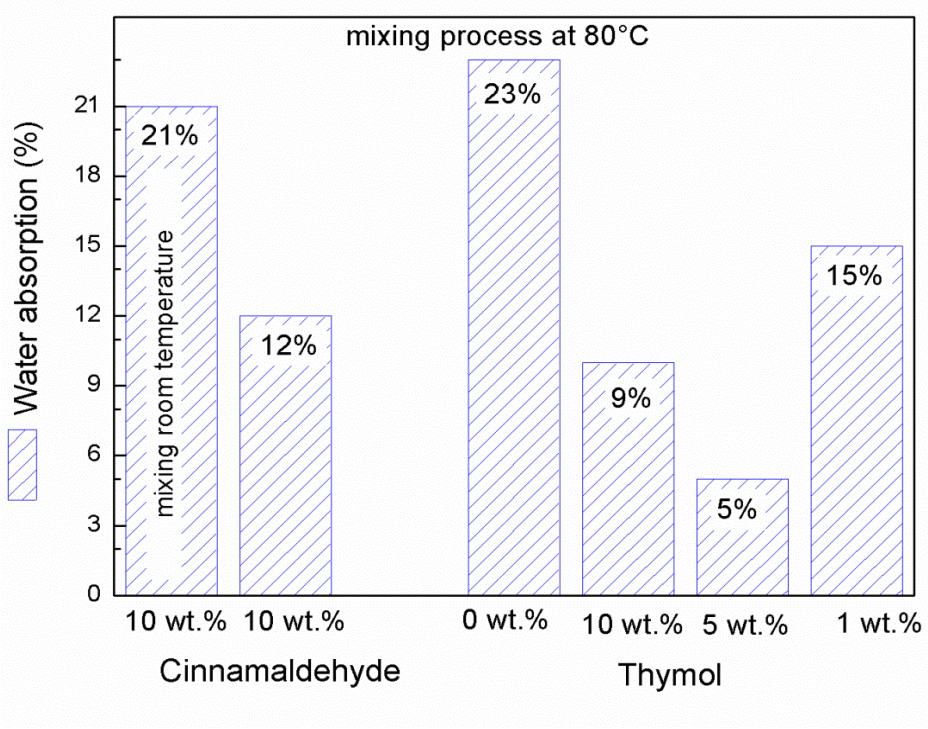

Figure 4.4.4 Water absorption of wheat gluten/potato protein blends with two different antimicrobial agents, mixed at 80°C and thermomoulded at 120°C.

Figure 4.4.4 shows the effect of cinnamaldehyde and thymol addition on the water absorption properties of wheat gluten/potato protein-based bioplastic mixed at 80°C. The thermal treatment during the mixing process, in combination with the addition of cinnamaldehyde or thymol, seems to produce a significant reduction in the water absorption. A reduction in water absorption of 10 wt.% can be observed for the sample with cinnamaldehyde compared to the one mixed at room temperature. This behaviour corresponds to the high modulus values (E*) observed in Figure 4.4.3, which might be due to crosslinking of the protein produced during the mixing process at high temperature. It seems that the high temperature during the mixing process helps to improve the interaction and/or reaction within potato protein.

The addition of thymol led to a significant decrease in water absorption compared to the sample without an antimicrobial agent, processed under the same temperature conditions. In this case, although the evolution in complex modulus with temperature was quite similar for different concentrations of thymol, the water absorption capacity displayed greater variation. Thus, the lowest reduction in water absorption was for the sample with 5 wt.% thymol (5 wt.%), while, the highest value was for the sample with 1 wt.% thymol (15 wt.%). These results provide us with evidence that even just a 1 wt.% addition of thymol might

significantly improve the water absorption properties of this material. Thymol is rich in phenolic compounds which may contain different numbers of hydroxyl groups capable of forming H-bonding with peptide carbonyl groups of proteins (Damodaran, 1996). These more hydrophobic compounds could modify the protein matrix structure and consequently improving the water barrier properties of the material.

V. CONCLUSIONS

1. The different formulations and process conditions evaluated in this study exhibited suitable rheological properties, thermosetting potentials and physical properties that make them suitable for two specific applications such as controlled release and packaging materials.

2. Rice and potato-based bioplastics showed higher viscoelastic moduli than wheat gluten based bioplastics. Both proteins led to materials with improved thermal resistance and higher degree of crosslinking in comparison with wheat gluten. Furthermore, these materials exhibited a water absorption below 50 wt.%, having the potato protein-based bioplastics the lowest values.

3. Thermal degradations of gluten and glycerol–gluten-based bioplastics have been simulated by models based on pseudocomponents which refer to the main gluten isolate and bioplastic compounds, i.e. water, glycerol, starch, glutenin and gliadin. As a result, modelling confirms the experimental bioplastic and gluten isolate compositions, e.g. bioplastic moist content, starch concentration and the expected gliadin/glutenin ratio. According to the simulation, the glycerol volatilisation is affected by bioplastic moist content and hindered by the protein matrix. A fact that points out that glycerol/water blend plays relevant plasticizing roles in the protein matrix through diverse physicochemical interactions.

4. Incorporating wheat gluten into rice and potato protein based bioplastics gave rise to materials with characteristics from both proteins, that is, the flexibility and thermomouldability of wheat gluten alongside the desirable water absorption properties of rice and/or potato proteins. The incorporation of rice protein to the wheat gluten blend led to a decrease in the sample viscosity, while potato protein led to an

increase. The viscosity of potato protein blend was even higher than that of low density polyethylene (LDPE) at 160ºC.

5. Thermoplastic processing at high temperature of wheat gluten/potato protein based bioplastics exhibited a considerable increase in the torque values in comparison with the one processed at room temperature. These blends proved to be more thermo-stable than wheat gluten, but returned complex modulus values lower than those for potato protein. The high temperature during the mixing led to a reduction in water absorption from 28 to 25 wt.%.

6. The extrusion process of wheat gluten/potato protein-based bioplastic led to a decrease in the complex modulus as screw speed increased for samples extruded with the temperature profiles P1 and P2. By contrast, for samples extruded at P3, an increase in the complex modulus was observed when the screw speed during the extrusion process was increased. These samples were less elastic than the non-extruded sample. The lowest swelling ratio was for the sample extruded with P1 (30 r.p.m.) followed by samples extruded at P3 (50 r.p.m.). Both samples absorbed less water than the non-extruded sample.

7. Lower water absorption and KCl release rates were obtained as more severe thermo-mechanical treatments were applied on the sample. On the contrary, citric acid addition to bioplastic formulations led to a remarkable decrease in the crosslinking degree of the protein network. Nonetheless, significantly higher water absorption and slower KCl release rate (both of them suitable properties for agricultural applications) have been found by adding citric acid.

8. An increase in molecular weight of the PEG plasticizer led to stiffer and more elastic materials, except for the bioplastic formulated with PEG 8000, which underwent a significant decrease in its complex modulus value. As PEG molecular weight increases, greater incompatibility between matrix and the plasticizer blend has been observed, which suggests different plasticizing roles for water and PEG in the bioplastics. On the whole, with the exception of PEG8000, glycerol replacement by PEG brought about a lower release of KCl (which takes place faster). However, water

absorption of materials plasticized with PEG increased with the molecular weight of plasticizer.

9. The addition of modifying agents to the system containing PEG4000 led to increased KCl release (M_∞) and reduced water absorption. Compared to the reference system and the other modifiers, citric acid seems to impart the most suitable balance between an enhanced protein/salt affinity and material mechanical properties, yielding slow release patterns, higher KCl leaching capacity and suitable water uptake.

10. Protein-based bioplastics have demonstrated their antimicrobial activity, with potential application in food packaging, when biocides were incorporated in their formulation. In terms of ability to inhibit growth of the selected microorganisms, the best results were obtained for samples containing cinnamaldehyde, carvacrol, white thyme, thymol, eugenol and linalol. The sample containing cinnamaldehyde produced the greatest degree of antimicrobial activity against all the microorganisms studied. Their ability to inhibit growth of the selected microorganisms decreased as antimicrobial agent concentration decreased, a lower threshold concentration was established at 5 wt.% biocide.

11. Thermoplastic processing of blends which mix both proteins (gluten/rice, gluten/potato and potato/egg-white protein) with antimicrobial agents showed a significant increase in viscosity and their viscoelastic properties compared to the sample without an antimicrobial agent. The addition of cinnamaldehyde and thymol led to a significant decrease in the water absorption for all the bioplastics studied. Moreover, the thermal treatment during the mixing process further reduced water absorption to values below 15 wt.%. The lowest value was obtained for the bioplastic having 5 wt.% thymol, mixed at 80ºC and themomoulded at 120ºC, for which water absorption dropped up to 5 wt.%.

VI. REFERENCES

A

Aguilera J.M. Gelation whey proteins. Food Technology. **1995**, 49, 83-89.

Ali, Y.; Ghorpade, V. M.; Hanna, M. A. Properties of thermally treated wheat gluten films. Industrial Crops and Products. **1997**, 6, 177-184.

Allen, A.K.; Bolwell, G.P.; Brown, D.S.; Sidebottom, C; Slabas, A.R. Potato lectin: A three domain glycoprotein with novel hydroxyproline-containing sequences and sequence similarities to wheatgerm agglutinin. International Journal of Biochemistry & Cell Biology. **1996**, 28,1285-1291.

Appendini, P., Hotchkiss J.H. Review of antimicrobial food packaging. Innovative Food Science & Emerging Technologies. **2002**, 3, 113-126.

Arora, D.S.; Kaur, J., Antimicrobial activity of spices. International Journal of Antimicrobial Agent. **1999**, 12, 257-262.

Archambault, Ê.; Bertrand, F.; Côtes, G.; Craig-Dupont, O.; Larivière, V.; Gagné, É.V. Canadian R & D Biostrategy: Toward a Canadian R & D Strategy for Bioproducts and Bioprocessed. Prepared for National Research Council of Canada. **2004**

Astarita, G. The engineering reality of the yield stress. Journal of Rheology. **1990**, 34, 275-277.

ASTM , Standard Test Methods for Determining the Biobased Content of Solid, Liquid, and Gaseous Samples Using Radiocarbon Analysis". Designation D6866 – 11. Astm.org. Retrieved **2011**, 08-14.

ASTM, Standard test method for Plastics: Dynamic Mechanical Properties: In Flexure (Three-Point Bending). Designation D 5023–01. In Annual book of ASTM standards Philadelphia, PA: American Society for Testing and Materials. **2001a.**

ASTM, Standard test method for Plastics: Water Absorption of Plastics Designation D 570 – 98. In Annual book of ASTM standards Philadelphia, PA: American Society for Testing and Materials. **2001b.**

B

Bachtsi, A.; Kiparissides, C. Synthesis and release studies of oil-containing poly (vinyl alcohol) microcapsules prepared by coacervation. Journal of Controlled Release. **1996**, 38, 49-58.

Balaguer, M.P.; Gomez-Estaca, J.; Gavara, R.; Hernandez-Munoz, P. Functional properties of bioplastics made from wheat gliadins modified with cinnamaldehyde. Journal of Agriculture and Food Chemistry. **2011**, 59, 6689-6695.

Barnes, H. The yield stress –a review or– everything flows? Journal of Non-Newtonian Fluid Mechanics. **1999**, 81, 213-217.

Barnes, H.A. Thixotropy - a review. Journal of Non-Newtonian Fluid Mechanics. **1997**, 70, 1-33.

Barnes H.A.; Walters K. The yield stress myth, Rheolycal Acta. **1985**, 24, 323-326.

Barnes, H.A., Hutton, J.F., Walters, K. An Introduction to Rheology, Elsevier, Amsterdam. **1993**.

Barneto, A.G.; Ariza, J.; Martín, J.E.; Jiménez, L. Use of autocatalytic kinetics to obtain composition of lignocellulosic materials. Bioresource Technology. **2009**, 100, 3963-3973.

Barneto, A.G.; Ariza, J.; Martín, J.E.; Sánchez, R. Simulation of the thermogravimetry analysis of three non-wood pulps. Bioresource Technology **2010**, 101, 3220-3229.

Bechtel, D.B. **;** Pomeranz, Y. The rice kernel*In* Y. Pomeranz, ed., Advances in Cereal Science and Technology, Vol. 3, Amer. Assoc. Cereal, Chem., Inc., St. Paul, MN. **1980**, pp. 73-113.

Beverlya, R.L.; Janes, M.E.; Prinyawiwatkula, W.; No, H.K. Edible chitosan films on ready-to-eat roast beef for the control of Listeria monocytogenes. Food Microbiology. **2008**, 25, 534-537.

bioplastics42.htm

Bloksma, A. H.;Bushuk, W. Rheology and chemistry of dough. In Pomeranz (Ed.), Wheat: chemistry and technology. St. Paul, MN, USA: AACC. **1998**, pp. 131–200.

Boger, D.V. Highly elastic constant-viscosity fluid. J. Non-Newtonian Fluid Mech. **1977**, 3, 87-91.

Brescia, F.; Arents, J.; Meislich, H.; Turk, A. Química. Nueva Editorial Interamericana S.A. D.F. México. **1977**, pp 654.

Bressani, R.; Elias, L.G; Juliano, B.O. Evaluation of the protein quality and milled rices differing in protein content. Journal of Agricultural and Food Chemistry. **1971**, 19, 1028-1034

Brody, A.L. Strupinsky ER, Kline, LR. Active packaging for food applications. Lancaster: Technomic Publishing Co., Inc. **2001**, pp 218.

Buchholz, F.L.; Graham, T. Modern superabsorbent polymer technology. Wiley-VCH, New York. **1998**, pp. 1 and 125.

Buonocore, G.; Del Nobile, M.A.; Panizza, A.; Corbo, M.R.; Nicolais, L. A general approach to describe the antimicrobial agent release from highly swellable films intended for food packaging applications. Journal of Controlled Release. **2003**, 90, 97-107.

Burdock, G.A.; Carabin, I.G. Safety assessment of coriander (Coriandrum sativum L.) essential oil as a food ingredient. Food and Chemical Toxicology. **2009**, 47 22-34

Burnham, A.K.; Braun, R.L.; Coburn, T.T.; Sandvik, E.I.; Curry, D.J.; Schmidt, B.J.; Noble, R.A. An Appropriate Kinetic Model for Well-Preserved Algal Kerogens. Energy & Fuels. **1996**, 10, 49-59

Burt, S. A.; Reinders, R. D. Antibacterial activity of selected plant essential oils against Escherichia coli O157:H7. Letters in Applied Microbiology. **2003**, 36, 162-167.

Burt, S. Essential oils: Their antibacterial properties and potential applications in foods-A review. International Journal of Food Microbiology. **2004**, 94, 223-253.

Byaruhanga, Y.B.; Erasmus, C.; Taylor, J.R.N. Effect of microwave heating of kafirin on the functional properties of kafirin films. Cereal Chemistry Journal. **2005**, 82, 565-573.

C

Cagampang, G.; Perdon, A.; Juliano, B. Changes in salt-soluble proteins of rice during grain development. Phytochemistry. **1976**, 15, 1425-1429.

Cagampang, G.B.; Cruz, L. J.; Espiritu, S.G.; Santiago, R.G.; Juliano, B.O. Studies on the extraction and composition of rice proteins. Cereal Chemistry Journal. **1966**, 43, 145-155.

Cagri, A.; Ustunol, Z.; Ryser, E. Antimicrobial edible films and coatings. Journal of Food Protection. **2004**, 67, 833-848.

Cao, N.; Yang, X.; Fu, Y. Effect of various plasticizers in mechanical and water barrier properties of gelatin films. Food Hydrocolloids. **2009**, 23, 729 -735.

Castro, G.; Panilaitis, B.; Kaplan, D. Emulsan, a tailorable biopolymer for controlled release. Bioresource Technology. **2008**, 99, 4566-4571.

Cava, R., Nowak, E.; Taboada. Antimicrobial activity of clove and cinnamon essential oils against Listeria monocytogenes in pasteurized milk. Journal of Food Protection. **2007**, 70, 2757-2763.

Chen, P.; Zhang, L.; Cao, F. Effects of Moisture on Glass Transition and Microstructure of Glycerol-Plasticized Soy Protein. Macromolecular Bioscience. **2005**, 5, 872-880

Chen, S.e.G.; Cheng, M.C. Characterization of storage proteins in indica rice, Bot. Bull. Acad. Sin. **1986**, 27, 147-162.

Chen, Y.; Tan H.M. Crosslinked carboxymethylchitosan-g-poly (acrylic acid) copolymer as a novel superabsorbent polymer. Carbohydrate Research. **2006**, 341, 887-896.

Chhabra, R.P.; Richardson, J.F. Chapter 1 - Non-Newtonian fluid behaviour. Non-Newtonian Flow in the process industries: Fundamentals and Engineering Applications. Butterworth-Heinemann, Oxford. **1999**, pp 1-36.

Ching, C.; Kaplan, D.L.; Thomas, E.L. Biodegradable polymer and packing. Technomic Publishing Company INC, Lancaster, Pennsylvania. **1993**, pp. 1-141.

Chothia, C.; Janin, J. Principles of protein-protein recognition. Nature. **1975**, 256, 705-708.

Chung, O. K.; Pomeranz, Y. in 'Digestibility and Amino Acid Availability in Cereals and Oilseeds'(J. W. Finley and D. T. Hopkins, cds) AACC, St Paul, MN. **1985**, pp 65-107.

Cocero, A. M.; Kokini, J. L. The study of the glass transition of glutenin using small amplitude oscillatory rheological measurements and differential scanning calorimetry. Journal of Rheology. **1991**, 35, 257-270.

Coma, V. Bioactive packaging technologies for extended shelf life of meat-based products. Meat Science. **2008**, 78 90-103.

Coma, V. Perspective for the active packaging of meat products. En Advanced Technologies For Meat Products (Nollet, L.M. & Toldrá, F. eds.). CRC press, Taylor & Francis Group. Boca Raton. FL. USA. **2006,** pp.449-472.

COPA; COGEGA. Committee of Agricultural Organisation in the European Union, General Committee for the Agricultural Cooperation in the European Union**. 2001**.

Cornec, M.; Popineau, Y.; Lefebvre, J. Characterisation of Gluten Subfractions by SE-HPLC and Dynamic Rheological Analysis in Shear. Journal of Cereal Science. **1994**, 19, 131-139.

Cunningham, P.; Ogale, A.A.; Dawson, P.L.; Acton, J.C. Tensile properties of soy protein isolate films produced by a thermal compaction technique. Journal of Food Science. **2000**, 65, 668-71.

Cuq B.; Gontard N.; Guilbert S. Proteins as agricultural polymers for packaging production. Cereal Chemistry Journal. **1998**, 75, 1-9.

Cuq, B.; Boutrot, F.; Redl, A.; Lullien-Pellerin, V. Study of the temperature effect on the formation of wheat gluten network: influence on mechanical properties and protein solubility. Journal of Agricultural and Food Chemistry. **2000**, 48, 2954-2959.

Cuq, B.; Gontard, N.; Cuq, J.L.; Guilbert, S. Thermoplastic properties of fish myofibrillar proteins: application to biopackaging fabrication. Polymer. **1997**, 38, 4071-4078.

Cutter, C.N . Opportunities for bio-based packaging technologies to improve the quality and safety of fresh and further processed muscle foods. Meat Science. **2006**, 74, 131-142.

D

Da silva, L.S.; Taylor, J.R.N. Sorghum bran as a potential source of kafirin.Cereal Chemistry Journal. **2004**, 81, 322-327.

Das, S.; Routray, M.; Nayak, P. Spectral, thermal, and mechanical properties of furfural and formaldehyde cross-linked soy protein concentrate: A comparative study. Polymer-Plastics Technology and Engineering. **2008**, 47, 576-582.

Dawson, P.L.; Carl, G.D.; Acton, J. C.; Han, I.Y. Effect of lauric acid and nisin-impregnated soy-based films on the growth of Listeria monocytogenes on turkey bologna. Poultry Science. **2002**, 81, 721-726.

Damodaran, S. . Amino acids, peptides, and proteins. In O. R. Fennema (Ed.), Food chemistry(3rd ed.). New York, USA: Marcel Dekker, Inc. **1996.**

De Almeida, A.; Ruiz, J.A.; López, N.I.; Pettinari, M.J. Bioplásticos: una alternativa ecológica. QuímicaViva. **2004**, 3, 3.

De Graaf, L. Denaturation of proteins from a non-food perspective. Journal of Biotechnology. **2000**, 79 299-306.

Dean, J.A. The Analytical Chemistry Handbook. New York: McGraw Hill, Inc.. ISBN 0-07-016197-6. **1995**, pp 15.1-15.5.

Derksen, J.T.P.; Cuperus, F.P.; Kolster, P. Paints and coatings from renewable resources. Industrial Crops and Products. **1995**, 3, 225-236.

Devlieghere, F.; Vermeiren, L.; Debevere, J. New preservation technologies: Possibilities and limitations. International Dairy Journal. **2004**, 14 273-285.

Di Gioia, L.; Cuq, B.; Guilbert, S. Effect of hydrophilic plasticizers on thermomechanical properties of corn gluten meal. Cereal Chemistry Journal. **1998**, 75, 514-519.

Di Gioia, L.; Guilbert, S. Corn protein-based thermoplastic resins: effect of some polar and amphiphilic plasticizers. Journal of Agricultural and Food Chemistry. **1999**, 47, 1254-1261.

Donhowe, I.G.; Fennema, O.R. The effects of plasticizers on crystallinity, permeability, and mechanical properties of methylcellulose films. Journal of Food Processing and Preservation. **1993**, 17, 247-257.

Dorman, H. J. D.; Deans, S. G. Antimicrobial agents from plants: antibacterial activity of plant volatile oils. Journal of Applied Microbiology. **2000**, 88, 308-316.

E

Eggum, B. O. in 'Proceedings of a Workshop on Chemical Aspects of Rice Grain Quality', International Rice Research Institute, Los Banos, Laguna, Philippines. **1979**, pp 91-111.

Ennadios, A.; Weller, C.L.; Testin, R.F. Temperature effect on oxygen permeability of edible protein-based films. Journal of Food Science. **1993**, 58, 212-219.

European Bioplastics e.V. European-Bioplastics.htm

Evans, I.D. On the nature of the yield stress. Journal of Rheology. **1992**, 36, 1313-1316.

F

Fitzsimons, S.M.; Mulvihill, D.M.; Morris, E.R. Denaturation and aggregation processes in thermal gelation of whey proteins resolved by differential scanning calorimetry. Food Hydrocolloids. **2007**, 21 638-644.

Floros, J.D., Dock, L.L.; Han, J.H. Active packaging technologies and applications. Food Cosmet Drug Packag. **1997**, 20, 10-7.

Foster, J. F.; Samsa, E.G. Streaming Orientation Studies on Denatured Proteins. I. Heat Denaturation of Ovalbumin in Acid Media. Journal of the American Chemical Society. **1951**, 73; 3187-3193.

Friedli, G. L. Interactions of deamidated soluble wheat protein (SWP) with other food proteins and metals. Ph.D. thesis, University of Surrey. **1996**.

G

Galicia-García, T.; Martínez-Bustos, F.; Jiménez-Arevalo, O.; Martínez, A.B.; Ibarra-Gómez, R.; Gaytán-Martínez, M.; Mendoza-Duarte, M. Thermal and microstructural characterization of biodegradable films prepared by extrusion–calendering process Thermomechanical manufacture of protein based bioplastics. Carbohydrate Polymers. **2011**, 83, 354-361.

Gammariello, D.; Di Giulio, S.; Conte, A.; Del Nobile, M.A. Effects of Natural Compounds on Microbial Safety and Sensory Quality of Fior di Latte Cheese, a Typical Italian Cheese. Journal of Dairy Science. **2008**, 91, 4138-4146.

Gennadios A.; Weller C.L.; Hanna M.A.; Froning, G.W. Mechanical and barrier properties of egg albumen films. Journal of Food Science. **1996**, 61, 585-589.

Gennadios, A.; Weller, C.L.; Testin, R.F. Modification of physical and barrier properties of edible wheat gluten-based films. Cereal Chemistry Journal **1993**, 70, 426-429.

Ghanbarzadeh, B.; Musavi, M; Oromiehie, A.R.; Rezayi, K.; Razmi Rad, E.; Milani, J. Effect of plasticizing sugars on water vapor permeability, surface energy and microstructure properties of zein films. LWT - Food Science and Technology. **2007**, 40 1191-1197.

Gillgren, T; Stading, M. Mechanical and barrier properties of avenin and kafirin films. Food Physics. **2008**, 3, 287-294.

Gómez-Estaca, J.; Montero, P.; Giménez, B.; Gómez -Guillén, M.C. Effect of functional edible films and high pressure processing on microbial and oxidative spoilage in cold-smoked sardine (Sardina pilchardus). Food Chemistry. **2007**, 105, 511-520.

Gomez-Martinez, D.P.; Partal, P.; Martinez, I.; Gallegos, C. Rheological behaviour and physical properties of controlled-release gluten-based bioplastics. Bioresource Technology. **2009**, 100, 1828-1832

Gontard, N., S. Guilbert and J. Cuq. Edible wheat gluten films: influence of the main process variables on film properties using response surface methodology. Journal of Food Science. **1992**, 57, 190-199.

Gontard, N.; Duchez, C.; Cuq, J.L.; Guilbert, S. Edible composite films of wheat gluten and lipids: water vapor permeability and other physical properties. International Journal of Food Science & Technology. **1994**, 29, 39-50.

Gontard, N.; Guilbert, S.; Cuq J.L. Water and glycerol as plasticizers affect mechanical and water vapor barrier properties of an edible wheat gluten film. Journal of Food Science. **1993**, 58, 206-211.

Gontard, N.; Guilbert, S.; Cuq, J.L. Edible wheat gluten films: influence of main process variables on films properties using response surface methodology. Journal of Food Science. **1991**, 57, 190-195.

Gontard, N.; Marchesseau, S.; Cuq, J.L.; Guilbert, S. Water vapor permeability of edible bilayer films of wheat gluten and lipids. International Journal of Food Science & Technology. **1995**, 30, 49-56.

Gontard, N.; Ring, S. Edible wheat gluten film: Influence of water content on glass transition temperature. Journal of Agricultural and Food Chemistry. **1996**, 44, 3474-3478.

Gonzalez-Gutierrez, J.; Partal, P.; Garcia-Morales, M.; Gallegos, C. Development of highly-transparent protein/starch-based bioplastics. Bioresource Technology. **2010**, 101, 2007-2013.

Gorinstein, S.; Zemser, M.; Friedman, M.; Rodrigues, W.A.; Martins, P.S.; Vello, N.A.; Tosello, G.A.; Paredes-López, O. Physicochemical characterization of the structural stability of some plant globulins. Food Chemistry. **1996**, 56, 131-138.

Goswamia, T.H.; Maitib, M.M. Thermal stability of cured gelatin±trimethylol phenol blends: effect of plasticizer. Polymer Degradation and Stability. **1998**, 62, 447-454.

Gujral, H.S.; Rosell, C.M. Improvement of the breadmaking quality of rice flour by glucose oxidase. Food Research International. **2004**, 37, 75-81.

Guo, J.H. Effects of Plasticizers on Water Permeation and Mechanical Properties of Cellulose Acetate: Antiplasticization in Slightly Plasticized Polymer Film. Drug Development and Industrial Pharmacy. **1993**, 19, 1541-1555.

Gutierrez, J.; Barry-Ryan, C.; Bourke, PAntimicrobial activity of plant essential oils using food model media: Efficacy, synergistic potential and interactions with food components. Food Microbiology. **2009**, 26, 142-150.

H

Hamada, J.S. Separation and molecular mass distribution of rice proteins by size-exclusion high-performance liquid chromatography in a dissociating buffer. Journal of Chromatography. **1996**, 734, 195-203.

Hammer, K.A.; Carson, C. F.; Riley, T. V. Antimicrobial activity of essential oils and other plant extracts. Journal of Applied Microbiology. **1999**, 86, 985−990.

Han, J. Antimicrobial food packaging. Food Technology. **2000**, 54, 56-65

Handa, A.; Gennadios, A.; Hanna, M.A.; Seller, C.L.; Kuroda, N. Physical and molecular properties of egg-white lipid films. Journal of Food Science. **1999**, 64, 860-864.

Hao, Y.Y.; Brackett, R.E.; Doyle, M.P. Efficacy of plant extracts in inhibiting Aeromonas hydrophila and Listeria monocytogenes in refrigerated, cooked poultry. Food Microbiology. **1998**, 15, 367-378.

Heinämäki, J. T.; Colarte, A. I.; Nordström., A. J.; and Yliruusi, J. K. Comparative evaluation of ammoniated aqueous and organic-solvent-based cellulose ester enteric coating systems: a study on free films. International Journal Pharmacy. **1994**, 109, 9-16.

Helander, I. M.; Alokomi, H.L.; Latva-Kala, K.; Mattila-Sandholm, T.; Pol, I.; Smid, E. J.; et al. Characterization of the action of selected essential oil components on Gram-negative bacteria. Journal of Agriculture and Food Chemistry. **1998**, 46, 3590-3595.

Hernandez-Izquierdo, VM. Thermal transitions, extrusion, and heat-sealing of whey protein edible films [dissertation]. Davis, Calif.: Univ. of California. **2007**, pp 110.

Hernandez-Munoz, P.; Villalobos, R.; Chiralt, A. Effect of crosslinking using aldehydes on properties of glutenin-rich films. Food Hydrocolloids. **2004**, 18, 403-411.

Hibino, T.; Kidzu, K.; Masumra, T.; Ohtsuki, K.; Tanaka, K.; Kawabata, M.; Fujii, S. Amino-acid composition of rice prolamin polypeptides. Agricultural and Biological Chemistry. **1989**, 53, 513-518.

Higuchi, W.; Fukazawa, C. A rice glutelin and a soybean glycinin have evolved from a common ancestral gene. Gene Journal **1987**, 55, 245-253.

Hoffman, K. L.; Han, I. Y.; Dawson, P. L. Antimicrobial effects of corn zein films impregnated with nisin, lauric acid, and EDTA. Journal of Food Protection. **2001**, 64, 885-889.

Houston, D.; Mohammad, A. Purification and partial characterization of a major globulin from rice endosperm. Cereal Chemistry Journal. **1970**, 47, 5-12.

I

Irissin-Mangata, J.; Bauduin, G., Boutevin, B.; Gontard, N. New plasticizers for wheat gluten films. European Polymer Journal. **2001**, 37, 1533-1541.

J

Jeon, Y. J.; Kamil, J. Y. V. A.; Shahidi, F. Chitosan as an edible film for quality preservation of Herring and Atlantic cod. Journal of Agricultural Food Chemistry. **2002**, 50, 5167-5178.

Jerez, A.; Partal, P.; Martínez, I.; Gallegos, C.;Guerrero, A. Rheology and processing of gluten based bioplastics. Biochemical Engineering Journal. **2005a**, 26, 131-138.

Jerez, A.; Partal, P.; Martínez, I.; Gallegos C.; Guerrero, A. Bioplástico y métodos para su preparación. Oficina Española de Patentes y Marcas. Patent, P200501556. **2005b.**

Jerez, A.; Partal, P.; Martínez, I.; Gallego, C.; Guerrero, A. Egg white-based bioplastics developed by thermomechanical processing. Journal of Food Engineering. **2007**, 82, 608-617.

Jiugao, Y.; Wang N.; Ma X. The effect of citric acid on the properties of thermoplastics starch plasticized by glycerol. Starch Journal. **2005**, 57, 494-504.

Jones, S.; Thornton, J. Protein-protein interactions: A review of protein dimer structures. Progress in Biophysics and Molecular Biology. **1995**, 63, 31-59,61-65.

Juliano, B. The rice caryopsis and its composition. In DF Houston, ed, Rice Chemistry and Technology. American Association of Cereal Chemists Inc, St. Paul. **1972**, pp 16-74.

Juliano, B. O. Metabolic evolution of rice protein. Food Chemistry. **1978**, 3 251-263.

Juliano, B. Polysaccharides, proteins and lipids of rice, in: B.O. Juliano (Ed.), Rice: Chemistry and Technology, edited by D.F. Houston. St. Paul, Minn.: American Association of Cereal Chemists. **1985**, pp. 59-174.

Juliano, B.O.; Antonio A.A.; Esmama, B.V. Effects of protein content on the distribution and properties of rice protein. Journal of the Science of food and agriculture. **1973**, 24, 295-306.

K

Kahovec, J.; Fox, R. B.; Hatada, K. Nomenclature of regular single-strand organic polymers. Pure and Applied Chemistry. **2002**, 74, 1921-1956.

Kalichevsky, M.T.; Blanshard, J.M.V. A study of the effect of water on the glass transition of 1:1 mixtures of amylopectin, casein and gluten using DSC and DMTA. Carbohydrate Polymers. **1992**, 19 271-278.

Kalichevsky, M. T.; Jaroszkiewicz, E. M.; Blanshard, J. M. V. Glass transition of gluten. 1: Gluten and gluten-sugar mixtures. International Journal of Biological Macromolecules. **1992**, 14, 257-266.

Kalichevsky, M.T.; Jaroszkiewicz, E.M.; Blanshard, J.M.V. A study of the glass transition of amylopectin—sugar mixtures. Polymer. **1993**, 34, 346-358.

Kasarda, D.D.; Autran, J.C.; Lew, E.J.L.; Nimmo, C.C.; Shewry, P.R. N-terminal amino acid sequences of ω-gliadins and ω-secalins; Implications for the evolution of prolamin genes. Biochimica et Biophysica Acta, **1983**, 747, 138-150.

Kauzmann, W. Some factors in the interpretation of Protein Denaturation. Advances in Protein Chemistry. **1959**, 14; 1-64.

Kayserilioğlu, B.Ş.; Bakir, U.; Yilmaz, L.;Akkaş, N. Drying temperature effects on wheat gluten film properties. Journal of Agricultural and Food Chemistry. **2003**, 51, 964-969.

Keith, S. Mechanics (Third ed.). Addison-Wesley. ISBN 0-201-07392-7. **1971**.

Keller, D.S.; Keller, Jr. D.V. An investigation of the shear thickening and antithixotropic behavior of concentrated coal-water dispersions. Journal of Rheology. **1990**, 34, 1267-1291.

Kennedy, B.M.; Schelstraete, M. Chemical, physical and nutritional properties of high-protein flours and residual kernel from over milling of uncoated milled rice. II. Amino acid composition and biological evaluation of the protein. Cereal Chemistry Journal. **1974**, 51, 448-457.

Khatkar, B.S.; Bell, A.E.; Schofield, J.D. The dynamic emphasising the positive role of gliadins in bread rheological properties of glutens and gluten sub-fractions from wheats of good and poor bread making quality. Journal of Cereal Science. **1995**, 22, 29-44.

Khoi, B. H.; Dicon, L. D.; Lasztity, R.; Salgo, A. The protein and the amino acid composition of some rice and maize varieties grown in North Vietnam. Journal of the Science of Food and Agriculture. **1987**, 39, 137-143.

Kim, W.K.; Okita, T.W. Nucleotide and primary sequence of a major rice prolamine. FEBS Lett. **1988**, 231, 308-310.

Kim, W.T. Ph.D. Dessertation, Washington State University. **1988**.

Kinney, A.B.; Scranton, A.B. Formulation and structure of crosslinked polyacrylates: methods for modeling network formation. In: Buchhloz FL, Peppas NA (eds.) Superabsorbent polymers: Sciencie and technology. ACS Symposium Series, American Chemical Society, Washington DC. **1994**, 573, 2-26.

Kokini, J.L.; Cocero, A.M.; Madeka, H.; de Graaf, E. The development of state diagrams for cereal proteins. Trends in Food Science & Technology. **1994**, 5, 281-288.

Kokini, J.L.; Cocero, A.M.; Madeka, H. State diagrams help predict rheology of cereal proteins. Food Technology. **1995**, 5, 74-82.

Krishnan, H.B.; Okita, T.W. Structural relationships among rice glutelin polypeptides. Plant Physiololy. **1986**, 81, 748-753.

Krochta, J.M., McHugh, T.H. Water-insoluble protein-based edible barrier coatings and films. US Pat. No. 5,543,164. **1996**.

L

Lai, H.M.; Padua, G.W. Water vapor barrier properties of zein films plasticized with oleic acid. Cereal Chemistry Journal. **1998**, 75, 194-199.

Langmuir, I. Protein Denaturation. Cold Spring Harb. Symposia on Quantitative Biology. **1938**, 6, 159.

Lefèvre, T.; Subirade, M. Interaction of β-lactoglobulin with phospholipid bilayers: a molecular level elucidation as revealed by infrared spectroscopy. International Journal of Biological Macromolecules. **2000**, 28, 59-67.

Lew, E.J.L.; Kuzmicky, D.D.; Kasarda, D.D. Characterization of low-molecular-weight glutenin subunits by reversed-phase highperformance liquid chromatography, sodium dodecyl sulfate-polyacrylamide gel electrophoresis, and N-terminal amino acid sequencing. Cereal Chemistry Journal. **1992**, 69, 508-515.

Li, M; Lee, TC. Effect of cysteine on the functional properties and microstructures of wheat flour extrudates. Journal of Agricultural and Food Chemistry. **1996**, 44, 1871-80.

Lim, L.T.; Mine, Y.; Tung, M.A. Barrier and tensile properties of transglutaminase cross-linked gelatin films as affected by relative humidity, temperature, and glycerol content. Journal of Food Science. **1999**, 64, 616-22.

Lis-Balchin, M; Hart, S. A preliminary study of the effect of essential oils on skeletal and smooth muscle in vitro. Journal of Ethnopharmacology. **1997**, 58 183-187.

Liu, L.; Kerry, J.F.; Kerry, J.P. Effect of food ingredients and selected lipids on the physical properties of extruded edible films/casings. International Journal of Food Science & Technology. **2006**, 41, 295–302.

López, P.; Sánchez, C.; Batlle, R.; Nerín, C. Vapor-phase activities of cinnamon, thyme, and oregano essential oils and key constituents against food borne microorganisms. Journal of Agricultural and Food Chemistry. **2007**, 55, 4348-4356.

López-Caballero, M.E.; Gómez-Guillén, M.C.; Pérez-Mateos, M.; Montero, P. A chitosan–gelatin blend as a coating for fish patties. Food Hydrocolloids. **2005**, 19 303-311.

Lopez-Rubio, A.; Almenar, E.; Hernandez-Munoz, P.; Lagaron, J. M.; Catala, R.; Gavara, R. Overview of active polymer-based packaging technologies for food applications. Food Reviews International. **2004**, 20, 357−387.

Lörck, J.; Pommeranz, W.; Schmidt, H. Biologically degradable polymer misture. United States Patent and trademark Office. WO96/31561. **2000.**

Lumry, R.; Eyring, H. Conformation changes of Proteins. Journal of Physical Chemistry. **1954**, 58; 110-120.

Luthe, D.S. Storage protein accumulation in developing rice (Oryza sativa L.) seeds Plant Science Letters. **1983**, 32, 147-158.

M

MacRitchie, F. Physicochemical processes in mixing. In: Blanshard, J.M.V., Frazier, P.J., Galliard, T. (Eds.), Chemistry and Physic of Baking. Royal Society of Chemistry, London, UK. **1986**, pp 132-146.

Madeka, H. ; Kokini, J.L. Changes in rheological properties of gliadin as a function of temperature and moisture: Development of a state diagram. Journal of Food Engineering. **1994**, 22 241-252.

Mandac, B.; Juliano, B. Properties of prolamin in mature and developing rice grain. Phytochemistry. **1978**, 17. 611-614.

Mangavel, C.; Rossignol, N.; Perronnet, A.; Barbot, J.; Popineau, Y.; Gueguen, J. Properties and microstructure of thermo-pressed wheat gluten films: A comparison with cast films. Biomacromolecules. **2004**, 5, 1596-1601.

Masci, S.; Lew, E.J.-L.; Lafiandra, D.; Porceddu, E.; Kasarda, D.D. Characterization of low-molecular-weight glutenin subunits in durum wheat by RP-HPLC and N-terminal sequencing. Cereal Chemistry. **1995**, 72, 100-104.

Matveev, Yu.I .; Grinberg, V.Ya.; Tolstoguzov, V.B. The plasticizing effect of water on proteins, polysaccharides and their mixtures. Glassy state of biopolymers, food and seeds. Food Hydrocolloids Journal. **2000**, 14, 425-437.

McMurry, J. Quimica organica. Mexico: grupo editorial iberoamerica. **1994**, pp 1278.

Min, B.J.; Oh, J.H. Antimicrobial activity of catfish gelatin coating containing origanum (Thymus capitatus) oil against gram-negative pathogenic bacteria. J. Food Sci. **2009**, 74, M143-M148.

Min, S.; Harris, L. J.; Han, J. H.; Krochta, J. M. Listeria monocytogenes inhibition by whey protein films and coatings incorporating lysozyme. Journal of Food Protection. **2005**, 68, 2317-2325.

Mine Y. Effect of dry heat and mild alkaline treatment on functional properties of egg white proteins. Journal of Agricultural and Food Chemistry. **1997**, 45, 2924-2928.

Mirsky, A.E. Sulfhydryl group of egg albumin in different denaturing agents. Journal Cell Biology. **1941**, vol. 24, 709-723.

Mitchell, J.R.; Areas, J.A.; Rasul, S.; Coloma, P.; Della Valle G. La cuisson Extrusion Technique et Documentation, Lavoiser, Paris. **1994**, pp. 88-108.

Mo, X. Q.; Sun, X. S.; Wang, Y. Q. Effects of molding temperature and pressure on properties of soy protein polymers. Journal of Applied Polymer Science. **1999**, 73, 2595-2602

N

Nanda, P.; Nayak, P;., Rao, K. Thermal degradation analysis of biodegradable plastics from urea-modified soy protein isolate. Polymer-Plastics Technology and Engineering. **2007**, 46, 207-211.

Nakatsu, T.; Lupo Jr., A.; Chinn Jr. J.; Kang, R. Biological activity of essential oils and their constituents. Bioactive Natural Products (Part B). **2000** , 21, 571-631.

Nelson, R. R. In vitro activities of five plants essential oils against methicillin resistant Staphylococcus aureus and vancomycin ressistant Enterococcus faecium. Journal of Antimicrobial Chemotherapy. **1997**, 40, 305-306.

Neurath, H.; Greenstein, J.P.; Putman, F.W.; Erickson, J.O. The chemistry of protein denaturation. Chemical Reviews. **1944**, 34: 157-265.

O

Ogawa, M., Kumamaru, T., Satoh, H., Iwata, N., Omura, T., Kasai, Z., Tanaka, K. Purification of protein body I of rice seed and its polypeptide composition. Plant and Cell Physiology. **1987**, 28, 1517-1527.

Okita, T.W.; Hwang, Y.S.; Hnilo, J., Kim, W.T.; Aryan, A.P.; Larson, R.; Krishnan, H.B. Structure and expression of the rice glutelin multigene family. Journal of Biological Chemistry. **1989**, 264, 12573-12581.

O'Neill, M.J. "The Analysis of a Temperature-ControlledScanning Calorimeter". Analytical Chemistry. **1964**, 36, 1238-1245.

Oszvald Domenek, S.; Morel, M.-H.; Bonicel, J.;Guilbert, S. Polymerization kinetics of wheat gluten upon thermosetting. A mechanical model. Journal of Agricultural and Food Chemistry. **2002**, 50,5947-5954

Oszvald, M.; Jenes, B.; Tömösközi, S.; Békés, F.; Tamás, L. Expression of the Dx5 high molecular weight glutenin subunit protein in transgenic rice. Cereal Research Communication. **2007a**, 35, 1543-1549.

Oszvald, M.; Tömösközi, S.; Tamás, L.; Békés, F. Developing method to study the effect of rice proteins for the functional properties. Acta Alimentaria. **2007b,** 37, 399-408.

Oszvald, M.; Tömösközi, S.; Larroque, O.; Kereszténvi, E.; Tamás, L.; Békés, F. Characterization of rice storage proteins by SE-HPLC and micro z-arm mixer.Journal of Cereal Science. **2008**, 48 68-76.

Oussalah, M.; Caillet, S.; Salmieri, S.; Saucier, L.; Lacroix, M. Antimicrobial and antioxidant effects of milk protein based film containing essential oils for the preservation of whole beef muscle. Journal of Agricultural and Food Chemistry. **2004**, 52, 5598-5605.

Oussalah, M.; Caillet, S.; Salmieri, S.; Saucier, L.; Lacroix, M. Antimicrobial and antioxidant effects of milk protein based film containing essential oils for the preservation of whole beef muscle. Journal of Agriculture and Food Chemistry. **2004**, 52, 5598-5605.

Oussallah, M.; Caillet, S.; Saucier, L.; Lacroix, M. Antimicrobial effects of selected plant essential oils on the growth of a Pseudomonas putida strain isolated from meat. Meat Science. **2006**, 73 236-244.

P

Padget, T.; Han, I. Y.; Dawson, P.L. Effect of lauric acid addition on the antimicrobial efficacy and water permeability of corn zein films containing nisin. Journal of Food Processing and Preservation. **2000**, 24, 423-432.

Padgett, T.; Han, I. Y.;Dawson, P.L. Incorporation of food grade antimicrobial compounds into biodegradable packaging films. Journal of Food Protection. **1998**, 61, 1330-1335.

Padhye, V.W.; Salunkhe, D.K. Extraction and characterization of rice proteins. chemistry journal. **1979**, 56, 389-393.

Pal R.K. Ripening and rheological properties of mango as influenced by ethereal and carbide. Journal of Food Science & Technology. **1998**, 35, 358-360.

Pallos F. M.; Robertson G.H.; Pavlath A.E.; Orts W.J. Thermoformed Wheat Gluten Biopolymers. Journal of Agricultural and Food Chemistry. **2006**, 54, 349-352

Park, J.W.; Testin, R.F.; Park, H.J.; Vergano, P.J.; Weller, C.L. Fatty acid concentration effect on tensile strength, elongation and water vapor permeability of laminated edible films. Journal of Food Science. **1994**, 59, 916–919.

Park, W.D. Tuber proteins of potato: a new and surprising molecular system. Plant Molecular Biology Reports. **1983**, 1, 61-66

Paster, N.; Calderon, M.; Menasherov, M.; Mora, M. Biogeneration of modified atmospheres in small storage containers using plant wastes. Crop Protection. **1990**, 9, 235-238.

Paster, N.; Menasherov, M.; Ravid, U.; Juven, B. Antifungal activity of oregano and thyme essential oils applied as fumigants against fungi attacking stored grain. Journal of Food Protection. **1995**, 58, 81-85.

Perdon, A.; Juliano, B. Properties of a major α-globulin of rice endosperm. Phytochemistry. **1978**, 17, 351-353.

Periago, P.M.; Delgado, B.; Fernández, P.S.; Palop, A. Use of carvacrol and cymene to control growth and viability of Listeria monocytogenes cells and predictions of survivors using frequency distribution functions. Journal of Food Protection. **2004**, 67, 1408-1416.

Pommet, M.; Redl, A., Guilbert, S.; Morel, M-H. Intrinsic influence of various plasticizers on functional properties and reactivity of wheat gluten thermoplastic materials. Journal of Cereal Science. **2005**, 42, 81-91.

Pommet, M.; Redl, A.; Morel, MH.; Domenek, S.; Guilbert, S. Thermoplastic processing of protein-based bioplastics: chemical engineering aspects of mixing, extrusion and hot molding. Macromolecular Symposia. **2003**, 197, 207-17.

Popineau, Y.; Cornec, M.; Lefebvre, J.; Marchylo, B. Influence of high Mr glutenin subunits on glutenin polymers and rheological properties of glutens and gluten subfractions of near-isogenic lines of wheat sicco. Journal of Cereal Science. **1994**, 19 231-241.

Pouplin, M.; Redl, A.; Gontard, N. Glass transition of wheat gluten plasticized with water, glycerol, or sorbitol. Journal of Agricultural and Food Chemistry. 1**999**, 47, 538–543.

Pouvreau, L.; Gruppen, H.; Piersma, S. R.; Van den Broek, L. A. M.; Van Koningsveld, G.A.; Voragen, A. G. J. Relative abundance and inhibitory distribution of protease inhibitors in potato fruit juice from c.v. Elkana. Journal of Agricultural and Food Chemistry. **2001**, 49, 2864-2874.

Pouvreau, L.; Gruppen, H.; van Koningsveld, G.; van den Broek, L.A.M.; Voragen, A.G.J. Conformational stability of the potato serine protease inhibitor group. Journal of Agricultural and Food Chemistry. **2005a**, 53, 3191-3196.

Pouvreau, L.; Kroef, T.; Gruppen, H.; van Koningsveld, G.; van den Broek, L. A.M.;Voragen, A.G.J. Structure and stability of the potato cysteine protease inhibitor group (Cv. Elkana). Journal of Agricultural and Food Chemistry. **2005b**, 53, 5739-5746.

Prilutski, G. .; Gupta, R.K.; Sridhar, T.; Ryan, M.E. Model viscoelastic liquids. Journal of Non-Newtonian Fluid Mechanics. **1983**, 12 233-241.

Privalov, P.L.; Khechinashvili, N.N. A thermodynamic approach to the problem of stabilization of globular protein structure: A calorimetric study. Journal of Molecular Biology. **1974**, 86 665-684.

Prout, E.G.; Tompkins, F.C. The thermal decomposition of potassium permanganate. Transactions of the Faraday Society. **1944**, 40, 488-498

Prout, E.G.; Tompkins, F.C.The thermal decomposition of silver permanganate. Transactions of the Faraday Society. **1946**, 42, 468-472

Pungor, E. A Practical Guide to Instrumental Analysis. Florida: Boca Raton. **1995**, pp 181-191.

Q

Quintavalla, S.; Vicini, L. Antimicrobial food packaging in meat industry. Meat Science. **2002**, 62 373-380.

R

Rebello, C. A.; Schaich, K. M. Extrusion chemistry of wheat flour proteins: II. Sulfhydryl–disulfide content and protein structural changes. Cereal Chemistry Journal. **1999**, 76, 756-763.

Redl, A.; Morel, M-H.; Bonicel, J.; Vergnes, B.; Guilbert, S. Extrusion of wheat gluten plasticized with glycerol: influence of process conditions on flow behavior, rheological properties, and molecular size distribution. Cereal Chemistry Journal. **1999a**, 76, 361-370.

Redl, A.; Morel, M.H.; Bonicel, J.; Vergnes B.; Guilbert S. Rheological properties of gluten plasticized with glycerol: dependence on temperature, glycerol content and mixing conditions. Rheolycal Acta. **1999b**, 38, 311-320.

Redl, A.; Guilbert, S.; Morel, M.H. Heat and shear mediated polymerisation of plasticized wheat gluten protein upon mixing. Journal of Cereal Science. **2003**, 38, 105-114.

Refstie, S; Tiekstra, H.A.J. Potato protein concentrate with low content of solanidine glycoalkaloids in diets for Atlantic salmon (Salmo salar). Aquaculture. **2003**, 16, 283-298.

Regulation (EC) No. 1935/2004 of the European Parliament and of the Council of 27 October 2004 on materials and articles intended to come into contact with food and repealing Directives 80/590/EEC and 89/109/EEC, Official Journal of the European Union. **2004,** L338, 4-17.

Regulation (EC) No. 450/2009. on active and intelligent materials and articles intended to come into contact with food. Official Journal of the European Union. **2009**, L 135, 3-11

Rice, S. A.; Wada, A.; Geidushek, E. P. Some comments on the Theory of Denaturation. Discussions of the Faraday Society. **1958**, 25, 130.

Rojas-Graü, M.; Avena-Bustillos, J.R.; Olsen, C.; Friedman, M.; Henika, P.R.; Martin-Belloso, O. Effects of plant essential oils and oil compounds on mechanical barrier and antimicrobial properties of alginate-apple puree edible films. Journal of Food Engineering. **2007**, 81, 634-641.

Rojas-Graü, M.A; Avena-Bustillos, R.J.; Mendel Friedman, C.O.; Henika, P.R.; Martín-Belloso, O.; Pan, Z.; McHugh, T.H. Effects of plant essential oils and oil compounds on mechanical, barrier and antimicrobial properties of alginate–apple puree edible films. Journal of Food Engineering. **2007**, 81 634-641.

Rooney, M. L. Active packaging in polymer films. In M. L. Rooney (Ed.), Active food packaging. Glasgow: Blackie Academic and Professional. **1995**, pp. 74-110

Rosell, C.M.; Rojas, J.A.; Benedito de Barber C. Influence of hydrocolloids on dough rheology and bread quality Food Hydrocolloids. **2001**, 15, 75-81.

Rouilly, A.; Jorda, J.; Rigal, L. Thermo-mechanical processing of sugar beet pulp. II. Thermal and rheological properties of thermoplastic SBP. Carbohydrate Polymers. **2006**, 66, 117-125.

S

Sarwin, R.; Laskawy, G.; GROSCH, W. Changes in the levels of glutathione and cysteine during the mixing of doughs with Lthreo- and D-erythro-ascorbic acid. Cereal Chemistry Journal. **1993**, 70, 553-557

Schaich, K. M.; Rebello, C. A. Extrusion chemistry of wheatflour proteins: II. Free radical formation. Cereal Chemistry Journal. **1999**, 7, 748-755.

Schluentz, E. J.; Steffe, J. F.; Ng, K.W.P. Rheology and microstructure of wheat dough developed with controlled deformation. Journal of Texture Studies. **2000**, 31, 41-54.

Schofield, J. D.; Bottomley, R. C.; Timms, M. F.; Booth, M. R. The effect of heat on wheat gluten and the involvement of sulphydryl–Disulphide interchange reaction. Journal of Cereal Science. **1983**, 1, 241-253.

Schurz, J. The yield stress - an empirical reality. Rheolycal Acta. **1990**, 29, 170-171.

Seydim, A. C.; Sarikus, G. Antimicrobial activity of whey protein based edible films incorporated with oregano, rosemary and garlic essential oils. Food Research International. **2006**, 39, 639-644.

Shawkat, H.; Li, H. The impact of the Asian crisis on the behavior of US and international petroleum prices. Energy Economics. **2004**, 26, 135-160.

Shellhammer, T.H.; Rumsey, T.R.; Krochta, J.M. Viscoelastic properties of edible lipids. Journal of Food Engineering. **1997**, 33, 305-320.

Shen, L.; Haufe, J.; Patel, M.K. Product overview and market projection of emerging bio-base bioplastic. PRO-BIP. **2009**

Shewry, P. R.; Tatham, A. S.; Forde, J.; Kreis, M.;Miflin, B. J. The classification and nomenclature of wheat gluten proteins:a reassessment. Journal of Cereal Science. **1986**, 4, 97-106.

Shyur, L-f.; Zia, K.K.; Chen, C-s. Purification and some properties of storage proteins in Japonica rice. Bot. Bull. Acad. Sin. **1988**, 29, 113-122.

Siepmann, F.; Siepmann, J.; Walther, M.; MacRae, R.J.; Bodmeier, R. Polymer blends for controlled release coatings. Journal of Controlled Release. **2008**, 125, 1-15.

Singh, J.; Kaur, L. Introduction: potato tuber. In Singh, J. Kaur, L. (Eds.). Advances in Potato Chemistry and Technology. Burlington, MA: Elsevier. **2009**, pp. 9-12.

Sivaramakrishnan, H.P.; Senge, B.; Chattopadhyay, P.K. Rheological properties of rice dough for making rice bread. Journal of Food Engineering. **2004**, 62, 37-45.

Skoog, D.A.,; Holler, F.J.; Nieman, T.A. Principles of Instrumental Analysis, 5th edition, Thomson Learning. **1998**, chapter 14, 16, 17.

Song, Y.; Zheng, Q. Improved tensile strength of glycerol-plasticized gluten bioplastic containing hydrophobic liquids. Bioresource Technology. **2008**, 99, 7665-7671.

Sothornvit, R.; Krochta, J.M. Plasticizer effect on mechanical properties of β-lactoglobulin films. Journal of Food Engineering, **2001**, 50, 149-155.

Sothornvit, R.; Krochta, J.M. Plasticizers in edible films and coatings. Innovations in Food Packaging. **2005**, 403-433.

Sothornvit, R.; Olsen, C.W.; McHugh, T.H.; Krochta, J.M. Tensile properties of compression-molded whey protein sheets: Determination of molding condition and glycerol-content effects and comparison with solution-cast films. Journal of Food Engineering. **2007**, 78 855-860.

Suppakul, P.; J. Miltz, J.; Sonneveld, K.; Bigger, S.W. Active Packaging Technologies with an Emphasis on Antimicrobial Packaging and its Applications. Journal of Food Science. **2003**, 68, 408-420.

Steffe, J.F. Rhelogical methods in food processing engineering. Freeman Press, East Lansing. **1996**.

Steg, I. ; Katz, D. Rheopexy in some polar fluids and in their concentrated solutions in slightly polar solvents. Journal of Applied Polymer Science. **1965**, 9, 3177-3193.

Stevens, MP. Polymer chemistry. An introduction. New York: Oxford Univ. Press. **1999**, pp 551.

Strecker, T. D.; Cavalieri, R. P.; Zollars, R. L.; Pomeranz, Y. Polymerization and mechanical degradation kinetics of gluten and glutenin at extruder melt-section temperatures and shear rates. Journal of Food Science. **1995**, 60, 532-537.

Suda, K.; Wararuk, C.; Manit, S. Radiation modification of water absorption of cassava starch by acrylic acid/acrylamide. Radiation Physics and Chemistry. **2000**, 59, 413- 427.

Sun, S.; Song, Y.; Zheng, Q. Morphologies and properties of thermo-molded biodegradable plastics based on glycerol-plasticized wheat gluten. Food Hydrocolloids. **2007**, 21, 1005-1013.

Swain, S.; Rao, K.; Nayak, P. Biodegragable Polymers. Part II. Thermal degradation of biodegradable plastics cross-linked from formaldehyde-soy protein concentrate. Journal of Thermal Analysis and Calorimetry. **2005**, 79, 33-38.

T

Takaiwa, F.; Ebinuma, H.; Kikuchi, S., Oono, K. Nucleotide sequence of a rice glutelin gene. FEBS Letters. **1987**, 221, 43-47.

Takaiwa, F.; Kikuchi, S., Oono, K. The structure of rice storage protein glutelin precursor deduced from cDNA. FEBS Letters. **1986**, 206, 33-35.

Talens, P.; Krochta, J.M. Plasticizing effects of beeswax and carnauba wax on tensile and water vapor permeability properties of whey protein films. Journal of Food Science. **2005**, 70, E239-E243.

Tanaka, T. Gels. Scientific American: Scientific American Magazine. **1981**, 244, 110-123.

Tanner, R.I. Engineering Rheology. Oxford University Press, Oxford. **1988**.

Tharanathan, R. N. Biodegradable films and composite coatings: past, present and future. Trends in Food Science Technology. **2003**, 14, 71-78.

The European Standard EN13432 "Requirements for packaging recoverable through composting and biodegradation - Testing scheme and evaluation criteria for the final acceptance of packaging". European standard, **2001**.

Timasheff, S. N.; Gibbs, R.J. The state of plasma albumin in acid pH. Archives of Biochemistry and Biophysics. **1957**, 70; 547-560.

Tolstoguzov, VB. Thermoplastic extrusion—the mechanism of the formation of extrudate structure and properties. Journal of the American Oil Chemists' Society. **1993**, 70, 417-24.

Torres, J.A. Edible films and coatings from proteins. in: Protein Functionality in Food Systems. N. S. Hettiarachchy and G. R. Ziegler, eds. Marcel Dekker: New York. **1994**, pp 467-507

Tropea, C.;Yarin, A.L.; Foss, J.F. Springer Handbook of Experimental Fluid Mechanics. Springer, Berlin. **2007**.

Tunç , S.; Duman , O. The effect of different molecular weight of poly(ethylene glycol) on the electrokinetic and rheological properties of Na-bentonite suspensions. Colloids and Surfaces A: Physicochemical and Engineering Aspects. **2008**, 31793-99.

Turhan, K. N.; Sahbaz, F.; Guner, A. A spectrophotometric study of hydrogen bonding in methylcellulose-based edible films plasticized by polyethylene glycol. Journal of Food Science. **2001**, 66, 59-62.

Turhan, K.N.; Şahbaz, F. Water vapor permeability, tensile properties and solubility of methylcellulose-based edible films. Journal of Food Engineering. **2004**, 61, 459-466.

V

Vallejo, B.; Barbosa, H.; Cortés, C.; Espinosa, A. Evaluación de la velocidad de liberación de un principio activo para acondicionamiento de suelos desde comprimidos matriciales con base en un higrogel de acrilamida. Revista colombiana de ciencias químico farmacéuticas. **2005**, 34, 155-171.

Van Koningsveld, G.A.; Walstra, P.; Voragen, A. G.J.; Kuijpers, I.J.; van Boekel, M.A.J.S.; Gruppen, H. Effects of protein composition and enzymatic activity on formation and properties of potato protein stabilized emulsions. Journal of Agricultural and Food Chemistry. **2006**, 54, 6419-6427.

Van Koningsveld, G.A.; Gruppen, H.; de Jongh, H. H. J.; Wijngaards, G.; van Boekel, M. A. J. S.; Walstra, P.; et al. Effects of pH and heat treatment on the structure and solubility of potato proteins in different preparations. Journal of Agricultural and Food Chemistry. **2001,** 49,4889-4897.

Van Koningsveld, G.A.; Gruppen, H.; de Jongh, H. H. J.; Wijngaards, G.; van Boekel, M. A. J. S.; Walstra, P.. Formation and stability of foam made with various potato protein preparations. Journal of Agricultural and Food Chemistry. **2002**, 50, 765-7659.

Van Vliet, T.; Lyklema, H. Rheology. Fundamentals of Interface and Colloid Science. **2005**, 4, 6.1-6.88.

Vázquez, B. I.; Gente, C.; Franco, C. M.; Vázquez, M. J.; Cepeda, A.Inhibitory effects of eugenol and thymol on Penicillium citrinum strains in culture media and cheese. International Journal of Food Microbiology. **2001**, 67, 157-163.

Vermeiren, L.; Devlieghere, F.; van Beest, M.; de Kruijf, N.; Debevere, J. Developments in the active packaging of foods.Trends in Food Science & Technology. **1999**, 10, 77-86.

Vidal, A. J.; Juliano, B. O. Comparative composition of waxy and norwaxy rice. Cereal Chemistry Journal. **1967**, 44, 86-91

W

Wang, C-S.; Shastri, K.; Wen, L.; Huang, J.K.; Santhayanon, B.; Muthukrishanan, S.; Reeck, G.R. Heterogeniety in cDNA clones enconding rice giutelin. FEBS Lett. **1987**, 222, 135-138.

Weegels, P.L.; Verhoek, J.A.; de Groot, A.M.G.; Hamer, R.J. Effects on Gluten of Heating at Different Moisture Contents. I. Changes in Functional Properties. Journal of Cereal Science. **1994a**, 19 31-38.

Weegels, P.L.; de Groot, A.M.G.; Verhoek, J.A.; Hamer, R.J. Effects on Gluten of Heating at Different Moisture Contents. II. Changes in Physico-Chemical Properties and Secondary Structure. Journal of Cereal Science. **1994b**, 19 39-47.

Weegels, P.L.; Orsel, R.; Van de Pijpekamp, A.M.; Lichtendonk, W.J.; Hamer, R. J. ; Schofield, J. D. Functional properties of low Mr wheat proteins. II. Effects on dough properties. Journal of Cereal Science. **1995**, 21, 117-126.

Wen, T.N.; Luthe, D.S. Biochemical characterization of rice glutelin. Plant Physioloy. **1985**, 78 172-177.

Weng, Y. M.; Hotchkiss, J. H. Inhibition of surface molds on cheese by polyethylene containing the antimycotic imazalil. Journal of Food Protection. **1992**, 55, 367-369.

Wirsenius, S.; Azar, C.; Berndes, G. How much land is needed for global food production under scenarios of dietary changes and livestock productivity increases in 2030?. Agricultural Systems. **2010**, 103, 621-638.

Wright, D.J.; Leach, L.B.; Wilding, P. Differential scanning calorimetric studies of muscle ant its constituent proteins. Journal of the Science of Food and Agriculture. **1977**, 28, 557.

Y

Yuan, J.; Shang, P.P.; Wu S.H. Effects of Polyethylene Glycol on Morphology, Thermomechanical Properties, and Water Vapor Permeability of Cellulose Acetate–Free Films. Pharmaceutical Technology. **2001**, 25, 62-74.

Z

Zárate-Ramírez, L.; Martínez, I.; Romero, A.; Partal, P.; Guerrero, A. Wheat gluten-based materials plasticised with glycerol and water by thermoplastic mixing and thermomoulding. Journal of the Science of Food and Agriculture. **2011**, 91, 625-633

Zhang, D.; Song, X.M.; Liang, F.X. Preparation, swelling behaviour, and slow-release properties of poly (acrylic acid-co-acrylamide)/sodium humate superabsorbent composite. Industrial & Engineering Chemistry Research. **2006**, 45, 48-53.

Zhang, J.; Mungara, P.; Jane, J. Mechanical and thermal properties of extruded soy protein sheets. Polymer. **2001**, 42, 2569-2578.

Zhao, W.M.; Gatehouse, J.A.; Boulter, D. The purification and partial amino acid sequence of a polypeptide from the glutelin fraction of rice grains: homology to pea legumin. FEBS Left. **1983**, 162, 96-102.

Zheng, H.; Tan, Z.; Zhan, YR.; Huang, J. Morphology and properties of soy protein plastics modified with chitin. Journal of Applied Polymer Science. **2002**, 90, 3676-3682.

Zivanovic, S.; Chi, S.; Draughon, A.F. Antimicrobial activity of chitosan films enriched with essential oils. Journal of Food Science. **2005**, 70, 45-50.

PUBLICACIONES

El capítulo de libro y los artículos publicados han sido retirados de la tesis debido a restricciones relativas a los derechos de autor. Dichos artículos han sido sustituidos por la referencia bibliográfica, enlace al texto completo (solo miembros de la UHU) y/o enlace Arias Montano, Repositorio Institucional de la Universidad de Huelva, así como resumen.

- Gómez Martínez, D.P., Partal López, P., Gallegos Montes, C.: "Gluten-based bioplastics with modified controlled-release and hydrophilic properties". Industrial Crops and Products. Vol. 43, págs. 704–710, (2013). DOI: 10.1016/j.indcrop.2012.08.007

RESUMEN:
Bioplastics made from renewable and biodegradable polymers are considered as promising materials for relevant industrial applications in agriculture, packaging, pharmacy, etc. Their added value would arise from their hydrophilic character and ability controlling the release of "active agents". On these grounds, this work deals with the development of protein-based bioplastics to be used as water resources (with improved water uptake) and able to control the release of an agricultural nutrient (KCl), both of them required for the suitable plant growth. Their thermo-mechanical and physico-chemical properties were determined through dynamic mechanical thermal analysis (DMTA), differential scanning calorimetry (DSC), water absorption and diffusion tests. The use of less hygroscopic plasticizers, in the new formulations proposed, has modified bioplastic release/swelling properties. Among the modifiers studied, citric acid achieved the most suitable balance between an enhanced protein/salt affinity and the material mechanical properties, yielding slow release patterns, higher KCl leaching capacity and suitable water uptake.

Enlace al texto complete del artículo (solo para miembros de la UHU):
http://dx.doi.org/10.1016/j.indcrop.2012.08.007

- Gómez Martínez, D.P., Barneto, A.G., Martínez García, I., Partal López, P.: "Modelling of pyrolysis and combustion of gluten–glycerol-based bioplastics". Bioresource Technology. Vol. 102, n. 10, págs. 6246–6253, (2011). DOI: 10.1016/j.biortech.2011.02.074

RESUMEN:

Non-isothermal thermogravimetric analysis, under nitrogen and air atmospheres, has been applied to study the thermal degradation of wheat gluten and gluten–glycerol-based bioplastics. In order to explain experimental data, thermal degradation has been simulated using the so-called pseudo-components, which are related to protein fraction (mainly gliadin and glutenin), residual starch and plasticiser. Thus, the proposed models have been used to shed some light on the thermal decomposition of these materials, which have been found affected by their compositions and microstructures. Modelling confirms the experimental bioplastic and gluten isolate compositions, e.g. bioplastic moisture content, starch concentration and the expected gliadin/glutenin ratio. According to the simulation, the glycerol volatilisation is affected by bioplastic moisture content and hindered by the protein matrix. A fact pointing out that glycerol/water blend plays relevant plasticizing roles in the protein matrix through diverse physicochemical interactions

Enlace al texto complete del artículo (solo para miembros de la UHU):
http://dx.doi.org/10.1016/j.biortech.2011.02.074

- Gómez Martínez, D.P., Partal López, P., Martínez García, I., Gallegos Montes, C.: "Rheological behaviour and physical properties of controlled-release gluten-based bioplastics". Bioresource Technology. Vol. 100, n. 5, págs. 1828-1832, (2009). DOI: 10.1016/j.biortech.2008.10.016

RESUMEN:

Bioplastics based on glycerol, water and wheat gluten have been manufactured in order to determine the effect that mechanical processing and further thermal treatments exert on different thermo-mechanical properties of the biomaterials obtained. An "active agent", KCl was incorporated in these matrices to develop controlled-release formulations. Oscillatory shear, dynamic mechanical thermal analysis (DMTA), diffusion and water absorption tests were carried out in order to study the influence of the above-mentioned treatments on the physico–chemical characteristics and rheological behaviour of these bioplastic samples. Wheat gluten protein-based bioplastics studied in this work present a high ability for thermosetting modification, due to protein denaturation, which may favour the development of a

wide variety of biomaterials. Bioplastic hygroscopic properties depend on plasticizer nature and processing procedure, and may be a key factor for industrial applications where water absorption is required. On the other hand, high water absorption and slow KCl release from bioplastic samples (both of them suitable properties in agricultural applications) may be obtained by adding citric acid to a given formulation, at selected processing conditions.

Enlace al texto complete del artículo (solo para miembros de la UHU):
http://dx.doi.org/10.1016/j.biortech.2008.10.016

- Gómez Martínez, D.P., Partal López, P., Martínez García, I., Gallegos Montes, C.: "Rhelogical and release behaviour of gluten-based bioplásticos ". En: A. Guerrero, J. Muñoz and J.M. Franco, ed. Rheology in product design and engineering. Sevilla : Grupo Español de Reología, 2008. P. 21-24